DISSERTATION

TUMOR MICROENVIRONMENT IN SPONTANEOUSLY OCCURING TUMORS AND *IN VITRO* EVALUATION OF HYPOXIA ASSOCIATED MUTAGENESIS

Submitted by

Nadira Trncic

Department of Environmental and Radiological Health Sciences

In partial fulfillment of the requirements
For the Degree of Doctor in Philosophy
Colorado State University
Fort Collins, Colorado
Spring 2008

COLORADO STATE UNIVERSITY

January 17, 2008

WE HEREBY RECOMMEND THAT THE DISSERTATION PREPARED UNDER OUR SUPERVISION BY NADIRA TRNCIC ENTITLED TUMOR MICROENVIRONMENT IN SPONTANEOUSLY OCCURING TUMORS AND *IN VITRO* EVALUATION OF HYPOXIA ASSOCIATED MUTAGENESIS BE ACCEPTED AS FULFILLING IN PART REQUIREMENTS FOR THE DEGREE OF DOCTOR OF PHILOSOPHY.

Committee on Graduate Work

Susan Kraft
Susan Kraft
Michael Fox
Michael Fox
William S Bennett
William S Bennett

Susan M LaRue
Susan M LaRue
Adviser

John D. Zumbrunnen
Department Head/Director

ABSTRACT OF DISSERTATION

TUMOR MICROENVIRONMENT IN SPONTANEOUSLY OCCURING TUMORS AND *IN VITRO* EVALUATION OF HYPOXIA ASSOCIATED MUTAGENESIS

The importance of the tumor oxygenation status in tumor progression and tumor response to radiation and other forms of treatment has been investigated in many experimental and clinical studies.

Oxygen status can impact cell killing associated with radiation treatment and, interestingly radiation can also impact subsequent oxygen levels. Part I of my dissertation is concerned with this phenomenon of reoxygenation. A multiparameter study was conducted in naturally occurring canine tumors to evaluate physiological changes in the tumor microenvironment following a 3 Gy fraction of radiation. Pre-treatment values of partial pressure of oxygen, interstitial fluid pressure, microvascular perfusion, level of apoptosis, and microvessel density were compared to the 24 hours post-radiation measurements in the same location. I analyzed changes in all parameters and evaluated the relationship between parameters and pO_2. In disagreement with my working hypothesis, I only found inverse correlation between changes in oxygen level and changes in IFP.

In Part II, I used the CHO A_L mutation assay to investigate the role of hypoxia alone in the induction of mutagenesis. After exposing cells to different hypoxic conditions I found that only severe hypoxia can cause mutations in human-hamster hybrid cells (A_L). Level of oxygen that induced mutations was less than 0.63 mm Hg. Both the complement-mediated A_L mutation assay and the flow cytometry mutation assay were done. Mutant cells were sorted from the mutant peak, and the clonal populations of cells were analyzed with the A_L flow cytometry assay to determine if cells were really mutated (negative for CD59) and not just downregulated in hypoxia. Quantitative analysis of mutations that were performed did not detect any changes in the CD59 gene.

Tumor reoxygenation, as shown here, may not be associated with improved tumor perfusion, but rather with other factors such as decreased oxygen consumption. These studies proved that severe hypoxia can cause mutations and possibly tumor genetic instability, and that those levels of oxygenation can be found in spontaneous tumors in dogs, which are a great tumor model for translating findings to human cancers.

Nadira Trncic
Environmental and Radiological Health Sciences Department
Colorado State University
Fort Collins, CO 80523
Spring 2008

ACKNOWLEDGEMENTS

The Department of Environmental and Radiological Health Sciences and the first professor I met here, Dr. Ed Gillette have given me the great opportunity of learning and supported me in my pursuit of the discovery of the world of research. I am truly indebted to all faculty and staff for years of help they offered through this incredible experience. First, I would like to express my gratitude to my advisor Dr. Susan LaRue for giving me the opportunity of pursuing graduate studies here at Colorado State University. I am thankful for her support and the various opportunities for improvement, including traveling, which allowed me to interact with other scientists in my field.

I would also like to thank my graduate committee members Dr. Michael Fox, Dr. William Dernell and Dr. Susan Kraft for their scientific contribution and their help in improving the quality of my work.

The support from radiation treatment staff was also very important, and included help with all my study patients, as well as with the scheduling and handling of the samples and help with the equipment when necessary. My special thanks to Billie Arceneaux, her patience and help with imaging, to Chana Fuller and Frank Conwey for their help and understanding.

I am very thankful to Diane Vannais for her selfless help with A_L assay, PCR, and providing me with advice and guidance in that part of my study.

I have to thank all my fellow graduate students who were tremendous support and helped me with my learning process that included a big task of learning science, English, American way of life: Elizabeth McNiel, Christine Anderson, Larry Dugan, Scott Pearson, Adam Holmes, Susan Hudachek, and my officemate Jenny Devitt.

Apart from the University, special thanks go to my family and friends: My parents who thought me the most important lectures in my life about honesty, respect, and constant search for knowledge; To my husband Sinisa, for his patience, understanding, and for being an example of integrity and perseverance; To my children Damir and Anja for being the most wonderful people in my life, and for their unconditional love. Also thanks to my brother Sejo and sister Nerma for their thoughtfulness; To Jasmina, Jean, Alex, Ana, and Valeria for their invaluable company during this journey.

Without all of the people mentioned here I would not be where I am today, and my journey would never go this far.

TABLE OF CONTENTS

PART I

THE IMPACT OF RADIATION ON TUMOR OXYGEN STATUS IN SPONTANEOUSLY OCCURING CANINE TUMORS

CHAPTER 1

INTRODUCTION

Cancer is the second leading cause of death in the US, exceeded only by heart disease. In 2007 it is estimated that more than 1500 Americans a day will die of cancer (about 559,650 people) and about 1.445 million new cancer cases would be diagnosed in the US, plus more than 1 million cases of basal and squamous cell skin cancers (Cancer Facts and Figures 2007, American Cancer Society).

Cancer is a disease resulting from genetic mutations, either inherited or acquired, that allow cells to grow uncontrolled. However, there is a significant physiological contribution to the development of a tumor.

Tumor microenvironment

Microenvironment within solid tumors is different from that in normal tissues (Dewhirst et al, 1995), with characteristic chaotic vasculature and deficient lymphatic system (Rockwell et al, 2001). Unrestricted growth of tumors is dependent upon angiogenesis (Folkman et al, 1971; Folkman and Klagsbrun, 1987).The formation of new blood vessels is necessary for a tumor to grow beyond a few millimeters in diameter (Folkman, 1985). Normal angiogenesis usually occurs in the embryo as remodeling of the

primary capillary plexus, created by the process of vasculogenesis. During this process, vessels are formed from endothelial cell precursors called angioblasts. Remodeling of the primary capillary plexus is done by the sprouting and branching of new vessels from preexisting ones in the process of angiogenesis (Papetti and Herman, 2002). Angiogenesis is also present in the adult during the ovarian cycle, in physiological repair processes such as wound healing, and in pathological non-neoplastic conditions as retrolental fibroplasia or diabetic retinopathy, arthritis, psoriasis, and duodenal ulcers (Folkman, 1995). Under non-neoplastic conditions, angiogenesis is a highly ordered process that strictly follows, and is limited, by the demand of growing tissues. Neovascularization is essential for tumor growth and progression (Folkman et al, 1989). Tumor-induced angiogenesis differs from that occurring in physiological situations and pathological nonmalignant conditions. Tumor-induced angiogenesis is not self-limited. Once induced, it continues indefinitely. Tumor blood vessels may form from preexisting capillaries in a process very similar to normal angiogenesis. It has been suggested recently that circulating endothelial precursors derived from bone marrow could be involved in tumor-derived vasculature formation. The induction of tumor neovascularization results from the interrupted balance between pro- and anti-angiogenic factors in the tumoral microenvironment. Some of these factors are well characterized as pro-angiogenic: vascular endothelial growth factor (VEGF), fibroblast growth factors (FGFs), heparinase, angiopoietin 2 (Ang2), and interleukin-8 (IL-8). In addition to the stimulators of angiogenesis there are more than 40 endogenous angiogenesis inhibitors: interferons (INF-α, -β, -γ), interleukins (IL-4), tissue inhibitors of metalloproteinases (TIMPs), photolytic fragments (angiostatin, endostatin), and others like

thrombospondin-1 (TSP-1) (Papetti and Herman, 2002). Tumor expansion after the onset of angiogenesis is dependant not only on delivery of oxygen and nutrients by new microvessels, but also on the release of anti-apoptotic and survival factors (at least 20 of them), from the endothelial cells in these new vessels, some of them being: acidic fibroblast growth factor (aFGF), basic fibroblast growth factor (bFGF), Interleukin-6 (IL-6), Insulin-like growth factor-1 (IGF-1), Platelet derived growth factor (PDGF) (Folkman, 2003).

As a tumor grows, a chaotic network of microvessels develops. Newly formed microvessels do not parallel the morphology of the host tissue vasculature as nicely shown in Fig.1.1. (Vaupel, 2004). Such microvessels are characterized by lack of smooth muscle cells and nervous components, tortuosity, dilatation, elongation, arterio-venous shunts, and blind ends (Jain, 1999). Tumor blood vessels have incomplete or even missing endothelial linings and basement membranes, resulting in increased leakiness. The extravasation of plasma and red blood cells results in an increase of the interstitial fluid space (Vaupel, 2004). The density of the tumor vascular network is expressed as intratumoral microvascular density (MVD). It is usually implied that MVD is directly related to tumor angiogenesis, but some non-specific factors, such as inflammation, can modify the vascular density within the tumor. The intratumoral vascular density was found to vary in the degree and spatial distribution between tumors, but even among tumors of the same histology (Koukourakis et al, 2000). Many studies on different tumor types have provided significant prognostic information with high vascularity associated with poor treatment outcome (Weidner et al, 1992; Alvarez et al, 1999; Guidi et al, 2000; West et al, 2001, Uzzan et al, 2004).

In addition, a functioning lymphatic system is absent in most solid tumors. Some recent findings (Stacker et al, 2001; Karkkainen et al, 2004) provide evidence that tumors can activate lymphangiogenesis, stimulated by VEGF-C and VEGF-D and the receptor, VEGFR-3.

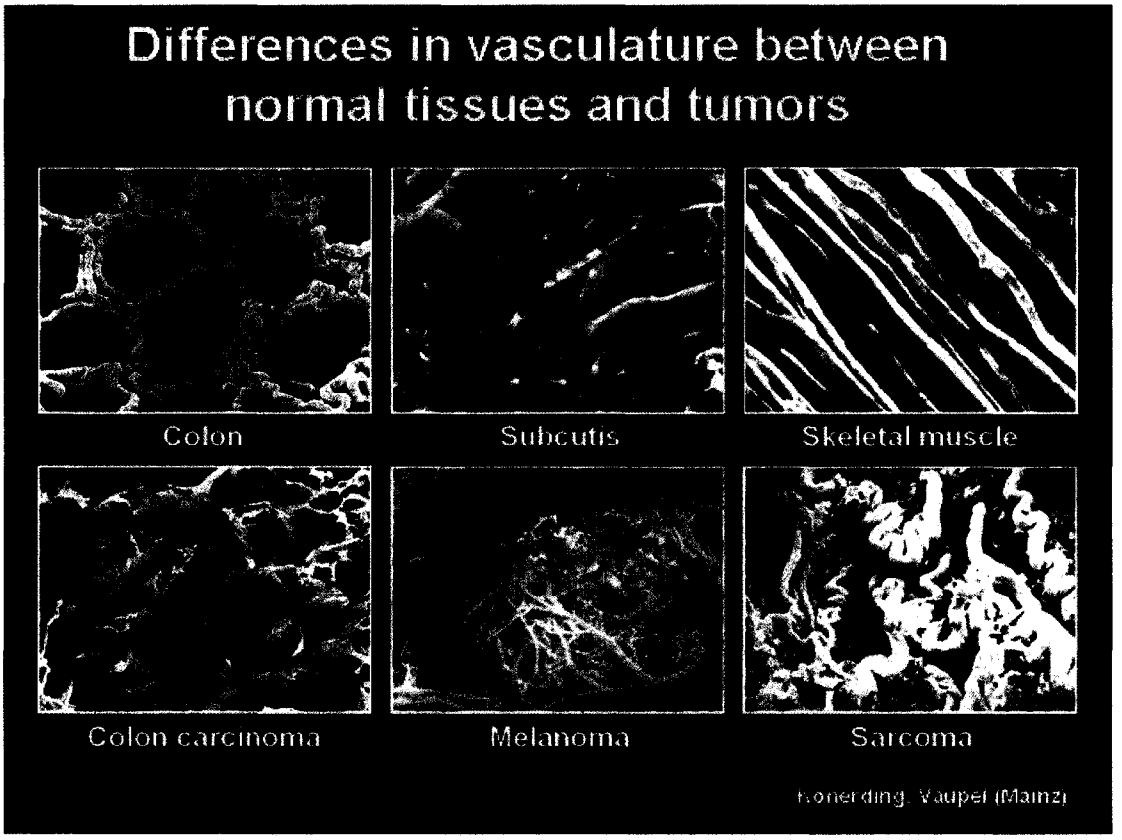

Figure 1.1 Differences in vasculature between normal tissues (upper panels) and malignant tumors (lower panels). (Vaupel from Konerding, 2004).

Tumor blood and lymphatic vessels are structurally and functionally abnormal, which results from an imbalance in molecular factors regulating growth and maturation of the

vessels, and from the compressive mechanical forces formed by proliferating tumor cells. These abnormalities can lead to hyperpermeable, tortuous vessels and compressive forces can cause vessel lumen collapse and hence influence blood flow.

The absence of properly functioning lymphatics results in decreased interstitial fluid drainage and increased values of interstitial fluid pressure (Dunn, 1997; Kuszyk et al, 2001). Elevated IFP in solid tumors was recognized as early as the 1950s (Young et al. 1950). Interstitial hypertension has been measured since then in animal and human solid tumors (Znati et al, 1996; Zachos et al, 2001; Milosevic et al, 2001). Normal IFP is close to atmospheric, but in tumors it is elevated. IFP has been measured in a variety of human tumors before treatment, and it was in a range from near zero to levels of 100mmHg (Boucher et al,1991; Gutmann et al,1992; Milosevic et al,1998; Cairns et al, 2006). Recent studies on a spontaneous carcinogenesis model (Hagendoorn et al, 2006) found that interstitial fluid pressure was already elevated in the hyperplastic/dysplastic stage (early stage of cancer development). There are two major ways that tumor IFP becomes elevated. First; the leakage of fluid and osmotic proteins from the blood into the interstitial space results in a reduction of hydrostatic pressure in the vessels and increase of colloid osmotic pressure in the interstitium. The lack of a lymphatic system enhances this problem. In addition to the influence of the architecture of the tumor vessels, there is also the role of the extracellular matrix and its contractile characteristics. The experiments have shown that normal fibroblasts grown in collagen gel will take on contractile characteristics and actively compress the gel (Steinberg et al, 1980). The process is mediated by stimulation from platelet-derived growth factor (PDGF),

transforming growth factor-β receptors and through the interactions of β1 integrin and collagen (Clark et al, 1989; Nakamura et al, 2002).

Hemoconcentration, found due to fluid loss from the tumor vasculature (Vaupel et al, 87; Sevick and Jain, 1988), causes elevated viscosity of the blood resulting in increased resistance to flow (Vaupel, 2004; Jain, 1988). A significant increase in the aggregation and rigidity of RBC (red blood cells), fibrinogen and globulin concentrations, and plasma and blood viscosity has been reported in melanoma patients (Dintenfass, 1978). This increase in RBC aggregation has been reported in lung and bowel cancers (Dintenfass and Forbes, 1973, 1975), breast cancer (Riley, 1976) and in various carcinomas (Tietjen et al, 1977). The resistance of blood is regulated by the viscosity of plasma and the number, size, and rigidity of blood cells. The increased RBC aggregation may explain increased blood viscosity, and the associated elevated fibrinogen and globulin concentrations may explain increased plasma viscosity (Jain, 1988). Therefore blood flow through a tumor is more sluggish and inadequate. Impaired blood flow leads to reduced oxygen delivery through the tumor and contributes to regions of tumor hypoxia. Deviant vasculature and vessel density lead to an increase in geometric resistance to flow (Vaupel, 2004), consequently contributing to deficient perfusion.

Poor perfusion and elevated metabolic rates are bases for the unique microenvironment characterized by regions of low oxygen (hypoxia) and low pH (acidosis) (Reynolds et al, 1996). The diffusion distances of glucose and other critical nutrients are similar to that of oxygen (Reynolds et al, 1996; Vaupel, 2004), and the uptake of glucose is limited by its delivery by the defective tumor blood flow (Kallinowski et al, 1988). Tumor characteristic vasculature is not only inefficient in the delivery of oxygen, but it can also

limit tumor tissue supply of energy sources and growth factors. Therefore, cells found at a distance from the nearest functional blood vessel may experience nutritional deprivation (Vaupel, 2004).

One of the properties of invasive cancers is altered glucose metabolism. Lysis of glucose, glycolysis, starts with conversion of glucose to pyruvate. In most mammalian cells, glycolysis is inhibited by the presence of oxygen, which allows mitochondria to oxidize pyruvate to CO_2 and H_2O. In cancer cells pyruvate is converted instead to a waste product, lactic acid (Figure 1.2). Conversion of glucose to lactic acid in the presence of oxygen is known as aerobic glycolysis or the Warburg effect, since this phenomenon was first observed by Warburg in the 1920s (Semenza et al, 2001). Increased aerobic glycolysis is specifically observed in cancers. Upregulation of glycolysis is likely to be an adaptation to hypoxia that develops as pre-malignant lesions grow further from the blood supply, and malignant cells in invasive cancers remain glycolytic even in the presence of oxygen (Gatenby and Gillies, 2004). Increased production of lactic acid results in acidic tumor microenvironment, with significantly lower pH of the extracellular space.

A significant amount of work has shown that tumor microenvironment enhances malignant progression and aggressiveness (Graeber et al, 1996; Kunz and Ibrahim, 2003). It has been shown that hypoxia, by selecting for mutant p53, tumor suppressor gene, may lead to more malignant phenotype of tumors (Graeber et al, 1996). Hypoxia is associated with metastasis of soft tissue sarcomas, cervix carcinomas, carcinomas of the head and neck (Brizel et al, 1997; Hockel et al, 1996, Flyes et al, 1998; Brizel et al, 1999; Nordsmark et al, 1996; Rofstad, 2000a). It has been shown experimentally that hypoxia can lead to increased mutations (Reynolds et al, 1996). Clinical data support the

conclusion that hypoxia is a strong prognostic factor selecting for tumor metastatic spread.

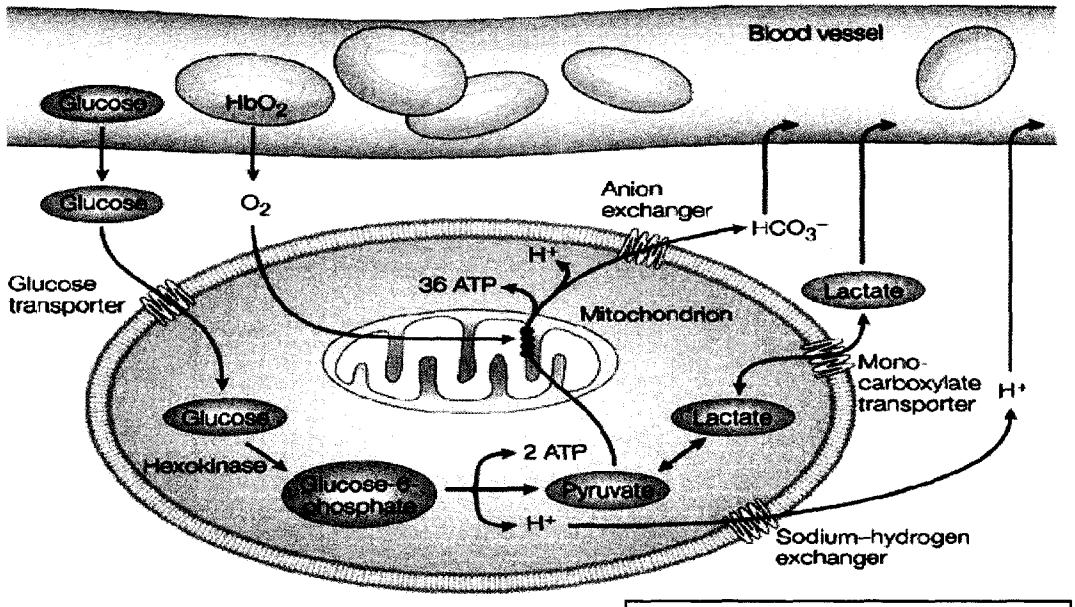

Afferent blood delivers glucose and oxygen (on haemoglobin) to tissues, where it reaches cells by diffusion. Glucose is taken up by specific transporters, where it is converted first to glucose-6-phosphate by hexokinase and then to pyruvate, generating 2 ATP per glucose. In the presence of oxygen, pyruvate is oxidized to HCO3, generating 36 additional ATP per glucose. In the absence of oxygen, pyruvate is reduced to lactate, which is exported from the cell. Note that both processes produce hydrogen ions (H+), which cause acidification of the extracellular space. HbO2, oxygenated haemoglobin.

Figure 1.2 Glucose metabolism in mammalian cells.

Tumor hypoxia also stimulates tumor progression through hypoxia-inducible transcription factor-1 (HIF-1), which regulates most genes induced by hypoxia stimulating their transcription. More than 60 HIF-1 target genes have been identified. A large number of them are involved in angiogenesis, glycolysis, cell survival, and erythropoiesis. Some of these genes are vascular endothelial growth factor (VEGF), glucose transporters (GLUT), glycolytic enzymes and erythropoietin (EPO). (Semenza, 2002; Lu et al, 2002).Also, high tumor lactate levels predict an elevated risk of metastasis in head and neck carcinoma (Brizel et al, 2001) and cervical cancers (Walenta et al, 2000; Rofstad, 2000a; Hockel et al, 1996).The upregulation of glycolysis resulting in elevated glucose consumption, and the subsequent microenvironmental acidosis, lead to the evolution of phenotypes resistant to acid-induced cell toxicity. These cells have great growth advantage that promotes uncontrolled proliferation and invasion. It has been shown in numerous studies that the extracellular pH in tumors is acidic and can reach values of almost 6.0. It was demonstrated that H^+ ions from acidic tumors diffuse into peritumoral normal tissue (along concentration gradients). Normal cells are unable to survive in this environment, while tumor cells continue to proliferate. Acidosis can alone be mutagenic through inhibition of DNA repair (Gatenby and Gillies, 2004).

It has been shown that overexpression of IL-8 caused by hypoxia and acidosis plays an important role in tumor angiogenesis and in the aggressive biology of human pancreatic cancer (Shi et al, 1999). The expression of IL-8 by human ovarian cancer cells correlates directly with disease progression. It has been shown that acidic pH activates nuclear factor-kappaB (NF-kappaB) and activator protein-1 (AP-1) and consequently induced elevated IL-8 gene expression by human ovarian carcinoma cells (Xu and Fidler, 2000).

While tumor specific vasculature is in part responsible for regions of tumor hypoxia along with acidosis and elevated interstitial fluid pressure, the cells within the tumor contribute to the characteristic tumor physiology by responding to these changes.

The inflammatory responses in solid tumors can alter tumor microenvironment. Tumor-associated inflammatory cells and fibroblasts contribute to neoplastic progression in the early stages, by modulating synthesis and degradation of the extracellular matrix components, and allowing tumor to produce mitogenic and angiogenic factors that promote tumor growth and metastasis (van Kampen et al, 2003).

Cellular responses to tumor microenvironment

In vitro studies have shown that cells exposed to hypoxia had decreased cellular adenosine thriphosphate (ATP) levels that are further decreased by exposure to low pH (Rotin et al, 1986). The concentration of ATP in human malignancies, consistent with these in vitro findings, was found to be lower than in normal tissues (Vaupel et al, 1989).

Cells exposed to conditions of tumor microenvironment and metabolic changes exhibit a reduced synthesis of the macromolecules. It has been shown that during hypoxia protein synthesis was reduced and protein degradation was increased (Pettersen et al, 1986). Hypoxia is also associated with a decrease in DNA synthesis (Graeber et al, 1994). One of the common cellular responses to environmental stress is reversible growth arrest by activation of the G1-phase check point. Probably G1/early S phase cell cycle arrest protects cells from advancing to S phase, when they are the most sensitive to killing by hypoxia (Amellem and Pettersen, 1991).

It has been demonstrated that hypoxia induces apoptosis (Graeber et al, 1996; Nelson et al, 2004). Apoptosis is a form of programmed cell death that is genetically encoded. The magnitude of apoptosis both in cell culture and in experimental tumors is promoted by the presence of functional p53. It has become apparent that the cellular inability to undergo apoptosis may have important consequences during neoplastic transformation. Damaged and possibly mutated cells that have lost the p53 tumor-suppressor gene or overexpressed the anti-apoptotic genes such as Bcl-2 are prevented from entering the apoptotic pathway. Instead, these cells survive and may go on to divide and expand the line of mutated cells, increasing carcinogenic risk. Hypoxia thus provides a physiological selective pressure in tumors for the cells that have lost apoptotic potential and particularly p53 mutants (Graeber et al, 1996).

Gene expression regulated by tumor microenvironment

To survive the extreme conditions of tumor microenvironment, tumor cells upregulate the expression of large number of genes as an adaptive mechanism. Some of these genes are, as categorized by their physiologic functions (Sutherland, 1998): glycolytic enzymes (phosphofructokinase, lactate dehydrogenase), glucose regulated proteins (GRP), glucose transporters, and growth factors that play an important role in tumor angiogenesis including vascular endothelial growth factor (VEGF), epidermal growth factor (EGF), transforming growth factor β (TGF-β), and platelet-derived endothelial growth factor (PDEGF). The gene products include proteins regulating the production of vasodilators, tumor suppressor genes and oncogenes, proteins involved in

maintaining redox homeostasis, and proteins involved in the regulation of signal transduction pathways (Dachs and Stratford, 1996).

Transcription factors are involved in expression of many cellular metabolism effectors. The most important such factor is hypoxia-inducible factor 1 (HIF-1). Many hypoxia-inducible genes are controlled by HIF-1 (Wang and Semenza, 1993) including genes involved in cell survival: insulin-like growth factor 2 (IGF2), transforming growth factor-α (TGF-α), and nitric oxide synthase 2 (NOS2). HIF-1 also increases glucose transport and anaerobic metabolism by activating glucose transporters (GLUT-1 and GLUT-3), and enzymes such as phosphoglycerate kinase-1 (PGK-1) and aldolase A (ALDA) (Wouters et al, 2004).

HIF functions also at the tissue level through up regulation of genes involved in angiogenesis and blood flow (VEGF and haem oxygenase-1) (Rofstad and Danielsen, 1999). Furthermore, HIF has an effect at the level of the whole organism by inducing erythropoietin (EPO) gene responsible for oxygen-carrying capacity of blood by involvement in the generation of hemoglobin (Wouters et al, 2004). HIF-1 is a heterodimer consisting of constitutively expressed HIF-1βsubunit and a HIF-1α subunit, whose expression is highly regulated by hypoxia (Semenza, 2003). Even though not as well investigated as HIF-1, there are other transcription factors that play role in adaptive responses to hypoxia including early growth response protein (Egr1), nuclear factor-κB (NF-κB), and activator-protein 1 (AP-1) (Papandreou et al, 2005).

Potential mechanisms of microenvironment-induced tumor progression are proposed to be by DNA damage induced by hypoxia and/or reoxygenation leading to deletions, amplifications and genomic instability; selecting for metastatic cell phenotypes

and induction of specific genes involved in metastasis like HIF-1α, VEGF, IL-8, TGF ß. High lactate concentration, low extracellular pH and low glucose concentration probably induce metastasis by similar mechanisms as hypoxia (Rofstad, 1999, 2000b).

Hypoxia

One of the most investigated features of the tumor microenvironment is reduced oxygen content or hypoxia. While the oxygen tension in normal tissue is in the range of 10 to 80 mmHg, depending on the tissue type (Cairns and Hill, 2004), many tumors contain regions of decreased partial pressure of oxygen (pO_2), less than 10 mmHg. The significance of 10 mmHg pO_2 is that is when radiation resistance starts to develop (Vaupel et al, 1989; Steen, 1991) with full resistance occurring at values of less than 0.5 mmHg (Wouters and Brown, 1997; Brown, 1999). The pO_2 value at which cellular radiation sensitivity is midway between fully oxygenated and anoxic is approximately 3-4 mmHg. The hypoxic cell radioresistance is a result of lack of oxygen in the radiochemical process by which ionizing radiation is interacting with cells (Hall, 2000). In the last decade the threshold was set even lower, reporting levels of pO_2 less than 5 or 2.5 mmHg as hypoxic (Thews et al, 1999; Haider et al, 2004; Cardenas-Navia et al, 2004; Vaupel and Harrison, 2004). Precisely, we are talking about radiobiological hypoxia. These are levels of oxygen enough for tumor cells to stay viable, but they become more resistant to killing by irradiation.

The existence of hypoxia in solid tumors was first reported by Thomlinson and Gray over 50 years ago (1955). Since than, many investigators have shown that animal tumors contain radioresistant hypoxic cells, and that these cells play a significant role in

reducing the response to radiation treatment (Powers, 1963; Thomlinson and Craddock, 1967). It is believed that tumor hypoxia results from imbalance between the supply and consumption of oxygen or poor and inefficient perfusion (Vaupel and Hockel, 2003; Gillies et al, 2002). Numerous studies have clearly shown the presence of hypoxic areas in different human malignancies including cancers of the breast, prostate, uterine cervix, head and neck, rectum, pancreas, brain tumors, malignant melanomas and soft tissue sarcomas (Vaupel et al, 1987; Vaupel, 2004). Hypoxic regions are found in a wide range of tumors with evident intra- and inter-tumoral variability in the extent of hypoxia. These findings are independent of clinical size, stage, and histopathologic type (Vaupel et al, 2001). Two forms of tumor cell hypoxia were initially identified in tumors.

Diffusion-limited or chronic hypoxia develops in areas distant from functional blood vessels. This mechanism was first proposed by Thomlinson and Gray after examination of tissue sections of human lung cancers, noticing viable cells around regions of oxygen supply, and necrosis at distances consistent with the limit of oxygen diffusion in tumor tissue (~150 μm) (Thomlinson and Gray, 1955). Perfusion-limited or acute hypoxia results from transient occlusion of blood vessels producing fluctuations in blood perfusion of tumor regions (Brown, 1979; Sutherland and Franko, 1980; Chaplin et al, 1986). Vaupel and Hockel introduced the terms anemic hypoxia and hypoxemic hypoxia as separate forms (Vaupel et al, 2001). Tumor-associated or therapy-induced anemia can reduce oxygen transport capacity of the blood and contribute to the development of hypoxia. Tumor microvessels can be perfused by plasma only, and hypoxia develops around those vessels rapidly because of inadequate supply. In the mammary carcinoma model (R3230AC) it has been found that approximately 8 to 9 % of microvessels are

plasma channels, vessels that don't carry red blood cells, or very few (Dewhirst et al, 1996). Considering the broad range of the factors that influence oxygen transport, and oxygen consumption rate, it is evident that the initial classification of only two types of hypoxia in tumors is oversimplified (Dewhirst, 2003). Some of these factors are: lowered vascular density, intravascular pO_2, blood viscosity. Dewhirst proposes a model to explain the bases for tumor hypoxia: in studies using skin-fold window chamber tissues they demonstrated a reduction in pO_2 in the longitudinal direction with respect to the arterioles that supply the tumor. Away from the arteriolar source microvascular pO_2 decreases, resulting in shorter diffusion distances and larger hypoxic zones between vessels. Tumor hypoxia has traditionally been thought to result from limitations of oxygen gradients in the radial direction from blood vessel (Thomlinson and Gray, 1955).

The rate of oxygen consumption is an important factor in tissue oxygenation since pO_2 depends on the supply of oxygen by the microvessels and on the local metabolic demand (Dewhirst et al, 1994; Thews et al, 1996). Malignant proliferation and aberrant metabolism increase the metabolic rate of tumors. Considering the demands involved in the replication of cellular organelles and chromosomes in addition to the physical division of a mother cell into two new ones, it is not surprising that the oxygen consumption rate of proliferating cells is three to five times higher than in cells not actively dividing (Vaupel et al, 1989).

Cancer cells display high rates of aerobic glycolysis known as the Warburg effect, where lactic acid is generated even in the presence of oxygen (Gatenby and Gillies, 2004). The upregulation of glycolysis and excessive production of lactate leads to an acidic environment within the tumor (Brizel et al, 2001). Across the cell membrane in

tumors there is a pH gradient with intracellular pH_i greater then extracellular pH_e (acidic outside, which is reverse of that found in normal tissue). The extracellular environment within tumor tissues has a median pH value 0.5 units below that of the surrounding normal tissues (Yuan and Glazer, 1998).

The presence of hypoxic cells in tumors is not only a major problem in radiation treatment but also leads to resistance to many anticancer drugs, and is associated with tumor progression and increased metastasis (Rofstad, 2000a), increased mutation rates (Reynolds et al, 1996), and increased expression of genes associated with angiogenesis and tumor invasion (Rofstad and Danielsen, 1999). Hypoxia-induced modification of gene expression may contribute to poor prognostic outlook, giving rise to more aggressive locoregional disease and enhanced invasive capacity. Low oxygen concentrations activate signaling pathways leading to the activation of transcription factors (Guillemin and Krasnow, 1997). As mentioned earlier, activated transcription factors are involved further in induction and control of many genes that play a role in adaptive responses to hypoxia. Even though there are numerous studies providing evidence that hypoxia is clinically associated with metastasis and poor prognosis, the underlying mechanisms remain unclear (Hockel and Vaupel, 2001). After finding that expression of extracellular matrix protein lysyl oxidase (LOX) in hypoxic human tumor cells is elevated (Denko et al, 2003), and its expression is regulated by HIF, in recent studies it has been shown that LOX correlates with metastatic disease and is essential for hypoxia-induced metastasis (Erler et al, 2006), and is good therapeutic target for the prevention of metastasis in breast cancer.

Experimental evidence suggested that hypoxia selects for tumor cells that have p53 mutations and consequently lost their apoptotic potential (Graeber et al, 1996; Kim et al, 1997). Hypoxia was found to induce apoptosis in tumor cells and further genetic alterations, such as loss of tumor suppressor gene p53 or overexpression of the apoptosis inhibitor protein Bcl-2. These observations lead to the suggestion that hypoxia provides a pressure in tumors selecting for cells with survival and growth advantage (Graeber et al, 1996). Following these findings, in human cervix carcinomas were identified tumors with a low apoptotic index that showed high probability for lymphatic spread and post-treatment recurrence (Hockel et al, 1999).

Numerous clinical studies performed in patients with soft tissue sarcomas (Brizel et al, 1996; Nordsmark et al, 2001), head and neck cancers (Brizel et al, 1997, 1999; Nordsmark et al, 1996, 2000), and carcinomas of the uterine cervix (Hockel et al, 1996; Fyles et al, 1998, 2002) indicated that presence of hypoxia adversely affects locoregional control and/or disease-free survival after primary radiation therapy. Therefore, hypoxia has a significant negative role in tumor prognosis. However, the low levels of oxygen are unique characteristic of tumors, which can be of therapeutic advantage. Targeting hypoxic regions of tumor, therapeutic strategies have potential to improve oxygenation or to kill tumor cells, relatively sparing normal tissues.

Correlation of tumor hypoxia to different treatment modalities:

As a Problem

The oxygen tension of tumors is an important determinant of their sensitivity to ionizing radiation. More than five decades ago Thomlinson and Gray established that

tumors contain oxygen-deprived regions, found beyond the limits of oxygen diffusion (Thomlinson and Gray, 1955). Pioneering studies of Gray and colleagues in early 50's (Gray et al, 1953) showed that hypoxic regions exhibited resistance to radiation damage. Numerous studies have confirmed that a dose of radiation kills oxygenated cells more efficiently than hypoxic cells. The difference in radiation sensitivity between aerobic and hypoxic cells expressed as the ratio of hypoxic to aerated doses needed to achieve the same biological effect, is known as the oxygen enhancement ratio and is normally 2.5-3 for sparsely ionizing radiations. The reason for this effect is that oxygen reacts with free radicals, the basic biochemical lesion produced by ionizing radiation. The consequences of radiation in the human body are mainly induction of DNA damage either by direct ionization of DNA or indirectly by the generation of free radicals. Free radicals are highly unstable and reactive due to their unpaired electron. Since 80 % of the cell is composed of water, free radicals induced by radiation are produced predominantly by the degradation of water molecules. As a consequence, reactive oxygen species (ROS) such as $OH^{\cdot}$, H_2O_2 or $O_2^{\cdot-}$ are generated. These free oxygenated radicals are strong oxidants that damage macromolecules such as DNA, but also cellular proteins and lipids. Oxygen reacts with the free electron of the free radical, "fixing" the damage, making it permanent (Hall, 2000). In hypoxic regions thus damage is not "fixed": it can be repaired.

There are different ways in which hypoxia might contribute to drug resistance. Oxygen concentration may have direct effect on drugs, such as mephalan, bleomycin, and etoposide, which require molecular oxygen for maximum efficiency (Koch et al, 2003). Hypoxia causes cells to slow their proliferation slowing their rate of progression through the cell cycle, likely as a result of hypoxia-induced specific proteins (Sciandra et

al, 1984; Heacock and Sutherland, 1986). Since most of anticancer drugs are more effective against rapidly proliferating cells, this slowing of cell proliferation with increased distance from the vasculature will lead to decreased cell killing (Tannock, 1968; Amellem and Pettersen, 1991). Drug concentrations are higher closer to blood vessels. Many anticancer drugs are limited in their diffusion from the blood vessel that is delivering them, not only because of the greater distances needed to be diffused, but also because of their reactivity. Many of them, such as intercalators, bind to DNA (Brown, 1999). Tumor hypoxia might contribute to drug resistance through amplification of genes leading to drug resistance (Rice et al, 1986, 1987) or through the induction of various hypoxic stress proteins that are responsible for resistance to some chemotherapeutics (Murphy et al, 1994). In addition to hypoxia, other features of the tumor microenvironment can impact effectiveness of chemotherapy.

The high interstitial fluid pressure in tumors can present a barrier to efficient drug delivery by decreasing transport from the bloodstream into the tumor interstitium. This is especially important for large molecules, such as antibodies and other proteins. Several clinical studies have shown that elevated IFP was a poor prognostic factor for patient outcome (Milosevic et al, 1998, 2001; Rofstad et al, 2002; Fyles et al, 2006).

Low pHe (extracellular) and resulting tumor cell trans-membrane pH gradient can impact the effectiveness of chemotherapy. Many commonly used chemotherapeutic agents are either weak bases or weak acids. While the uncharged form of the drug equalizes in concentration across both sides of the plasma membrane, the uptake and activity of charged forms is altered. This leads to increased uptake of weak acids such as chlorambucil, while that of weak bases like vinblastine can be decreased. For some

chemotherapeutic agents, such as the anthracyclines, this pH gradient can lead to a 50% reduction in intracellular drug levels comparing to extracellular drug levels, allowing for "physiological drug resistance" (Evelhoch et al, 2000).

Hypoxia is also a problem in cancer treatment with photodynamic therapy. Photodynamic therapy (also known as a photoradiation therapy or photochemotherapy) is a treatment modality that is a combination of light and light sensitive agents, photosensitizers, in an oxygen-rich environment. The photosensitizer is administered systemically or locally and preferentially taken up by tissues having strong mitotic activity and achieving higher concentrations in tumor than in normal tissue. This drug is activated with light at a particular wavelength that has to match the absorption maximum of the drug. It does not react directly with cells. Instead, it passes its energy to oxygen to create a chemical radical "singlet oxygen". PDT produces cytotoxic effects through photodamage to subcellular organelles and biomolecules only in the presence of oxygen (Figure 1.3).

As mentioned earlier, hypoxia is associated with the metastatic phenotype of cancers. Hypoxia may also decrease local control such as curability of tumors by surgery. This was observed in cervical cancer patients who underwent radical surgical treatment. It was found that tumors with a median $pO_2<10$ mmHg had larger tumor extensions, more frequent infiltrations and lymph-vascular space involvement comparing to tumors with a median $pO_2>10$ mmHg. Tumor oxygen status has been observed to be the most important prognostic factor for treatment outcome and metastatic free survival in cervical carcinoma after radiotherapy as well as surgery (Hockel et al, 1996).

Overall, hypoxia presents a barrier to the curability of solid tumors, regardless of treatment modality, and is an important biological consideration in cancer research.

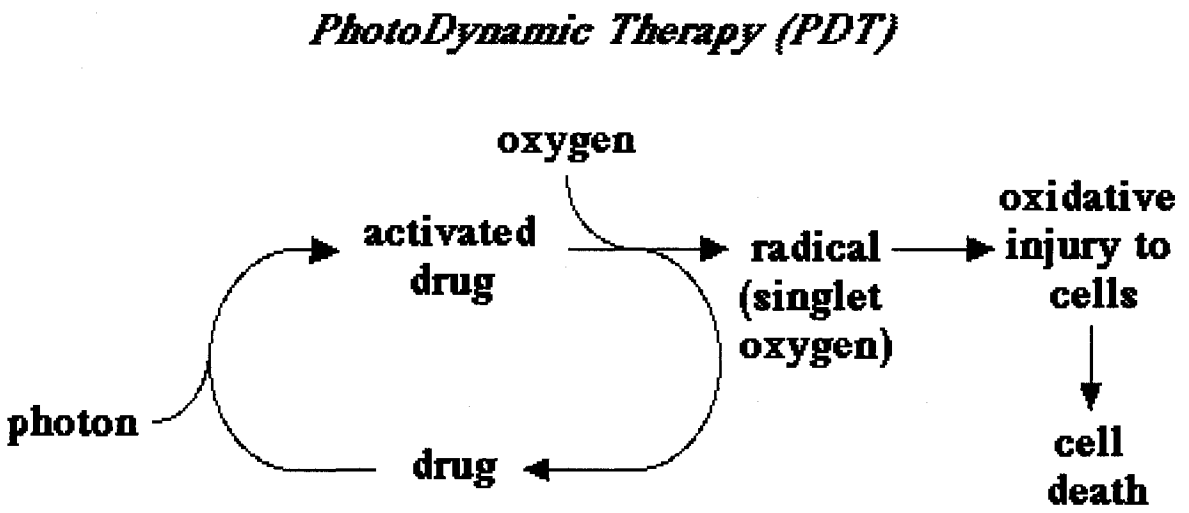

Figure 1.3. Schematics of the mechanism of action of Photodynamic Therapy.

Correlation of tumor hypoxia to different treatment modalities:

As an Advantage

Studying hypoxia in tumors has led to possibilities to use it as an advantage in a treatment of cancer. Two main strategies to overcome tumor hypoxia are to increase oxygen delivery or use oxygen-mimetic drugs, or to exploit tumor hypoxia for targeted therapy. The first strategy includes hyperbaric oxygen breathing, the administration of

carbogen and nicotinamide, and utilization of chemical radiosensitizers. The other strategy, using bioreductive drugs and hypoxia-targeted gene therapy, activates cytotoxic agents at the tumor site sparing normal tissues.

One of the first attempts to overcome the resistance of hypoxic tumor cells to radiation was to increase the oxygen level in the blood. This was performed by having patients breathe 100% oxygen at a pressure of 3 atmospheres in a hyperbaric oxygen chamber (Henk, 1986; Dische, 1991). Multicenter clinical trials showed an increase in locoregional control and survival in patients with cervix or advanced head and neck carcinoma treated with radiation and hyperbaric oxygen, compared with radiotherapy given to air breathing patients. However, these studies were discontinued mainly because of patient compliance (Greco et al, 2003).

A strategy has been devised to overcome both chronic and acute hypoxia, namely the combination of carbogen (95% O_2 and 5% CO_2), effective against chronic hypoxia and vitamin B derivative nicotinamide, which is believed to prevent transient blood flow fluctuation, has been tested in experimental models with success (Kjellen et al, 1991; Horsman et al, 1997). In clinical studies, this dual strategy was combined with radiation and has had some therapeutic efficacy, especially in treatment of bladder and head and neck malignancies. The treatment use was limited by gastro-intestinal toxicity of nicotinamide (Hoskin et al, 1997, 1999; Kaanders et al, 2002).

Hyperthermia has been shown to enhance radiation therapy (Thrall et al, 1996). It is well known that the delivery of hyperthermia therapy depends on the tumor vascularization: hyperthermia is more effective in poorly vascularized regions of the malignant tissue (Dewhirst et al, 1997).The mechanisms for the enhancement of radiation

therapy by hyperthermia varies based on the tumor temperature. Treatment with high temperatures >42-43°C, may impact blood flow and actually increase tumor hypoxia. Treatment with mild hyperthermia (41-42°C) has been shown to improve tumor oxygenation and has been used in number of studies (Vujaskovic and Song, 2004; Jones et al, 2004; Dewhirst et al, 2005). It has been suggested that this increase in oxygenation is due an increase in perfusion and also a decrease in oxygen consumption (Vujaskovic et al, 2000). Mild hyperthermia given before radiation may be effective in overcoming hypoxic radioresistance. There is evidence that addition of heat increased the effect of radiation therapy in many of the randomized studies (Perez et al, 1991; Overgaard et al, 1995; Vernon et al, 1996). Furthermore, the heat-induced increase in tumor oxygenation may significantly increase the effectiveness of thermoradiotherapy in combination with some chemotherapy drugs, which is also oxygen dependant. The results of phase I/II clinical trials show that trimodality treatment, consisting of hyperthermia, cisplatin, and radiation therapy is effective and feasible in different cancer types with tolerable toxicity (Bergs et al, 2007).

Radiosensitizers have been developed to sensitize hypoxic tumor cells. The first radiation sensitizer was 2-nitroimidazole. Results from studies on experimental animals with these drugs were quite striking (Sheldon et al, 1974; Brown, 1975), but human clinical trials showed severe neuropathy with multiple doses of misonidazole. This side effect restricted the dose of drug that could be used clinically with radiation treatment (Dische, 1985). Then more effective 5-nitroimidazole, known as nimorazole, was reported to improve the effect of radiation therapy in some head and neck cancers, with only mild toxicity (Overgaard et al, 1998).

Hypoxia can be used to advantage in treating tumors by selectively killing the hypoxic tumor cells. Bioreductive drugs such as mitomycin C have been utilized as hypoxia selective cytotoxins. For bioreductive drugs to be activated, the cells need to be hypoxic and to produce appropriate reductase enzymes. Bioactivation is restricted by the presence of oxygen in normal tissue. These drugs specifically kill cells resistant to radiation and chemotherapeutics, adding to their cytotoxicity. It also affects fluctuating hypoxia, and could be very effective if given with every radiation dose. However, drug mitomycin C could be given only twice during the radiation treatments. Nevertheless, clinical trials using this bioreductive drug in conjunction with radiation have shown the benefit of this combination (Weissberg et al, 1989).

The first hypoxic cytotoxin used in the clinic is from the benzotriazine di-N-oxide class of agents, known as tirapazamine or TPZ (Brown, 1999). Since TPZ is relatively ineffective in killing oxygenated cells it is not effective to be used alone in cancer treatment. TPZ in combination with fractionated radiation has been shown to potentiate cell killing by radiation (Brown and Lemmon, 1990). Combination of TPZ with cisplatin, however, had the most clinical success (Brown, 1999). Since the dose that can be administered in clinical trials during chemo or radiation treatment has been limited by toxicity like neutropenia, there is a need for improved hypoxia-induced prodrugs. Another hypoxic cytotoxin, the anthraquinone AQ4N is promising and currently in clinical trials. AQ4N is a prodrug that gets activated in hypoxic cells to a stable cytotoxic product. Compared to TPZ, AQ4N shows an advantage since it can diffuse from hypoxic cells to kill the surrounding oxygenated cells, producing a bystander effect (Patterson and McKeown, 2000).

Besides using drugs that are toxic only to hypoxic cells, there are other ways to exploit tumor hypoxia in cancer treatment. One such approach is targeting some of the hypoxia-induced proteins such as transcription factor HIF-1 (hypoxia-inducible factor 1). The importance of the HIF pathway in tumorigenesis is very well established thanks to numerous experiments and a great amount of data in that field. Even though first discovered in 1993 (Wang and Semenza, 1993) this whole new field has become a topic of numerous investigations. Its role in angiogenesis, glucose metabolism, tumor cell survival and invasion, make it a potential tumor-specific target. Many of the enzymes involved in this pathway are potential therapeutic targets such as HIF-prolyl hydroxylases. Some of the proposed approaches to target high levels of HIF-1α are: inhibition of transactivation of HIF-1 target genes, like vascular endothelial growth factor VEGF; suppression of HIF-1 protein levels by its destabilization or inhibiting its production; or find agents potentially toxic to cells expressing HIF-1α (Brown and Wilson, 2004).

Another promising strategy is hypoxia-targeted gene therapy. Gene therapy can be explained as the transfer of genetic material (DNA or RNA) to modify the genetic repertoire of target cells for therapeutic purposes. Initially designed to treat inherited disorders caused by single gene defects (genetic diseases), the first clinical protocol was approved in1989 (Rosenberg et al, 1990). Since cancer develops as the result of gene mutations, it might be effectively treated with gene therapy. Interest in research in cancer gene therapy has grown so that more than half of clinical trials now are cancer related. As an antitumor approach, gene therapy has the possibility to target tumor cells selectively by combining highly specific gene delivery and highly specific gene expression (Greco et

al, 2002). The successful gene therapy is dependent on the development of vectors with maximum efficiency and minimum toxicity. Its major limitation is the lack of specificity of the gene-delivery system. Instead of delivering vectors directly into the tumor by needle injection, it is better to have the therapeutic gene transcribed or translated by a tumor-specific property. HIF-1 is expressed in high levels in tumors but not in normal tissues, and stimulates the transcription of a number of genes via the binding of HIF-1 to sequences known as hypoxia-responsive elements (HREs) in the promoter regions of target genes. This fact is used to get hypoxia-specific transcription of a therapeutic gene by developing a promoter highly responsive to HIF-1. This way the expression of the therapeutic gene would be specifically obtained in tumors (Brown, 2002). The major approaches in the design of therapeutic genes for cancer gene therapy are genetic immunopotentiation, mutation compensation and molecular chemotherapy. In the first case, the insertion of genes that encode cytokines enhances tumor immunogenicity; mutation compensation is targeted towards inactivation of oncogenes or induces the expression of tumor suppressor genes. In molecular chemotherapy a "suicide" gene is delivered to the tumor cells (Dachs et al, 1997). The enzyme expressed by the therapeutic gene is not toxic, but is able to convert prodrug (non-toxic compound) into a cytotoxin. The latter system is known as gene-directed enzyme/prodrug therapy, GDEPT. This has advantages in both the amplification effect (each enzyme activates many prodrug molecules) and the bystander effect. The bystander effect can extend killing effects of the active drug to untransfected neighboring cells (Greco et al, 2000). The combination of hypoxia gene therapy and ionizing radiation is a promising approach in exploiting resistant hypoxic tumor cells.

Reoxygenation

Low oxygen level regions within tumors play an important role in tumor progression and tumor spread, and determine tumor susceptibility to killing by various anti- cancer agents. Since about half of all US cancer patients are treated with radiation therapy (Moeller et al, 2004), the possibility that tumor hypoxia may limit the response of fractionated radiotherapy has been very closely evaluated. Tumor hypoxia has been the subject of interest in many experimental and clinical studies and its role in resistance to radiation therapy, as well as the other treatment modalities, has been well documented. Hypoxic cells require up to three times more radiation than normoxic cells to reach the same level of cell killing (Gray et al, 1953). Clinically it has been reported that pretreatment oxygenation of different tumors predicts the tumor response to radiotherapy (Kolstad, 1968; Getenby et al, 88; Hockel et al, 1993; Nordsmark et al, 1996; Brizel et al, 1997).

Tumor oxygen status has been proven to be very important for the outcome of patients treated with radiation. However, radiation itself also changes tumor oxygenation status. The phenomenon of hypoxic cells becoming oxygenated after a dose of radiation, known as reoxygenation, was first demonstrated in the late 1960's by work of van Putten and Kallman (1968). Since then it has been shown to occur in many experimental murine tumors (Olive, 1994; Horsman et al, 1995; Goda et al, 1995; Milas et al, 1995; Speke and Hill, 1995; Murata et al, 1996; Olsen and Rofstad, 1999; Bussink et al, 2000). Clinically it has been monitored by several authors in various human tumor types. Reoxygenation has been shown to occur in breast cancers (Pappova et al, 1982), carcinoma of the cervix (Sheridan et al, 2000; Cooper et al, 1999), and head and neck cancers (Brizel et al, 1999;

Lyng et al, 1999).The magnitude and time course of reoxygenation after radiation have been investigated in many experimental tumor models, revealing that the reoxygenation pattern could vary widely with the tumor type (Speke and Hill, 1995; Goda et al, 1995; Hockel et al, 1993), tumor size (Rofstad, 1989), irradiation conditions (Shibamoto et al, 1987), and dose of radiation (Hockel et al, 1996).

In many solid tumors reoxygenation appears within hours following radiation (Olive, 1994). Mechanisms governing tumor reoxygenation still remain unknown. Proposed explanations include extensive cell loss by apoptosis and tumor shrinkage (Milas et al, 1995; Kocher and Treuer, 1995), and consequently increased availability of oxygen to the surviving cells, decreased metabolic rate, decrease in oxygen consumption rates by radiation damaged cells (Kallman, 1972; Olive, 1994), reduced interstitial fluid pressure (Milosevic et al, 1998) as the tumor shrinks and improved microcirculation (Brown, 1979). It is also not known whether reoxygenation takes place primarily in chronic or acutely hypoxic tumor regions. It has been proposed that rapid reoxygenation may be present as a result of the resumed blood flow in acutely hypoxic areas of tumor (Brown, 1979), but that slow or inadequate reoxygenation is most likely the product of the slow process of removal of dead cells and tumor shrinkage (Horsman et al, 1995; Kocher and Treuer, 1995; Speke and Hill, 1995) with improvements in nutrient and oxygen status for chronically hypoxic areas. In the experimental tumors (SCC-VII tumors, Kitakabu et al, 1991) reoxygenation has been found to be biphasic after a single dose of 13 Gy, with rapid phase occurring within 1 hour, and a slow phase lasting 12-72 hours. With smaller doses, if applied in a number of 4 Gy fractions, more rapid reoxygenation was seen in 24 hour intervals between fractions. The work from the other

investigators, using different schedules of dose fractionation in experimental tumors, indicated that reoxygenation may not be rapid after an initial dose, but may improve over the course of fractionated radiation (Kallman et al, 1970; Rofstad, 1989).

Based on results obtained in numerous studies that measured the oxygen status of solid tumors before and post-radiation, it can be concluded that the radiocurability of tumors is probably influenced by the pretreatment hypoxic fraction as well as the reoxygenation pattern. Therefore, there is interest in knowing the extent to which reoxygenation occurs in radiation treated tumors. A better understanding of the changes in tumor oxygenation after radiation would allow for better planning of fractionated radiotherapy and its combination with modifiers of tumor microenvironmental parameters (blood flow, oxygenation, angiogenesis).

BIBLIOGRAPHY

1. Achermann R, Ohlerth S, Fidel J, Gardelle O, Gassmann M, Roos M, Saunders HM, Scheid A, Wergin M, Kaser-Hotz B (2002) Ultrasound guided, pre-radiation oxygen measurements using polarographic oxygen needle electrodes in spontaneous canine soft tissue sarcomas. *In Vivo* 16: 431-437

2. Achermann RE, Ohlerth SM, Rohrer BC, Gassmann M, Inteeworn N, Roos M, Scharz M, Wergin MC, Kaser-Hotz B (2004) Oxygenation of spontaneous canine tumors during fractionated radiation therapy. *Strahlentherapie und Onkologie* 180: 297-305

3. Adam MF, Gabalski EC, Bloch DA, Oehlert JW, Brown JM, Elsaid AA, Pinto HA, Terris DJ (1999) Tissue oxygen distribution in head and neck cancer patients. *Head & Neck* 21: 146-153

4. Alvarez AA, Krigman HR, Whitaker RS, Dodge RK, Rodriguez GC (1999) The prognostic significance of angiogenesis in epithelial ovarian carcinoma. *Clinical Cancer Research* 5: 587-591

5. Amellem O, Pettersen EO (1991) Cell inactivation and cell cycle inhibition as induced by extreme hypoxia: the possible role of cell cycle arrest as a protection against hypoxia-induced lethal damage. *Cell Proliferation* 24: 127-141

6. Axelson H, Fredlund E, Ovenberger M, Landberg G, Pahlman S (2005) Hypoxia-induced dedifferentiation of tumor cells--a mechanism behind heterogeneity and aggressiveness of solid tumors. [Review] [55 refs]. *Seminars in Cell & Developmental Biology* 16: 554-563

7. Bergs JW, Franken NA, Haveman J, Geijsen ED, Crezee J, van Bree C (2007) Hyperthermia, cisplatin and radiation trimodality treatment: a promising cancer treatment? A review from preclinical studies to clinical application. [Review] [132 refs]. *International Journal of Hyperthermia* 23: 329-341

8. Bindra RS, Schaffer PJ, Meng A, Woo J, Maseide K, Roth ME, Lizardi P, Hedley DW, Bristow RG, Glazer PM (2004) Down-regulation of Rad51 and decreased homologous recombination in hypoxic cancer cells. *Molecular & Cellular Biology* 24: 8504-8518

9. Bindra RS, Glazer PM (2005) Genetic instability and the tumor microenvironment: towards the concept of microenvironment-induced mutagenesis. [Review] [79 refs]. *Mutation Research* 569: 75-85

10. Boucher Y, Kirkwood JM, Opacic D, Desantis M, Jain RK (1991) Interstitial hypertension in superficial metastatic melanomas in humans. *Cancer Research* 51: 6691-6694

11. Brizel DM, Scully SP, Harrelson JM, Layfield LJ, Bean JM, Prosnitz LR, Dewhirst MW (1996) Tumor oxygenation predicts for the likelihood of distant metastases in human soft tissue sarcoma. *Cancer Research* 56: 941-943

12. Brizel DM, Sibley GS, Prosnitz LR, Scher RL, Dewhirst MW (1997) Tumor hypoxia adversely affects the prognosis of carcinoma of the head and neck. *International Journal of Radiation Oncology, Biology, Physics* 38: 285-289

13. Brizel DM, Dodge RK, Clough RW, Dewhirst MW (1999) Oxygenation of head and neck cancer: changes during radiotherapy and impact on treatment outcome. *Radiotherapy & Oncology* 53: 113-117

14. Brizel DM, Schroeder T, Scher RL, Walenta S, Clough RW, Dewhirst MW, Mueller-Klieser W (2001) Elevated tumor lactate concentrations predict for an increased risk of metastases in head-and-neck cancer. *International Journal of Radiation Oncology, Biology, Physics* 51: 349-353

15. Brown JM (1975) Selective radiosensitization of the hypoxic cells of mouse tumors with the nitroimidazoles metronidazole and Ro 7-0582. *Radiation Research* 64: 633-647

16. Brown JM (1979) Evidence for acutely hypoxic cells in mouse tumours, and a possible mechanism of reoxygenation. *British Journal of Radiology* 52: 650-656

17. Brown JM, Lemmon MJ (1990) Potentiation by the hypoxic cytotoxin SR 4233 of cell killing produced by fractionated irradiation of mouse tumors. *Cancer Research* 50: 7745-7749

18. Brown JM, Giaccia AJ (1998) The unique physiology of solid tumors: opportunities (and problems) for cancer therapy. [Review] [112 refs]. *Cancer Research* 58: 1408-1416

19. Brown JM (1999) The hypoxic cell: a target for selective cancer therapy--eighteenth Bruce F. Cain Memorial Award lecture. [Review] [106 refs]. *Cancer Research* 59: 5863-5870

20. Brown JM (2002) Tumor microenvironment and the response to anticancer therapy. [Review] [69 refs]. *Cancer Biology & Therapy* 1: 453-458

21. Brown JM, Wilson WR (2004) Exploiting tumour hypoxia in cancer treatment. [Review] [140 refs]. *Nature Reviews* Cancer. 4: 437-447

22. Bruehlmeier M, Kaser-Hotz B, Achermann R, Bley CR, Wergin M, Schubiger PA, Ametamey SM (2005) Measurement of tumor hypoxia in spontaneous canine sarcomas. *Veterinary Radiology & Ultrasound* 46: 348-354

23. Bussink J, Kaanders JH, Rijken PF, Raleigh JA, van der Kogel AJ (2000) Changes in blood perfusion and hypoxia after irradiation of a human squamous cell carcinoma xenograft tumor line. *Radiation Research* 153: 398-404

24. Cairns R, Papandreou I, Denko N (2006) Overcoming physiologic barriers to cancer treatment by molecularly targeting the tumor microenvironment. [Review] [125 refs]. *Molecular Cancer Research: MCR* 4: 61-70

25. Cairns RA, Hill RP (2004) Acute hypoxia enhances spontaneous lymph node metastasis in an orthotopic murine model of human cervical carcinoma. *Cancer Research* 64: 2054-2061

26. Cardenas-Navia LI, Yu D, Braun RD, Brizel DM, Secomb TW, Dewhirst MW (2004) Tumor-dependent kinetics of partial pressure of oxygen fluctuations during air and oxygen breathing. *Cancer Research* 64: 6010-6017

27. Chaplin DJ, Durand RE, Olive PL (1986) Acute hypoxia in tumors: implications for modifiers of radiation effects. *International Journal of Radiation Oncology, Biology, Physics* 12: 1279-1282

28. Clark RA, Folkvord JM, Hart CE, Murray MJ, McPherson JM (1989) Platelet isoforms of platelet-derived growth factor stimulate fibroblasts to contract collagen matrices. *Journal of Clinical Investigation* 84: 1036-1040

29. Cooper RA, West CM, Logue JP, Davidson SE, Miller A, Roberts S, Statford IJ, Honess DJ, Hunter RD (1999) Changes in oxygenation during radiotherapy in carcinoma of the cervix. *International Journal of Radiation Oncology, Biology, Physics* 45: 119-126

30. Dachs GU, Stratford IJ (1996) The molecular response of mammalian cells to hypoxia and the potential for exploitation in cancer therapy. [Review] [82 refs]. *British Journal of Cancer - Supplement* 27: S126-S132

31. Dachs GU, Dougherty GJ, Stratford IJ, Chaplin DJ (1997) Targeting gene therapy to cancer: a review. [Review] [105 refs]. *Oncology Research* 9: 313-325

32. Denko NC, Fontana LA, Hudson KM, Sutphin PD, Raychaudhuri S, Altman R, Giaccia AJ (2003) Investigating hypoxic tumor physiology through gene expression patterns. [Review] [86 refs]. *Oncogene* 22: 5907-5914

33. Dewhirst MW, Secomb TW, Ong ET, Hsu R, Gross JF (1994) Determination of local oxygen consumption rates in tumors. *Cancer Research* 54: 3333-3336

34. Dewhirst MW, Larue SM, Gerweck L (1995) Tumor physiology and cell kinetics. [Review] [47 refs]. *Seminars in Veterinary Medicine & Surgery (Small Animal)* 10: 148-157

35. Dewhirst MW, Kimura H, Rehmus SW, Braun RD, Papahadjopoulos D, Hong K, Secomb TW (1996) Microvascular studies on the origins of perfusion-limited hypoxia. *British Journal of Cancer - Supplement* 27: S247-S251

36. Dewhirst MW, Prosnitz L, Thrall D, Prescott D, Clegg S, Charles C, MacFall J, Rosner G, Samulski T, Gillette E, LaRue S (1997) Hyperthermic treatment of malignant diseases: current status and a view toward the future. [Review] [56 refs]. *Seminars in Oncology* 24: 616-625

37. Dewhirst MW (2003) Mechanisms underlying hypoxia development in tumors. [Review] [24 refs]. *Advances in Experimental Medicine & Biology* 510: 51-56

38. Dewhirst MW, Vujaskovic Z, Jones E, Thrall D (2005) Re-setting the biologic rationale for thermal therapy.[see comment]. [Review] [67 refs]. *International Journal of Hyperthermia* 21: 779-790

39. Dintenfass L, Forbes CD (1973) About increase of aggregation of red cells with an increase of temperature in normal and abnormal blood (i.e. cancer). Effect of ABO blood groups and proteins. *Biorheology* 10: 383-391

40. Dintenfass L, Forbes CD (1975) Effect of fibrinogen on aggregation of red cells and on apparent viscosity of artificial thrombi in haemophilia, myocardial infarction, thyroid disease, cancer and control systems: effect of ABO blood groups. *Microvascular Research* 9: 107-118

41. Dintenfass L (1978) Elevation of plasma viscosity and of aggregation of red cells in melanoma metastasis. *Biorheology* 15: 99-110

42. Dische S (1985) Chemical sensitizers for hypoxic cells: a decade of experience in clinical radiotherapy. [Review] [81 refs]. *Radiotherapy & Oncology* 3: 97-115

43. Dische S (1991) What have we learnt from hyperbaric oxygen? *Radiotherapy & Oncology* 20 Suppl 1: 71-74

44. Dunn T (1997) Oxygen and cancer. [Review] [13 refs]. *North Carolina Medical Journal* 58: 140-143

45. Erler JT, Bennewith KL, Nicolau M, Dornhofer N, Kong C, Le QT, Chi JT, Jeffrey SS, Giaccia AJ (2006) Lysyl oxidase is essential for hypoxia-induced metastasis. *Nature* 440: 1222-1226

46. Evelhoch JL, Gillies RJ, Karczmar GS, Koutcher JA, Maxwell RJ, Nalcioglu O, Raghunand N, Ronen SM, Ross BD, Swartz HM (2000) Applications of magnetic

resonance in model systems: cancer therapeutics. [Review] [116 refs]. *Neoplasia (New York)* 2: 152-165

47. Folkman J, Merler E, Abernathy C, Williams G (1971) Isolation of a tumor factor responsible for angiogenesis. *Journal of Experimental Medicine* 133: 275-288

48. Folkman J (1985) Tumor angiogenesis. [Review] [152 refs]. *Advances in Cancer Research* 43: 175-203

49. Folkman J, Klagsbrun M (1987) Vascular physiology. A family of angiogenic peptides. *Nature* 329: 671-672

50. Folkman J, Watson K, Ingber D, Hanahan D (1989) Induction of angiogenesis during the transition from hyperplasia to neoplasia. *Nature* 339: 58-61

51. Folkman J (1995) Angiogenesis in cancer, vascular, rheumatoid and other disease. [Review] [72 refs]. *Nature Medicine* 1: 27-31

52. Folkman J (2003) Angiogenesis and apoptosis. [Review] [79 refs]. *Seminars in Cancer Biology* 13: 159-167

53. Fyles A, Milosevic M, Hedley D, Pintilie M, Levin W, Manchul L, Hill RP (2002) Tumor hypoxia has independent predictor impact only in patients with node-negative cervix cancer.[see comment]. *Journal of Clinical Oncology* 20: 680-687

54. Fyles A, Milosevic M, Pintilie M, Syed A, Levin W, Manchul L, Hill RP (2006) Long-term performance of interstial fluid pressure and hypoxia as prognostic factors in cervix cancer. *Radiotherapy & Oncology* 80: 132-137

55. Fyles AW, Milosevic M, Wong R, Kavanagh MC, Pintilie M, Sun A, Chapman W, Levin W, Manchul L, Keane TJ, Hill RP (1998) Oxygenation predicts radiation response and survival in patients with cervix cancer.[erratum appears in Radiother Oncol 1999 Mar;50(3):371]. *Radiotherapy & Oncology* 48: 149-156

56. Garcia-Barros M, Paris F, Cordon-Cardo C, Lyden D, Rafii S, Haimovitz-Friedman A, Fuks Z, Kolesnick R (2003) Tumor response to radiotherapy regulated by endothelial cell apoptosis.[see comment]. *Science* 300: 1155-1159

57. Gatenby RA, Kessler HB, Rosenblum JS, Coia LR, Moldofsky PJ, Hartz WH, Broder GJ (1988) Oxygen distribution in squamous cell carcinoma metastases and its relationship to outcome of radiation therapy. *International Journal of Radiation Oncology, Biology, Physics* 14: 831-838

58. Gatenby RA, Gillies RJ (2004) Why do cancers have high aerobic glycolysis?. [Review] [96 refs]. *Nature Reviews* Cancer. 4: 891-899

59. Gillies RJ, Ogino T, Shulman RG, Ward DC (1982) 31P nuclear magnetic resonance evidence for the regulation of intracellular pH by Ehrlich ascites tumor cells. *Journal of Cell Biology* 95: 24-28

60. Gillies RJ, Raghunand N, Karczmar GS, Bhujwalla ZM (2002) MRI of the tumor microenvironment.[erratum appears in J Magn Reson Imaging 2002 Dec;16(6):751]. [Review] [225 refs]. *Journal of Magnetic Resonance Imaging* 16: 430-450

61. Goda F, O'Hara JA, Rhodes ES, Liu KJ, Dunn JF, Bacic G, Swartz HM (1995) Changes of oxygen tension in experimental tumors after a single dose of X-ray irradiation. *Cancer Research* 55: 2249-2252

62. Graeber TG, Peterson JF, Tsai M, Monica K, Fornace AJ, Jr., Giaccia AJ (1994) Hypoxia induces accumulation of p53 protein, but activation of a G1-phase checkpoint by low-oxygen conditions is independent of p53 status. *Molecular & Cellular Biology* 14: 6264-6277

63. Graeber TG, Osmanian C, Jacks T, Housman DE, Koch CJ, Lowe SW, Giaccia AJ (1996) Hypoxia-mediated selection of cells with diminished apoptotic potential in solid tumours.[see comment]. *Nature* 379: 88-91

64. Gray L.H, Conger A.D., Ebert M., Hornsey S., Scott O.C. (1953) The concentration of oxygen dissolved in tissues at the time of irradiation as a factor in radiotherapy. *British Journal of Radiology* 26: 638-648

65. Greco O, Patterson AV, Dachs GU (2000) Can gene therapy overcome the problem of hypoxia in radiotherapy?. [Review] [53 refs]. *Journal of Radiation Research* 41: 201-212

66. Greco O, Scott SD, Marples B, Dachs GU (2002) Cancer gene therapy: 'delivery, delivery, delivery' . [Review] [84 refs]. *Frontiers in Bioscience* 7: d1516-d1524

67. Greco O, Marples B, Joiner MC, Scott SD (2003) How to overcome (and exploit) tumor hypoxia for targeted gene therapy. [Review] [202 refs]. *Journal of Cellular Physiology* 197: 312-325

68. Guidi AJ, Berry DA, Broadwater G, Perloff M, Norton L, Barcos MP, Hayes DF (2000) Association of angiogenesis in lymph node metastases with outcome of breast cancer. *Journal of the National Cancer Institute* 92: 486-492

69. Guillemin K, Krasnow MA (1997) The hypoxic response: huffing and HIFing. [Review] [21 refs]. *Cell* 89: 9-12

70. Gutmann R, Leunig M, Feyh J, Goetz AE, Messmer K, Kastenbauer E, Jain RK (1992) Interstitial hypertension in head and neck tumors in patients: correlation with tumor size. *Cancer Research* 52: 1993-1995

71. Hagendoorn J, Tong R, Fukumura D, Lin Q, Lobo J, Padera TP, Xu L, Kucherlapati R, Jain RK (2006) Onset of abnormal blood and lymphatic vessel function and interstitial hypertension in early stages of carcinogenesis. *Cancer Research* 66: 3360-3364

72. Haider MA, Milosevic M, Fyles A, Sitartchouk I, Yeung I, Henderson E, Lockwood G, Lee TY, Roberts TP (2005) Assessment of the tumor microenvironment in cervix cancer using dynamic contrast enhanced CT, interstitial fluid pressure and oxygen measurements. *International Journal of Radiation Oncology, Biology, Physics* 62: 1100-1107

73. Hall EJ (2000) *Radiobiology for the radiologist.* Lippincot: Philadelphia

74. Harris AL (2002) Hypoxia--a key regulatory factor in tumour growth. [Review] [117 refs]. *Nature Reviews* Cancer. 2: 38-47

75. Heacock CS, Sutherland RM (1986) Induction characteristics of oxygen regulated proteins. *International Journal of Radiation Oncology, Biology, Physics* 12: 1287-1290

76. Henk JM (1986) Late results of a trial of hyperbaric oxygen and radiotherapy in head and neck cancer: a rationale for hypoxic cell sensitizers? *International Journal of Radiation Oncology, Biology, Physics* 12: 1339-1341

77. Hockel M, Knoop C, Schlenger K, Vorndran B, Baussmann E, Mitze M, Knapstein PG, Vaupel P (1993) Intratumoral pO2 predicts survival in advanced cancer of the uterine cervix. *Radiotherapy & Oncology* 26: 45-50

78. Hockel M, Schlenger K, Aral B, Mitze M, Schaffer U, Vaupel P (1996) Association between tumor hypoxia and malignant progression in advanced cancer of the uterine cervix. *Cancer Research* 56: 4509-4515

79. Hockel M, Schlenger K, Hockel S, Vaupel P (1999) Hypoxic cervical cancers with low apoptotic index are highly aggressive. *Cancer Research* 59: 4525-4528

80. Hockel M, Vaupel P (2001) Tumor hypoxia: definitions and current clinical, biologic, and molecular aspects. [Review] [162 refs]. *Journal of the National Cancer Institute* 93: 266-276

81. Horsman MR, Grau C, Overgaard J (1995) Reoxygenation in a C3H mouse mammary carcinoma. The importance of chronic rather than acute hypoxia. *Acta Oncologica* 34: 325-328

82. Horsman MR, Siemann DW, Chaplin DJ, Overgaard J (1997) Nicotinamide as a radiosensitizer in tumours and normal tissues: the importance of drug dose and timing. *Radiotherapy & Oncology* 45: 167-174

83. Hoskin PJ, Saunders MI, Phillips H, Cladd H, Powell ME, Goodchild K, Stratford MR, Rojas A (1997) Carbogen and nicotinamide in the treatment of bladder cancer with radical radiotherapy. *British Journal of Cancer* 76: 260-263

84. Hoskin PJ, Saunders MI, Dische S (1999) Hypoxic radiosensitizers in radical radiotherapy for patients with bladder carcinoma: hyperbaric oxygen, misonidazole, and accelerated radiotherapy, carbogen, and nicotinamide. *Cancer* 86: 1322-1328

85. Jain RK (1988) Determinants of tumor blood flow: a review. [Review] [165 refs]. *Cancer Research* 48: 2641-2658

86. Jain RK (1999) Transport of molecules, particles, and cells in solid tumors. [Review] [177 refs]. *Annual Review of Biomedical Engineering* 1: 241-263

87. Jones EL, Prosnitz LR, Dewhirst MW, Marcom PK, Hardenbergh PH, Marks LB, Brizel DM, Vujaskovic Z (2004) Thermochemoradiotherapy improves oxygenation in locally advanced breast cancer. *Clinical Cancer Research* 10: 4287-4293

88. Kaanders JH, Pop LA, Marres HA, Bruaset I, van den Hoogen FJ, Merkx MA, van der Kogel AJ (2002) ARCON: experience in 215 patients with advanced head-and-neck cancer. *International Journal of Radiation Oncology, Biology, Physics* 52: 769-778

89. Kallinowski F, Vaupel P, Runkel S, Berg G, Fortmeyer HP, Baessler KH, Wagner K, Mueller-Klieser W, Walenta S (1988) Glucose uptake, lactate release, ketone body turnover, metabolic micromilieu, and pH distributions in human breast cancer xenografts in nude rats. *Cancer Research* 48: 7264-7272

90. Kallman RF, Jardine LJ, Johnson CW (1970) Effects of different schedules of dose fractionation on the oxygenation status of a transplantable mouse sarcoma. *Journal of the National Cancer Institute* 44: 369-377

91. Kallman RF (1972) The phenomenon of reoxygenation and its implications for fractionated radiotherapy. *Radiology* 105: 135-142

92. Karkkainen MJ, Haiko P, Sainio K, Partanen J, Taipale J, Petrova TV, Jeltsch M, Jackson DG, Talikka M, Rauvala H, Betsholtz C, Alitalo K (2004) Vascular endothelial growth factor C is required for sprouting of the first lymphatic vessels from embryonic veins.[see comment]. *Nature Immunology* 5: 74-80

93. Khosravani H, Chugh B, Milosevic MF, Norwich KH (2004) Time response of interstitial fluid pressure measurements in cervix cancer. *Microvascular Research* 68: 63-70

94. Kim CY, Tsai MH, Osmanian C, Graeber TG, Lee JE, Giffard RG, DiPaolo JA, Peehl DM, Giaccia AJ (1997) Selection of human cervical epithelial cells that possess reduced apoptotic potential to low-oxygen conditions. *Cancer Research* 57: 4200-4204

95. Kitakabu Y, Shibamoto Y, Sasai K, Ono K, Abe M (1991) Variations of the hypoxic fraction in the SCC VII tumors after single dose and during fractionated radiation therapy: assessment without anesthesia or physical restraint of mice. *International Journal of Radiation Oncology, Biology, Physics* 20: 709-714

96. Kjellen E, Joiner MC, Collier JM, Johns H, Rojas A (1991) A therapeutic benefit from combining normobaric carbogen or oxygen with nicotinamide in fractionated X-ray treatments. [Review] [45 refs]. *Radiotherapy & Oncology* 22: 81-91

97. Koch S, Mayer F, Honecker F, Schittenhelm M, Bokemeyer C (2003) Efficacy of cytotoxic agents used in the treatment of testicular germ cell tumours under normoxic and hypoxic conditions in vitro. *British Journal of Cancer* 89: 2133-2139

98. Kocher M, Treuer H (1995) Reoxygenation of hypoxic cells by tumor shrinkage during irradiation. A computer simulation. *Strahlentherapie und Onkologie* 171: 219-230

99. Kolstad P (1968) Intercapillary distance, oxygen tension and local recurrence in cervix cancer. *Scandinavian Journal of Clinical and Laboratory Investigation Supplement* 106: 145-157

100. Koong AC, Denko NC, Hudson KM, Schindler C, Swiersz L, Koch C, Evans S, Ibrahim H, Le QT, Terris DJ, Giaccia AJ (2000) Candidate genes for the hypoxic tumor phenotype. *Cancer Research* 60: 883-887

101. Koukourakis MI, Giatromanolaki A, Sivridis E, Fezoulidis I (2000) Cancer vascularization: implications in radiotherapy? *International Journal of Radiation Oncology, Biology, Physics* 48: 545-553

102. Kunz M, Ibrahim SM (2003) Molecular responses to hypoxia in tumor cells. [Review] [111 refs]. *Molecular Cancer* 2: 23

103. Kuszyk BS, Corl FM, Franano FN, Bluemke DA, Hofmann LV, Fortman BJ, Fishman EK (2001) Tumor transport physiology: implications for imaging and imaging-guided therapy. [Review] [46 refs]. *AJR* American Journal of Roentgenology. 177: 747-753

104. Le QT, Denko NC, Giaccia AJ (2004) Hypoxic gene expression and metastasis. [Review] [183 refs]. *Cancer & Metastasis Reviews* 23: 293-310

105. Leo C, Giaccia AJ, Denko NC (2004) The hypoxic tumor microenvironment and gene expression. [Review] [68 refs]. *Seminars in Radiation Oncology* 14: 207-214

106. Lu H, Forbes RA, Verma A (2002) Hypoxia-inducible factor 1 activation by aerobic glycolysis implicates the Warburg effect in carcinogenesis. *Journal of Biological Chemistry* 277: 23111-23115

107. Lyng H, Tanum G, Evensen JF, Rofstad EK (1999) Changes in oxygen tension during radiotherapy of head and neck tumours. *Acta Oncologica* 38: 1037-1042

108. Lyng H, Sundfor K, Trope C, Rofstad EK (2000) Disease control of uterine cervical cancer: relationships to tumor oxygen tension, vascular density, cell density, and frequency of mitosis and apoptosis measured before treatment and during radiotherapy. *Clinical Cancer Research* 6: 1104-1112

109. Mihaylova VT, Bindra RS, Yuan J, Campisi D, Narayanan L, Jensen R, Giordano F, Johnson RS, Rockwell S, Glazer PM (2003) Decreased expression of the DNA mismatch repair gene Mlh1 under hypoxic stress in mammalian cells. *Molecular & Cellular Biology* 23: 3265-3273

110. Milas L, Hunter NR, Mason KA, Milross CG, Saito Y, Peters LJ (1995) Role of reoxygenation in induction of enhancement of tumor radioresponse by paclitaxel. *Cancer Research* 55: 3564-3568

111. Milosevic M, Fyles A, Hedley D, Pintilie M, Levin W, Manchul L, Hill R (2001) Interstitial fluid pressure predicts survival in patients with cervix cancer independent of clinical prognostic factors and tumor oxygen measurements. *Cancer Research* 61: 6400-6405

112. Milosevic M, Fyles A, Hedley D, Hill R (2004) The human tumor microenvironment: invasive (needle) measurement of oxygen and interstitial fluid pressure. [Review] [72 refs]. *Seminars in Radiation Oncology* 14: 249-258

113. Milosevic MF, Fyles AW, Wong R, Pintilie M, Kavanagh MC, Levin W, Manchul LA, Keane TJ, Hill RP (1998) Interstitial fluid pressure in cervical carcinoma: within tumor heterogeneity, and relation to oxygen tension. *Cancer* 82: 2418-2426

114. Milosevic MF, Fyles AW, Hill RP (1999) The relationship between elevated interstitial fluid pressure and blood flow in tumors: a bioengineering analysis. *International Journal of Radiation Oncology, Biology, Physics* 43: 1111-1123

115. Moeller BJ, Cao Y, Li CY, Dewhirst MW (2004) Radiation activates HIF-1 to regulate vascular radiosensitivity in tumors: role of reoxygenation, free radicals, and stress granules.[see comment]. *Cancer Cell* 5: 429-441

116. Moolten FL (1986) Tumor chemosensitivity conferred by inserted herpes thymidine kinase genes: paradigm for a prospective cancer control strategy. *Cancer Research* 46: 5276-5281

117. Murata R, Shibamoto Y, Sasai K, Oya N, Shibata T, Takagi T, Abe M (1996) Reoxygenation after single irradiation in rodent tumors of different types and sizes. *International Journal of Radiation Oncology, Biology, Physics* 34: 859-865

118. Murphy BJ, Laderoute KR, Chin RJ, Sutherland RM (1994) Metallothionein IIA is up-regulated by hypoxia in human A431 squamous carcinoma cells. *Cancer Research* 54: 5808-5810

119. Nakamura Y, Hirano S, Suzuki K, Seki K, Sagara T, Nishida T (2002) Signaling mechanism of TGF-beta1-induced collagen contraction mediated by bovine trabecular meshwork cells. *Investigative Ophthalmology & Visual Science* 43: 3465-3472

120. Nelson DA, Tan TT, Rabson AB, Anderson D, Degenhardt K, White E (2004) Hypoxia and defective apoptosis drive genomic instability and tumorigenesis. *Genes & Development* 18: 2095-2107

121. Nordsmark M, Overgaard M, Overgaard J (1996) Pretreatment oxygenation predicts radiation response in advanced squamous cell carcinoma of the head and neck. *Radiotherapy & Oncology* 41: 31-39

122. Nordsmark M, Overgaard J (2000) A confirmatory prognostic study on oxygenation status and loco-regional control in advanced head and neck squamous cell carcinoma treated by radiation therapy. *Radiotherapy & Oncology* 57: 39-43

123. Nordsmark M, Alsner J, Keller J, Nielsen OS, Jensen OM, Horsman MR, Overgaard J (2001) Hypoxia in human soft tissue sarcomas: adverse impact on survival and no association with p53 mutations. *British Journal of Cancer* 84: 1070-1075

124. Olive PL (1994) Radiation-induced reoxygenation in the SCCVII murine tumour: evidence for a decrease in oxygen consumption and an increase in tumour perfusion. *Radiotherapy & Oncology* 32: 37-46

125. Olsen DR, Rofstad EK (1999) Monitoring of tumor reoxygenation following irradiation by 31P magnetic resonance spectroscopy: an experimental study of human melanoma xenografts. *Radiotherapy & Oncology* 52: 261-267

126. Overgaard J, Gonzalez GD, Hulshof MC, Arcangeli G, Dahl O, Mella O, Bentzen SM (1995) Randomised trial of hyperthermia as adjuvant to radiotherapy for recurrent or metastatic malignant melanoma. European Society for Hyperthermic Oncology.[see comment]. *Lancet* 345: 540-543

127. Overgaard J, Hansen HS, Overgaard M, Bastholt L, Berthelsen A, Specht L, Lindelov B, Jorgensen K (1998) A randomized double-blind phase III study of nimorazole as a hypoxic radiosensitizer of primary radiotherapy in supraglottic larynx and pharynx carcinoma. Results of the Danish Head and Neck Cancer Study (DAHANCA) Protocol 5-85.[see comment]. *Radiotherapy & Oncology* 46: 135-146

128. Overgaard J (2007) Hypoxic radiosensitization: adored and ignored. [Review] [74 refs]. *Journal of Clinical Oncology* 25: 4066-4074

129. Papandreou I, Krishna C, Kaper F, Cai D, Giaccia AJ, Denko NC (2005) Anoxia is necessary for tumor cell toxicity caused by a low-oxygen environment. *Cancer Research* 65: 3171-3178

130. Papandreou I, Powell A, Lim AL, Denko N (2005) Cellular reaction to hypoxia: sensing and responding to an adverse environment. [Review] [113 refs]. *Mutation Research* 569: 87-100

131. Papetti M, Herman IM (2002) Mechanisms of normal and tumor-derived angiogenesis. [Review] [266 refs]. *American Journal of Physiology - Cell Physiology* 282: C947-C970

132. Pappova N, Siracka E, Vacek A, Durkovsky J (1982) Oxygen tension and prediction of the radiation response. Polarographic study in human breast cancer. *Neoplasma* 29: 669-674

133. Patterson LH, McKeown SR (2000) AQ4N: a new approach to hypoxia-activated cancer chemotherapy. [Review] [29 refs]. *British Journal of Cancer* 83: 1589-1593

134. Perez CA, Pajak T, Emami B, Hornback NB, Tupchong L, Rubin P (1991) Randomized phase III study comparing irradiation and hyperthermia with irradiation alone in superficial measurable tumors. Final report by the Radiation Therapy Oncology Group. *American Journal of Clinical Oncology* 14: 133-141

135. Pettersen EO, Juul NO, Ronning OW (1986) Regulation of protein metabolism of human cells during and after acute hypoxia. *Cancer Research* 46: 4346-4351

136. POWERS WE, TOLMACH LJ (1963) A multicomponent x-ray survival curve for mouse lymphosarcoma cells irradiated in vivo. *Nature* 197: 710-711

137. Reynolds TY, Rockwell S, Glazer PM (1996) Genetic instability induced by the tumor microenvironment. *Cancer Research* 56: 5754-5757

138. Rice GC, Hoy C, Schimke RT (1986) Transient hypoxia enhances the frequency of dihydrofolate reductase gene amplification in Chinese hamster ovary cells. *Proceedings of the National Academy of Sciences of the United States of America* 83: 5978-5982

139. Rice GC, Ling V, Schimke RT (1987) Frequencies of independent and simultaneous selection of Chinese hamster cells for methotrexate and doxorubicin (adriamycin) resistance. *Proceedings of the National Academy of Sciences of the United States of America* 84: 9261-9264

140. Riley V (1976) Breast cancer patients: substance in blood causing acceleration of erythrocyte sedimentation rate. *Science* 191: 86-88

141. Rockwell S, Yuan J, Peretz S, Glazer PM (2001) Genomic instability in cancer. [Review] [41 refs]. *Novartis Foundation Symposium* 240: 133-142

142. Rofstad EK (1989) Hypoxia and reoxygenation in human melanoma xenografts. *International Journal of Radiation Oncology, Biology, Physics* 17: 81-89

143. Rofstad EK, Danielsen T (1999) Hypoxia-induced metastasis of human melanoma cells: involvement of vascular endothelial growth factor-mediated angiogenesis. *British Journal of Cancer* 80: 1697-1707

144. Rofstad EK (2000a) Microenvironment-induced cancer metastasis. [Review] [216 refs]. *International Journal of Radiation Biology* 76: 589-605

145. Rofstad EK, Halsor EF (2000b) Vascular endothelial growth factor, interleukin 8, platelet-derived endothelial cell growth factor, and basic fibroblast growth factor promote angiogenesis and metastasis in human melanoma xenografts. *Cancer Research* 60: 4932-4938

146. Rofstad EK, Tunheim SH, Mathiesen B, Graff BA, Halsor EF, Nilsen K, Galappathi K (2002) Pulmonary and lymph node metastasis is associated with primary tumor interstitial fluid pressure in human melanoma xenografts. *Cancer Research* 62: 661-664

147. Rosenberg SA, Aebersold P, Cornetta K, Kasid A, Morgan RA, Moen R, Karson EM, Lotze MT, Yang JC, Topalian SL (1990) Gene transfer into humans--immunotherapy of patients with advanced melanoma, using tumor-infiltrating lymphocytes modified by retroviral gene transduction.[see comment]. *New England Journal of Medicine* 323: 570-578

148. Rotin D, Robinson B, Tannock IF (1986) Influence of hypoxia and an acidic environment on the metabolism and viability of cultured cells: potential implications for cell death in tumors. *Cancer Research* 46: 2821-2826

149. Sciandra JJ, Subjeck JR, Hughes CS (1984) Induction of glucose-regulated proteins during anaerobic exposure and of heat-shock proteins after reoxygenation. *Proceedings of the National Academy of Sciences of the United States of America* 81: 4843-4847

150. Semenza GL, Artemov D, Bedi A, Bhujwalla Z, Chiles K, Feldser D, Laughner E, Ravi R, Simons J, Taghavi P, Zhong H (2001) 'The metabolism of tumours': 70 years later. [Review] [47 refs]. *Novartis Foundation Symposium* 240: 251-260

151. Semenza GL (2002) Involvement of hypoxia-inducible factor 1 in human cancer. *Internal Medicine* 41: 79-83

152. Semenza GL (2003) Targeting HIF-1 for cancer therapy. [Review] [107 refs]. *Nature Reviews* Cancer. 3: 721-732

153. Sevick EM, Jain RK (1988) Blood flow and venous pH of tissue-isolated Walker 256 carcinoma during hyperglycemia. *Cancer Research* 48: 1201-1207

154. Sheldon PW, Foster JL, Fowler JF (1974) Radiosensitization of C3H mouse mammary tumours by a 2-nitroimidazole drug. *British Journal of Cancer* 30: 560-565

155. Sheridan MT, West CM, Cooper RA, Stratford IJ, Logue JP, Davidson SE, Hunter RD (2000) Pretreatment apoptosis in carcinoma of the cervix correlates with changes in tumour oxygenation during radiotherapy. *British Journal of Cancer* 82: 1177-1182

156. Shi Q, Abbruzzese JL, Huang S, Fidler IJ, Xiong Q, Xie K (1999) Constitutive and inducible interleukin 8 expression by hypoxia and acidosis renders human pancreatic cancer cells more tumorigenic and metastatic. *Clinical Cancer Research* 5: 3711-3721

157. Shibamoto Y, Sasai K, Abe M (1987) The radiation response of SCCVII tumor cells in C3H/He mice varies with the irradiation conditions. *Radiation Research* 109: 352-354

158. Speke AK, Hill RP (1995) The effects of clamping and reoxygenation on repopulation during fractionated irradiation. *International Journal of Radiation Oncology, Biology, Physics* 31: 857-863

159. Stacker SA, Caesar C, Baldwin ME, Thornton GE, Williams RA, Prevo R, Jackson DG, Nishikawa S, Kubo H, Achen MG (2001) VEGF-D promotes the metastatic spread of tumor cells via the lymphatics.[see comment]. *Nature Medicine* 7: 186-191

160. Steen RG (1991) Characterization of tumor hypoxia by 31P MR spectroscopy. [Review] [40 refs]. *AJR* American Journal of Roentgenology. 157: 243-248

161. Sutherland RM, Franko AJ (1980) On the nature of the radiobiologically hypoxic fraction in tumors. [Review] [34 refs]. *International Journal of Radiation Oncology, Biology, Physics* 6: 117-120

162. Sutherland RM (1998) Tumor hypoxia and gene expression--implications for malignant progression and therapy. *Acta Oncologica* 37: 567-574

163. Tannock IF (1968) The relation between cell proliferation and the vascular system in a transplanted mouse mammary tumour. *British Journal of Cancer* 22: 258-273

164. Thews O, Kelleher DK, Vaupel P (1996) In vivo oxygen consumption rate of DS sarcoma cells on inhibition of DNA synthesis. *Cancer Research* 56: 2009-2012

165. Thews O, Zywietz F, Lecher B, Vaupel P (1999) Quantitative changes of metabolic and bioenergetic parameters in experimental tumors during fractionated irradiation. *International Journal of Radiation Oncology, Biology, Physics* 45: 1281-1288

166. Thomlinson R.H., Gray L.H. (1955) The histologiacal structure of some human lung cancers and the possible implications for radiotherapy. *British Journal of Cancer* 9: 539-549

167. Thomlinson RH, Craddock EA (1967) The gross response of an experimental tumour to single doses of x-rays. *British Journal of Cancer* 21: 108-123

168. Thrall DE, Prescott DM, Samulski TV, Rosner GL, Denman DL, Legorreta RL, Dodge RK, Page RL, Cline JM, Lee J, Case BC, Evans SM, Oleson JR, Dewhirst MW (1996) Radiation plus local hyperthermia versus radiation plus the combination of local and whole-body hyperthermia in canine sarcomas. *International Journal of Radiation Oncology, Biology, Physics* 34: 1087-1096

169. Tietjen GW, Chien S, Scholz P, Gump FE, Kinney JM (1977) Changes in blood viscosity and plasma proteins in carcinoma. *Journal of Surgical Oncology* 9: 53-59

170. Uzzan B, Nicolas P, Cucherat M, Perret GY (2004) Microvessel density as a prognostic factor in women with breast cancer: a systematic review of the literature and meta-analysis. [Review] [114 refs]. *Cancer Research* 64: 2941-2955

171. van Kempen LC, Ruiter DJ, van Muijen GN, Coussens LM (2003) The tumor microenvironment: a critical determinant of neoplastic evolution. [Review] [105 refs]. *European Journal of Cell Biology* 82: 539-548

172. Van Putten LM, Kallman RF (1968) Oxygenation status of a transplantable tumor during fractionated radiation therapy. *Journal of the National Cancer Institute* 40: 441-451

173. Vaupel P, Fortmeyer HP, Runkel S, Kallinowski F (1987) Blood flow, oxygen consumption, and tissue oxygenation of human breast cancer xenografts in nude rats. *Cancer Research* 47: 3496-3503

174. Vaupel P, Kallinowski F, Okunieff P (1989) Blood flow, oxygen and nutrient supply, and metabolic microenvironment of human tumors: a review. [Review] [214 refs]. *Cancer Research* 49: 6449-6465

175. Vaupel P, Kelleher DK, Hockel M (2001) Oxygen status of malignant tumors: pathogenesis of hypoxia and significance for tumor therapy. [Review] [24 refs]. *Seminars in Oncology* 28: 29-35

176. Vaupel P, Hockel M (2003) Tumor oxygenation and its relevance to tumor physiology and treatment. *Advances in Experimental Medicine & Biology* 510: 45-49

177. Vaupel P (2004) Tumor microenvironmental physiology and its implications for radiation oncology. [Review] [55 refs]. *Seminars in Radiation Oncology* 14: 198-206

178. Vaupel P, Harrison L (2004) Tumor hypoxia: causative factors, compensatory mechanisms, and cellular response. [Review] [29 refs]. *Oncologist* 9 Suppl 5: 4-9

179. Vaupel P, Mayer A (2005) Hypoxia and anemia: effects on tumor biology and treatment resistance. [Review] [34 refs]. *Transfusion Clinique et Biologique* 12: 5-10

180. Vernon CC, Hand JW, Field SB, Machin D, Whaley JB, van der ZJ, van Putten WL, van Rhoon GC, van Dijk JD, Gonzalez GD, Liu FF, Goodman P, Sherar M (1996) Radiotherapy with or without hyperthermia in the treatment of superficial localized breast cancer: results from five randomized controlled trials. International Collaborative Hyperthermia Group.[see comment]. *International Journal of Radiation Oncology, Biology, Physics* 35: 731-744

181. Vujaskovic Z, Poulson JM, Gaskin AA, Thrall DE, Page RL, Charles HC, MacFall JR, Brizel DM, Meyer RE, Prescott DM, Samulski TV, Dewhirst MW (2000) Temperature-dependent changes in physiologic parameters of spontaneous canine soft tissue sarcomas after combined radiotherapy and hyperthermia treatment. *International Journal of Radiation Oncology, Biology, Physics* 46: 179-185

182. Vujaskovic Z, Song CW (2004) Physiological mechanisms underlying heat-induced radiosensitization. [Review] [55 refs]. *International Journal of Hyperthermia* 20: 163-174

183. Walenta S, Wetterling M, Lehrke M, Schwickert G, Sundfor K, Rofstad EK, Mueller-Klieser W (2000) High lactate levels predict likelihood of metastases, tumor recurrence, and restricted patient survival in human cervical cancers. *Cancer Research* 60: 916-921

184. Wang GL, Semenza GL (1993) Characterization of hypoxia-inducible factor 1 and regulation of DNA binding activity by hypoxia. *Journal of Biological Chemistry* 268: 21513-21518

185. Weidner N, Folkman J, Pozza F, Bevilacqua P, Allred EN, Moore DH, Meli S, Gasparini G (1992) Tumor angiogenesis: a new significant and independent prognostic indicator in early-stage breast carcinoma.[see comment]. *Journal of the National Cancer Institute* 84: 1875-1887

186. Weissberg JB, Son YH, Papac RJ, Sasaki C, Fischer DB, Lawrence R, Rockwell S, Sartorelli AC, Fischer JJ (1989) Randomized clinical trial of mitomycin C as an adjunct to radiotherapy in head and neck cancer. *International Journal of Radiation Oncology, Biology, Physics* 17: 3-9

187. West CM, Cooper RA, Loncaster JA, Wilks DP, Bromley M (2001) Tumor vascularity: a histological measure of angiogenesis and hypoxia. *Cancer Research* 61: 2907-2910

188. Wouters BG, Brown JM (1997) Cells at intermediate oxygen levels can be more important than the "hypoxic fraction" in determining tumor response to fractionated radiotherapy. *Radiation Research* 147: 541-550

189. Wouters BG, van den BT, Magagnin MG, Lambin P, Koumenis C (2004) Targeting hypoxia tolerance in cancer. [Review] [173 refs]. *Drug Resistance Updates* 7: 25-40

190. Xu L, Fidler IJ (2000) Acidic pH-induced elevation in interleukin 8 expression by human ovarian carcinoma cells. *Cancer Research* 60: 4610-4616

191. Young JS, Lumsden CE, Stalker AL (1950) The significance of the tissue pressure of normal testicular and of neoplastic (Brown-Pearce carcinoma) tissue in the rabbit. *Journal of Pathology & Bacteriology* 62: 313-333

192. Yuan J, Glazer PM (1998) Mutagenesis induced by the tumor microenvironment. [Review] [47 refs]. *Mutation Research* 400: 439-446

193. Yuan J, Narayanan L, Rockwell S, Glazer PM (2000) Diminished DNA repair and elevated mutagenesis in mammalian cells exposed to hypoxia and low pH. *Cancer Research* 60: 4372-4376

194. Zachos TA, Aiken SW, DiResta GR, Healey JH (2001) Interstitial fluid pressure and blood flow in canine osteosarcoma and other tumors. *Clinical Orthopaedics & Related Research* 230-236

195. Znati CA, Rosenstein M, Boucher Y, Epperly MW, Bloomer WD, Jain RK (1996) Effect of radiation on interstitial fluid pressure and oxygenation in a human tumor xenograft. *Cancer Research* 56: 964-968

CHAPTER 2

MULTIPARAMETER ANALYSIS OF TUMOR REOXYGENATION

INTRODUCTION

Ionizing radiation used as a therapy (radiation therapy) is one of the three major cancer treatment modalities, besides surgery and conventional chemotherapy. About half of all cancer patients are treated with radiation therapy, either alone or in combination with other types of cancer treatment. The therapeutic effect of radiation depends in part on the oxygenation status of the tumor. Hypoxic regions within tumors play an important role in tumor progression and tumor susceptibility to killing by various anticancer agents. Tumor hypoxia and its role in resistance to radiation therapy have been evaluated in many experimental (Grayet al, 1953; Kallman and Dorie, 1986; Rofstad, 1989; Murata et al, 1996; Goda et al, 1995; Fenton et al, 2001) and clinical studies (Getenby et al, 1988; Hockel et al, 1993; Nordsmark et al, 1996; Brizel et al, 1997).

Interestingly, radiation itself may change the tumor oxygenation status. The phenomenon of reoxygenation has been investigated since its first demonstration in the late 1960's (van Putten and Kallman, 1968). Reoxygenation has been shown to occur in experimental murine tumors (Olive, 1994; Horsman et al, 1995; Milas et al, 1995; Murata et al, 1996; Bussink et al, 2000), and in various human tumor types (Pappova et al, 1982; Sheridan et al, 2000; Cooper et al, 1999; Lyng et al, 1999; Brizel et al, 1999).

Mechanisms responsible for reoxygenation have not been clearly established. We evaluated multiple physiological parameters in spontaneously developing canine tumors before and 24 hours after 3 Gy fractions.

In many solid tumors the increase in pO_2 begins within hours following irradiation (Olive, 1994; Crokart et al, 2005). Some experiments found reoxygenation in murine tumors to be biphasic following a single large dose of 13 Gy. The rapid phase of reoxygenation appeared within one hour of radiation, with a slower phase that lasted up to 72 hours (Kitakabu et al, 1991). With smaller doses applied in a number of daily fractions, more rapid reoxygenation was seen in between fractions. Clearly, the pattern of reoxygenation differs between different tumor types and among tumors of the same type. Even though extensively investigated, mechanisms underlying tumor reoxygenation remain unknown. Figure 2.1 is a diagram of suggested biological parameters that could impact tumor oxygen status following irradiation. We hypothesized that tumor reoxygenation was due to reperfusion of collapsed vessels after apoptotic cell death decreased interstitial fluid pressure.

To test this hypothesis , partial pressure of oxygen (pO_2), microvascular perfusion, apoptosis, interstitial fluid pressure (IFP), and microvessel density (MVD) were evaluated in the same tumor, before and 24 hours following the first fraction of radiation in 14 canine tumors. The aim was to investigate the relationship among tumor microenvironmental biological parameters and the oxygen level of tumors, looking at the changes of each of these parameters following a clinically relevant radiation dose (3 Gy). Understanding of the underlying physiological changes after radiation helps us develop strategies to exploit these changes to gain a therapeutic advantage.

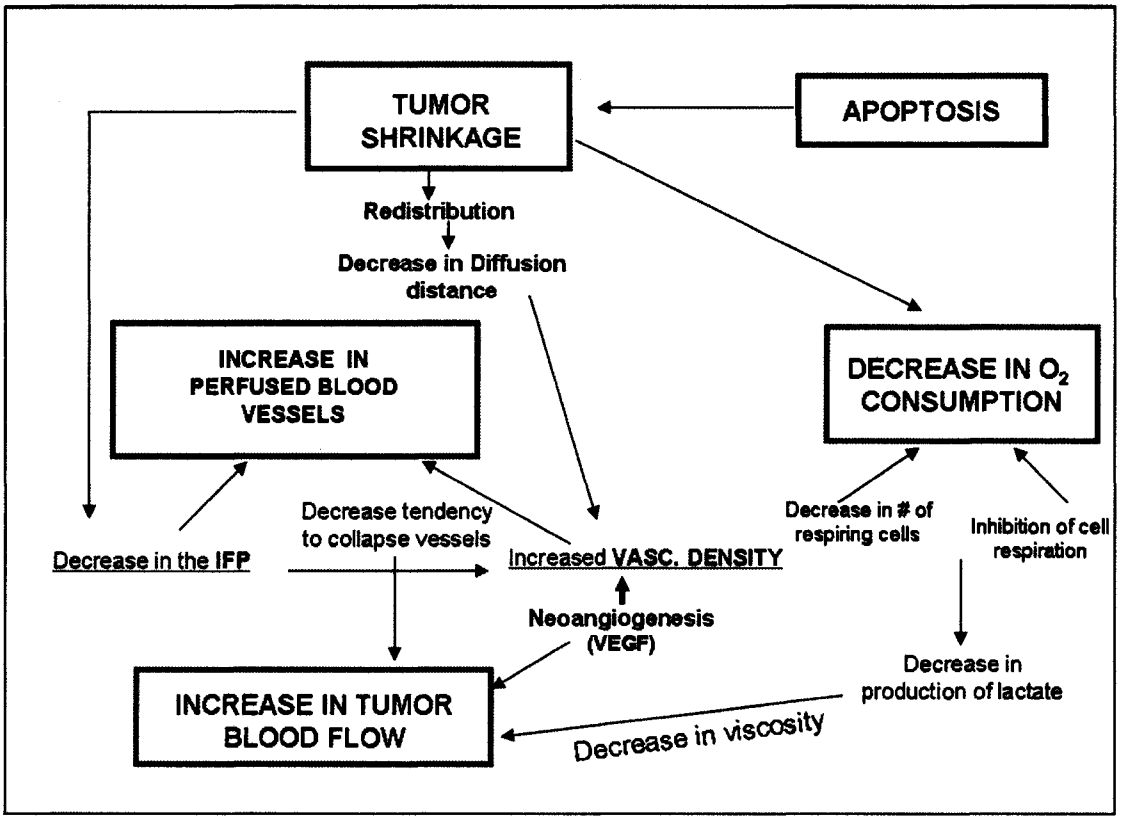

Figure 2.1. Interactions induced by radiation, resulting in tumor reoxygenation. Suggested mechanisms include reduced oxygen consumption by irradiated cells, rapid cell loss leading to tumor shrinkage, migration of cells from hypoxic to oxygenated areas and improvements in tumor blood flow. Tumor shrinkage as a result of apoptosis relieves pressure on blood vessels and reduces the level of intermittent hypoxia. A decrease in the interstitial fluid pressure of the tumor may result in redistribution of blood between the systemic circulation and the tumor, and filling of previously collapsed tumor vessels. This would improve microvessel density.
(The abbreviations used are: O_2, oxygen; IFP, interstitial fluid pressure; Vasc. Density, vascular density; VEGF, vascular endothelial growth factor)

MATERIALS AND METHODS

Research model

The Animal Cancer Center (ACC) at CSU is a great resource for cancer related research. Spontaneously occurring tumors in dogs are an excellent model for cancer research. Unlike experimental tumor models, canine tumors are heterogeneous. Most canine tumors have a histological counterpart in human cancer. The biological behavior and progression are often similar. The tumors also have similar tumor size to body mass ratios as found in human beings. Dogs are large enough to undergo sophisticated monitoring and the tumors are large enough for sequential biopsying.

In this study canine patients with solid tumors accessible for probe placement were eligible for the study. We entered 14 dogs into a study, 8 had soft tissue sarcoma (STS), 3 osteosarcoma (OSA), 2 carcinoma, and 1 mast cell tumor. Client consent was obtained for patient's entry into the study. Approval for the study was obtained from CSU Animal Care and Use Committee and the Hospital Clinical Review Board.

All of the measurements were made with dogs under general anesthesia. Dogs were premedicated with subcutaneously injected fentanyl at 0.006-0.008 mg/kg +/- atropine at 0.02mg/kg. Anesthesia was induced with a combination of midazolam or diazepam at 0.2 mg/kg and propofol 3 mg/kg to effect. Dogs were intubated and anesthesia was maintained with an admixture of Isoflurane and oxygen. Normosol-R solution was administered at 5-10 ml/kg/h during anesthesia. Irradiation was administered with a 6 MV photon beam from a clinical linear accelerator (Siemens, New York, NY).

The dose delivered was 3 Gy and all measurements were performed immediately before and 24 hours after irradiation.

Oxygen measurements

Simultaneous measurements of pO_2, temperature and microvascular perfusion were obtained with Oxford Optronix system (Oxford Optronix Ltd, Oxford, UK) OxyLite and OxyFlow.

Tumor oxygenation measurements were obtained using OxyLite. This is a time-resolved luminescence-based optical sensory system. This system uses a fiber-optic probe that contains a fluorescent dye (a platinum-based fluorophore) immobilized at the tip. Light is emitted along the probe to excite a fluorophore at the tip. The resulting emission of fluorescent light, quenched by the presence of oxygen molecules, travels back along the fiber and is detected by the instrument. The lifetime of the fluorescent dye is inversely proportional to the concentration of dissolved oxygen in tissue, providing the value for pO_2 in mmHg. The fluorescent lifetime is longest at low pO_2, making probes most sensitive under conditions of tumor tissue hypoxia. Because these sensors do not show significant consumption of oxygen, they are a better choice for measuring tissue oxygenation than paleographic electrodes. Not only conventional paleographic techniques consume oxygen that is most evident under conditions of tissue hypoxia, but require complex and time consuming calibration procedure which is avoided with OxyLite sensors by providing pre-calibrated probes. Another advantage of this system is the possibility to combine it with laser Doppler blood perfusion monitors for

simultaneous multi-parameter monitoring. We used combined probes for pO_2, microvessel perfusion and temperature measurements from the same tumor microregion. To perform measurements at multiple locations across the tumor a digitalized caliper was adopted to pull back the probes. The probes were introduced through microdialysis split tubing (CMA/Microdialysis AB, North Chelmsford,MA), placed in the tumor with a 20-gauge catheter. After initial stabilization of recording measurements, the probe was withdrawn 0.2mm each 5sec and measurements were displayed using a data-acquisition system Chart v.4.2.4 (AD Instruments, Inc., Colorado Springs, CO). Histograms were created using SigmaPlot v.7.101 software (Systat Software Inc., San Jose, CA) (Figure 2.2).

Interstitial fluid pressure measurements

The interstitial fluid pressure (IFP) was measured using a modified "wick-in-needle" technique (Fadnes et al, 1977). Wick-in-needle probes were custom made from 22-gauge spinal needle with a 3 mm side hole located 5mm from the tip. Standard cotton thread was threaded into each needle before sterilization. The needle was connected to a pressure transducer by polyethylene tubing filled with heparinized saline solution (100 IU/ml) to prevent clotting. Instrumentation was calibrated to zero at room air before each measurement. A zero reference was obtained by placing the needle at tumor height and by resetting the system. Measurements were recorded at 0.5 cm intervals across the tumor starting at the periphery of tumor under the skin.

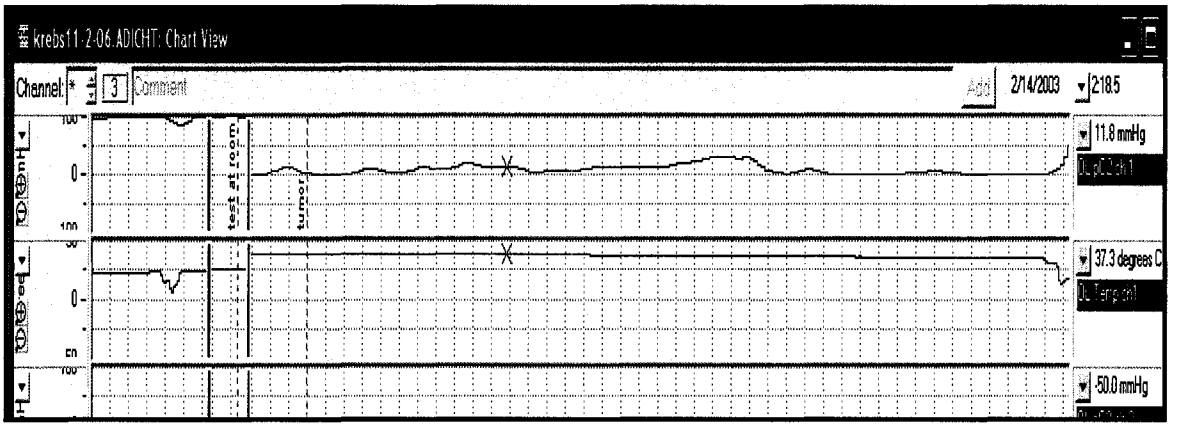

A.

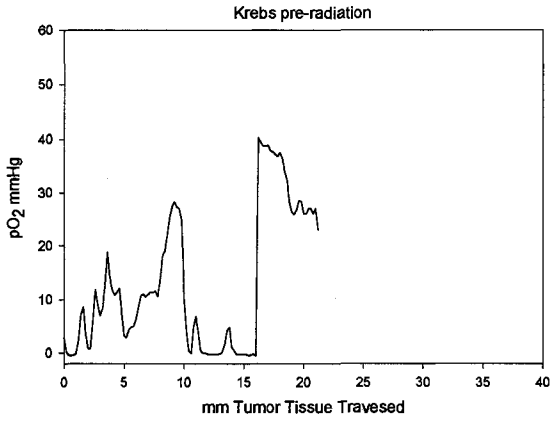

B.

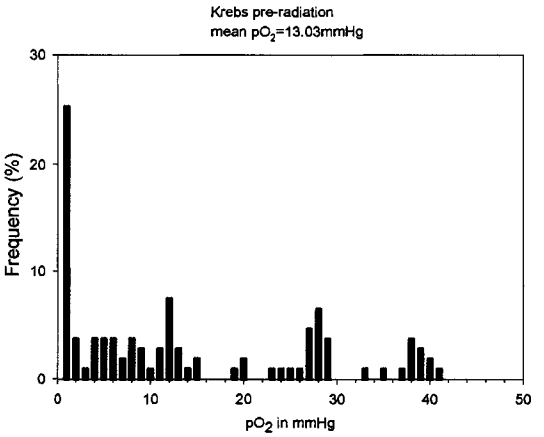

C.

Figure 2.2. Data obtained with Chart (A), and processed in SigmaPlot to present pO_2 track of measurement (B) and pO_2 histogram (C). Histogram represents percent frequency of pO_2 values measured at 0.2 mm intervals.

Microvascular perfusion measurements

Tumor perfusion was assessed by two complementary techniques: laser Doppler flowmetry (LDF) and dynamic contrast-enhanced (DCE) imaging. In the first five tumors, DCE was done using computed tomography (DCE-CT) and upon availability of

magnetic resonance imaging at the Animal Cancer Center we used dynamic contrast-enhanced MRI (DCE-MRI).

Laser Doppler Flowmetry

OxyFlow is part of the Oxford Optronix system that measures microvascular perfusion with laser Doppler flowmetry (LDF). It contains the laser source, sensitive photo detection and signal processor. Probes contain optical fibers that direct stable low power laser light to the tissue and collect scattered light to a photo detector. The presence of moving red blood cells in capillaries, arterioles, and venules in the tissue cause a Doppler shift in the fraction of returned light and it is this shift which constitutes the output signal. The signal is more correctly described as related to tissue perfusion rather than blood flow, as it cannot be directly calibrated in units such as ml/min.

Perfusion is indicated on a display in relative blood perfusion units (BPU) defined using a carefully controlled motility standard. Microvascular perfusion is proportional to the number of red blood cells moving in the tissue sampling volume under illumination from the probe, and mean velocity of these cells. The mean tumor blood flow was presented as a graph using SigmaPlot v.7.101 software (as an example given in Figure 2.3).

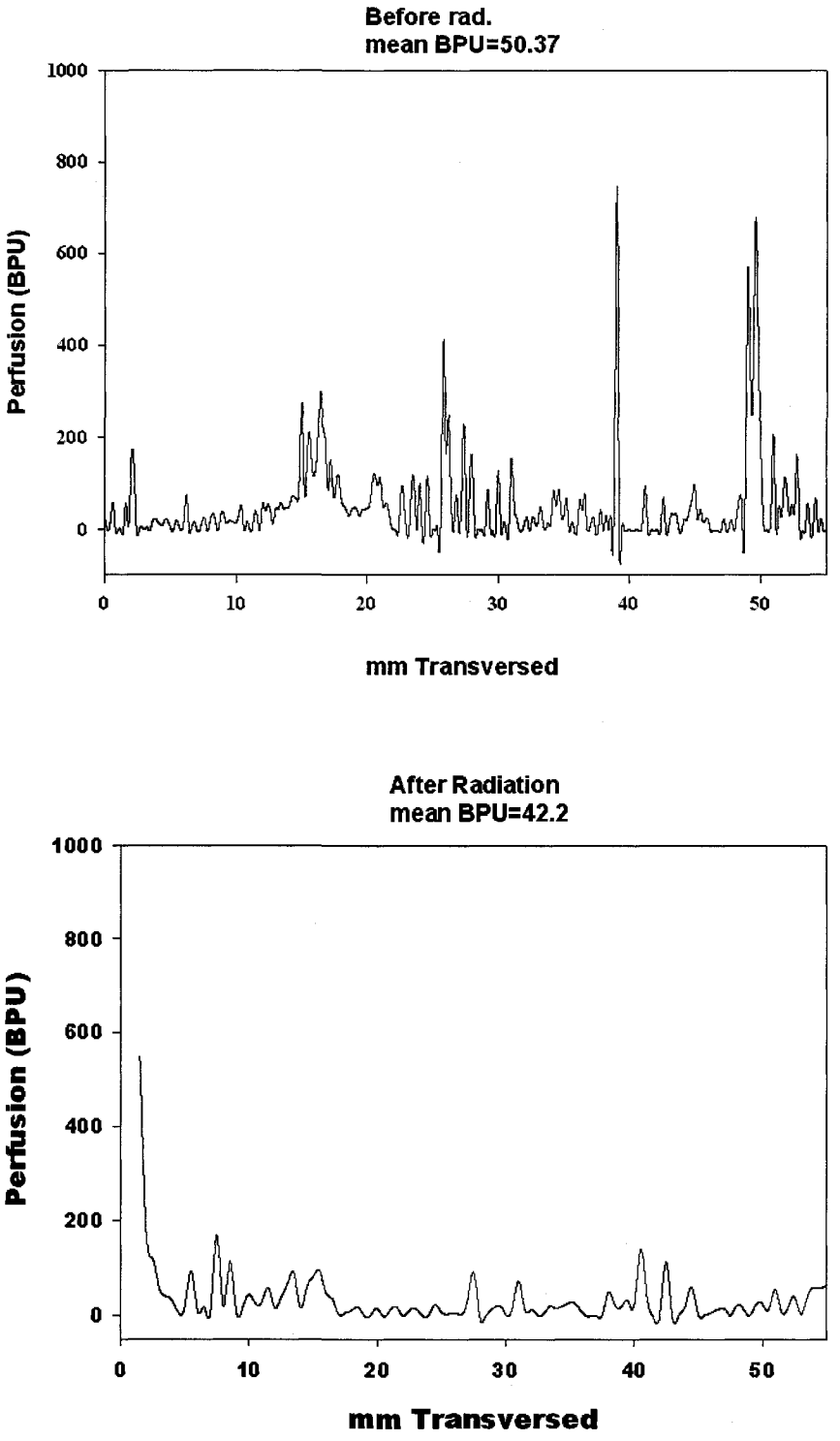

Figure 2.3. The changes in microvascular perfusion (measured via laser Doppler) along the probe track both before (left graph) and 24 h after radiation (right graph) in a canine tumor.

Dynamic contrast-enhanced CT

We also evaluated perfusion using quantitative dynamic contrast-enhanced computed tomography (DCE-CT). The use of wash-in kinetics of contrast medium was utilized to estimate perfusion. Images were acquired using a Picker PQ 2000 CT (Picker International, Highland Heights, OH).

An initial non-contrast CT scan was performed to evaluate the extent of tumor involvement. The imaging plane was repositioned at the central location of tumor (this slice was also the location of oxygen and interstitial fluid pressure measurements that were performed after CT).

Contrast agent was injected in the cephalic vein using a pressure injector at the rate of 3 ml/sec, 100 psi maximum, using a dose of 1 ml/lb body weight of sodium diatrizoate (370 mg/ml iodine) with a maximum dose of 60 ml. Tissue and vessel attenuation ("density") changes were observed during the first pass of the agent by rapid image acquisition. Image acquisition started just prior to contrast injection. Dynamic acquisition was performed using one image per 2 seconds for total of 40 images. Slice thickness was 5 mm (Figure 2.4).

Perfusion was estimated by assessing the uptake of contrast medium into the tumor compared to the concentration in the arterial supply as an input factor. Time-density (Hounsfield units) curves were constructed for regions of interest (ROI) drawn over the nearest major artery and the tumor (Figure 2.5). Tumor ROIs were drawn at the locations of tumor oxygen measurements. Arterial ROIs were chosen for an artery within the scan plane during the dynamic acquisition.

Tumor perfusion estimation was calculated as described in Van Camp et al. 2000.

Tumor perfusion was expressed as rate of rise of attenuation (Hounsfield units) in the tumor over the arterial attenuation (Hounsfield units) value over the same time points (Figure 2.6). Values obtained for perfusion are in units of ml/sec/ml.

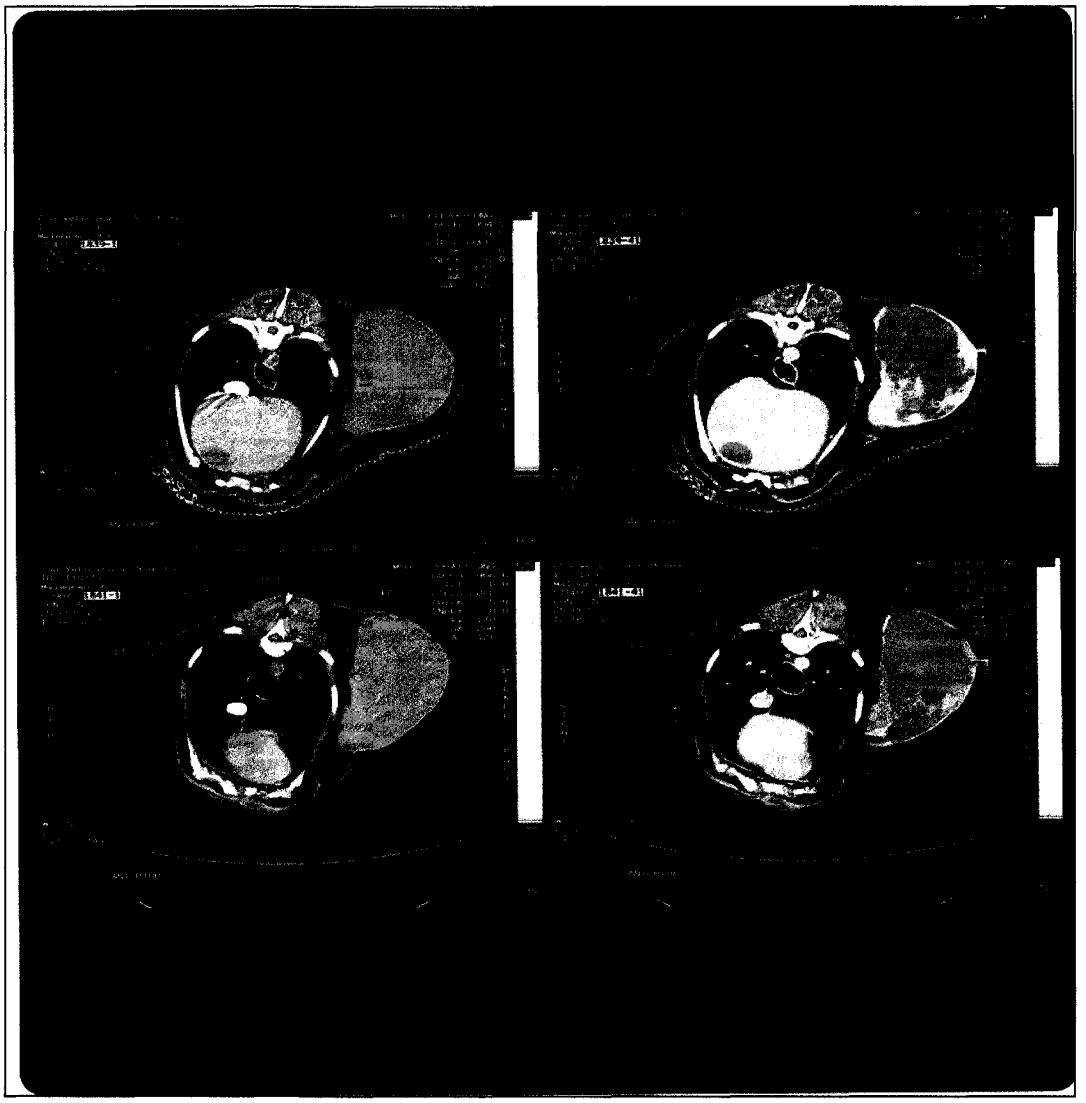

Figure 2.4. Tumor CT images of a large canine extrathoracic tumor show at the location of perfusion measurements. The tumor is the large grey area along the left side of the thorax (patients left is on the images on the right side). The heart and diaphragm are visible centrally in the chest on each image. Iodinated contrast medium was administered intravenously using pressure injector. Images are taken before (upper images), and 24h after irradiation (lower images). Images on the left were obtained at the beginning of the contrast injection, while images on the right were later in the series. Note the needle positioned to assist probe placement for subsequent measurements.

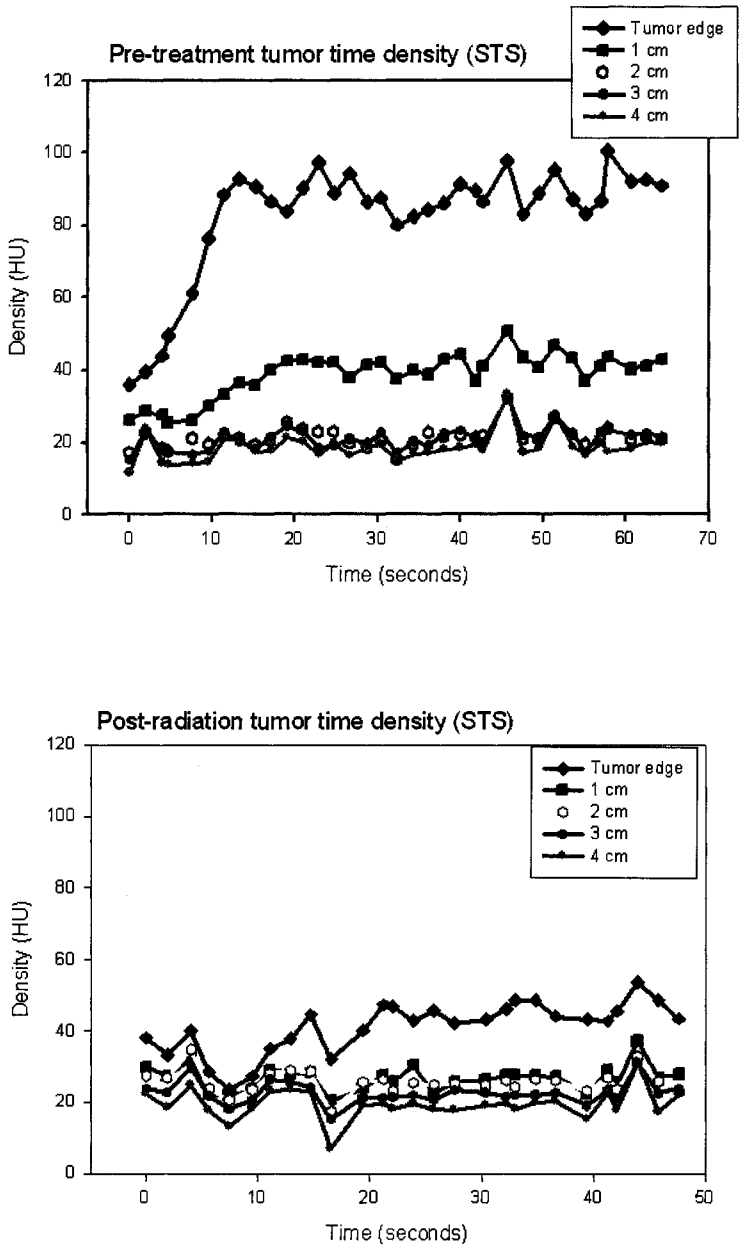

Figure 2.5. Time-density curves of tumor Hounsfield units (HU) plotted as a function of time after contrast injection are constructed for various regions of interest (ROI). ROIs are drawn at different depths along the needle position seen in figure 2.3.

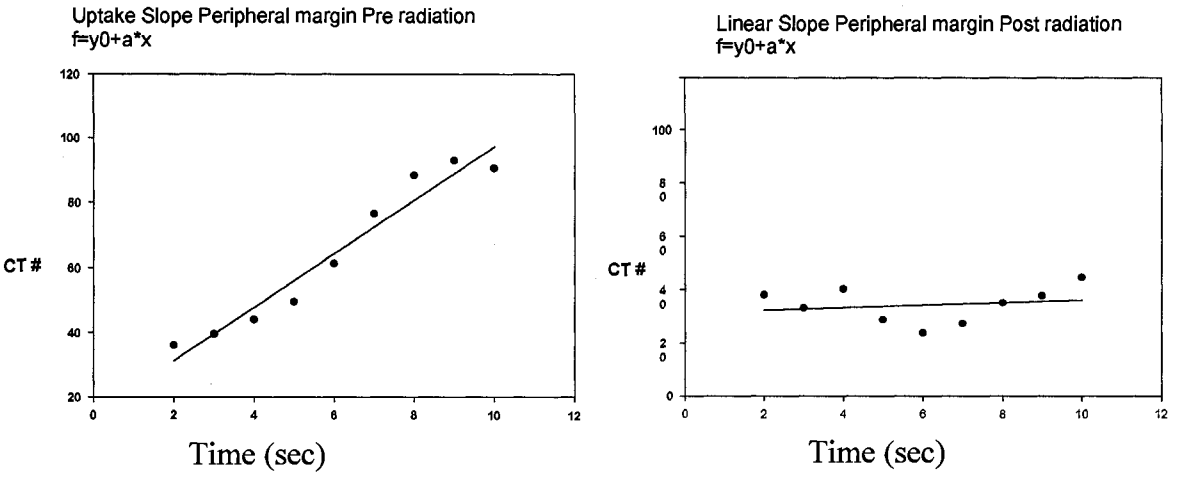

Figure 2.6. DCE-CT data was calculated as Δ tumor HU / Δ arterial HU derived from CT time density curves. Time-density curves were generated for the tumor ROIs and the largest artery in the imaging field. The slope of increasing tumor density was divided by the peak arterial density to obtain an estimate of perfusion.

Dynamic contrast-enhanced MRI

After the first five tumors entered our study we continue to measure tumor perfusion with dynamic contrast enhanced magnetic resonance imaging DCE-MRI instead of DCE-CT, still followed by LDF measurement. Tumors were imaged with dogs under general anesthesia, with a 1.5T GE Signa LX 9.0 MRI instrument (Signa, GE Medical Systems, Milwaukee,WI) using a coil appropriate for the body region. Anatomic T2 and T1 weighted pulse sequences were obtained to first evaluate tumor morphology. The dynamic contrast-enhanced scan was aquired as a T1 fast spin echo sequence (TR 400 ms, TE 15 ms, matrix 256X128, NEX 0.5) and the entire tumor volume was imaged repeatedly in 30-35 second phases for a total of 15 transverse slices, with thickness of slice from 5-10 mm. The field of view (FOV) was as small as possible. Gadolinium DTPA (Magnevist, Berlex Laboratories, Trenton NJ) contrast medium was administered

intravenously as a bolus using a pressure injector at 0.1 mmol/kg at a rate of 2.5ml/sec. The dynamic acquisition was done after contrast injection for a total of 30 minutes. Afterwards the skin on the tumor was marked for the probe placement for the subsequent physiological measurements and biopsy.

Analysis of the DCE-MRI was done using an "intensity based" method (Belfi et al. 1994). Time-intensity curves were generated for regions of interest (ROIs) that were drawn at the location of subsequent probe placement, for interstitial fluid pressure and partial pressure of oxygen measurements. Similar ROIs and slices were analyzed before and after radiation (Figure 2.7).

The ROI signal intensities were first converted into percent intensity values (%IE) by subtracting out baseline intensity (from pre-injection) and dividing by that pre-contrast intensity value:

%IE= (new intensity- background intensity)/background X 100

This signal intensity data was than fitted to a two compartmental analysis (done by Dr. Susan Kraft) to derive α, β, and A using the formula:

$$\%IE = A\,(1-e^{-\alpha t})\,e^{-\beta t}$$

with a standard commercial software package SigmaPlot 8.0.

A Relative Perfusion Index (RPI) was then calculated as: $RPI = \alpha A$, to characterize the uptake portion of the contrast dynamic curve. RPI was compared for each ROI before and after radiation (Figure 2.9).

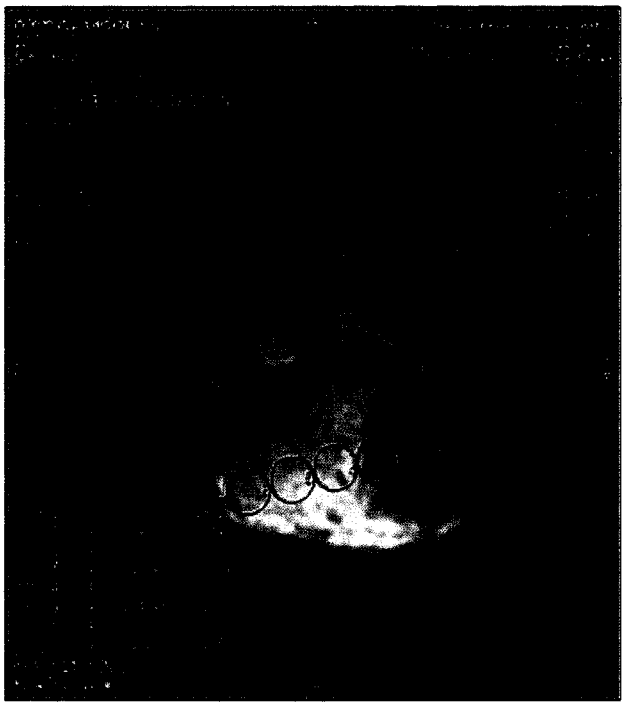

Figure 2.7. MRI image of a soft tissue sarcoma of the forelimb of a dog at the location of perfusion measurement, correlating to other parameters of interest. Regions of interest (ROI's) (numbered circles on the image) were drawn at the LDF probe placement location. Corresponding ROIs were drawn on post-radiation image and graphs obtained for the uptake of the contrast at different depths of tumor, as in figure 2.7.
The contrast-enhancing tumor is hyperintense (white). The circular darker area is a necrotic center to the tumor. Normal musculature (dark grey in upper left) and cross sections of the normal radius and ulna are included in this image.

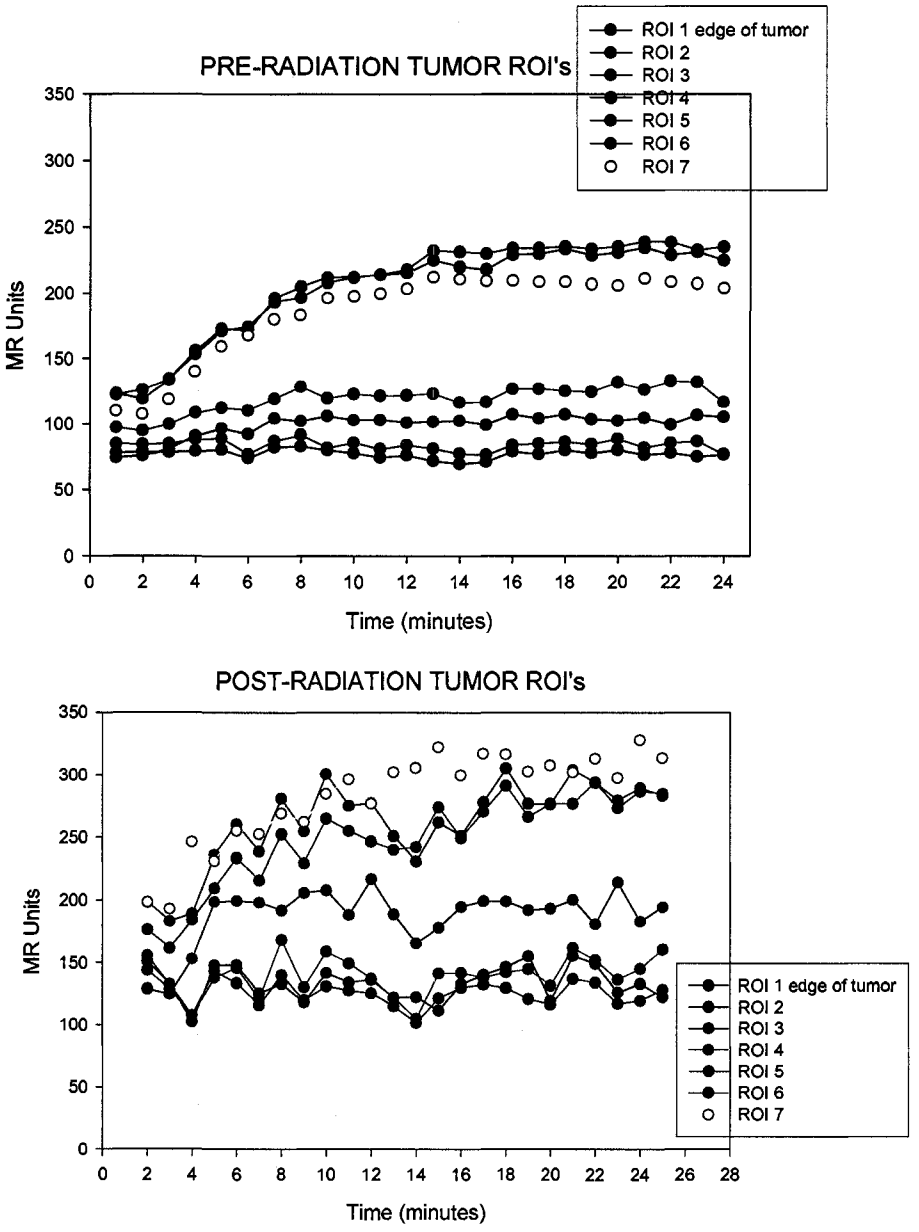

Figure 2.8. The ROI signal intensities: Curves of tumor MR units plotted as a function of time after contrast injection, were constructed for various regions of interest (ROI). ROIs are drawn at different depths, along OxyFlow probe placement, before and after radiation.

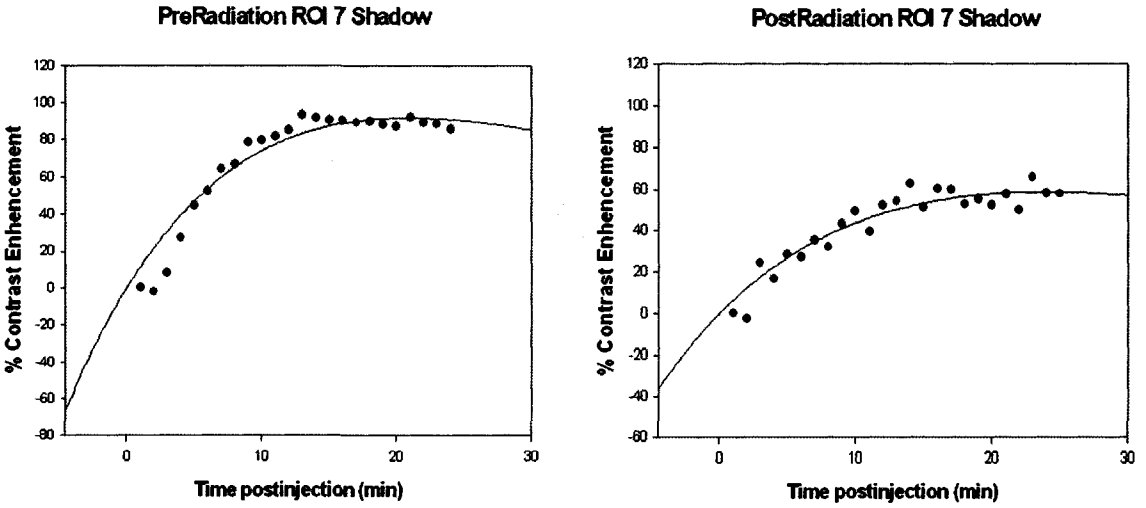

Figure 2.9. DCE-MRI data was calculated as a Relative Perfusion Index and compared for each ROI before and after radiation. The ROI signal intensities were first converted into % intensity values (Belfi et al. 1994): %IE= [(Ipost – Ipre) / Ipre] X 100%. This is the same tumor shown in MRI image in figure 2.7 and in ROI signal intensity curves in figure 2.8.

Apoptosis quantification

Needle biopsies were performed after each probe measurement to obtain tumor samples for quantification of apoptosis and microvessel density. In the first 4 dogs the biopsies were taken before, and 24 hours after radiation. Starting with dog 5 an additional time point at 6 hours after radiation was included. Paraffin embedded slides for immunohistochemistry, and hematoxylin and eosin stained slides were obtained from the tumor biopsies.

Apoptosis was measured in paraffin embedded histological sections of the tumor. Sections were stained by use of the In Situ cell death detection kit, Fluorescein (Roshe Molecular Biochemicals, Indianapolis, IN). The staining was based on the terminal

deoxynucleotidyl transferase (TdT)-mediated deoxyuridine triphosphate (dUTP)-biotin nick end labeling (TUNEL) method.

Using the TUNEL assay, the apoptotic fraction was expressed as percentage of TUNEL positive cells. Analysis was performed using KS 400 system software (Carl Zeiss MicroImaging, Inc., Thornwood, NY). For each tissue section images were taken using a Carl Zeiss Axioplan 2 imaging microscope coupled with an AxioCam HRc Carl Zeiss camera.Nine to ten areas of the tumor specimen were identified, counting was performed at X 200 magnification and the percentage of the apoptotic cells was calculated. It was expressed as an apoptotic index (AI):

$$AI = \frac{\text{\# of Fluorescein labeled cells X 100}}{\text{\# Fluorescein labeled + DAPI labeled cells}} \quad \%$$

For standardization, the measured fields were size 150X100 microns.

TUNEL Protocol

This protocol is used for detection and quantification of apoptosis at single cell level, based on labeling of DNA strand breaks. One of the characteristics of the apoptosis is the fragmentation of nuclear chromatin which results in a multitude of 3'-OH (hydroxyl) termini of DNA ends. These DNA strand breaks can be identified by labeling free 3'-OH terminal with modified nucleotides in an enzymatic reaction. This is the modified protocol used in this study:

1. Deparaffinize slides in HemoDe, 2 times for 5 min.
2. Rehydrate in a series of EtOH (100, 95, 90, 80 70%) for 5 min each.
3. Wash in PBS for 2 min.

4. Incubate slides in Proteinase K (PK) in a water bath for 30 min @ 37°C. To prepare PK: 66.5 µl/50ml 10mM Tris HCl. Tris HCl 10mM= 0.1576 g/100ml diH_2O.
5. Wash in PBS 2 times for 2 min each.
6. Centrifuge PN buffer and milk (to take off background noise), 5-7 min. Dry around the tissue and circle with PapPen. Add 30 µl of supernatant on slide, place a cover slip and keep 5 min at room temperature.
7. Prepare TnT in dark: take out 100 µl from vial 2 (Label solution) and add all 50 µl of vial 1 (Enzyme) from the TUNEL kit. Add 100 µl to each slide.
8. Incubate in a humidified chamber (box with wet paper and covered with foil), at 37°C for 60 min.
9. Wash in PBS, 3 times for 2 min. each.
10. Prapere 10 µl RNase + 90 µl PBS (100 µl). Apply 100 µl on each slide and leave for 60 min in humidified box at room temperature.
11. Dry around the sample and apply AntiFade and DAPI (counterstain). (SlowFade light AntiFade kit, Molecular Probes, Inc., Eugene, OR and Sigma-Aldrich, St. Louis, MO, respectively). DAPI stock solution: 10 mg/ml in dH_2O. Use 1 µg/ml stock solution in SlowFade. Place cover slip.
12. Dry in dark overnight. Then keep slides at -20°C.

Microvessel Density

Quantification of microvessel density (MVD) was performed using immunohistochemical staining of endothelial cells for factor VIII-related antigen (von Willebrand factor). Immunohistochemical staining was performed in the Diagnostic lab of The Veterinary Teaching Hospital, using standard immunoperoxidase technique on an automated stainer (Discovery System, Ventanna Medical Systems, Tucson, AZ).All reagents were purchased from Ventanna Medical Systems, and incubated at 37° C. Briefly, 4 micron sections were cut and mounted on positively charged slides. The sections were deparaffinized then rehydrated with descending alcohol concentrations to buffer. Antigen retrieval was with protease 1 incubation for 8 minutes. The sections were then incubated in the primary antibody anti factor VIIR, polyclonal, 32 min at 37°C. A pre-diluted, universal biotinylated secondary antibody, an alkaline phosphatase red basic kit detection system, and fast red as chromogen were utilized to detect the immunoreactive complexes. The slides were counterstained with hematoxylin and bluing for 4 min each. Image analysis was performed using KS 400 system software (Carl Zeiss MicroImaging, Inc., Thornwood, NY). Microvessel density was assessed in areas of highest neovascularisation found by scanning the tumor sections, "hot spot" technique (Weidner N.'91). Microvessel counts of these areas were performed at high-power field (X 200). Any brown stained endothelial cell or endothelial cell cluster that was clearly separated from adjacent microvessels, tumor cells, and connective elements was counted as one microvessel, irrespective of the presence of a vessel lumen. For the consistency in the MVD analysis the grid containing 100X150 micrometer squares was placed over the

images while counting. The vessels were counted in five to seven squares, depending on the tissue slice size, and the mean count was taken as the MVD (Figure 2.10).

Statistical analysis

Five pO_2 parameters were calculated for each tumor from pre and post radiation measurements: mean pO_2, median pO_2, fractions of pO_2 readings < 2.5 mmHg, 5 mmHg, and 10 mmHg. Two microvascular perfusion methods were performed for each tumor for pre and post radiation measurements: LDF and DCE CT/MRI. All tumors were divided in two groups regarding pO_2 measurements before treatment: hypoxic tumors with median pO_2 values < 10mmHg, and non-hypoxic tumors with median pO_2 before radiation ≥ 10mmHg.

Statistical analyses were performed to explore whether there was an association between changes in tumor oxygen levels and changes in other microenvironmental parameters obtained in all pre- and post-radiation measurements in all tumors. For normality p-value, paired t-test p-value, signed rank test p-value, and mean and standard deviation of the difference between measurements after and before radiation, Shapiro-Wilk tests were performed. Pearson and Spearman correlation coefficients and p-values for the association between changes in pO_2 and changes in microvascular perfusion, MVD, IFP, and apoptotic index were calculated. Pearson and Spearman correlation coefficients and p-values were used to compare pre and post radiation perfusion measurements performed by LDF and measurements by CT/MRI.

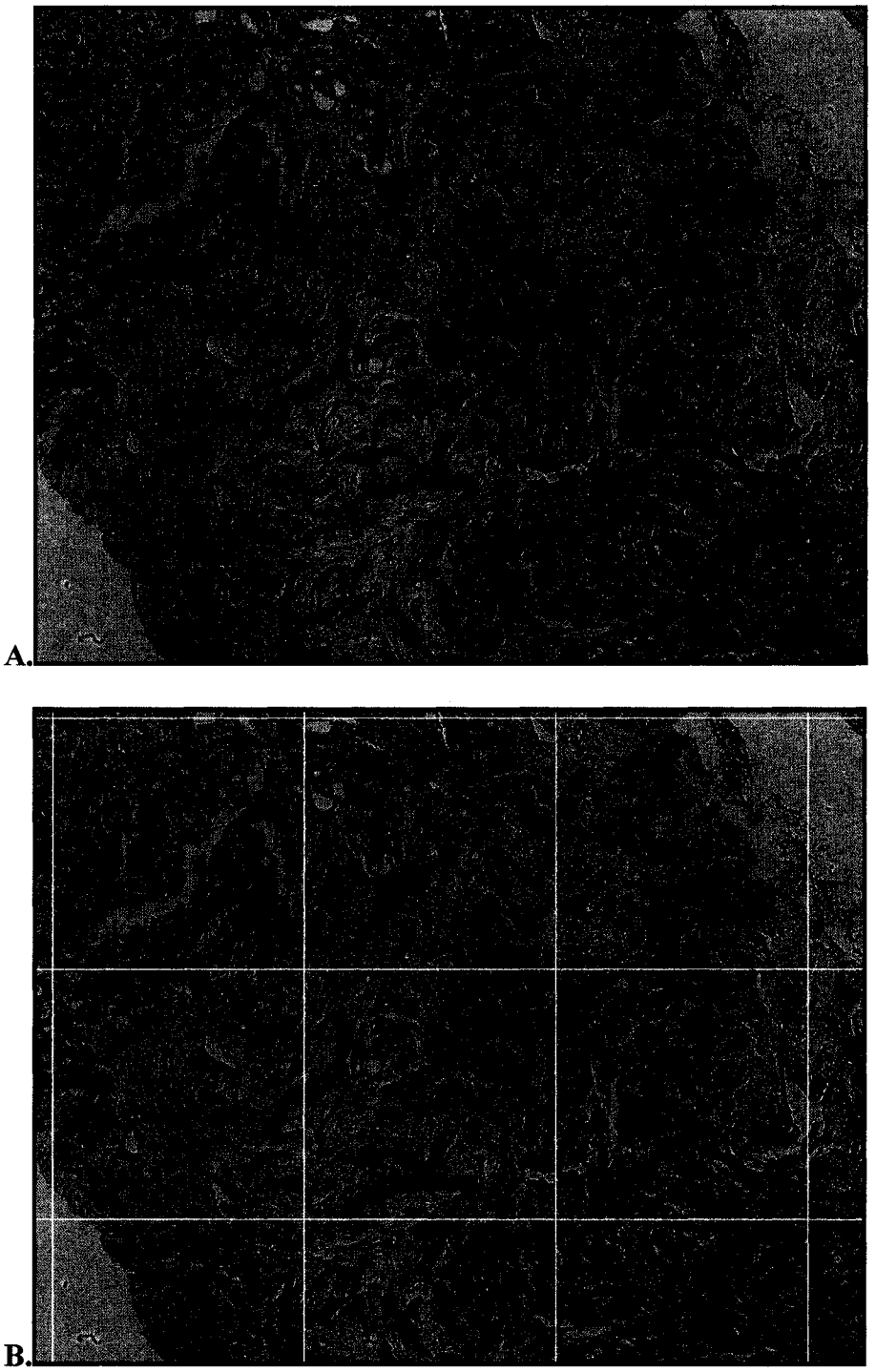

Figure 2.10. Immunohistochemical visualization of microvessels (arrows) in a dog mammary carcinoma. The section of tumor was stained for factor VIII-related antigen. Selected field (A) is a "hot spot" where counting was performed using a known size grid overlapping the field (B).

Chi Square test and Fisher's exact test were used for the changes in median pO_2 vs. other parameters, and for the changes in mean pO_2 vs. other parameters (microvascular perfusion, MVD, IFP, AI) to complete the statistical analysis.

RESULTS

Oxygen measurements

Oxygen measurements were analyzed along the track of a probe that was placed into a tumor and withdrawn toward the edge. All pO_2 values were expressed as mean and median pO_2 in mmHg. Tumors with mean/median O_2 levels above 10 mmHg were defined as normoxic. The fraction of measurements along the track with pO_2 values < 10 mmHg, <5 mmHg, and < 2.5 mmHg was calculated (Table 2.2). The pO_2 changed after radiation; in 9 tumors it increased, and in 5 tumors it decreased (both mean and median pO_2). Tumors that were pre-radiation hypoxic mostly reoxygenated: 6 out of 7 hypoxic tumors showed increased level of oxygen measured after radiation (3Gy) compared to measurements before treatment. In the same 6 initially hypoxic tumors the percent of the measurements less than 10, 5, and 2.5 mmHg decreased after radiation. The magnitude of the change differed among the tumors. For the 7 initially well oxygenated tumors: 3 of them had increased pO_2 after radiation, while 4 of them had decreased pO_2 but still in the range of oxygenated regions (not becoming hypoxic). For the best comparison each tumor pO_2 measurements are presented in histograms, before and after radiation, set next to each other on the same scale and analyzing the same track of the measurements length

in Figure 2.14, Figure2.15, Figure 2.16, Figure 2.17, Figure 2.18, Figure 2.19, Figure 2.20, Figure 2.21, Figure 2.22, Figure 2.23, Figure 2.24, Figure 2.25, Figure 2.26.

Table 2.2. Partial pressure of oxygen measurements in 14 tumors.

	O	X	Y	G	E	N		pO2		
DOG #	Before Mean	After Mean	Before Median	After Median	%<10 mmHg Before	%<10 mmHg After	%<5 mmHg Before	%<5 mmHg After	%<2.5 Before	%<2.5 After
1	2.2	12.3	-0.5	-0.1			88.1	62.1	86.2	61.1
2	7.2	2.8	-0.8	-2.4			63.8	86.4	63.4	84.5
3	8.7	38.9	-0.6	37.8			77	0	76.5	0
4	21.9	28.1	22.3	26.9			0	0	0	0
5	19.4	10.9	21.8	11			5	18.3	0	16.7
6	30.5	21	32.1	14.8			8	39.1	2.5	35.9
7	19.5	13.3	17.8	15.4			0	19.6	0	15.8
8	9.2	23.2	0.4	14.2			52.6	0	51.5	0
9	22.2	25	23.2	25.5			0	0	0	0
10	3.6	22.2	2.9	19.5			60.4	27.5	47.2	25.7
11	18.6	27.7	20.9	26.1			30.1	6.4	26	4.5
12	17.1	13.1	18	12.7			0	18.9	0	17.2
13	10.6	29.6	8.1	34.3			46.5	8	36.6	4.5
14	7.2	31.2	1.8	31			63.5	0	55.3	0

Table 2.2 Data were collected before and 24 hours after dose of 3Gy radiation. Results are expressed as mean and median values for the respective tracks of probe placement and recording. Percentages of measurements in hypoxic regions which are less than 10, 5, and 2.5 mmHg are also calculated for tracks of measurement before and after radiation for each tumor. Red numbers in mean and median columns represent increased pO_2 values, while red in % columns mean decrease in hypoxic fractions (i.e. increased oxygenation).

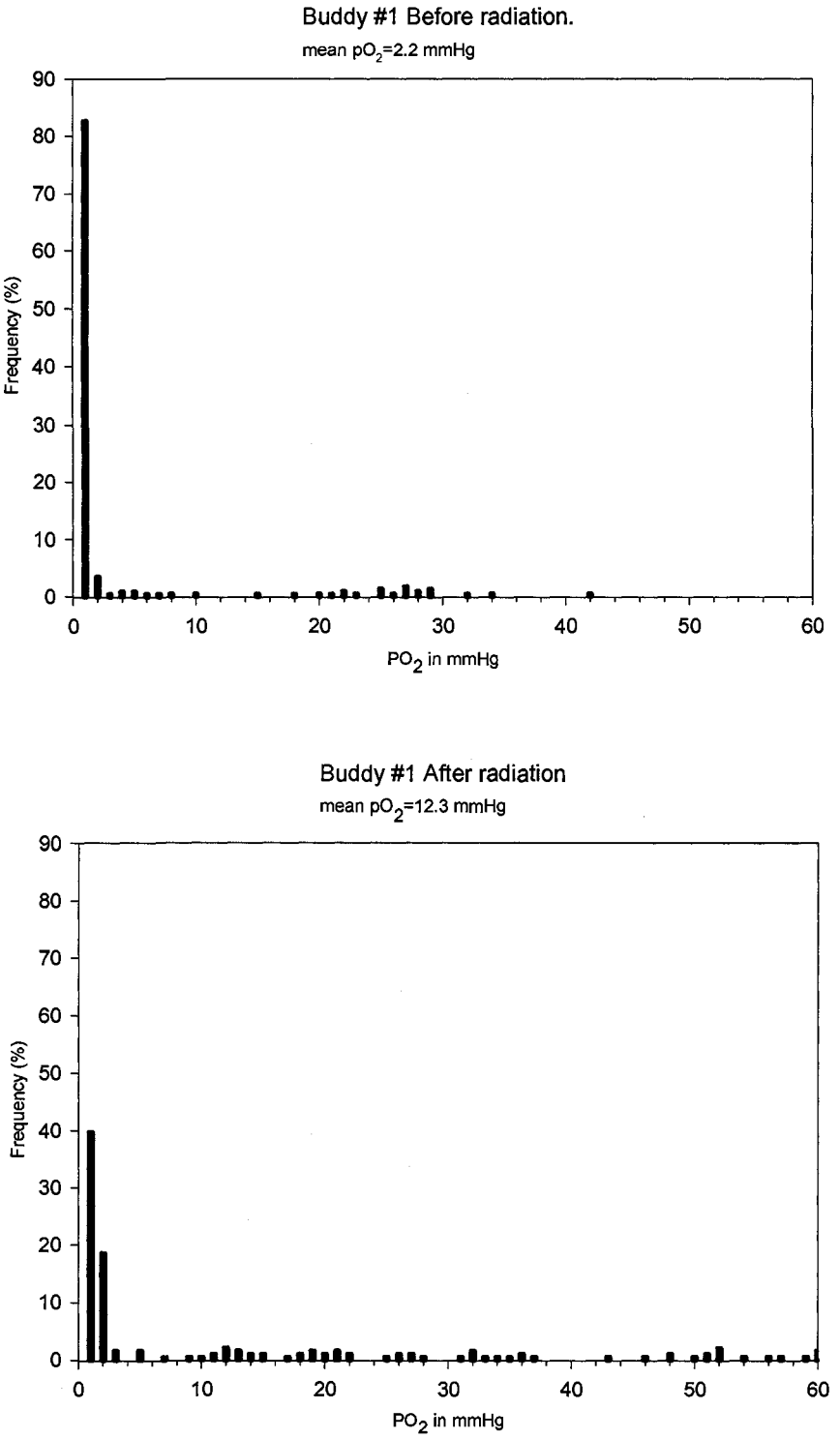

Figure 2.13. Oxygen measurements in tumor #1, soft tissue sarcoma, at the same location before and after radiation

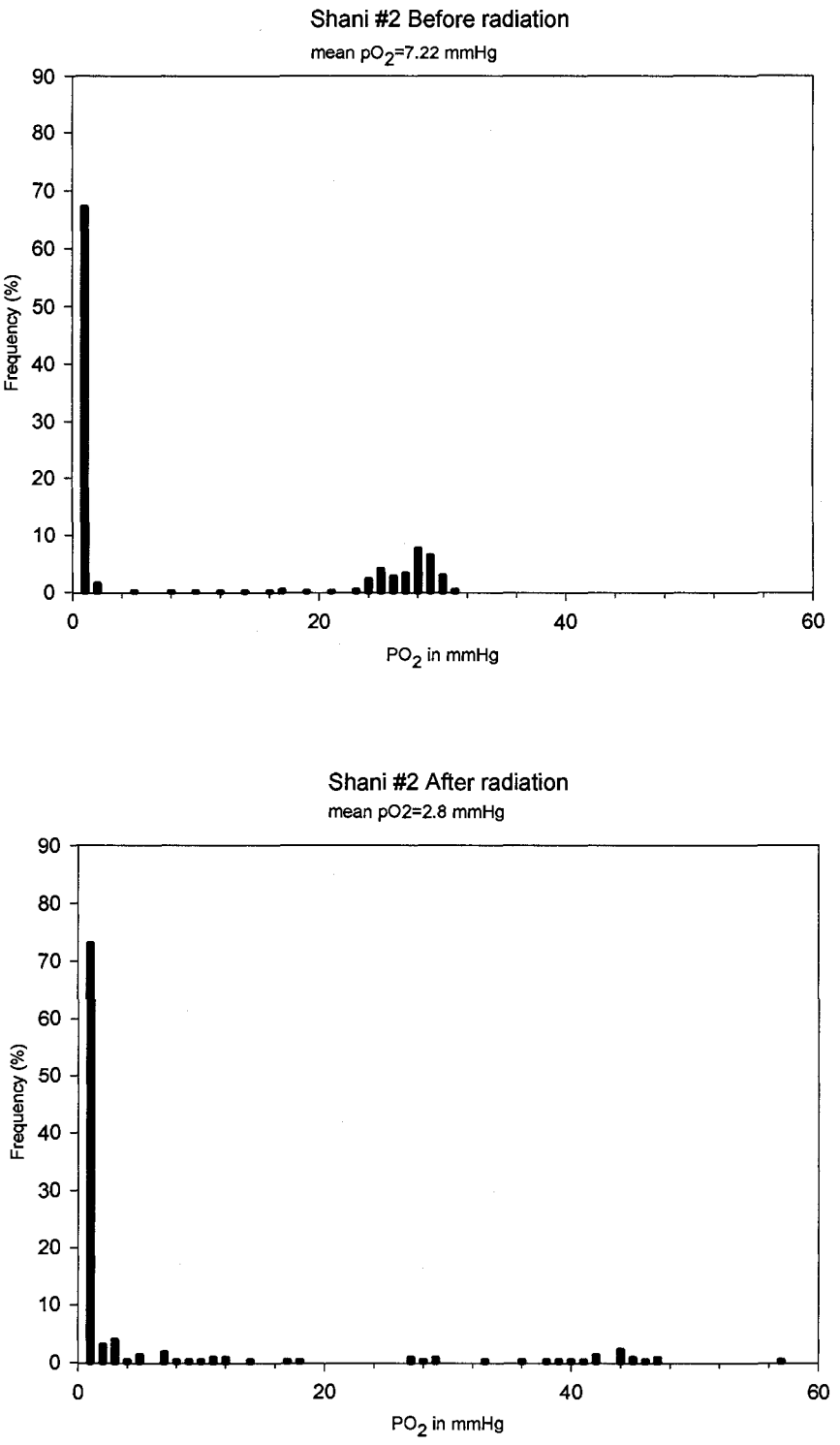

Figure 2.14. Oxygen measurements in tumor #2, soft tissue sarcoma, at the same location before and after radiation

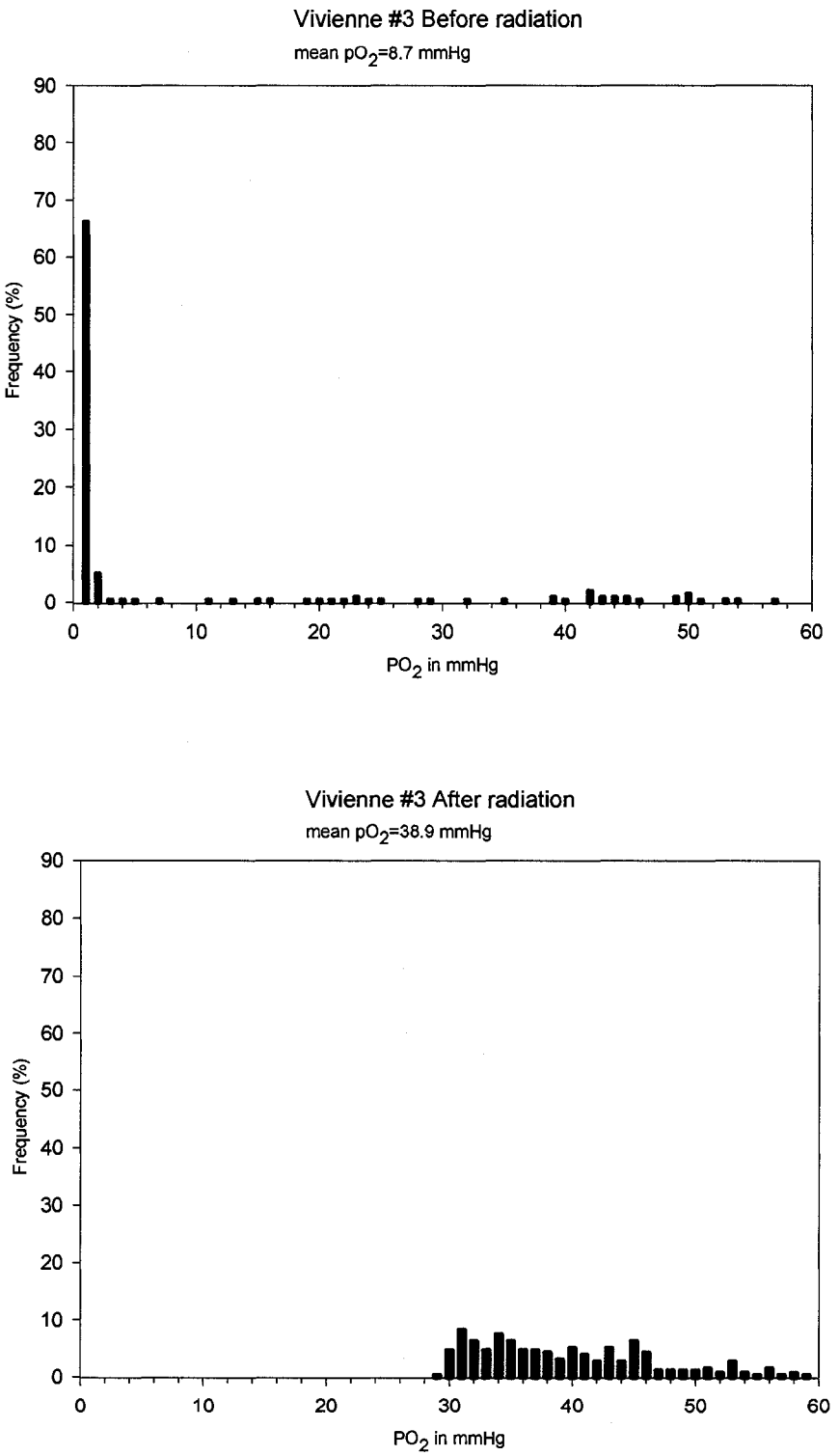

Figure 2.15. Oxygen measurements in tumor #3, osteosarcoma, at the same location before and after radiation

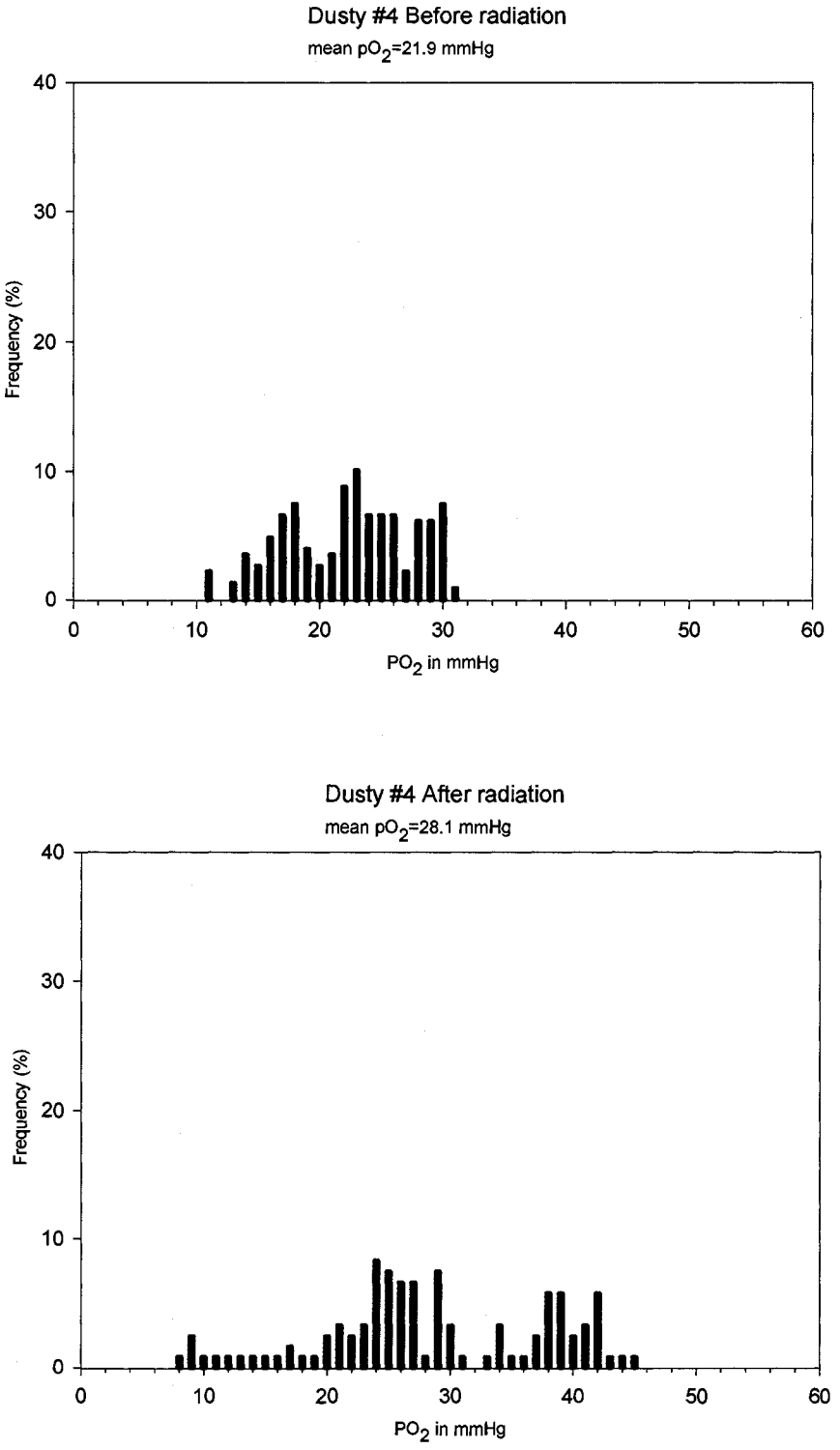

Figure 2.16. Oxygen measurements in tumor #4, osteosarcoma, at the same location before and after radiation

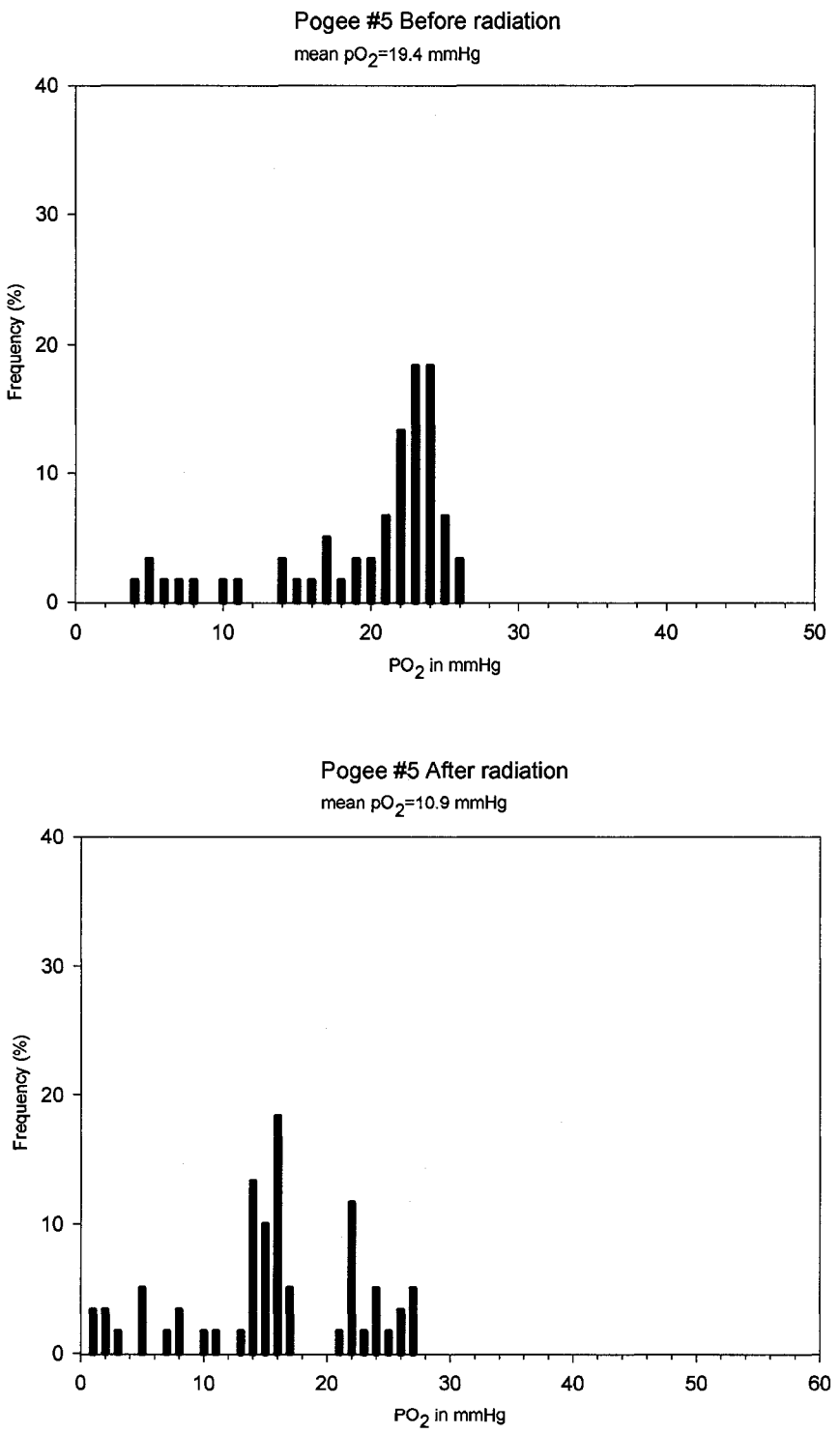

Figure 2.17. Oxygen measurements in tumor #5, soft tissue sarcoma, at the same location before and after radiation

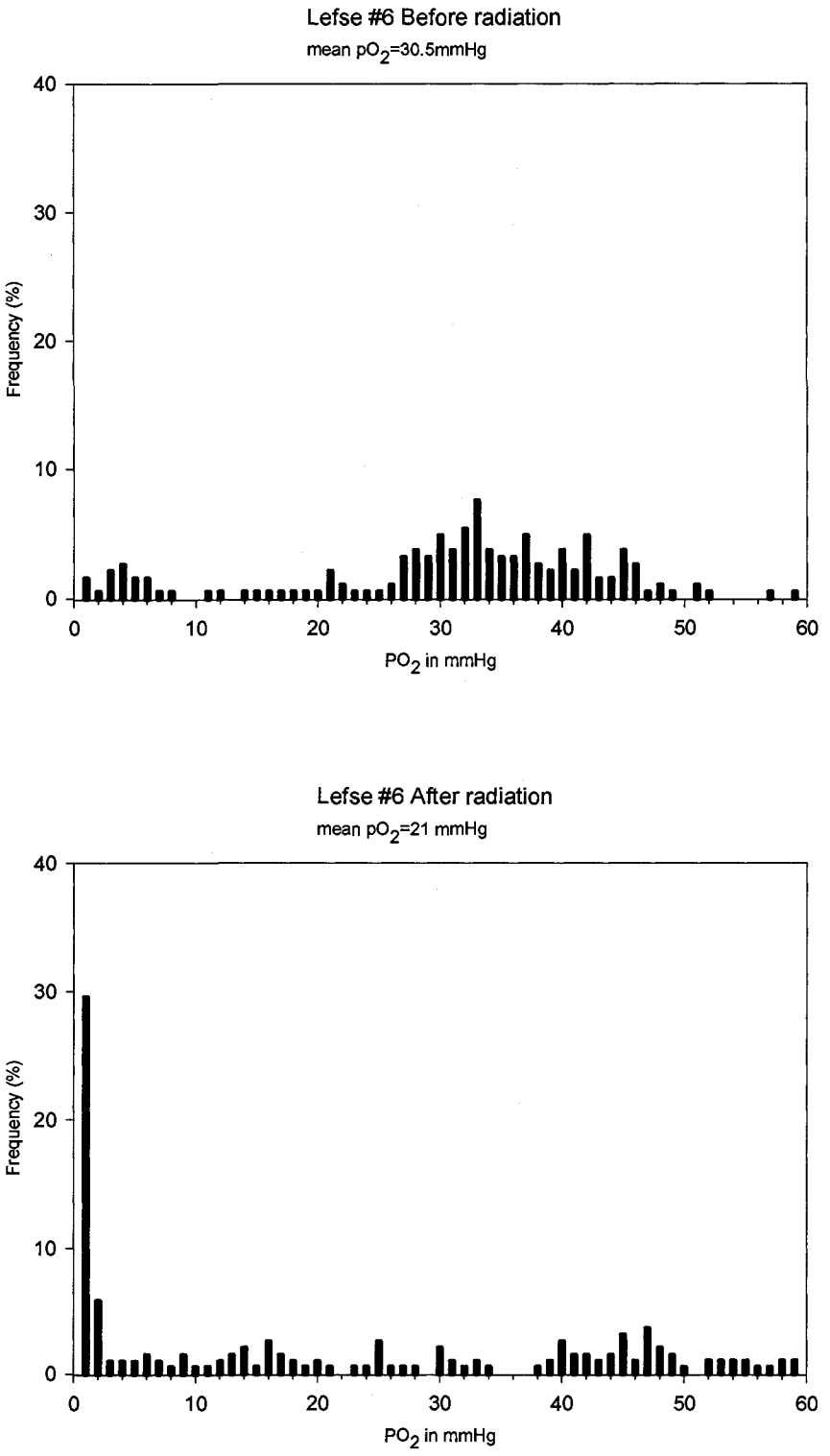

Figure 2.18. Oxygen measurements in tumor #6, mast cell tumor, at the same location before and after radiation.

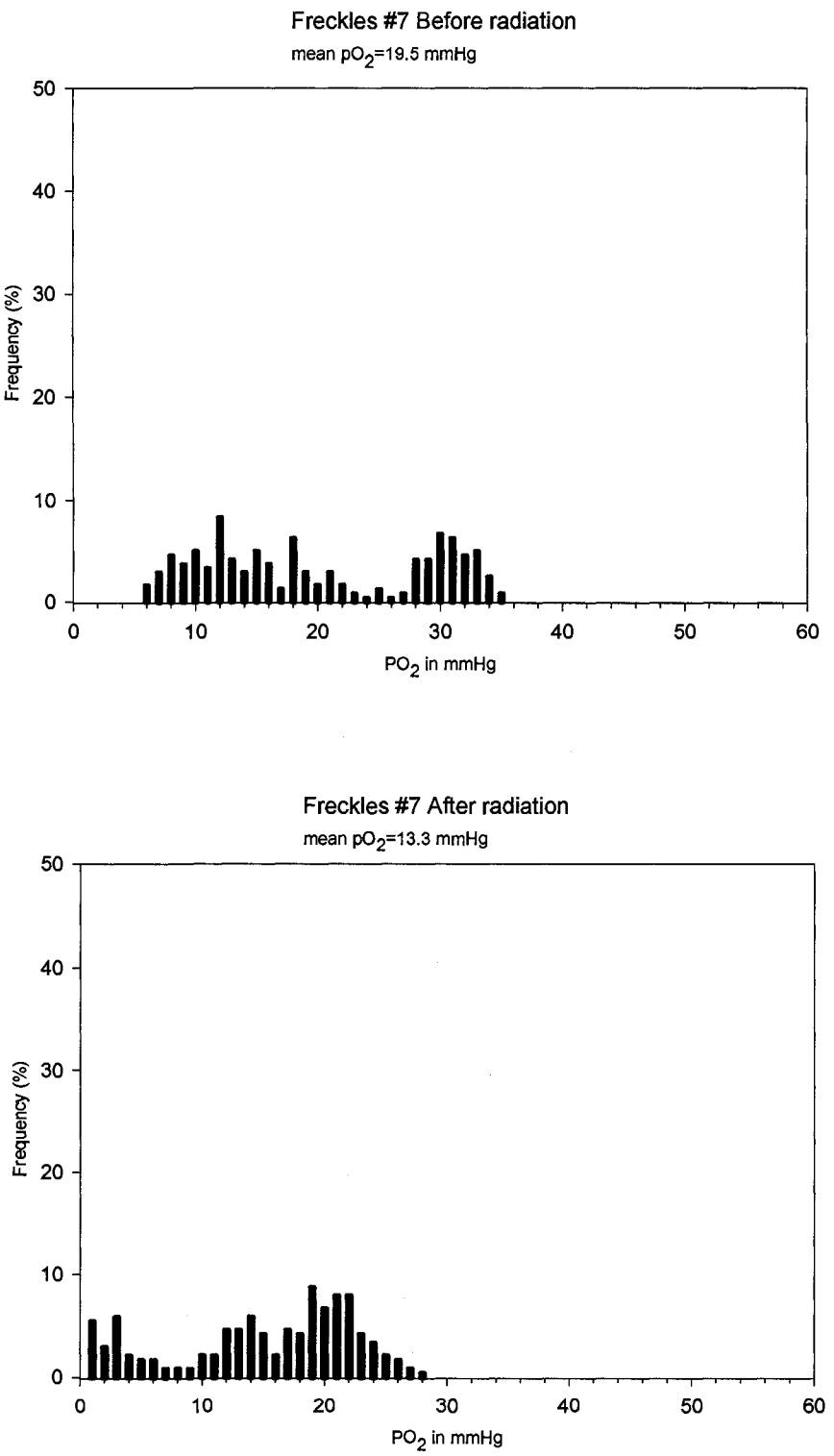

Figure 2.19. Oxygen measurements in tumor #7, adenocarcinoma, at the same location before and after radiation.

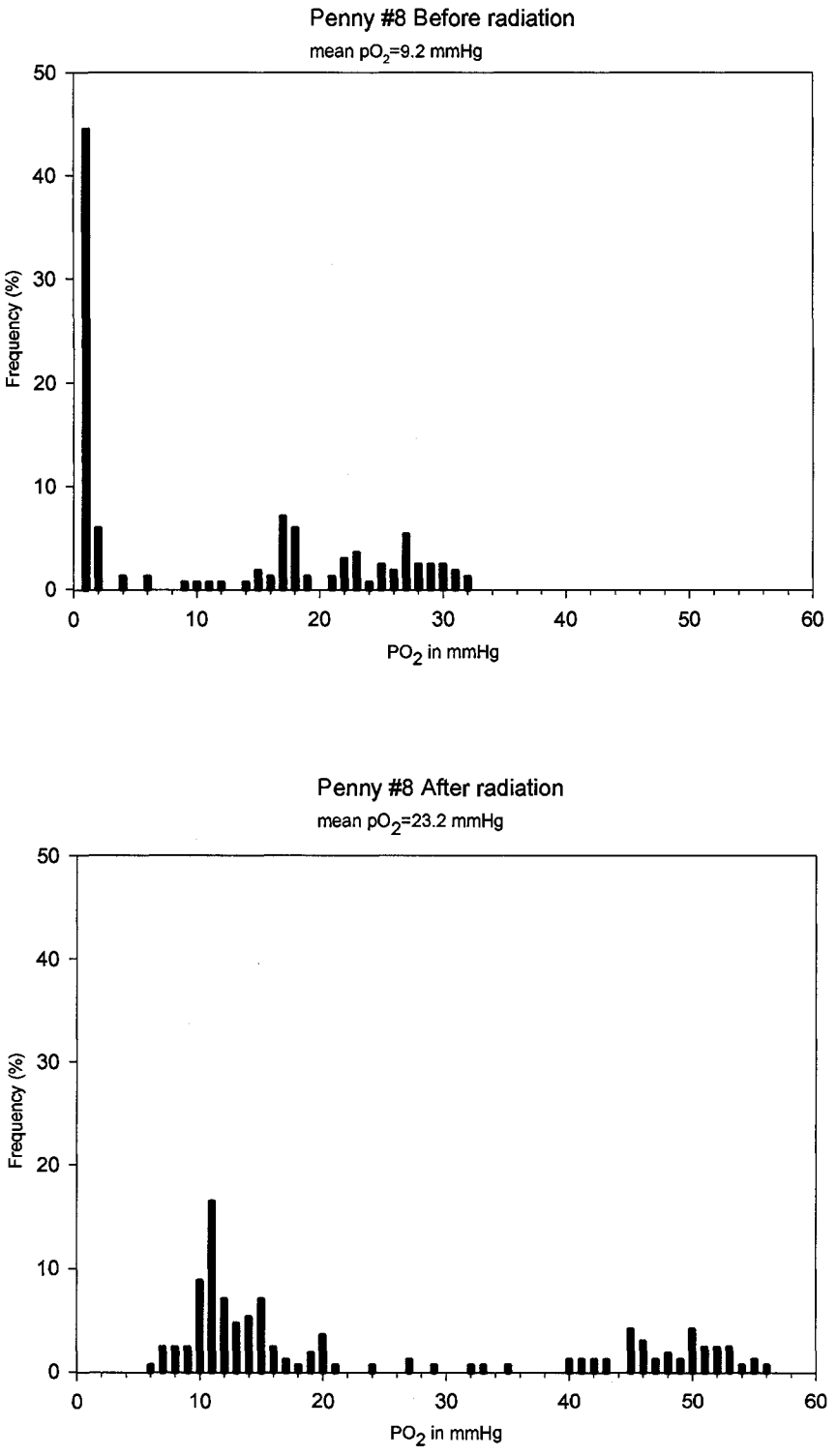

Figure 2.20. Oxygen measurements in tumor #8, mammary carcinoma, at the same location before and after radiation.

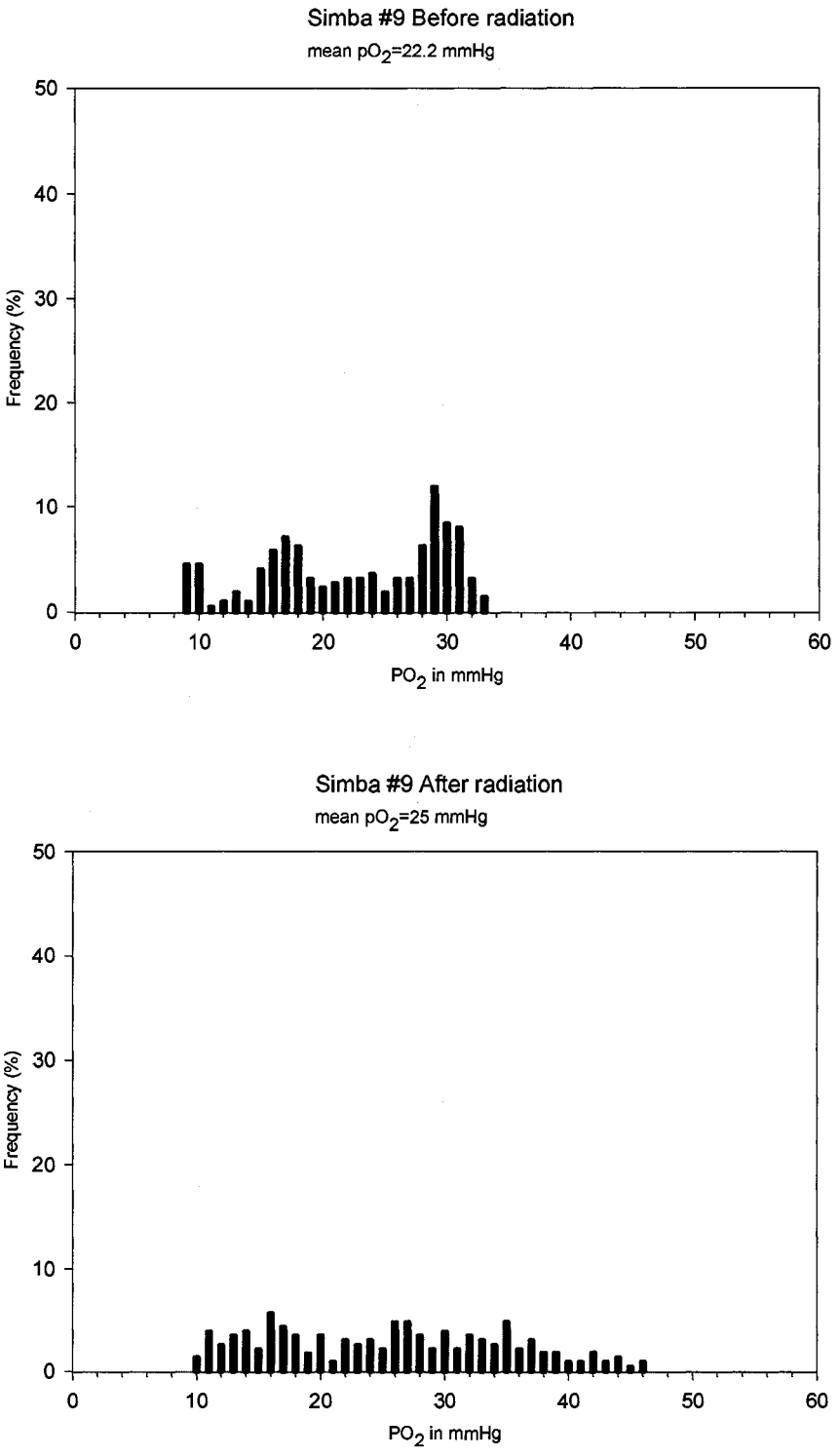

Figure 2.21. Oxygen measurements in tumor #9, multilobular osteochondrosarcoma, at the same location before and after radiation.

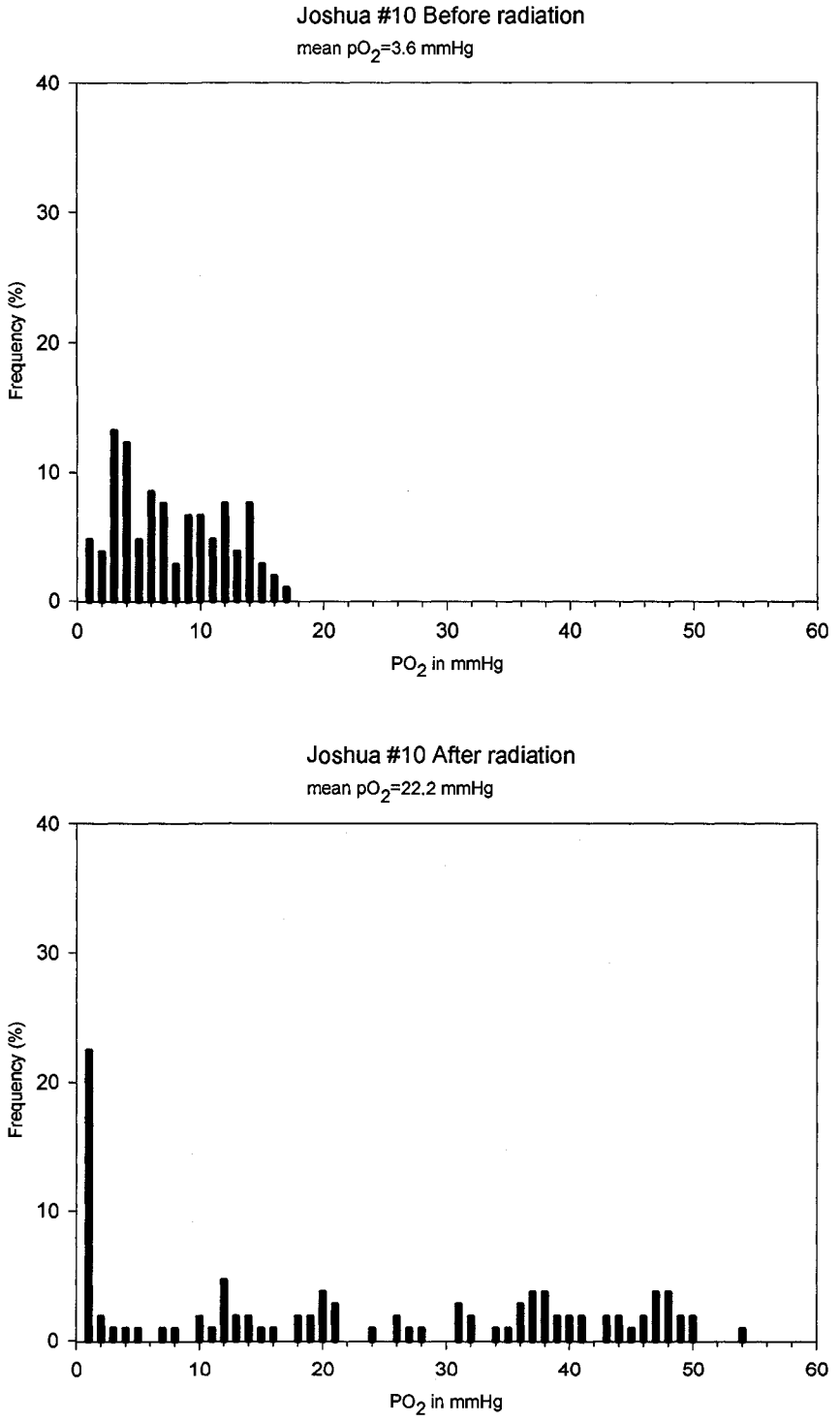

Figure 2.22. Oxygen measurements in tumor #10, soft tissue sarcoma, at the same location before and after radiation.

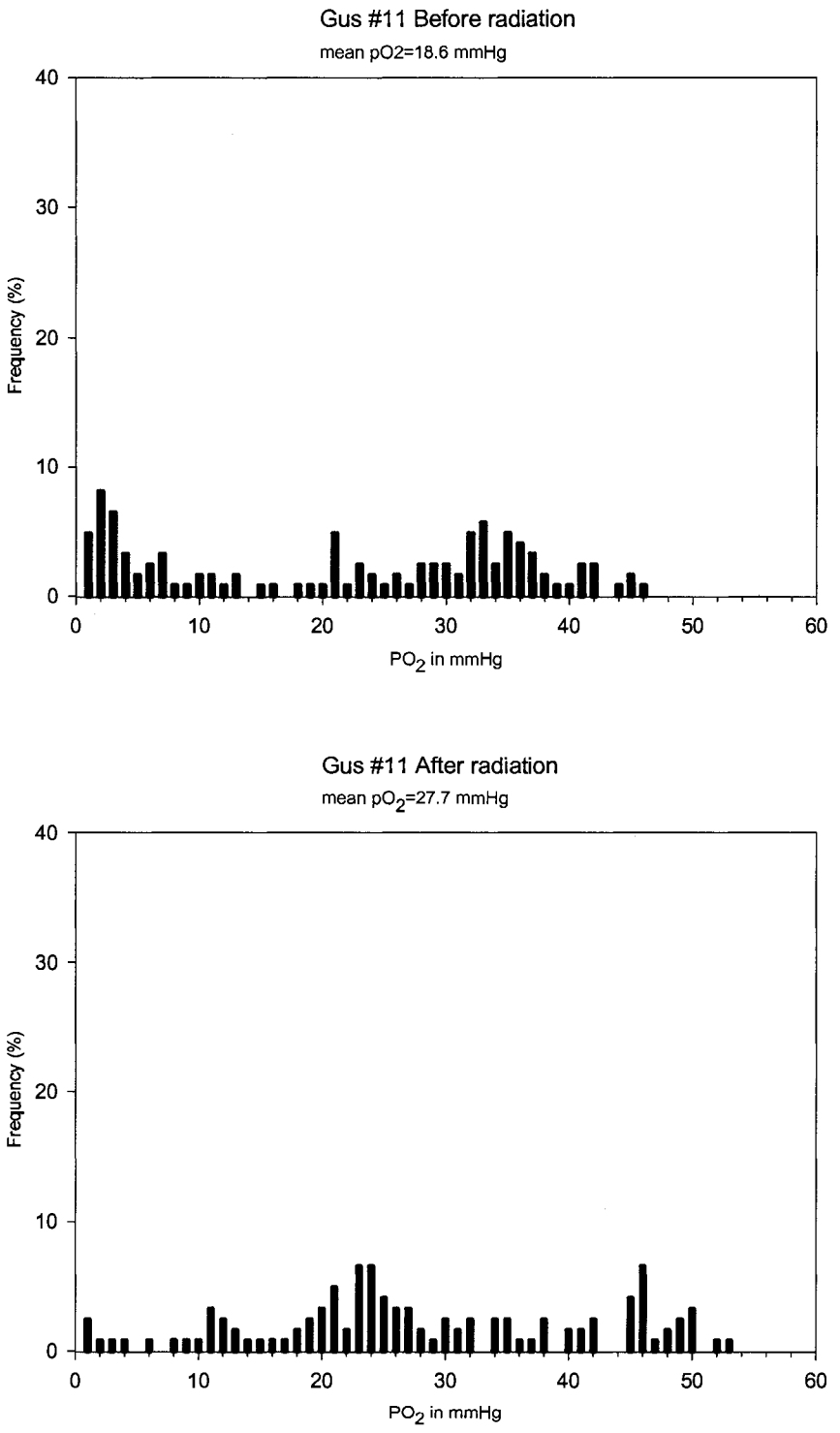

Figure 2.23. Oxygen measurements in tumor #11, fibrosarcoma, at the same location before and after radiation.

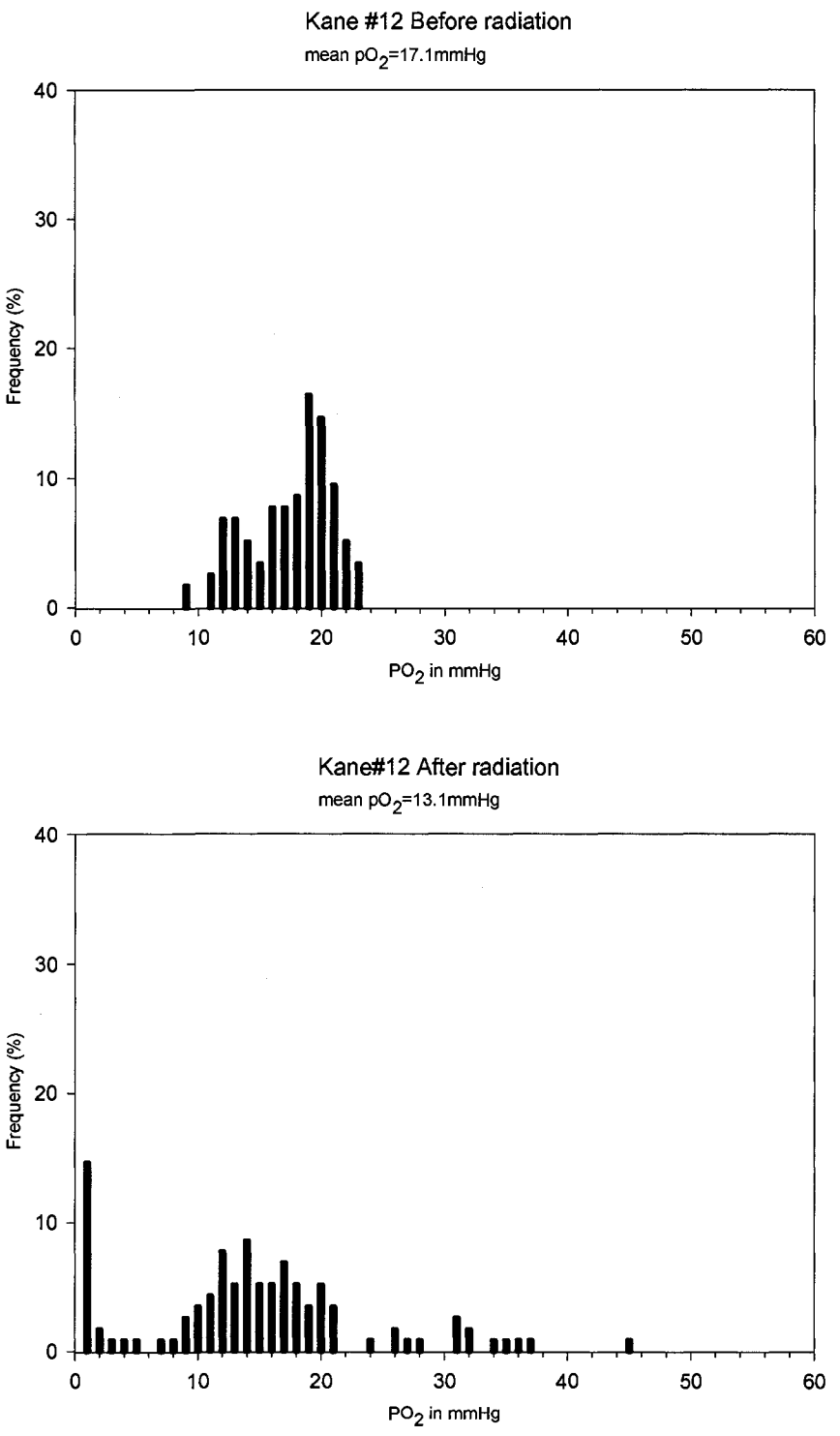

Figure 2.24. Oxygen measurements in tumor #12, liposarcoma, at the same location before and after radiation.

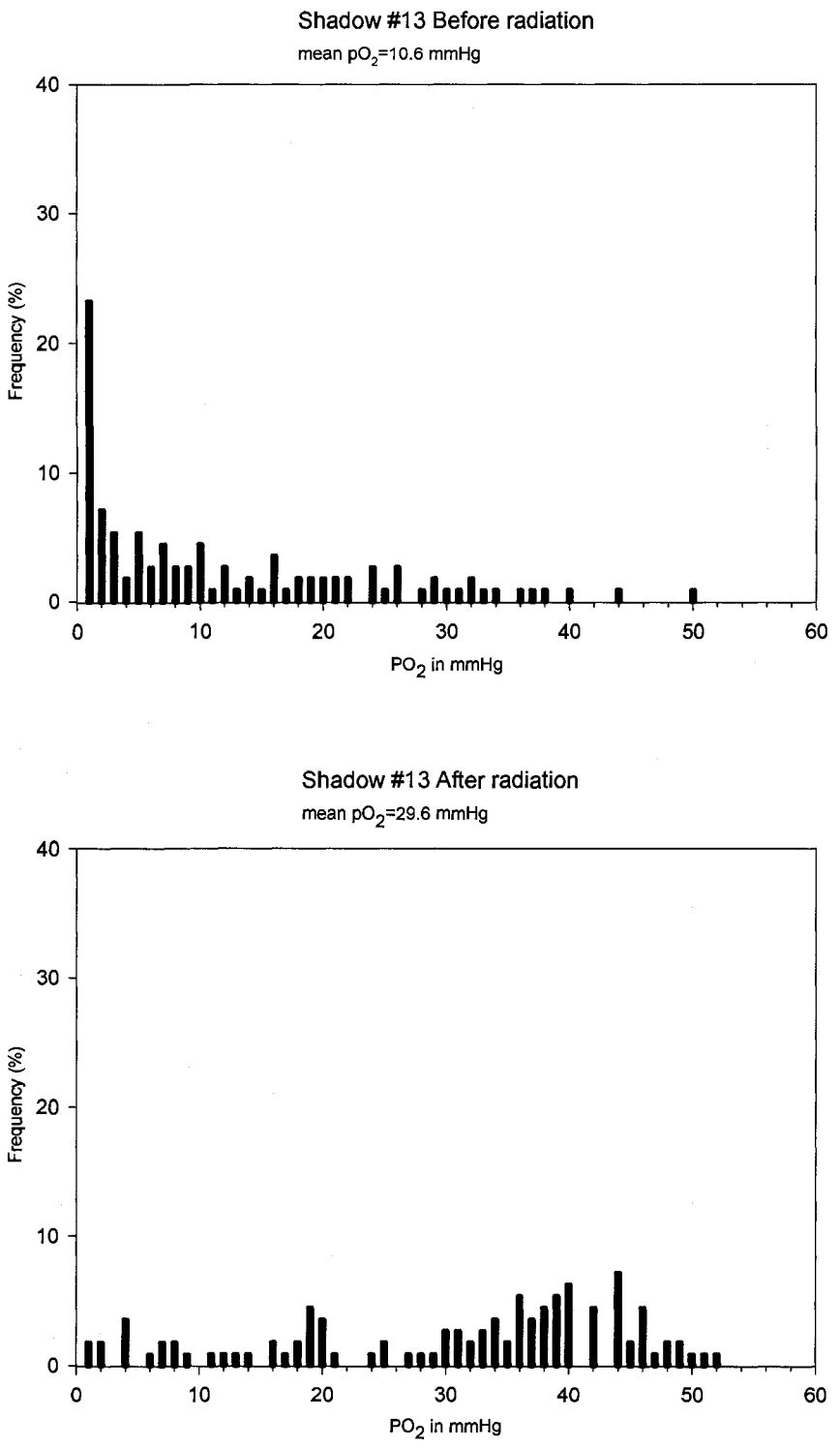

Figure 2.25. Oxygen measurements in tumor #13, soft tissue sarcoma, at the same location before and after radiation.

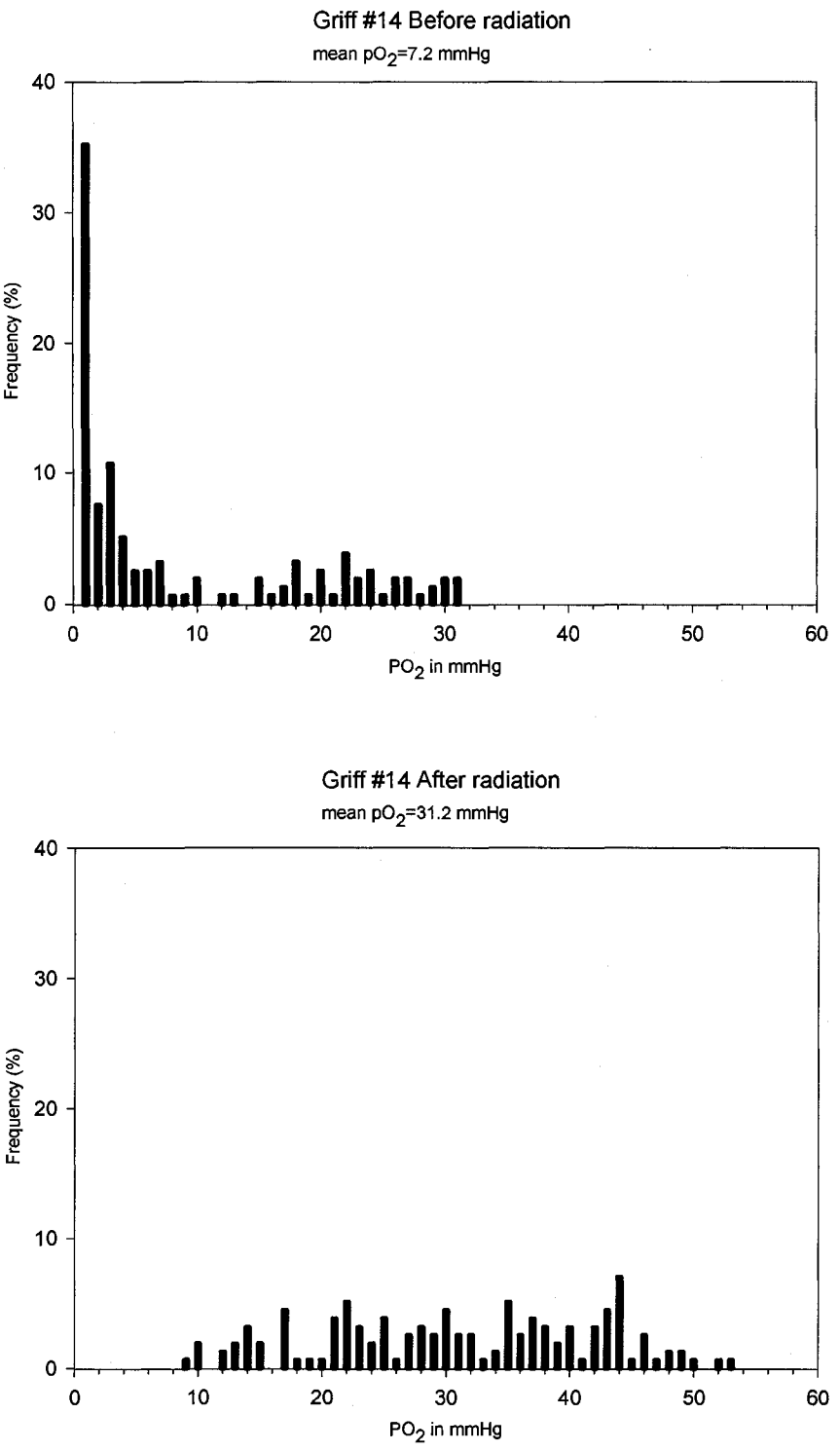

Figure 2.26. Oxygen measurements in tumor #14, fibrosarcoma, at the same location before and after radiation.

Interstitial fluid pressure

Mean IFP decreased after radiation in 9 out of 14 tumors. In 4 of the remaining tumors it did not change more than 0.05-0.12mmHg, and only one tumor had increased IFP post-radiation (Table 2.1).

Table 2.1. IFP measurements presented as means of measurements before and after radiation.

IFP Measurements		
Dog #	Before	After
1	8.8	4.99
2	0.26	0.37
3	3.37	1.56
4	-0.59	-3.41
5	-7.11	-7.21
6	-0.48	-0.53
7	1.02	0.9
8	1.03	0.34
9	1.58	-0.18
10	3.33	-0.68
11	9.83	3.85
12	-0.65	-7.45
13	8.6	0.63
14	1.8	10.45

In Figure 2.11, 2.12, and 2.13 the before and after pressure data from each tumor is graphed.

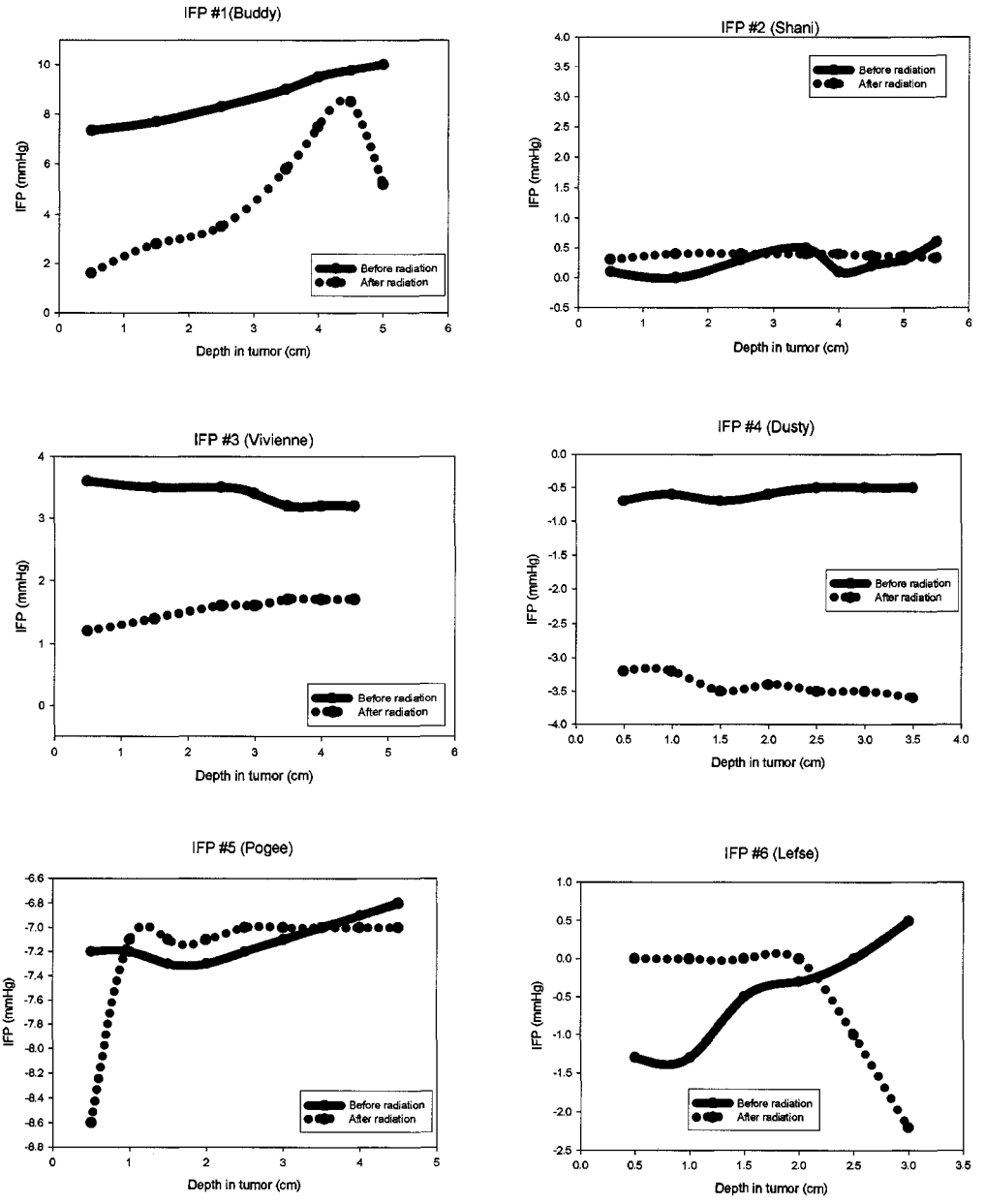

Figure 2.11. IFP before (full line) and after radiation (dotted line) for six tumors.

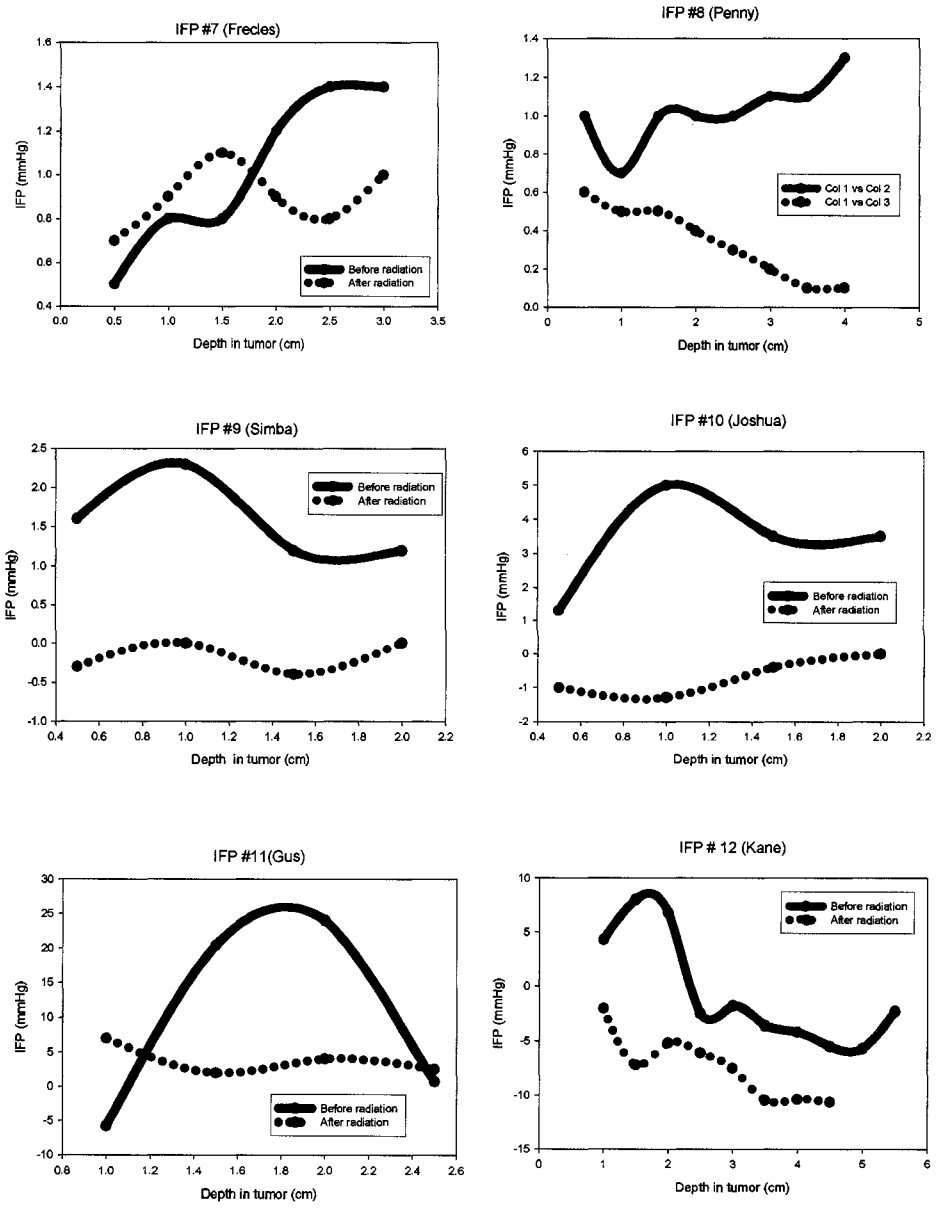

Figure 2.12. IFP before (full line) and after radiation (dotted line) for six tumors.

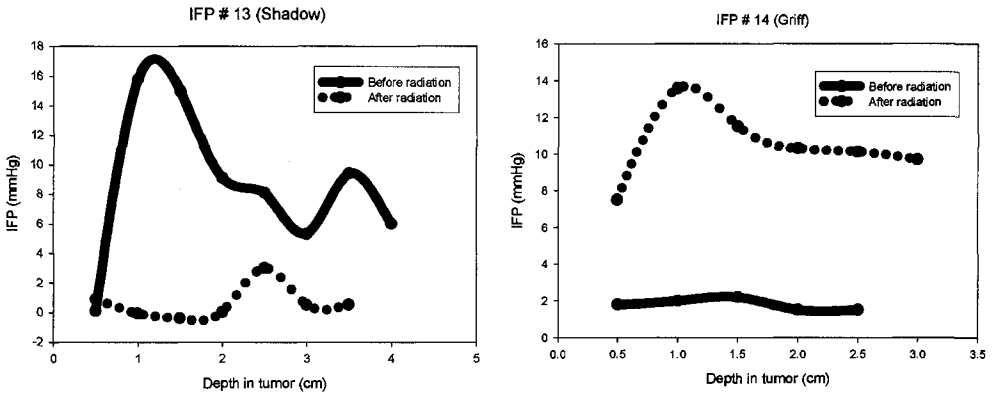

Figure 2.13. IFP before (full line) and after radiation (dotted line) for two tumors.

Microvascular perfusion measurements

Laser Doppler flowmetry data are expressed in relative blood pressure units (BPU) and was obtained in 13 out of 14 dogs. LDF showed an increased mean BPU after radiation in 5 tumors, and decreased mean BPU after radiation in 8 tumors. DCE CT was performed in 5 tumors and indicated an increase in tumor perfusion after radiation in 1 tumor (results that do not correlate to LDF data in this one case). DCE MRI for microvascular perfusion was obtained in 9 tumors and indicated that it was decreased in all 9 tumors after radiation (in four cases these data did not correlate to LDF results). Microvascular perfusion data obtained for each tumor are summarized in Table 2.3.

Table 2.3. Microvascular perfusion estimates in 14 tumors using two techniques for each tumor. Laser Doppler means of measurements are in BPU, and DCE CT/MRI measurements are presented as relative perfusion indexes (RPIs).

	LDF PERFUSION		CT/MRI PERFUSION	
DOG#	BPU before	BPU after	RPI before	RPI after
1	101.88	73.63	0.050335	0.047402
2	50.37	42.22	0.037031	0.004243
3	27.12	8.11	0.370206	0.173572
4	495.41	288.71	0.181723	0.253197
5	191.74	227.5	0.032	-0.0336
6	214.18	128.93	14.26	8.21
7	92.47	193.85	11	-3.3477
8	97.12	136.9	23.72	-0.5478
9	132.8	94.7	21.04	16.813
10	244.4	159.7	34.73	16.25
11	204.81	N/A	9.52	7.68
12	123.63	422.46	9.33	4.18
13	340.03	235.99	16.34	9.38
14	119.44	132.08	24.31	20.42

Microvascular perfusion data obtained for each tumor by LDF are also presented in graphs in Figures 2.27, 2.28, 2.29, 2.30, and 2.31.

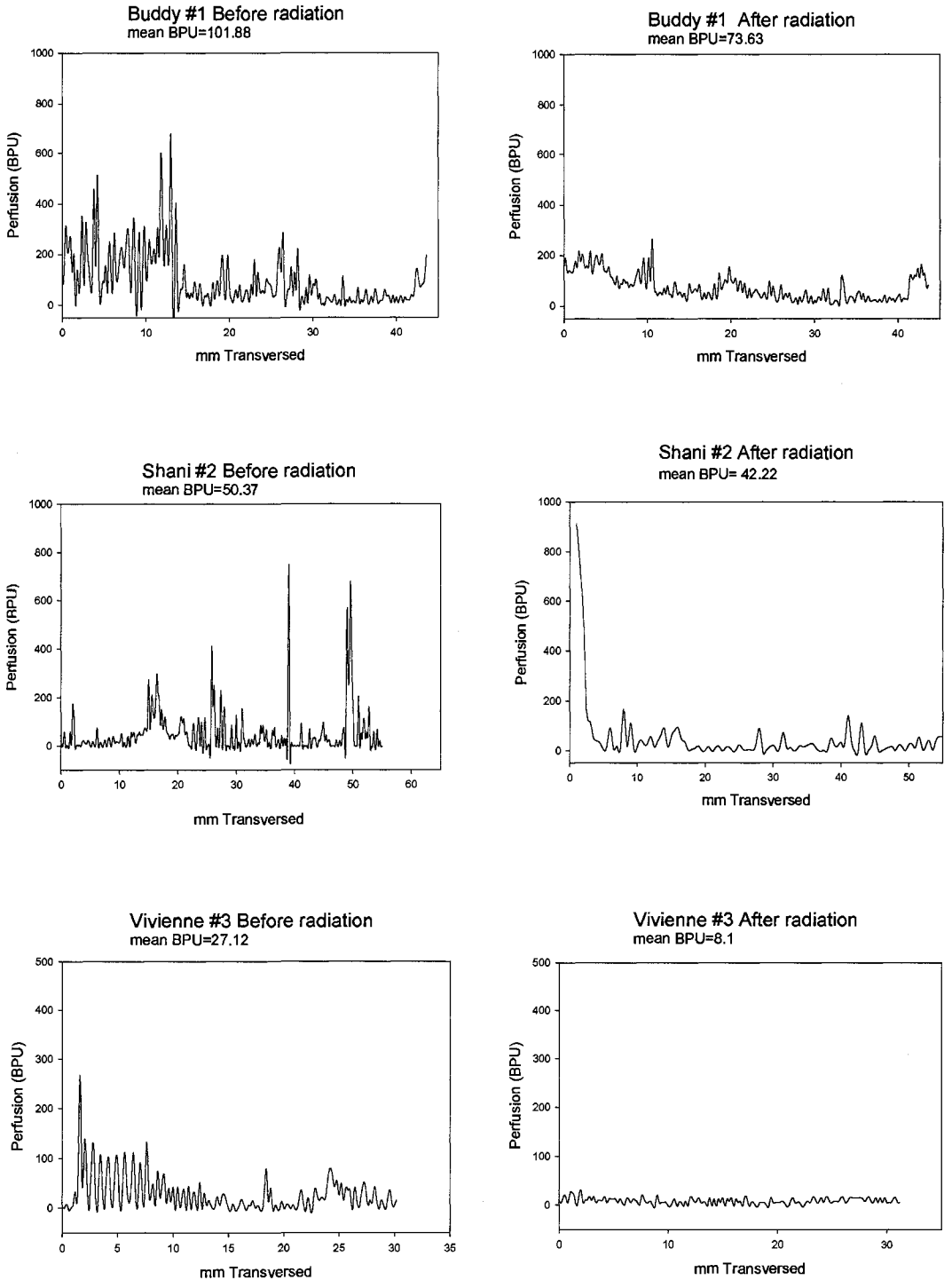

Figure 2.27. LDF perfusion measured with OxyFlow at the time of the pO_2 measurement with OxyLite, using combined perfusion/oxygen/temperature probes, before and after radiation dose of 3Gy in three different tumors.

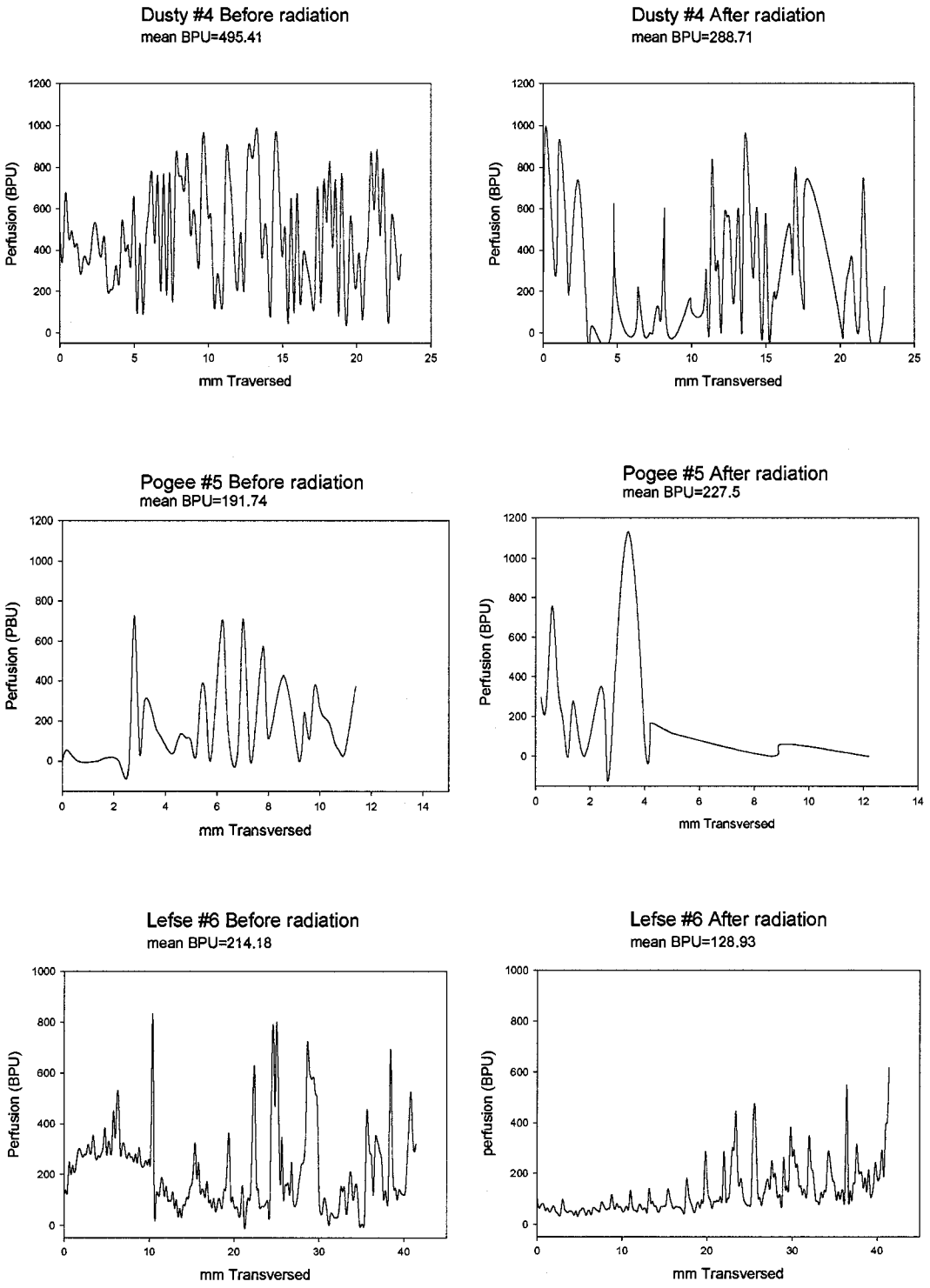

Figure 2.28. LDF perfusion measured with OxyFlow at the time of the pO_2 measurement with OxyLite, using combined perfusion/oxygen/temperature probes, before and after radiation dose of 3Gy in three different tumors.

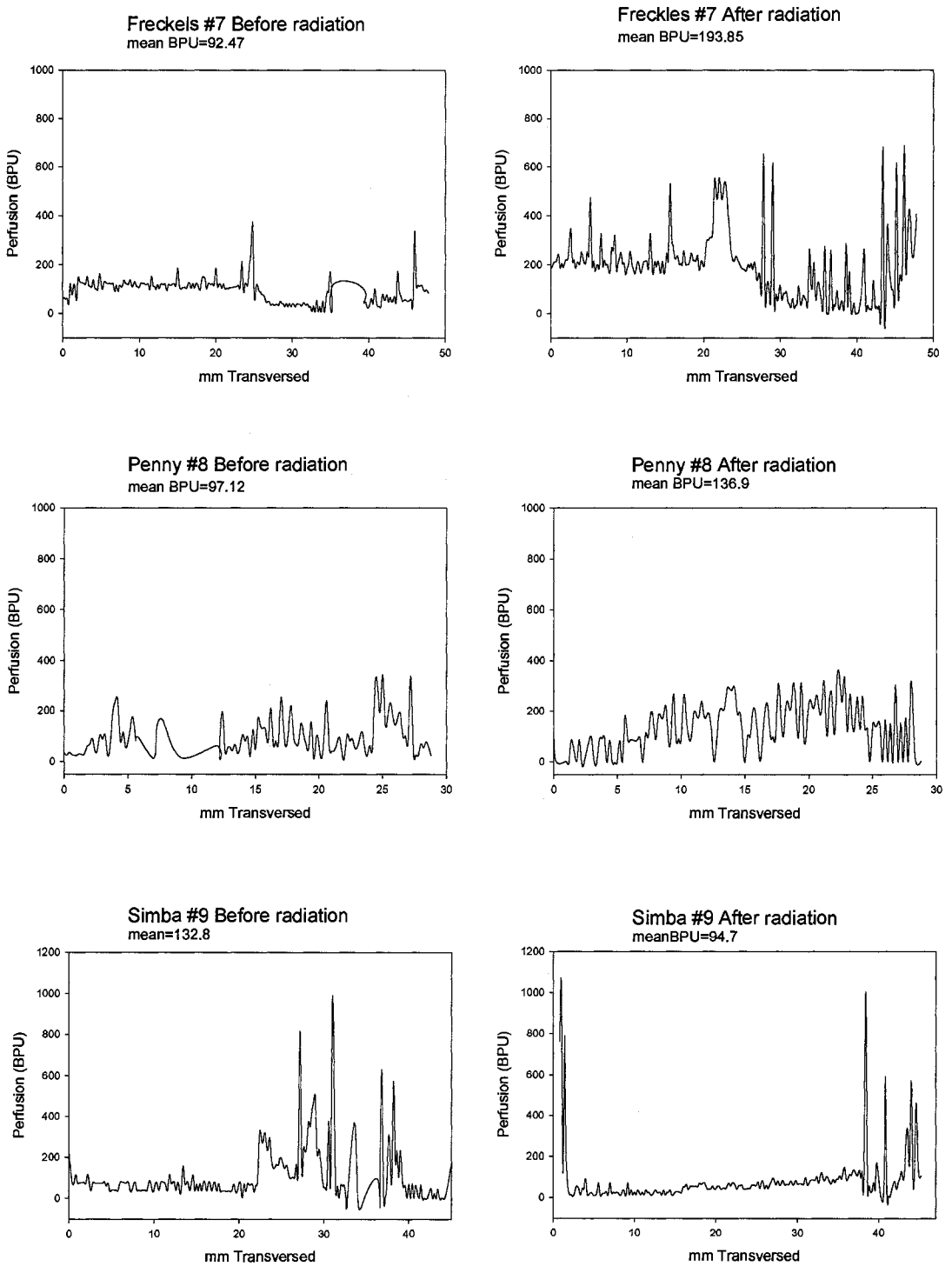

Figure 2.29. LDF perfusion measured with OxyFlow at the time of the pO_2 measurement with OxyLite, using combined perfusion/oxygen/temperature probes, before and after radiation dose of 3Gy in three different tumors.

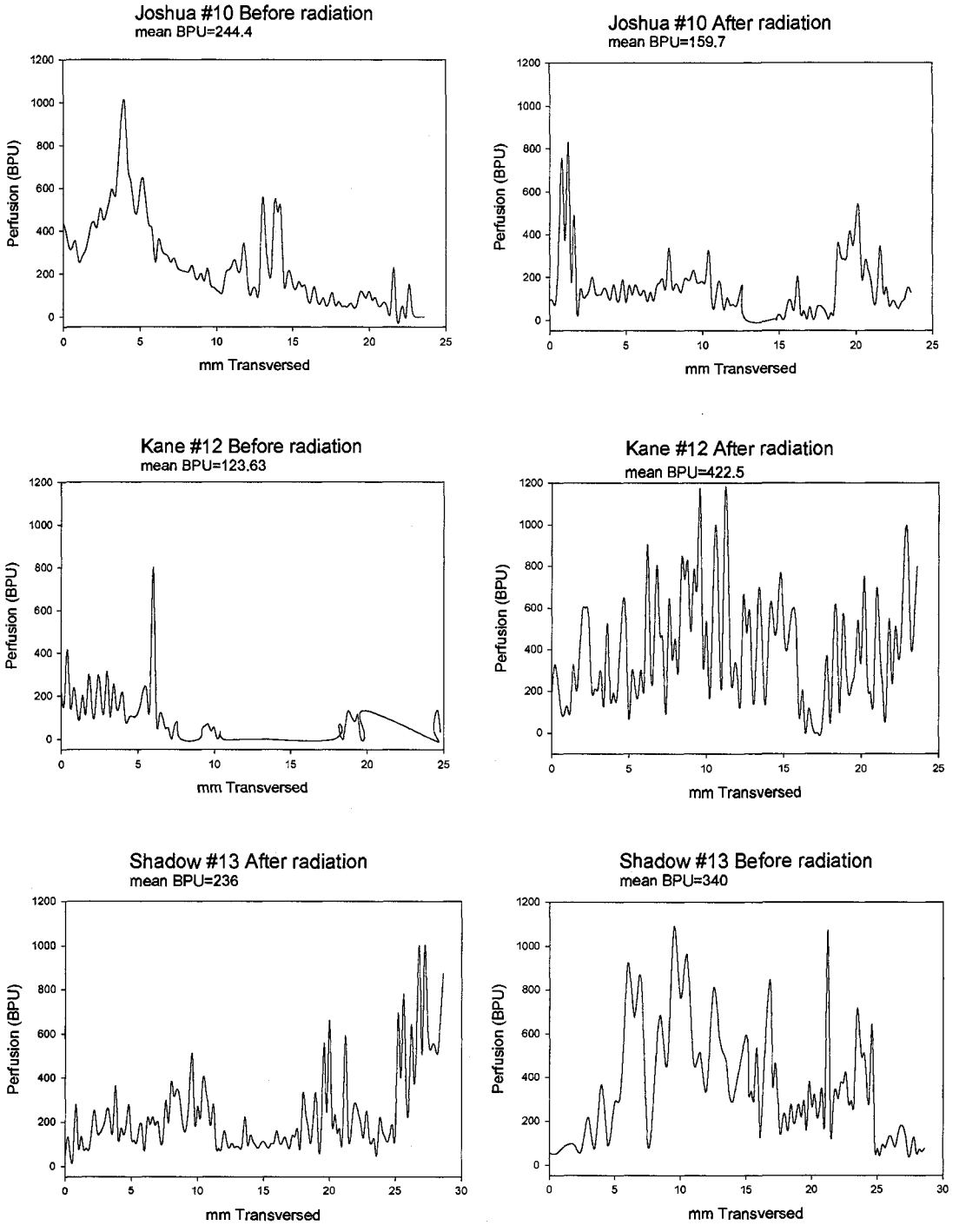

Figure 2.30. LDF perfusion measured with OxyFlow at the time of the pO_2 measurement with OxyLite, using combined perfusion/oxygen/temperature probes, before and after radiation dose of 3Gy in three different tumors.

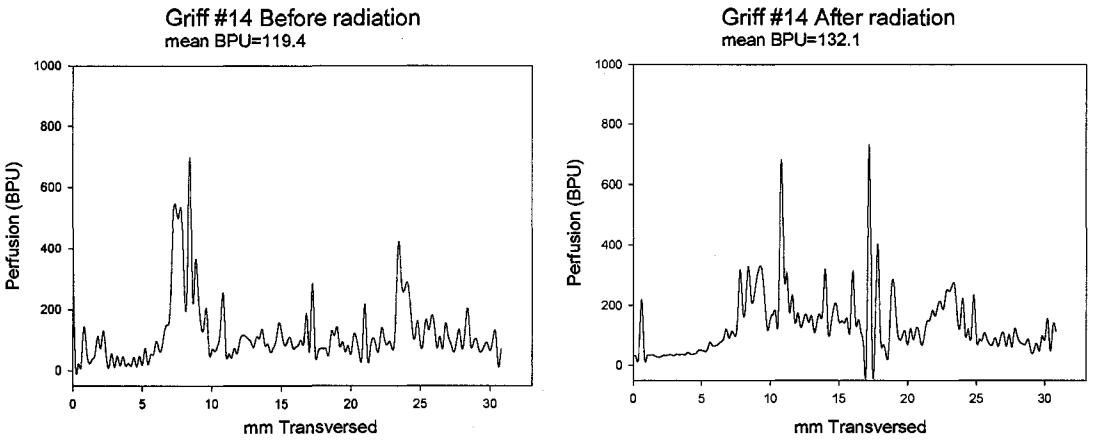

Figure 2.31. LDF perfusion measured with OxyFlow at the time of the pO_2 measurement with OxyLite, using combined perfusion/oxygen/temperature probes, before and after radiation dose of 3Gy.

Dynamic contrast enhanced CT and MRI were done along with LDF measurements in all tumors. RPIs were calculated and presented in Table 2.3. Graphs for average RPI for the entire tumor (for all tumors) and each tumor RPIs for regions of interest are presented in figures 2.32, 2.33, 2.34, 2.35, 2.36, and 2.37 provided by Dr. Susan Kraft.

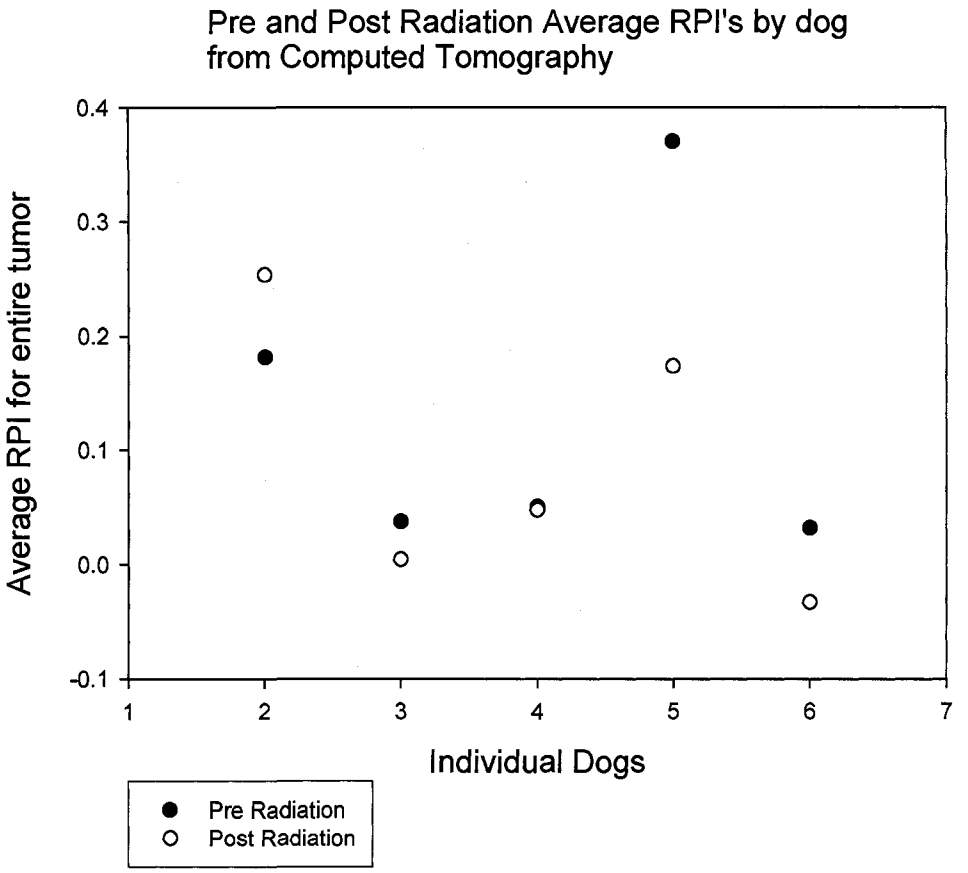

Figure 2.32. Average RPIs for whole tumor in 5 dogs, calculated from DCE CT pre- and post-radiation.

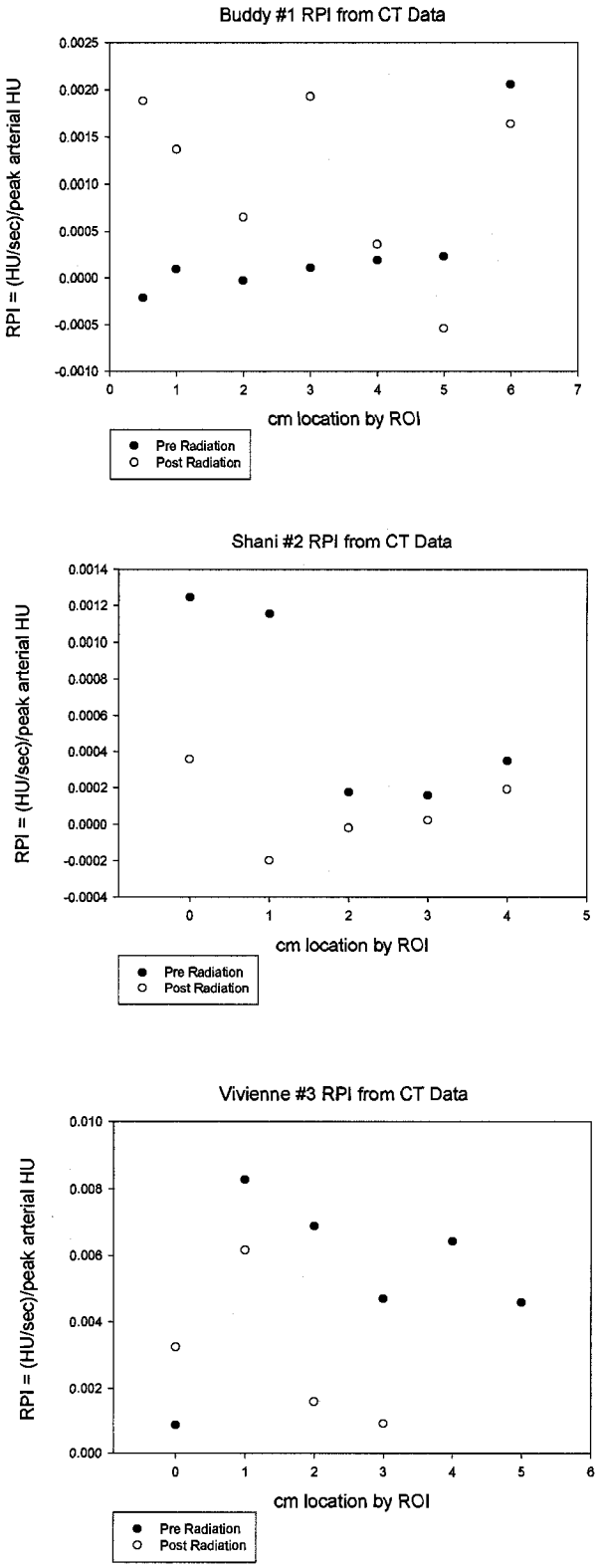

Figure 2.33. Individual tumors RPI calculated for ROIs at different depths in tumors, pre- and post-radiation.

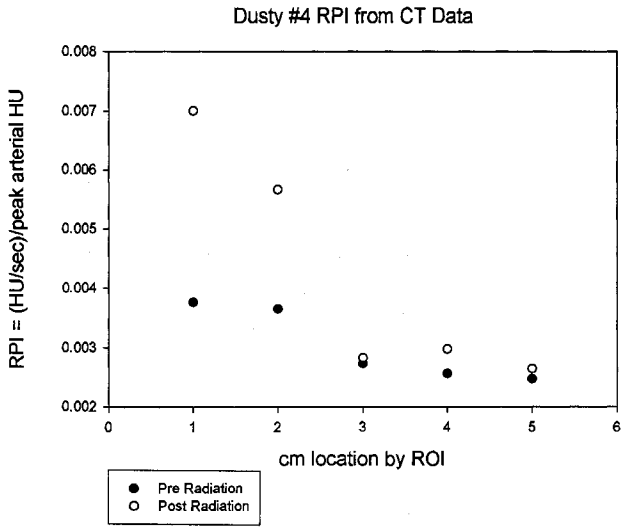

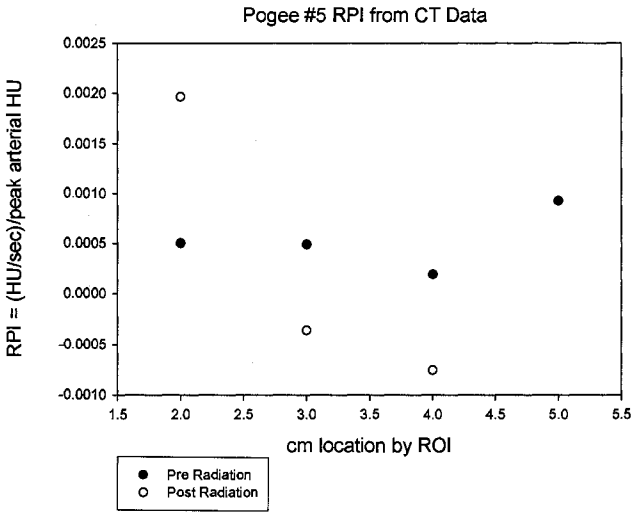

Figure 2.34. Individual tumors RPI calculated for ROIs at different depths in tumors, pre- and post-radiation.

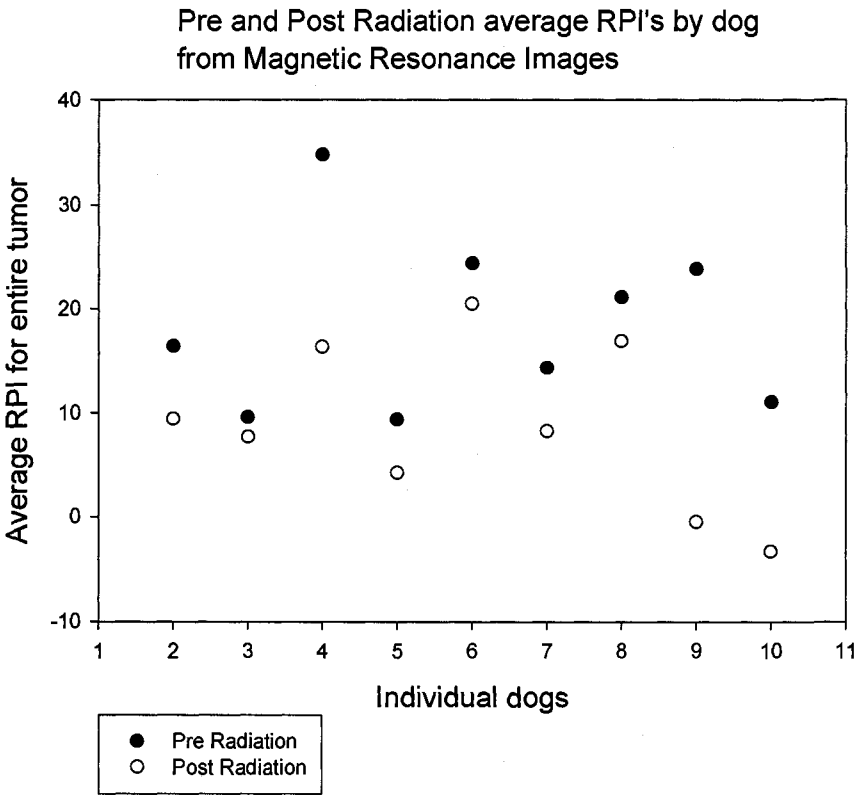

Figure 2.35. Average RPIs for whole tumor in 9 dogs, calculated from DCE MRI pre- and post-radiation.

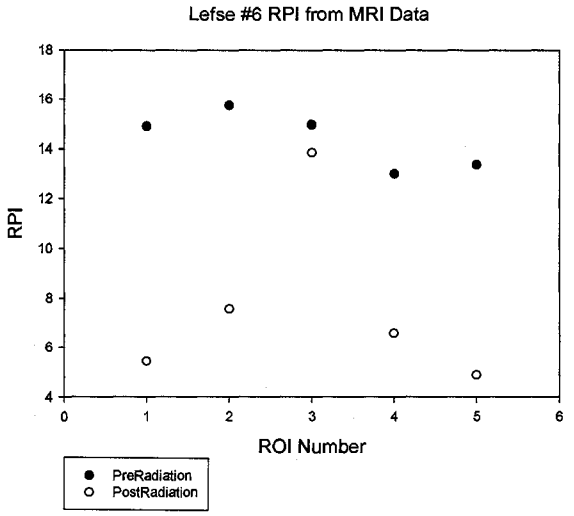
Lefse #6 RPI from MRI Data
RPI
ROI Number
PreRadiation
PostRadiation

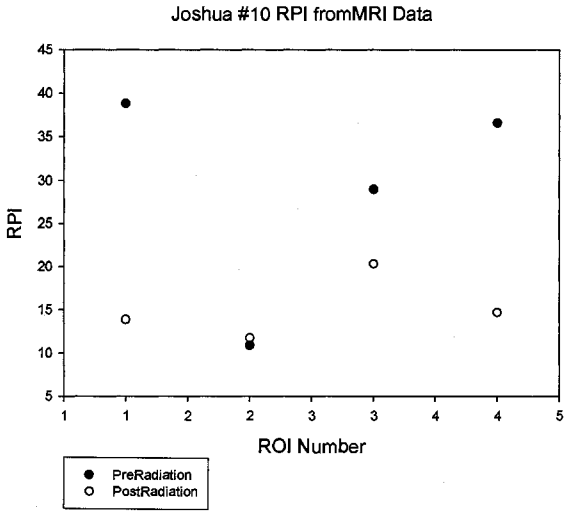
Joshua #10 RPI fromMRI Data
RPI
ROI Number
PreRadiation
PostRadiation

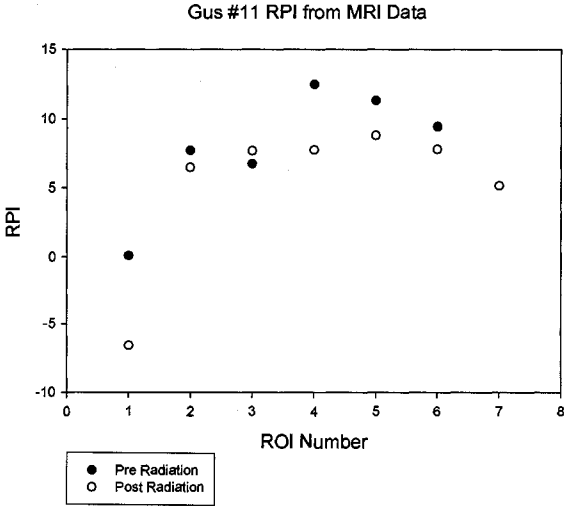
Gus #11 RPI from MRI Data
RPI
ROI Number
Pre Radiation
Post Radiation

Figure 2.36. Individual tumors RPI calculated for ROIs at different depths in tumors, pre- and post-radiation.

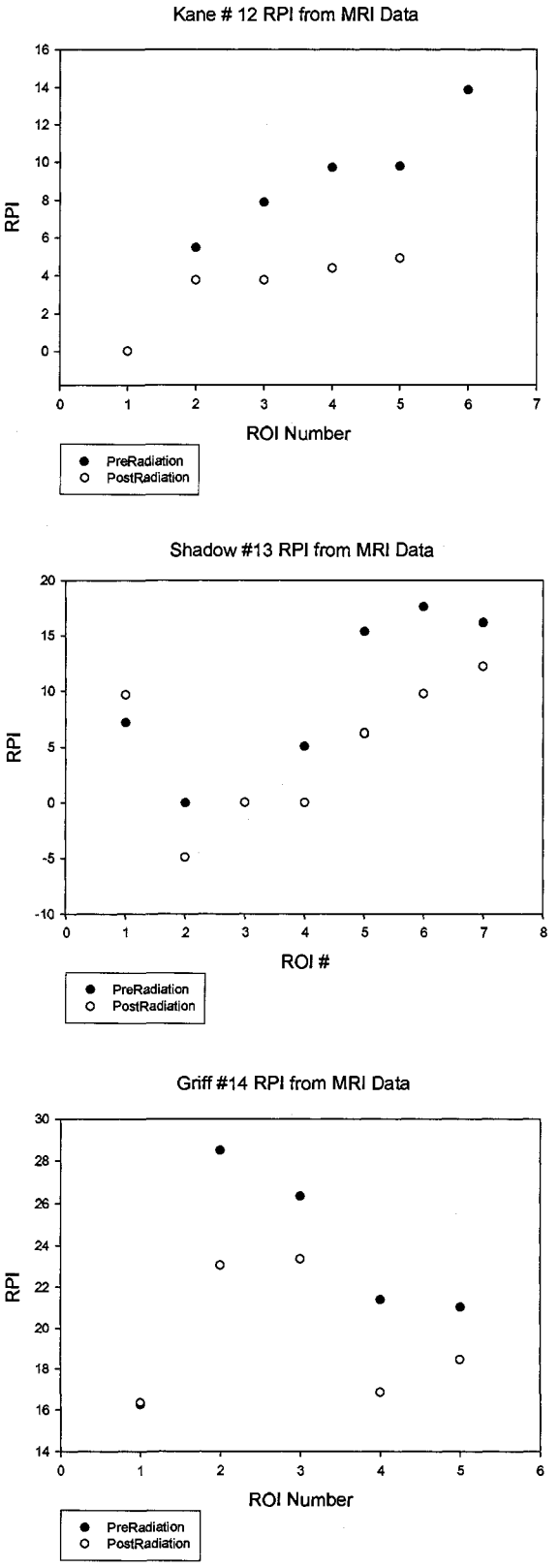

Figure 2.37. Individual tumors RPI calculated for ROIs at different depths in tumors, pre- and post-radiation.

Quantification of tumor cell apoptosis

Pretreatment frequency of apoptosis differed among the tumors (Table 2.4). After radiation, the apoptotic index was significantly increased in all tumors at both 6 and 24 hours (at 24 hours P=0.0015). The apoptotic index (AI) was greatest at 6 hours after radiation (P= 0.00093, two-tailed *t* test) (Figure 2.38).

Table 2.4. Apoptotic Indexes for 14 tumors

Dog #	AI %		
1	12.2		39.7
2	4.3		8.5
3	4.5		17.8
4	3.4		10.1
5	18.9	21.1	19.6
6	6.5	20.8	13.5
7	10.9	33.1	11.39
8	4.2	13.1	13.8
9	13.1	20.1	17
10	13.3	17.2	16.5
11	6.7	23.3	22.3
12	4.9	15.6	16.2
13	8.5	15	9.8
14	7	11.5	12.1
	before IR	6 h after	24 h after

Table 2.4 AI for 14 tumors analyzed from biopsy sections taken before radiation and 6 and 24 hours after dose of 3Gy. First 4 tumors had only before and 24h after radiation results.

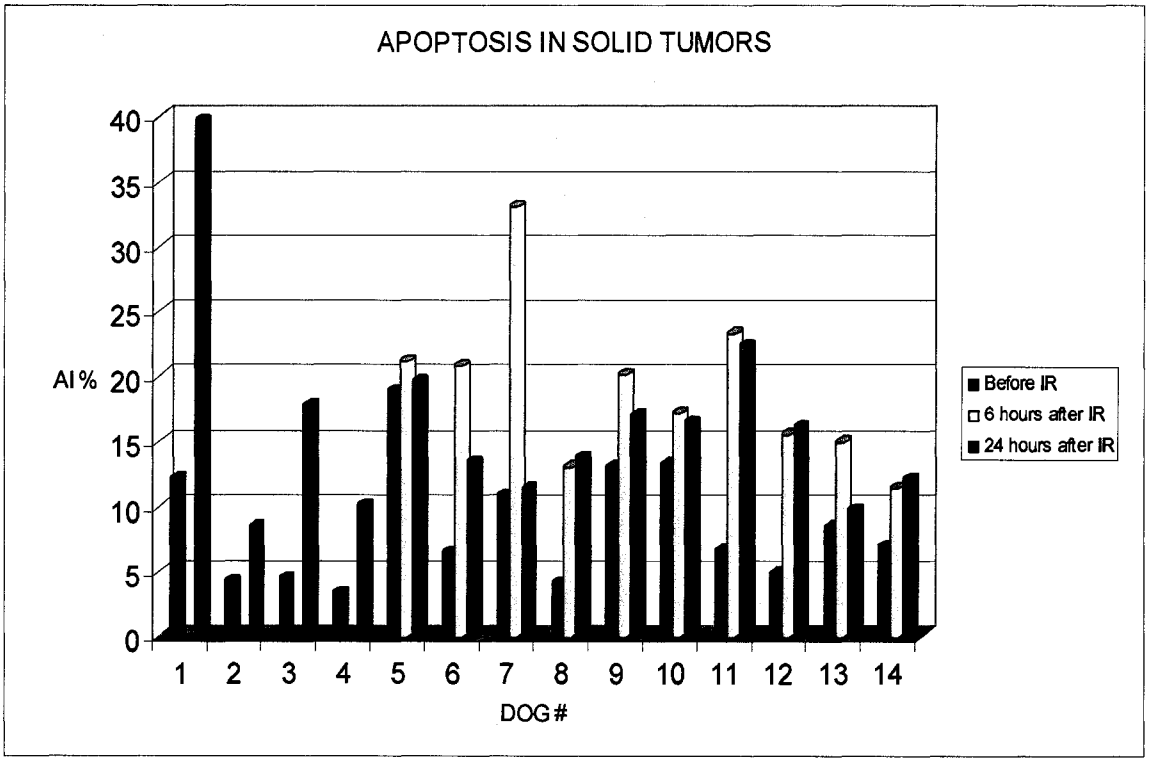

Figure 2.38. Apoptotic Index for each of 14 tumors showing values before (black), 6 hours (yellow), and 24 hours (red) after radiation.

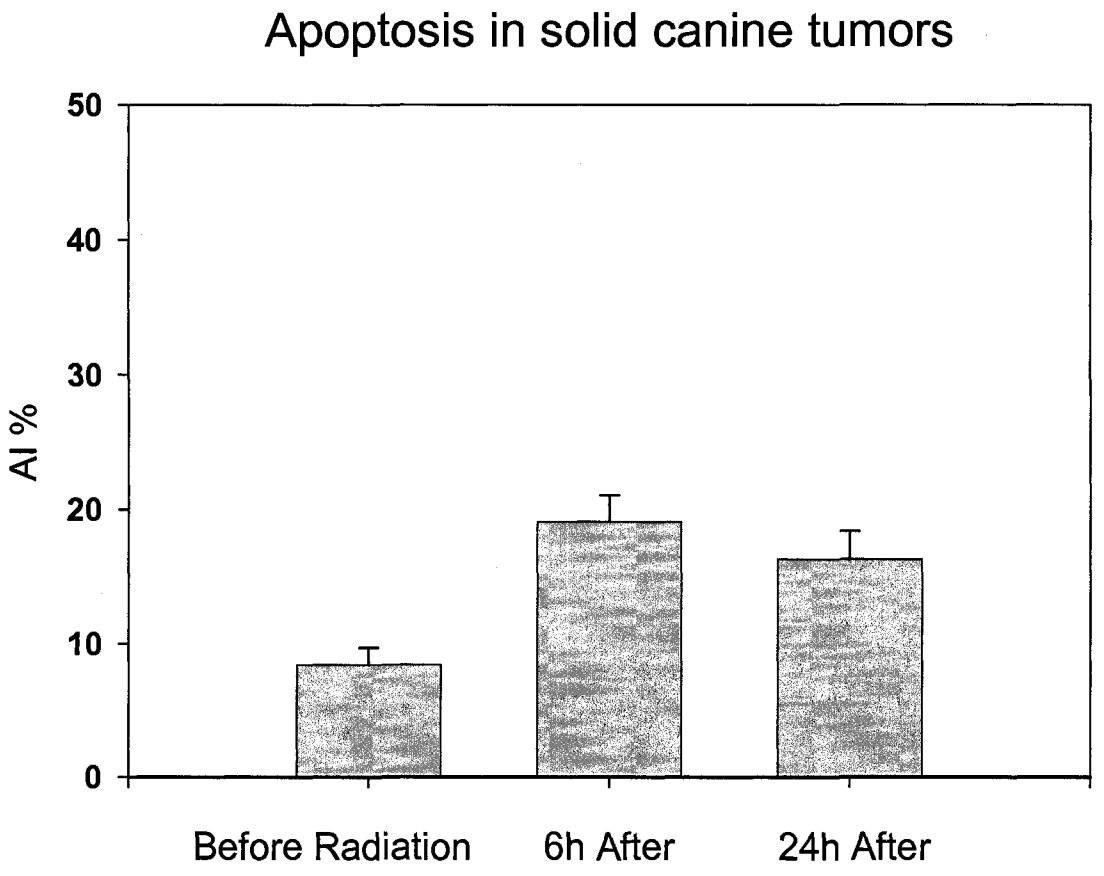

Figure 2.39. Tumor cell apoptosis. Mean values of AI for 14 tumors before, 6 hours, and 24 hours after radiation. Bars=SEM.

Figure 2.40. Adenocarcinoma tumor sections were stained with TUNEL as described earlier. Green fluorescence marked TUNEL positive apoptotic cells in tumor tissue before radiation (left panel), and after dose of 3 Gy radiation (right panel).

Microvascular density

Microvessels immunohistochemically detected using staining of endothelial cells for factor VIII-related antigen, showed a wide range of counts for different tumors, from 6 to 44 microvessels per field (Table 2.5).

After radiation MVD increased in 6 tumors and decreased in 8 tumors (Figure 2.41) with no correlation to changes in oxygen or other parameters investigated in this study.

Table 2.5. MVD for 14 tumors analyzed from biopsy sections taken before radiation and 24 hours after dose of 3Gy.

	VASCULAR DENSITY	
Dog #	Before	After
1	27	19
2	53	46
3	29	26
4	6	3
5	14	18
6	44	17
7	15	23
8	17	11
9	11	9
10	10	14
11	31	17
12	38	50
13	8	14
14	22	32

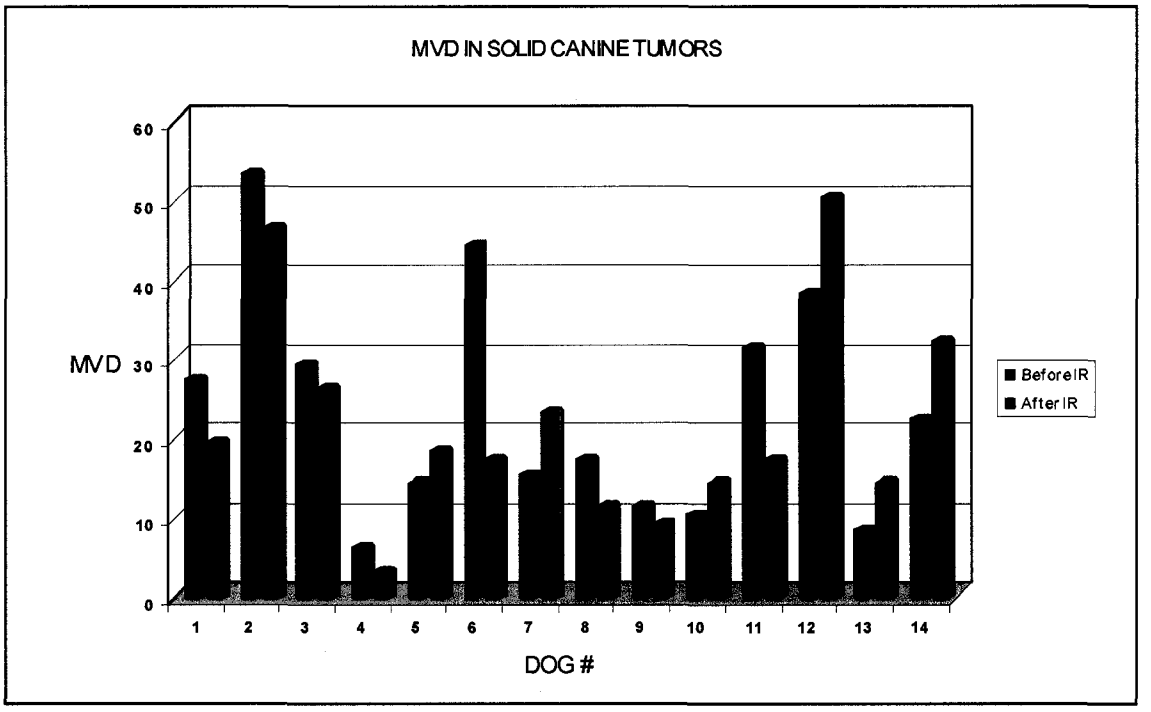

Figure 2.41. Microvessel density for each of 14 tumors showing values before (black), and 24 hours (red) after radiation.

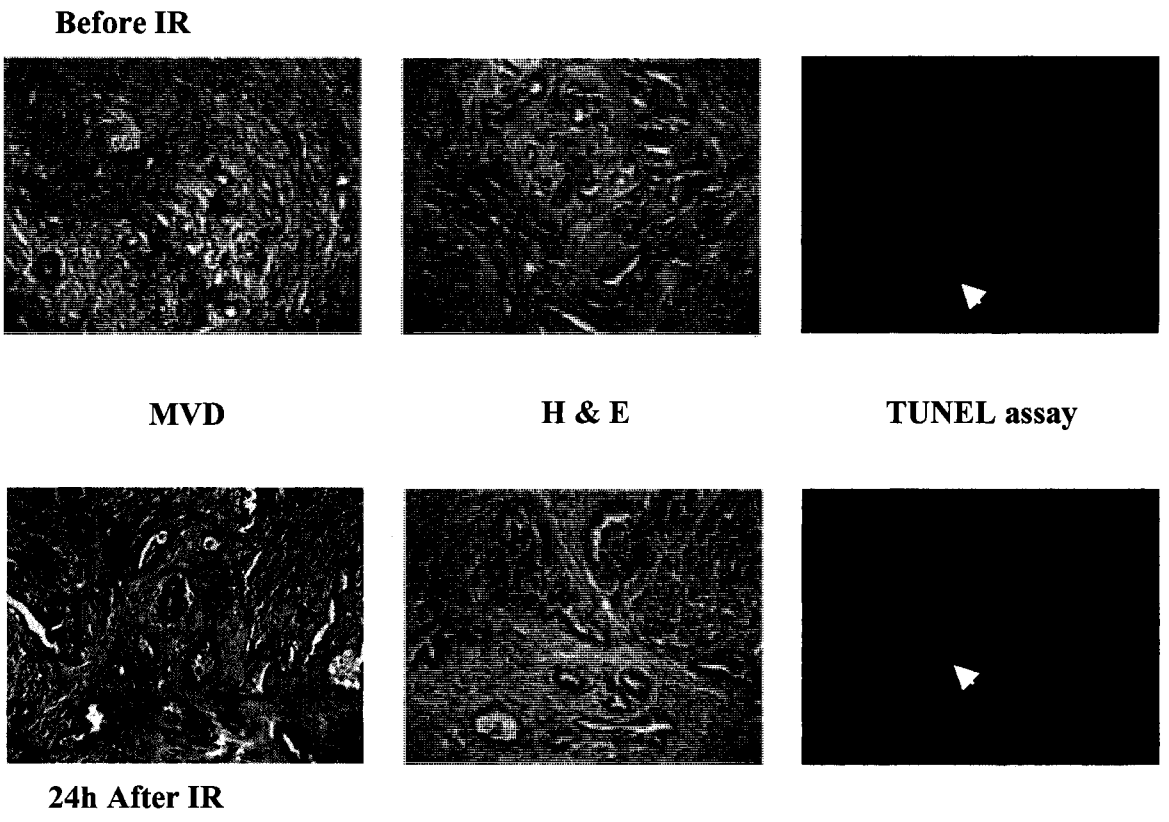

Figure 2.42. Immunohistochemical stainings in adenocarcinoma biopsy specimens pretreatment (upper panel), and 24 hours after irradiation (lower panel). Tumor sections were stained with anti-factor VIII related antibody for MVD quantification, H&E, and TUNEL as described in Materials and Methods.

Integrated Results

Statistical analysis integrating all parameters was provided with assistance from Dr. Annette Bachand and is included in this chapter with original tables, and summaries. As a summary of the study the table with all results for each tumor and each parameter included in this study is presented here (Table 2.6).

Table 2.6. Summary of all results for 14 dogs in the reoxygenation multiparameter study

	O	X	Y	G	E	N	pO2				LDF PERFUSION		CT/MRI PERFUSION		VASCULAR DENSITY		IFP Measurements		APOPTOSIS	
DOG #	Before meanO 2	After mean O2	Before median O2	After median O2	%<10 mmHg Before	%<10 mmHg After	%<5m mHg Before	%<5m mHg After	%<2.5 before	%<2.5 after	BPU before	BPU after	RPI before	RPI after	Before	After	Befoore	After	Before	After
1	2.2	12.3	0.5	0.1			88.1	62.1	86.2	61.1	101.88	73.63	0.050335	0.047402	27	19	8.8	4.99	12.2	39.7
2	7.2	2.8	0.6	2.4			63.8	86.4	63.4	84.5	50.37	42.22	0.037031	0.004243	53	46	0.26	0.37	4.3	8.5
3	8.7	38.9	6.8	37.8			77	0	76.5	0	27.12	8.11	0.370206	0.173572	29	26	3.37	1.56	4.5	17.8
4	21.9	28.1	22.3	26.9			0	0	0	0	495.41	288.71	0.181723	0.253197	6	3	-0.59	-3.41	3.4	10.1
5	19.4	10.9	21.5	11			5	16.3	0	16.7	191.74	227.5	0.032	-0.0336	14	18	-7.11	-7.21	18.9	19.6
6	30.5	21	32.1	14.8			8	39.1	2.5	35.9	214.18	128.93	14.26	8.21	44	17	-0.48	-0.53	6.5	13.5
7	19.5	13.3	17.8	15.4			0	19.6	0	15.8	92.47	193.85	11	-3.3477	15	23	1.02	0.9	10.9	11.39
8	9.2	23.2	0.4	14.2			52.6	0	51.5	0	97.12	136.9	23.72	-0.5478	17	11	1.03	0.34	4.2	13.8
9	22.2	25	23.2	25.5			0	0	0	0	132.8	94.7	21.04	16.813	11	9	1.58	-0.18	13.1	17
10	3.6	22.2	2.8	19.9			60.4	27.5	47.2	25.7	244.4	159.7	34.73	16.25	10	14	3.33	-0.68	13.3	16.5
11	18.6	27.7	20.9	26.1			30.1	6.4	26	4.5	204.81	N/A	9.52	7.68	31	17	9.83	3.85	6.7	22.3
12	17.1	13.1	18	12.7			0	18.9	0	17.2	123.63	422.46	9.33	4.18	38	50	-0.65	-7.45	4.9	16.2
13	10.6	29.6	8.1	34.3			45.5	8	36.6	4.5	340.03	235.99	16.34	9.38	8	14	8.6	0.63	8.5	9.8
14	7.2	31.2	1.8	31			53.5	0	55.3	0	119.44	132.08	24.31	20.42	22	32	1.8	10.45	7	12.1

Table 2.6 All mean and median pO_2 for 14 canine tumors, with percent measurements less than 10, 5, and 2,5 mmHg, microvascular perfusion estimates measured with laser Doppler flowmetry (LDF), and with dynamic contrast enhanced (DCE)computed tomography (CT) (first 5 dogs) and magnetic resonance imaging (MRI), microvessel density, interstitial fluid pressure (IFP), and apoptotic index before and after 3 Gy radiation. Red numbers in the oxygen measurements indicate increase in mean/median pO_2, and decrease in hypoxic fractions presented as percentages of measurements less than 10, 5, and 2,5 mmHg.

In Tables 2.7 through 2.16, statistical analyses are presented with interpretations and conclusions.

Table 2.7. Shapiro-Wilk test for normality p-value, paired t-test p-value, signed rank test p-value, and mean and Standard deviation of the difference between measurements taken after radiation and measurements taken prior to radiation – all 14 dogs.

Variable	Shapiro-Wilk p-value	Paired t-test p-value	Signed Rank test p-value	Mean	Std
post-pre O_2 mean	0.4891	0.0538	0.0701	7.24	12.78
post-pre O_2 median	0.5491	0.1105	0.1763	7.29	15.93
post-pre O_2 1st quartile	0.9291	0.2214	0.2749	4.89	14.23
post-pre O_2 3rd quartile	0.9996	0.0507	0.0676	10.23	17.78
post-pre % O_2 < 10 mmHg	0.3134	0.1579	0.2676	-15.3	38.08
post-pre % O_2 < 5 mmHg	0.3608	0.1350	0.0923	-14.8	34.83
post-pre % O_2 < 2.5 mmHg	0.4652	0.1713	0.1294	-12.8	33.09
post-pre perfusion (LDF)	0.1871	0.8461	0.5879	-6.60	120.0
post-pre perfusion (CT/MRI)	0.0045	0.0106	0.0009	-6.10	7.66
post-pre microvascular density	0.3626	0.5183	0.7964	-1.86	10.47
post-pre interstitial fluid pressure	0.0898	0.0963	0.0245	-1.94	4.05
post-pre % apoptosis	0.0281	0.0015	0.0001	7.85	7.33
ln (post-pre % apoptosis)	0.4788	0.0002	0.0012	1.57	1.17

Table 2.8. Shapiro-Wilk test for normality p-value, paired t-test p-value, signed rank test p-value, and mean and Standard deviation of the difference between measurements taken after radiation and measurements taken prior to radiation – 7 hypoxic dogs (median pO_2 before radiation <10mmHg)

Variable	Shapiro-Wilk p-value	Paired t-test p-value	Signed Rank test p-value	Mean	Std
post-pre O_2 mean	0.7484	0.0089	0.0313	15.93	11.08
post-pre O_2 median	0.4677	0.0177	0.0625	17.94	14.66
post-pre O_2 1st quartile	0.3315	0.0438	0.0625	12.26	12.74
post-pre O_2 3rd quartile	0.0494	0.0465	0.1094	19.57	20.71
post-pre % O_2 < 10 mmHg	0.3935	0.0192	0.0469	-40.8	33.98
post-pre % O_2 < 5 mmHg	0.5732	0.0203	0.0313	-38.1	32.22
post-pre % O_2 < 2.5 mmHg	0.7980	0.0267	0.0313	-34.4	31.20
post-pre perfusion (LDF)	0.6960	0.2065	0.2969	-27.4	51.18
post-pre perfusion (CT/MRI)	0.0503	0.0840	0.0156	-7.69	9.83
post-pre microvascular density	0.2847	0.8398	0.8438	-0.57	7.16
post-pre interstitial fluid pressure	0.3840	0.5112	0.3750	-1.36	5.16
post-pre % apoptosis	0.0716	0.0366	0.0156	9.17	9.06
ln (post-pre % apoptosis)	0.9945	0.0031	0.0156	1.81	1.00

Table 2.9. Shapiro-Wilk test for normality p-value, paired t-test p-value, signed rank test p-value, and mean and Standard deviation of the difference between measurements taken after radiation and measurements taken prior to radiation in 7 non-hypoxic dogs (median pO_2 before radiation ≥10mmHg)

Variable	Shapiro-Wilk p-value	Paired t-test p-value	Signed Rank test p-value	Mean	Std
post-pre O_2 mean	0.3588	0.6259	0.6250	-1.44	7.43
post-pre O_2 median	0.4849	0.3311	0.4688	-3.36	8.40
post-pre O_2 1st quartile	0.9643	0.6102	0.5781	-2.49	12.23
post-pre O_2 3rd quartile	0.6708	0.7569	0.8125	0.89	7.23
post-pre % O_2 < 10 mmHg	0.5489	0.2555	0.2188	10.27	21.62
post-pre % O_2 < 5 mmHg	0.6299	0.2605	0.4375	8.46	18.01
post-pre % O_2 < 2.5 mmHg	0.6235	0.2342	0.4375	8.80	17.61
post-pre perfusion (LDF)	0.9514	0.8130	1.0000	17.65	173.5
post-pre perfusion (CT/MRI)	0.1523	0.0526	0.0469	-4.52	4.96
post-pre microvascular density	0.5888	0.5604	0.8125	-3.14	13.50
post-pre interstitial fluid pressure	0.0860	0.0579	0.0156	-2.52	2.85
post-pre % apoptosis	0.5895	0.0203	0.0156	6.53	5.52
ln (post-pre % apoptosis)	0.1801	0.0403	0.0781	1.33	1.35

Summary:

In hypoxic dogs the mean, median, 1st and 3rd quartile of the pO_2 measurements increased significantly and the percentage of pO_2 measurements below 10 mmHg, 5 mmHg and 2.5 mmHg decreased significantly, but a similar trend was not observed in non-hypoxic dogs. In all dogs (hypoxic, non-hypoxic and combined) microvascular perfusion decreased significantly when microvascular perfusion was measured by CT/MRI but not when it was measured by LDF In all dogs (hypoxic, non-hypoxic and combined) microvascular

density did not change significantly. In all dogs (hypoxic, non-hypoxic and combined) interstitial fluid pressure decreased, but the decrease was not significant in hypoxic dogs. In all dogs (hypoxic, non-hypoxic and combined) percent apoptosis increased significantly.

	Variables	Pearson correlation coefficient	Pearson p-value	Spearman correlation coefficient	Spearman p-value
post-pre O_2 mean	post-pre perfusion (LDF)	-0.29330	0.3308	-0.19780	0.5171
	post- perfusion (CT/MRI)	-0.12304	0.6752	-0.09011	0.7593
	post-pre microvascular density	0.21014	0.4709	0.16520	0.5725
	post-pre IFP	0.04081	0.8898	-0.33626	0.2398
	post-pre % apoptosis	0.22957	0.4298	0.27473	0.3418
	ln (post-pre % apoptosis)	0.32657	0.2545	0.27473	0.3418
post-pre O_2 median	post-pre perfusion (LDF)	-0.22037	0.4694	-0.25860	0.3936
	post-pre perfusion (CT/MRI)	-0.12011	0.6825	-0.11881	0.6858
	post-pre microvascular density	0.35638	0.2111	0.14774	0.6142
	post-pre IFP	0.08529	0.7719	-0.22662	0.4359
	post-pre % apoptosis	0.00249	0.9932	0.12101	0.6803
	ln (post-pre % apoptosis)	0.11636	0.6920	0.12101	0.6803
post-pre O_2 1st quartile	post-pre perfusion (LDF)	-0.15327	0.6171	-0.23659	0.4364
	post-pre perfusion (CT/MRI)	0.05273	0.8579	-0.00440	0.9881
	post-pre microvascular density	0.28931	0.3157	0.06836	0.8164
	post-pre IFP	0.04966	0.8661	-0.22662	0.4359
	post-pre % apoptosis	0.14898	0.6112	0.21782	0.4544
	ln (post-pre % apoptosis)	0.21261	0.4655	0.21782	0.4544
post-pre O_2 3rd quartile	post-pre perfusion (LDF)	-0.29740	0.3237	-0.31319	0.2974
	post-pre perfusion (CT/MRI)	-0.21310	0.4645	-0.20000	0.4930
	post-pre microvascular density	0.06819	0.8168	0.00881	0.9762
	post-pre IFP	-0.04414	0.8809	-0.29670	0.3030
	post-pre % apoptosis	0.31071	0.2796	0.33187	0.2464
	ln (post-pre % apoptosis)	0.37650	0.1846	0.33187	0.2464
pre perfusion (LDF)	pre perfusion (CT/MRI)	0.03564	0.9037	0.21319	0.4643
post perfusion (LDF)	post perfusion (CT/MRI)	-0.05481	0.8588	0.01099	0.9716

	Variables	Pearson correlation coefficient	Pearson p-value	Spearman correlation coefficient	Spearman p-value
post-pre O_2 mean	post-pre perfusion (LDF)	-0.13566	0.7718	-0.10714	0.8192
	post-pre perfusion (CT/MRI)	-0.08792	0.8513	-0.25000	0.5887
	post-pre microvascular density	0.56200	0.1892	0.75000	0.0522
	post-pre IFP	0.08776	0.8516	-0.07143	0.8790
	post-pre % apoptosis	-0.03433	0.9418	-0.03571	0.9394
	ln (post-pre % apoptosis)	0.01710	0.9710	-0.03571	0.9394
post-pre O_2 median	post-pre perfusion (LDF)	-0.15559	0.7391	-0.07207	0.8780
	post-pre perfusion (CT/MRI)	0.00799	0.9864	-0.27028	0.5577
	post-pre microvascular density	0.64014	0.1215	0.77481	0.0408
	post-pre IFP	0.11970	0.7982	-0.01802	0.9694
	post-pre % apoptosis	-0.34906	0.4428	-0.10811	0.8175
	ln (post-pre % apoptosis)	-0.26852	0.5604	-0.10811	0.8175
post-pre O_2 1st quartile	post-pre perfusion (LDF)	0.10289	0.8263	0.10811	0.8175
	post-pre perfusion (CT/MRI)	0.19526	0.6748	-0.30632	0.5040
	post-pre microvascular density	0.40367	0.3692	0.70273	0.0782
	post-pre IFP	0.22970	0.6203	0.09009	0.8477
	post-pre % apoptosis	-0.14497	0.7565	0.00000	1.0000
	ln (post-pre % apoptosis)	-0.02576	0.9563	0.00000	1.0000
post-pre O_2 3rd quartile	post-pre perfusion (LDF)	-0.16105	0.7301	0.00000	1.0000
	post-pre perfusion (CT/MRI)	-0.25324	0.5837	-0.42857	0.3374
	post-pre microvascular density	0.36804	0.4166	0.53571	0.2152
	post-pre interstitial fluid pressure	-0.09667	0.8367	-0.07143	0.8790
	post-pre % apoptosis	0.17227	0.7119	0.07143	0.8790
	ln (post-pre % apoptosis)	0.18666	0.6886	0.07143	0.8790
pre perfusion (LDF)	pre microvascular perfusion (CT/MRI)	0.55729	0.1937	0.57143	0.1802
post perfusion (LDF)	post microvascular perfusion (CT/MRI)	0.55644	0.1945	0.32143	0.4821

	Variables	Pearson correlation coefficient	Pearson p-value	Spearman correlation coefficient	Spearman p-value
post-pre O_2 mean	post-pre perfusion (LDF)	-0.42967	0.3952	-0.20000	0.7040
	post-pre perfusion (CT/MRI)	0.42441	0.3426	0.50000	0.2532
	post-pre microvascular density	-0.09710	0.8359	-0.10714	0.8192
	post-pre IFP	-0.57471	0.1771	-0.78571	0.0362
	post-pre % apoptosis	0.56758	0.1838	0.42857	0.3374
	ln (post-pre % apoptosis)	0.55325	0.1977	0.42857	0.3374
post-pre O_2 median	post-pre perfusion (LDF)	-0.17530	0.7397	-0.25714	0.6228
	post-pre perfusion (CT/MRI)	0.15667	0.7373	0.42857	0.3374
	post-pre microvascular density	0.26113	0.5716	-0.14286	0.7599
	post-pre IFP	-0.48098	0.2745	-0.64286	0.1194
	post-pre % apoptosis	0.30444	0.5068	0.25000	0.5887
	ln (post-pre % apoptosis)	0.23998	0.6042	0.25000	0.5887
post-pre O_2 1st quartile	post-pre perfusion (LDF)	-0.11465	0.8288	-0.25714	0.6228
	post-pre perfusion (CT/MRI)	0.25210	0.5855	0.42857	0.3374
	post-pre microvascular density	0.20839	0.6539	-0.14286	0.7599
	post-pre IFP	-0.54117	0.2097	-0.64286	0.1194
	post-pre % apoptosis	0.41012	0.3608	0.25000	0.5887
	ln (post-pre % apoptosis)	0.23571	0.6109	0.25000	0.5887
post-pre O_2 3rd quartile	post-pre perfusion (LDF)	-0.67128	0.1443	-0.77143	0.0724
	post-pre perfusion (CT/MRI)	0.64918	0.1146	0.53571	0.2152
	post-pre microvascular density	-0.56464	0.1866	-0.67857	0.0938
	post-pre IFP	-0.44502	0.3170	-0.42857	0.3374
	post-pre % apoptosis	0.66766	0.1012	0.67857	0.0938
	ln (post-pre % apoptosis)	0.80674	0.0283	0.67857	0.0938
pre perfusion (LDF)	pre perfusion (CT/MRI)	-0.58323	0.1693	-0.21429	0.6445
post perfusion (LDF)	post perfusion (CT/MRI)	-0.47717	0.3386	-0.42857	0.3965

Summary:

In all dogs (hypoxic, non-hypoxic and combined) no consistent statistically significant correlations were observed between changes in tumor pO_2 levels (mean, median, 1st or 3rd quartile) and changes in microvascular perfusion, microvascular density, interstitial fluid pressure or percent apoptosis.

While in hypoxic dogs the association between changes in tumor pO_2 levels (mean, median and 1st quartile) and changes in microvascular density was borderline significant based on the Spearman correlation coefficients, it was not significant based on the Pearson correlation coefficients.

While in non-hypoxic dogs the association between changes in mean tumor pO_2 levels and changes in interstitial fluid pressure was significant based on the Spearman correlation coefficient, it was not significant based on the Pearson correlation coefficient. Furthermore, no significant association was observed between changes in interstitial fluid pressure and changes in median, 1st quartile or 3rd quartile tumor pO_2 levels.

While in non-hypoxic dogs, the associations between changes in the 3rd quartile of tumor pO_2 levels and several other variables were significant at the 0.1 level based on the Spearman correlation coefficient, all but one of these associations were not significant based on the Pearson correlation coefficient. There were no statistically significant corresponding associations observed when changes in the mean, median or 1st quartile of tumor pO_2 levels were considered.

In all dogs (hypoxic, non-hypoxic and combined) no significant correlation was observed between before and after microvascular perfusion measured by LDF and measured by CT/MRI.

To further explore whether there was an association between changes in tumor pO_2 levels and changes in microvascular perfusion, microvascular density, interstitial fluid pressure and percent apoptosis, all variables were dichotomized. The cutpoints (table 2.14) were determined based on the data shown in table 2.13.

Table 2.13. Changes in mean and median tumor pO_2 levels and changes in microvascular perfusion, microvascular density, interstitial fluid pressure and percent apoptosis for all 14 dogs

id	post-pre O_2 mean	post-pre O_2 median	post-pre perfusion (LDF)	post-pre perfusion (CT/MRI)	post-pre microvascular density	post-pre IFP	post-pre % apoptosis
1	10.1	0.0	-28.25	-0.0029	-8	-3.81	27.50
2	-4.4	0.0	-8.15	-0.0328	-7	0.11	4.20
3	30.2	37.8	-19.01	-0.1966	-3	-1.81	13.30
4	6.2	4.6	-206.70	0.0715	-3	-2.82	6.70
5	-8.5	-10.8	35.76	-0.0656	4	-0.10	0.70
6	-9.5	-17.3	-85.25	-6.0500	-27	-0.05	7.00
7	-6.2	-2.2	101.38	-14.3477	8	-0.12	0.49
8	14.0	13.8	39.78	-24.2678	-6	-0.69	9.60
9	2.8	2.3	-38.10	-4.2270	-2	-1.76	3.90
10	18.6	16.6	-84.70	-18.4800	4	-4.01	3.20
11	9.1	5.2	.	-1.8400	-14	-5.98	15.60
12	-4.0	-5.3	298.83	-5.1500	12	-6.80	11.30
13	19.0	28.2	-104.04	-6.9600	6	-7.97	1.30
14	24.0	29.2	12.64	-3.8900	10	8.65	5.10

Table 2.14. Cutpoints for dichotomizing the change in O_2 levels, microvascular perfusion, microvascular density, interstitial fluid pressure and percent apoptosis variables

Variable	0 if	1 if
post-pre O_2 mean	≤0	>0
post-pre O_2 median	≤0	>0
post-pre microvascular perfusion (LDF)	≤0	>0
post-pre microvascular perfusion (CT/MRI)	≤ -0.2	> -0.2
post-pre microvascular density	≤0	>0
post-pre interstitial fluid pressure	≤ -0.2	> -0.2
post-pre % apoptosis	≤ 1.5	> 1.5

Table 2.15. Observed and expected number of observations and Chi Square test and Fisher's Exact test p-values for the change in mean pO_2 vs. the change in microvascular perfusion, microvascular density, interstitial fluid pressure and percent apoptosis for all 14 dogs

post-pre O_2 mean		Obs	Exp	Obs	Exp	Chi Square test p-value	Fisher's Exact Test p-value
	post-pre microvascular perfusion (LDF)	*0*		*1*		0.2070	0.2929
0		2	3.07692	3	1.92308		
1		6	4.92308	2	3.07692		
	post-pre microvascular perfusion (CT/MRI)	*0*		*1*		0.8030	1.0000
0		3	3.21429	2	1.78571		
1		6	5.78571	3	3.21429		
	post-pre microvascular density	*0*		*1*		0.3340	0.5804
0		2	2.85714	3	2.14286		
1		6	5.14286	3	3.85714		
	post-pre interstitial fluid pressure	*0*		*1*		0.0099	0.0230
0		1	3.21429	4	1.78571		
1		8	5.78571	1	3.21429		
	post-pre % apoptosis	*0*		*1*		0.2069	0.5055
0		2	1.07143	3	3.92857		
1		1	1.92857	8	7.07143		

Table 2.16. Observed and expected number of observations and Chi Square test and Fisher's Exact test p-values for the change in median pO_2 vs. the change in microvascular perfusion, microvascular density, interstitial fluid pressure and percent apoptosis for all 14 dogs

post-pre O_2 median		Obs	Exp	Obs	Exp	Chi Square test p-value	Fisher's Exact Test p-value
	post-pre microvascular perfusion (LDF)	*0*		*1*		0.4285	0.5921
0		3	3.69231	3	2.30769		
1		5	4.30769	2	2.69231		
	post-pre microvascular perfusion (CT/MRI)	*0*		*1*		0.3340	0.5804
0		3	3.85714	3	2.14286		
1		6	5.14286	2	2.85714		
	post-pre microvascular density	*0*		*1*		0.6400	1.0000
0		3	3.42857	3	2.57143		
1		5	4.57143	3	3.42857		
	post-pre interstitial fluid pressure	*0*		*1*		0.0363	0.0909
0		2	3.85714	4	2.14286		
1		7	5.14286	1	2.85714		
	post-pre % apoptosis	*0*		*1*		0.3472	0.5385
0		2	1.28571	4	4.71429		
1		1	1.71429	7	6.28571		

Summary

There was evidence of a statistically significant association between the change in mean tumor pO_2 levels (≤ 0 vs. >0) and the change in interstitial fluid pressure (≤ -0.2 vs. > -0.2), and there was evidence of a statistically significant association between the change in median tumor pO_2 levels (≤ 0 vs. >0) and the change in interstitial fluid pressure (≤ -0.2 vs. > -0.2).

Among dogs with a post-pre mean $pO_2 \leq 0$, fewer than expected (based on an assumption of independence) experienced a change in interstitial fluid pressure of ≤ -0.2 and more than expected experienced a change in interstitial fluid pressure of > -0.2.

Among dogs with post-pre pO_2 mean >0, more than expected (based on an assumption of independence) experienced a change in interstitial fluid pressure of ≤ -0.2 and fewer than expected experienced a change in interstitial fluid pressure of > -0.2.

Results for the change in median pO_2 levels were similar.

In other words, dogs that experienced an increase in mean (median) tumor pO_2 levels had an increased likelihood of experiencing a decrease of more than 0.2 in interstitial fluid pressure, whereas dogs who experienced a decrease in mean (median) tumor pO_2 levels had a decreased likelihood of experiencing a decrease of more than 0.2 in interstitial fluid pressure.

DISCUSSION

Changes in partial pressure of oxygen (pO_2) of canine tumors following a fraction of radiation were evaluated. These tumors were heterogeneous, and the initial oxygen levels in the tumors as well as the changes post-radiation varied but there were two general patterns. Hypoxic tumors became better oxygenated, while well oxygenated tumors did not change out of normoxic range. These changes were analyzed in relation with changes in interstitial fluid pressure, microvascular perfusion, frequency of apoptosis, and microvessel density. Multiparameter analysis was used to try to elucidate underlying mechanisms of tumor reoxygenation. Different tumor microenvironmental

parameters did not interact as hypothesized prior the study. The only evident relationship was the inverse correlation between values of oxygen levels and interstitial fluid pressures.

Oxygen tension

The pO_2 was increased 24 hours after 3 Gy in 9 tumors, and decreased in 5 tumors. More importantly, oxygen levels increased in hypoxic tumors, and only in 1 hypoxic tumor pO_2 decreased (#2, soft tissue sarcoma). All tumors that reoxygenated in our study had a significantly decreased fraction of pO_2 measurements below 10 mm Hg, 5 mm Hg, and 2.5 mm Hg, meaning that the hypoxic fraction of these tumors decreased after radiation. Changes in well oxygenated tumors were not relevant for the treatment outcome since after radiation the mean/median pO_2 in these tumors if decreased, did not decrease below 10 mm Hg. Similar observations have been reported in studies on human cervix tumors, breast tumors, head and neck tumors, and nonsmall cell lung tumors (Lyng et al, 2000; Pappova et al, 1982; Lartigau et al, 1998; Lyng et al, 1999; Koh et al, 1995). As was reported in studies in human cervical tumors (Lyng et al, 2000; Dunst et al, 1999), hypoxic tumors may became better oxygenation during radiation therapy, whereas the oxygenation most often decreased in well-oxygenated tumors, similar to our results. Most of the studies of changes in oxygenation status are reporting different doses used, different tumor models, different time points of measurements. All this makes it very difficult to compare results from all these different studies and to make general conclusions about tumor microenvironment behavior following irradiation. In human tumors measurements were made during fractionated radiation therapy after two weeks of

radiation therapy (Lartigau et al, 1998; Gabalski et al, 1998; Lyng et al, 2000), after four weeks of radiation (Fyles et al, 1998; Cooper et al, 1999), or at the end of the treatment. A benefit of the spontaneous tumor model in dogs allowed me to look at oxygen levels at a time point that may be more relevant.

There is evidence that the reoxygenation of tumors occurs 24-72 hours after irradiation (Vaupel et al, 1984; Kallman et al, 1986; Koutcher et al, 1992; Goda et al, 1995; Znati et al, 1996; Bussink et al, 2000). This is closer to the time point we chose in our study. However, most of these studies obtained data after single high irradiation dose and in experimental animal tumors. Some studies that reported oxygen changes up to 24 hours following clinically relevant dose (2 Gy) were also in experimental murine tumors that are not heterogeneous as naturally developing tumors in. Nevertheless, some studies reported no significant change in pO_2 post-radiation in regard to pre-treatment values (Fyles et al, 1998) or decrease in the overall oxygenation of the tumors after radiation treatment (Gabalski et al, 1998; Achermann et al, 2004).

The discrepancy between findings of the different studies may have a number of reasons. The timing of the post-radiation measurement may be important, as well as the fractionation scheme used. Another contribution to the differences in these findings may be measurement related, consisting of intratumor heterogeneity, measurement method and operator variability.

I investigated the changes of oxygenation level and other relevant microenvironmental parameters in tumors following a fraction of radiation using a fraction size similar to those applied to human malignancies. I chose to look after a single time point to focus on the underlying mechanisms of reoxygenation. Changes of oxygen levels after single dose

of fractionated treatment are of relevance for the eventual manipulation in subsequent fractionation scheduling. Our findings are in agreement with earlier reported observations that these changes vary among different tumors (even same type tumors) and the extent of the reoxygenation is different.

Interstitial fluid pressure

Interstitial fluid pressure in this study was shown to decrease in most tumors after irradiation. It decreased in 9 out of 14 tumors. In 4 tumors it did not change more then 0.2 mm Hg, and in one tumor IFP increased after irradiation. A significant inverse correlation existed between changes in IFP and changes in oxygen levels in tumors after irradiation. This was the only significant relationship among microenvironmental parameters in this study. We did not see a relationship between the other parameters and IFP in this study. This may be due to the large number of factors that play a role in tumor IFP such as capillary pressure, the resistance of fluid leakage across the capillary walls, and the resistance of fluid percolation through the interstitium (Milosevic et al, 1999; Baxter et al, 1989; Tufto et al, 1999).

An inverse relation between tumor IFP and oxygenation was first suggested based on measurements taken in three patients with cervical carcinoma (Roh et al, 1991). A later study with a much larger population of patients (77 cervical carcinoma patients) demonstrated an inverse association between these parameters (Milosevic et al, 1998). However, with further increase of the number of patients in the study, the strength of this association diminished, but this study was the first to demonstrate a strong independent prognostic effect of IFP (Milosevic et al, 2001). Studies of IFP and the oxygenation in

animal tumors have similarly failed to show a correlation between them (Boucher et al, 1995; Tufto et al, 1996; Znati et al, 1996).

Our study demonstrated moderate negative correlation between the changes in pO_2 and the changes in the IFP in solid canine tumors after single dose of radiation. Considering the size of our patient population and reviewing studies previously mentioned here, it may be necessary to obtain more data for more conclusive demonstration of the pO_2-IFP relationship we found here.

It was reported from work with human tumor xenografts in mice (Znati et al, 1996), that irradiation with doses smaller than 10 Gy (delivered in 2.5 and 5 Gy fractions) did not affect the IFP of the tumor. The association between IFP and pO_2 is presumed to be due to changes in tumor blood flow and oxygen delivery (Jain et al, 1988; Boucher et al, 1992). It is also possible that IFP provides information about tumor physiology that is unrelated to perfusion (Milosevic et al, 2001). Some of the characteristics of tumors that lead to elevated IFP include abnormal vessel structure and organization, and high vascular permeability. My study found that perfusion actually decreased in most tumors after irradiation, and that decreased IFP and increased oxygenation were not related to increase of perfusion. A possible explanation may be a change of vascular permeability. Decrease in vascular permeability consequently could increase transvascular resistance, which would decrease the amount of fluid entering the interstitium. Understanding how tumor vasculature responds to irradiation seems important for understanding the relationship between IFP and tumor vasculature. It has been demonstrated recently that irradiation induces secretion of VEGF, a potent angiogenic protein, and that VEGF

enhances endothelial cell radioresistance, protecting tumors from radiation damage by minimizing vascular damage (Gorski et al, 1999; Moeller et al, 2004).

Tumor microvascular perfusion

Two different techniques used to estimate perfusion in each tumor, LDF and DCE (CT/MRI), did not show the same pattern of changes in perfusion in irradiated tumors. More uniform findings were obtained from dynamic contrast enhancement techniques: in 13 out of 14 tumors, they indicated decreased perfusion 24 hours after irradiation. Data obtained from LDF were different: 8 out of 13 tumors showed decreased perfusion post-radiation. In one of the tumors post-radiation data were not obtained (dog #11).

For the dogs #7, 8, and 9, individual RPI graphs could not be obtained. This is because there were motion artifacts on either the pre or post-radiation MRI scan, making it invalid to calculate RPI measurements for individual ROI's. The ROI's at the edges of those tumors could not be compared due to excess motion. Instead, Dr. Kraft calculated RPI for a central tumor ROI, which was a similar tissue region before and after irradiation. Those are the RPI numbers included in the results table (Table 2.3) and for those three dogs the average RPIs are included in the Figure 2.35.

The data obtained from LDF were difficult to present and analyze. There were numerous out of range values caused by both movement of the patient and movement of the probe during sampling. Most of the data reported in the literature was generated from stationary measurements (Lan et al, 2000; Thews et al, 2002) utilizing a constant probe location. A laser is used as the stable source of light in these instruments so that Doppler shift (i.e. the frequency change that light undergoes when reflected by object in motion, such as red

blood cells) could be utilized. We used a combined pO_2/ temperature/ LDF probe and in order to record tumor spatial heterogeneity, we moved the probe along the track of measurements. There were measurement artifacts as a result of the probe movements that manifested in the sudden changes of the total backscattered light. I excluded those values from the final evaluation. When that happens in a few instances during the recording it did not change the outcome of the evaluation of the measurements. We had probe withdrawn each 5 seconds for 0.2mm, and removing many of the spikes in flow signal, compromised the accuracy of the LDF tumor perfusion estimate.

Non-invasive tumor perfusion measurements by DCE-CT have been reported in studies in head and neck squamous cell carcinoma in human patients (Hermans et al, 1997, 1999; Brix et al, 1999), and in canine nasal tumors (Van Camp et al, 2000). They proved that CT-determined perfusion measurements are feasible; the procedure is safe and easy to perform. Studies using Gd-DTPA as MRI contrast agent in experimental murine tumors demonstrated the sensitivity of the DCE-MRI technique and its capability of providing estimates of blood perfusion in normal and tumor tissues (Belfi et al, 1992, 1994). Results were reported from the studies with experimental animal models (Bjornaes et al, 2000; Bhujwalla et al, 2001, 2003; Crokart et al, 2005) and DCE-MRI measurements of cervical tumors of human patients (Lyng et al, 2001; Haider et al, 2007).These studies show a spatial-temporal heterogeneity of perfusion in tumors, consistent with chaotic vascular architecture.

Our finding of decreased tumor perfusion did not support our hypothesis that reoxygenation occurs due to increased microvascular perfusion and reopening of collapsed vessels post-radiation. This finding was in agreement with recently reported

results from the study of the effect of irradiation of single 10 Gy dose in experimental tumors in mice using perfusion markers (Bussink et al, 2000; Fenton et al, 2001). In a study utilizing irradiation with 2 Gy dose in experimental tumors assessing tumor perfusion with LDF and DCE-MRI (Crokart et al, 2005) measurements were made 4 hours after irradiation and showed increased pO_2, which remained elevated for at least 24 hours, and increased tumor perfusion at 4 hours. Bussink also reported an early increase in perfused blood vessels at 2-7 hours after irradiation) followed by significant decrease, with a minimum value at 26 hours after irradiation. The decrease in tumor blood perfusion has been attributed to radiation-induced edema, thrombosis (Falkvoll, 1990), and an increase in damaged capillaries as a direct effect of irradiation (Goda et al, 1996). Other investigators have suggested that increases in tumor blood flow might be responsible for reoxygenation (Kallman, 1972; Brown, 1979; Rofstad, 1989). Some authors tried to explain reoxygenation, depending on time after radiation it occurred, to be due to acutely or due to chronically hypoxic cells. In the SCCVII murine tumor reoxygenation was found to be very rapid (within the first 6 hours after a13 Gy radiation). Tumor perfusion increased and was explained by a temporary decrease in perfusion-limited acute hypoxia (Olive, 1994; Kim et al, 1994). Rapid reoxygenation has been believed to be due to acutely hypoxic cells and slow reoxygenation due to chronically hypoxic cells (Brown, 1979; Coleman, 1988). Reoxygenation in C3H mouse mammary carcinoma occurred about 12 hours after a large dose of irradiation and was reported as a slow reoxygenation of the chronic hypoxic population (Horsman et al, 1995).

Apoptosis

Our study found increased levels of apoptosis in all irradiated tumors. These changes in levels of apoptosis were not correlated to any other parameters in the study. We also demonstrated that cell loss due to apoptosis was significant early after radiation, since the apoptotic index was higher at 6 hours post-radiation than at 24 hours.

It has been suggested that the elimination of tumor cells by radiation-induced apoptosis can result in tumor reoxygenation. This has been identified in animal models (Meyn et al, 1993; Milas et al, 1995; Rupnow et al, 1998). It was proposed that tumor shrinkage caused by apoptosis would relieve pressure on blood vessels and reduce the level of intermittent hypoxia. However, in the study with human squamous cell carcinoma of the cervix (Sheridan et al, 2000) no relationship was found between tumor shrinkage and the level of pretreatment apoptosis or the change in oxygenation during radiation therapy. Since it has been shown that a reduction in IFP can lead to increased tumor oxygenation (Milosevic et al, 1998), Sheridan et al. hypothesized that reoxygenation may be due to reduced IFP as a result of cell loss via apoptosis. This may relieve pressure on vessels, increase blood flow, and oxygen delivery, without affecting tumor size, which may correlate to our study.

Microvessel density

The change in vascular density did not have significance in the relation with any of tumor microenvironmental parameters, including oxygenation of tumors. MVD was increased in 6 and decreased in 8 tumors post-radiation. Previously reported results are not indicating the importance of the MVD changes in tumor reoxygenation. As shown by

Hittmair and coworkers (Hittmair et al, 1994) radiation therapy caused decreased cell density, while vascular density remained unchanged. The changes in oxygenation during radiation therapy of human breast cancer (Papova et al, 1982) and non-small cell lung cancer (Koh et al, 1995) coincided also with changes in cell density, but were not related to changes in MVD. Radiation-induced changes in the functionality of capillaries may occur (Brown, 1979; Dewhirst et al, 1990), leading to tumor perfusion changes independent of changes in vascular density (Lyng et al, 1999). Lyng et al. also reported no change in vascular density during radiation therapy in human uterine cervical cancer (Lyng et al, 2000).

Mechanisms of the changes in oxygenation

Changes in tumor oxygenation are reported to occur due to changes in the oxygen supply and/or oxygen consumption (Gulledge and Dewhirst, 1996). This study did not answer the question of the mechanisms of the tumor reoxygenation. Increased apoptosis was seen in the reoxygenated tumors, but also in the ones that did not have increased oxygen level after irradiation. If apoptosis played any role in the reoxygenation it was not the main cause for it. Microvessel density may not be associated with early change of oxygenation. The role of the microvascular perfusion is not clear. It could be possible that much earlier post-radiation perfusion increased and reoxygenated tumor tissue, which stayed oxygenated up to 24 hour point of our measurement. A possible explanation may be that the increased blood flow and oxygen supply are due to apoptosis and decreased IFP, but irradiation-damaged vessels are unable to deliver to the tumor tissue. It is important to understand that blood flow is blood movement through the vessels, and

perfusion is a delivery of the blood (with oxygen and nutrients) from the vessels to the mass of tissue in time. Thus the perfusion depends not only on blood flow, but also on the other factors such as resistance to flow through the vessel, pressure difference across its length, viscosity of the blood (Poiseuille's law for the flow of the liquids in tubes), vascular permeability, and pressure gradients between intra-vascular and extra-vascular spaces.

Some factors that we did not include in our study have been investigated by others. The occurrence of an inflammatory process has been reported to occur rapidly after irradiation, causing an increase in blood flow by vasorelaxation (el- Ghazaly et al, 1985; Moore et al, 2004). In their study Crokart et al. (2005) used an anti-inflammatory agent, and found a significant decrease in the level of tumor oxygenation 4 h after irradiation. They also found a significant decrease in the oxygen consumption rate, due to cell loss and reduced oxygen metabolism. 35 years ago, Kallman (1972) pointed out that decreased oxygen consumption by tumor cells allows for improved oxygenation even in the absence of increased perfusion. Decreased oxygen consumption was shown in the study by Olive et al. (1994), and suggested by many investigators as one of the factors playing role in the tumor reoxygenation (Secomb et al, 1995; Bussink et al, 2000). These are the parameters that have been investigated in relation to oxygen changes post-radiation: inflammation, oxygen consumption, and bioenergetic and metabolic status in tumor (distribution of ATP, lactate, and glucose (Thews et al, 1999)). They also may play a role in the changes in tumor microenvironment, and could be considered for some future multiparameter reoxygenation studies.

For the improvement of this study I would propose a better patients selection in regard to tumor location. We have learned that thoracic wall tumors were difficult to analyze by DCE-MRI. There was large movement of the thorax due to respiration, and consequently motion artifacts. For microvascular perfusion estimates I would choose DCE techniques. Even though there is now available artifact rejection technology from the Oxford Optronix, whose laser Doppler flowmetry equipment we use, my experience with constantly moving probes does not promise much more reliable LDF results. Since changes in MVD did not influence oxygenation status in tumors 24 hours post-radiation, as well as apoptosis was not related to changes in oxygenation, evaluation of these parameters could be omitted in eventual future study. I would more carefully evaluate a standardization of repeated procedures: precise localization and guidance of probe placements. Sampling in the same tumor region is a very important factor to overcome tumor heterogeneity since difference in the measurements may occur between very small intratumoral distances. I would like to include non-invasive techniques for assessment of tumor pH and tumor bioenergetic status by magnetic resonance spectroscopy (^{31}P-MRS, phosphorus MRS).

It is important to incorporate a combination of parameters to adequately describe the mechanisms underlying the changes in tumor after irradiation, since all parameters of the tumor microenvironment interact very closely and the change in one of them influences many other in this very complex system.

BIBLIOGRAPHY

1. Achermann RE, Ohlerth SM, Rohrer BC, Gassmann M, Inteeworn N, Roos M, Scharz M, Wergin MC, Kaser-Hotz B (2004) Oxygenation of spontaneous canine tumors during fractionated radiation therapy. *Strahlentherapie und Onkologie* 180: 297-305

2. Baxter LT, Jain RK (1989) Transport of fluid and macromolecules in tumors. I. Role of interstitial pressure and convection. [Review] [58 refs]. *Microvascular Research* 37: 77-104

3. Belfi CA, Ting LL, Hassenbusch SJ, Tefft M, Ngo FQ (1992) Determination of changes in tumor blood perfusion after hydralazine treatment by dynamic paramagnetic-enhanced magnetic resonance imaging. *International Journal of Radiation Oncology, Biology, Physics* 22: 477-482

4. Belfi CA, Paul CR, Shan S, Ngo FQ (1994) Comparison of the effects of hydralazine on tumor and normal tissue blood perfusion by MRI. *International Journal of Radiation Oncology, Biology, Physics* 29: 473-479

5. Bhujwalla ZM, Artemov D, Natarajan K, Ackerstaff E, Solaiyappan M (2001) Vascular differences detected by MRI for metastatic versus nonmetastatic breast and prostate cancer xenografts. *Neoplasia (New York)* 3: 143-153

6. Bhujwalla ZM, Artemov D, Natarajan K, Solaiyappan M, Kollars P, Kristjansen PE (2003) Reduction of vascular and permeable regions in solid tumors detected by macromolecular contrast magnetic resonance imaging after treatment with antiangiogenic agent TNP-470. *Clinical Cancer Research* 9: 355-362

7. Bjornaes I, Lyng H, Dahle GA, Kaalhus O, Rofstad EK (2000) Intratumor heterogeneity in perfusion in human melanoma xenografts measured by contrast-enhanced magnetic resonance imaging. *Magnetic Resonance Imaging* 18: 997-1002

8. Boucher Y, Lee I, Jain RK (1995) Lack of general correlation between interstitial fluid pressure and oxygen partial pressure in solid tumors. *Microvascular Research* 50: 175-182

9. Brix G, Bahner ML, Hoffmann U, Horvath A, Schreiber W (1999) Regional blood flow, capillary permeability, and compartmental volumes: measurement with dynamic CT--initial experience. *Radiology* 210: 269-276

10. Brizel DM, Sibley GS, Prosnitz LR, Scher RL, Dewhirst MW (1997) Tumor hypoxia adversely affects the prognosis of carcinoma of the head and neck. *International Journal of Radiation Oncology, Biology, Physics* 38: 285-289

11. Brizel DM, Dodge RK, Clough RW, Dewhirst MW (1999) Oxygenation of head and neck cancer: changes during radiotherapy and impact on treatment outcome. *Radiotherapy & Oncology* 53: 113-117

12. Brown JM (1979) Evidence for acutely hypoxic cells in mouse tumours, and a possible mechanism of reoxygenation. *British Journal of Radiology* 52: 650-656

13. Bussink J, Kaanders JH, Rijken PF, Raleigh JA, van der Kogel AJ (2000) Changes in blood perfusion and hypoxia after irradiation of a human squamous cell carcinoma xenograft tumor line. *Radiation Research* 153: 398-404

14. Coleman CN (1988) Hypoxia in tumors: a paradigm for the approach to biochemical and physiologic heterogeneity. [Review] [70 refs]. *Journal of the National Cancer Institute* 80: 310-317

15. Cooper RA, West CM, Logue JP, Davidson SE, Miller A, Roberts S, Statford IJ, Honess DJ, Hunter RD (1999) Changes in oxygenation during radiotherapy in carcinoma of the cervix. *International Journal of Radiation Oncology, Biology, Physics* 45: 119-126

16. Crokart N, Jordan BF, Baudelet C, Ansiaux R, Sonveaux P, Gregoire V, Beghein N, DeWever J, Bouzin C, Feron O, Gallez B (2005) Early reoxygenation in tumors after irradiation: determining factors and consequences for radiotherapy regimens using daily multiple fractions. *International Journal of Radiation Oncology, Biology, Physics* 63: 901-910

17. Dewhirst MW, Oliver R, Tso CY, Gustafson C, Secomb T, Gross JF (1990) Heterogeneity in tumor microvascular response to radiation. *International Journal of Radiation Oncology, Biology, Physics* 18: 559-568

18. Dunst J, Hansgen G, Lautenschlager C, Fuchsel G, Becker A (1999) Oxygenation of cervical cancers during radiotherapy and radiotherapy + cis-retinoic acid/interferon. *International Journal of Radiation Oncology, Biology, Physics* 43: 367-373

19. el Ghazaly M, Kenawy S, Khayyal MT, Roushdy H, Saleh S (1985) Effect of exposure to radiation on the inflammatory process and its influence by diclofenac. *British Journal of Pharmacology* 85: 45-50

20. Fadnes HO, Reed RK, Aukland K (1977) Interstitial fluid pressure in rats measured with a modified wick technique. *Microvascular Research* 14: 27-36

21. Falkvoll KH (1990) Histological study of the regrowth of a human melanoma xenograft exposed to single dose irradiation. *APMIS* 98: 758-764

22. Fenton BM, Lord EM, Paoni SF (2001) Effects of radiation on tumor intravascular oxygenation, vascular configuration, development of hypoxia, and clonogenic survival. *Radiation Research* 155: 360-368

23. Fyles AW, Milosevic M, Pintilie M, Hill RP (1998) Cervix cancer oxygenation measured following external radiation therapy. *International Journal of Radiation Oncology, Biology, Physics* 42: 751-753

24. Gabalski EC, Adam M, Pinto H, Brown JM, Bloch DA, Terris DJ (1998) Pretreatment and midtreatment measurement of oxygen tension levels in head and neck cancers. *Laryngoscope* 108: 1856-1860

25. Gatenby RA, Kessler HB, Rosenblum JS, Coia LR, Moldofsky PJ, Hartz WH, Broder GJ (1988) Oxygen distribution in squamous cell carcinoma metastases and its relationship to outcome of radiation therapy. *International Journal of Radiation Oncology, Biology, Physics* 14: 831-838

26. Goda F, O'Hara JA, Rhodes ES, Liu KJ, Dunn JF, Bacic G, Swartz HM (1995) Changes of oxygen tension in experimental tumors after a single dose of X-ray irradiation. *Cancer Research* 55: 2249-2252

27. Goda F, Bacic G, O'Hara JA, Gallez B, Swartz HM, Dunn JF (1996) The relationship between partial pressure of oxygen and perfusion in two murine tumors after X-ray irradiation: a combined gadopentetate dimeglumine dynamic magnetic resonance imaging and in vivo electron paramagnetic resonance oximetry study. *Cancer Research* 56: 3344-3349

28. Gorski DH, Beckett MA, Jaskowiak NT, Calvin DP, Mauceri HJ, Salloum RM, Seetharam S, Koons A, Hari DM, Kufe DW, Weichselbaum RR (1999) Blockage of the vascular endothelial growth factor stress response increases the antitumor effects of ionizing radiation. *Cancer Research* 59: 3374-3378

29. Gray L.H, Conger A.D., Ebert M., Hornsey S., Scott O.C. (1953) The concentration of oxygen dissolved in tissues at the time of irradiation as a factor in radiotherapy. *British Journal of Radiology* 26: 638-648

30. Gulledge CJ, Dewhirst MW (1996) Tumor oxygenation: a matter of supply and demand. [Review] [68 refs]. *Anticancer Research* 16: 741-749

31. Haider MA, Sitartchouk I, Roberts TP, Fyles A, Hashmi AT, Milosevic M (2007) Correlations between dynamic contrast-enhanced magnetic resonance imaging-derived measures of tumor microvasculature and interstitial fluid pressure in patients with cervical cancer. *Journal of Magnetic Resonance Imaging* 25: 153-159

32. Hall EJ (2000) *Radiobiology for the radiologist*. Lippincott: Philadelphia

33. Hermans R, Lambin P, Van den BW, Haustermans K, Van der GA, Baert AL (1997) Non-invasive tumour perfusion measurement by dynamic CT: preliminary results. *Radiotherapy & Oncology* 44: 159-162

34. Hermans R, Lambin P, Van der GA, Van den BW, Verbist B, Weltens C, Delaere PR (1999) Tumoural perfusion as measured by dynamic computed tomography in head and neck carcinoma. *Radiotherapy & Oncology* 53: 105-111

35. Hittmair K, Gomiscek G, Langenberger K, Recht M, Imhof H, Kramer J (1994) Method for the quantitative assessment of contrast agent uptake in dynamic contrast-enhanced MRI. *Magnetic Resonance in Medicine* 31: 567-571

36. Hockel M, Knoop C, Schlenger K, Vorndran B, Baussmann E, Mitze M, Knapstein PG, Vaupel P (1993) Intratumoral pO2 predicts survival in advanced cancer of the uterine cervix. *Radiotherapy & Oncology* 26: 45-50

37. Horsman MR, Grau C, Overgaard J (1995) Reoxygenation in a C3H mouse mammary carcinoma. The importance of chronic rather than acute hypoxia. *Acta Oncologica* 34: 325-328

38. Kallman RF (1972) The phenomenon of reoxygenation and its implications for fractionated radiotherapy. *Radiology* 105: 135-142

39. Kallman RF, Dorie MJ (1986) Tumor oxygenation and reoxygenation during radiation therapy: their importance in predicting tumor response. *International Journal of Radiation Oncology, Biology, Physics* 12: 681-685

40. Kim IH, Brown JM (1994) Reoxygenation and rehypoxiation in the SCCVII mouse tumor.[see comment]. *International Journal of Radiation Oncology, Biology, Physics* 29: 493-497

41. Kitakabu Y, Shibamoto Y, Sasai K, Ono K, Abe M (1991) Variations of the hypoxic fraction in the SCC VII tumors after single dose and during fractionated radiation therapy: assessment without anesthesia or physical restraint of mice. *International Journal of Radiation Oncology, Biology, Physics* 20: 709-714

42. Koh WJ, Bergman KS, Rasey JS, Peterson LM, Evans ML, Graham MM, Grierson JR, Lindsley KL, Lewellen TK, Krohn KA (1995) Evaluation of oxygenation status during fractionated radiotherapy in human nonsmall cell lung cancers using [F-18]fluoromisonidazole positron emission tomography. *International Journal of Radiation Oncology, Biology, Physics* 33: 391-398

43. Koutcher JA, Alfieri AA, Devitt ML, Rhee JG, Kornblith AB, Mahmood U, Merchant TE, Cowburn D (1992) Quantitative changes in tumor metabolism, partial pressure of oxygen, and radiobiological oxygenation status postradiation. *Cancer Research* 52: 4620-4627

44. Lan J, Hunter CJ, Murata T, Power GG (2000) Adaptation of laser-Doppler flowmetry to measure cerebral blood flow in the fetal sheep. *Journal of Applied Physiology* 89: 1065-1071

45. Lartigau E, Lusinchi A, Weeger P, Wibault P, Luboinski B, Eschwege F, Guichard M (1998) Variations in tumour oxygen tension (pO2) during accelerated radiotherapy of head and neck carcinoma.[see comment]. *European Journal of Cancer* 34: 856-861

46. Lyng H, Tanum G, Evensen JF, Rofstad EK (1999) Changes in oxygen tension during radiotherapy of head and neck tumours. *Acta Oncologica* 38: 1037-1042

47. Lyng H, Sundfor K, Rofstad EK (2000) Changes in tumor oxygen tension during radiotherapy of uterine cervical cancer: relationships to changes in vascular density, cell density, and frequency of mitosis and apoptosis.[see comment]. *International Journal of Radiation Oncology, Biology, Physics* 46: 935-946

48. Lyng H, Vorren AO, Sundfor K, Taksdal I, Lien HH, Kaalhus O, Rofstad EK (2001) Intra- and intertumor heterogeneity in blood perfusion of human cervical cancer before treatment and after radiotherapy. *International Journal of Cancer* 96: 182-190

49. Meyn RE, Stephens LC, Ang KK, Hunter NR, Brock WA, Milas L, Peters LJ (1993) Heterogeneity in the development of apoptosis in irradiated murine tumours of different histologies. *International Journal of Radiation Biology* 64: 583-591

50. Milas L, Hunter NR, Mason KA, Milross CG, Saito Y, Peters LJ (1995) Role of reoxygenation in induction of enhancement of tumor radioresponse by paclitaxel. *Cancer Research* 55: 3564-3568

51. Milosevic MF, Fyles AW, Wong R, Pintilie M, Kavanagh MC, Levin W, Manchul LA, Keane TJ, Hill RP (1998) Interstitial fluid pressure in cervical carcinoma: within tumor heterogeneity, and relation to oxygen tension. *Cancer* 82: 2418-2426

52. Milosevic MF, Fyles AW, Hill RP (1999) The relationship between elevated interstitial fluid pressure and blood flow in tumors: a bioengineering analysis. *International Journal of Radiation Oncology, Biology, Physics* 43: 1111-1123

53. Moeller BJ, Cao Y, Li CY, Dewhirst MW (2004) Radiation activates HIF-1 to regulate vascular radiosensitivity in tumors: role of reoxygenation, free radicals, and stress granules.[see comment]. *Cancer Cell* 5: 429-441

54. Molls M. VP (1998) *Blood perfusion and microenvironment of human tumors.* Springer: Berlin

55. Moore AH, Olschowka JA, Williams JP, Paige SL, O'Banion MK (2004) Radiation-induced edema is dependent on cyclooxygenase 2 activity in mouse brain. *Radiation Research* 161: 153-160

56. Murata R, Shibamoto Y, Sasai K, Oya N, Shibata T, Takagi T, Abe M (1996) Reoxygenation after single irradiation in rodent tumors of different types and sizes. *International Journal of Radiation Oncology, Biology, Physics* 34: 859-865

57. Nordsmark M, Overgaard M, Overgaard J (1996) Pretreatment oxygenation predicts radiation response in advanced squamous cell carcinoma of the head and neck. *Radiotherapy & Oncology* 41: 31-39

58. Olive PL (1994) Radiation-induced reoxygenation in the SCCVII murine tumour: evidence for a decrease in oxygen consumption and an increase in tumour perfusion. *Radiotherapy & Oncology* 32: 37-46

59. Pappova N, Siracka E, Vacek A, Durkovsky J (1982) Oxygen tension and prediction of the radiation response. Polarographic study in human breast cancer. *Neoplasma* 29: 669-674

60. Rofstad EK (1989) Hypoxia and reoxygenation in human melanoma xenografts. *International Journal of Radiation Oncology, Biology, Physics* 17: 81-89

61. Roh HD, Boucher Y, Kalnicki S, Buchsbaum R, Bloomer WD, Jain RK (1991) Interstitial hypertension in carcinoma of uterine cervix in patients: possible correlation with tumor oxygenation and radiation response. *Cancer Research* 51: 6695-6698

62. Rupnow BA, Murtha AD, Alarcon RM, Giaccia AJ, Knox SJ (1998) Direct evidence that apoptosis enhances tumor responses to fractionated radiotherapy. *Cancer Research* 58: 1779-1784

63. Secomb TW, Hsu R, Ong ET, Gross JF, Dewhirst MW (1995) Analysis of the effects of oxygen supply and demand on hypoxic fraction in tumors. *Acta Oncologica* 34: 313-316

64. Sheridan MT, West CM, Cooper RA, Stratford IJ, Logue JP, Davidson SE, Hunter RD (2000) Pretreatment apoptosis in carcinoma of the cervix correlates with changes in tumour oxygenation during radiotherapy. *British Journal of Cancer* 82: 1177-1182

65. Thews O, Vaupel P (1996) Relevant parameters for describing the oxygenation status of solid tumors. *Strahlentherapie und Onkologie* 172: 239-243

66. Thews O, Hummel M, Kelleher DK, Lecher B, Vaupel P (2002) Nifedipine improves blood flow and oxygen supply, but not steady-state oxygenation of tumours in perfusion pressure-controlled isolated limb perfusion. *British Journal of Cancer* 87: 1462-1469

67. Tufto I, Lyng H, Rofstad EK (1996) Interstitial fluid pressure, perfusion rate and oxygen tension in human melanoma xenografts. *British Journal of Cancer - Supplement* 27: S252-S255

68. Tufto I, Rofstad EK (1999) Interstitial fluid pressure and capillary diameter distribution in human melanoma xenografts. *Microvascular Research* 58: 205-214

69. Van Camp S, Fisher P, Thrall DE (2000) Dynamic CT measurement of contrast medium washin kinetics in canine nasal tumors. *Veterinary Radiology & Ultrasound* 41: 403-408

70. Van Putten LM, Kallman RF (1968) Oxygenation status of a transplantable tumor during fractionated radiation therapy. *Journal of the National Cancer Institute* 40: 441-451

71. Vaupel P, Frinak S, O'Hara M (1984) Direct measurement of reoxygenation in malignant mammary tumors after a single large dose of irradiation. *Advances in Experimental Medicine & Biology* 180: 773-782

72. Weidner N, Semple JP, Welch WR, Folkman J (1991) Tumor angiogenesis and metastasis--correlation in invasive breast carcinoma. *New England Journal of Medicine* 324: 1-8

73. Znati CA, Rosenstein M, Boucher Y, Epperly MW, Bloomer WD, Jain RK (1996) Effect of radiation on interstitial fluid pressure and oxygenation in a human tumor xenograft. *Cancer Research* 56: 964-968

PART II

MUTAGENIC EFFECT OF HYPOXIA ON A_L HYBRID CELLS

CHAPTER 3

GENETIC INSTABILITY AND THE TUMOR MICROENVIRONMENT

Genetic Instability

Genetic instability is a characteristic feature of malignancy. Over the past two decades investigations have identified numerous genetic alterations in the genes that control tumor cells growth. Tumor progression has been correlated with genetic instability (Nowell, 1976; Loeb, 1991). Specific gene defects that lead to genomic instability include the DNA mismatch repair genes associated with hereditary colon cancer (Bronner et al, 1994), and the p53 gene, which is inactivated more frequently than any other gene in a wide range of human cancers (Greenblatt et al, 1994). Mutations in critical genes contribute to genetic instability through alterations in DNA repair and alterations in the cell cycle. Environmental factors like carcinogen exposure also play role in DNA damage.

In addition to these endogenous and environmental factors, tumor microenvironment itself is shown to be mutagenic leading to tumor progression and evolution of malignant phenotype (Reynolds et al, 1996). The tumor microenvironment is characterized by regions of hypoxia, nutrient deprivation and acidity (Moulder and Rockwell, 1987; Rockwell, 1992). Since this specific microenvironment influences tumor

metabolism and physiology, it may also cause increased spontaneous damage to DNA or inhibit DNA repair processes needed to maintain their genomic integrity (Yuan and Glazer, 1998).

Hypoxia

Hypoxia, the most extensively studied of microenvironmental factors, may lead to significant genomic alterations, and evidence exists suggesting that tumor hypoxia plays a key role in the development of aggressive tumor phenotypes and genetic instability. Tumor hypoxia is associated with increased DNA damage and impairments in DNA repair pathways. Several studies using both reporter genes and endogenous loci have demonstrated increased mutation rates in cells grown in tumors relative to those in identical cells grown in cultures (Reynolds et al, 1996; Paquette and Little, 1994; Li et al, 2001). One of the first experiments examining the role of tumor microenvironment in genetic instability used the mouse cell line carrying a chromosomally based lambda phage shuttle vector that was implanted subcutaneously into the flanks of nude mice to generate tumors. At the same time, an equal number of cells from the same cell line (LN12) was grown *in vitro* under standard culture conditions. A five-fold increase in the mutation frequency in cells grown in tumors compared to the same cells grown in culture was found (Reynolds et al, 1996). Several other studies also provided evidence of increased mutagenesis following growth of cells in solid tumors (Li et al, 2001). The mutation frequency in the hypoxanthine guanine phosphoribosyl transferase (HGPRT) gene in tumors was also reported to be higher than that found in cultured cells (Wilkinson et al, 1995).

Studies trying to characterize hypoxia-induced DNA damage have shown that hypoxia alone does not induce double-strand breaks (DSBs) (Hammond, 2002). It was shown that reoxygenation, on the other hand, induces significant DNA damage with DSBs mediated by ROS production during post-hypoxia reoxygenation (Hammond et al, 2003). Based on the studies of reperfusion injury, DNA damage is attributed to production of reactive oxygen species (ROS) and increased levels of antioxidant enzyme, superoxide dismutase (Welbourn et al, 1991). For example, oxidative injury may generate excessive levels of 8-oxoguanine, which miscode for A, leading to C: G to A: T transversions (Cheng et al, 1992). Investigations of the effect of hypoxia on cell cycle provided evidence that hypoxia induces G1-phase arrest (Graeber et al, 1994; Gardner et al, 2001), and severe hypoxia (approximately 0.02% O_2) results in an S-phase arrest which is reversible upon reoxygenation (Hammond et al, 2002).

Under low oxygen conditions DNA synthesis is inhibited, due to the suppression of initiation (Probst et al, 1988). Interruption of DNA synthesis is associated with single-strand breaks and double-strand breaks. Since double-strand breaks are not seen after exposure to hypoxia, it seems that hypoxia may only suppress initiation of replication, and not directly cause extensive DNA damage (Bindra and Glazer, 2005). Hypoxia may damage DNA indirectly by inducing endonucleases leading to DNA strand breakage (Russo et al, 1995). Induction of aberrant DNA synthesis following hypoxia-reoxygenation results in DNA overreplication and gene amplification. Many studies have reported DNA overreplication after exposure to hypoxia (Rice et al, 1985, 1986, 1987), and its association with tumor metastasis (Young et al, 1988; Young and Hill, 1990). Gene amplification has been reported to be the most frequent genetic alteration in cancer

cells. Being associated with the overexpression of many oncogenes, this phenomenon is linked to tumor progression (Brison, 1993; Teicher, 1994).

Cells with overreplicated DNA were shown to acquire drug resistance. In one of early investigations by Rice et al. (Rice et al, 1986), exposure of Chinese hamster ovary (CHO) cells to hypoxia followed by recovery in the presence of oxygen led to increased methotrexate resistance resulting from amplification of the dihydrofolate reductase gene. In subsequent studies, it was found that gene amplification caused adriamycin and doxorubicin resistance observed after exposure to hypoxia in several cell lines (Rice et al, 1987; Luk et al, 1990). In these studies hypoxic exposure was followed by a reoxygenation period, and gene amplification has been observed during reoxygenation. Besides these studies that were focusing on large chromosomal rearrangements, there are studies done to detect small-scale mutations that may be induced by hypoxia. It was demonstrated that transient hypoxia resulted in increased mutation frequencies compared to normoxic controls (Reynolds et al, 1996). Furthermore, multiple hypoxia-reoxygenation exposures resulted in even greater mutation frequency.

Low pH and nutrient deprivation

Even though less investigated, other microenvironmental factors can alter cell metabolism and potentially contribute to genomic instability. Low pH has been shown to alter structure and function of proteins involved in DNA replication such as helicases and polymerases (Eckert and Kunkel, 1993a, 1993b). It has been demonstrated that both nutrient deprivation and acidosis can enhance metastatic potential of murine tumor cells (Cuvier et al, 1997; Schlappack et al, 1991). When cells were exposed to pH 6.5 or

starved for glucose followed by recovery in normal growth medium, some cells were found with overreplicated DNA, similar to the effect of hypoxia. Exposure to acidosis even led to a small increase in methotrexate resistance in a murine tumor cell line (Schlappack et al, 1991).

It was shown that serum deprivation can induce increase in mutations. The incubation of CHO cells in serum concentrations below 0.25% resulted in an almost five-fold increase in the mutation rate, and was also associated with a rise in intracellular oxidants (Goncharova et al, 1996). When the low serum was supplemented with antioxidants, the mutation rate was reduced in a dose-dependent manner, suggesting that ROS may be involved in induction of mutagenesis. Serum starvation was associated with increased genetic instability in 4T1 cells, as well (Li et al, 2001). According to the work done in this area, it has been demonstrated that other factors of tumor microenvironment, in addition to hypoxia, may play a role in inducing DNA damage and causing genetic instability.

Alterations in DNA repair pathways under hypoxia

The characteristic tumor microenvironment has been shown to contribute to genetic instability. Intratumoral hypoxia induces alterations in numerous physiological processes, including altered glucose metabolism, up-regulated angiogenesis, increased invasive capacity, and deregulation of apoptosis (Subarsky and Hill, 2003). All the specific changes in cell physiology may lead to conditions that cause either increased damage to DNA or inhibition of DNA repair processes. Decrease in expression of DNA repair genes is a possible mechanism for this effect. Specifically, it has been

demonstrated that hypoxia leads to functional decreases in both the nucleotide excision repair (NER) and mismatch repair (MMR) pathways.

Using UV-induced damage Yuan et al. examined the effects of hypoxia and low pH on the nucleotide excision repair (NER) pathway (Yuan et al, 2000).They reported that exposure of irradiated cells to hypoxia and pH 6.5 exhibited a decrease in DNA repair capacity.

DNA mismatches arise from errors in replication and repair and from intermediates produced during recombinational processes (Modrich and Lahue, 1996; Kolodner, 1996). Those genetic aberrations are repaired via mismatch repair pathway (MMR). MMR is carried out by a series of proteins, including MSH2, MSH3, MSH6, and MLH1 and PMS2 (Kolodner, 1996).The expression of MMR proteins was examined after exposure to hypoxia. It was found that severe hypoxia ($0.01\%O_2$) specifically down-regulates the expression of the MLH1 gene at the level of transcription (at the mRNA level) (Mihaylova et al, 2003). PMS2 protein levels were reduced under hypoxia, probably due to instability of PMS2 in the absence of its heterodimer partner, MLH1 (Chang et al, 2000). It has been proposed that metabolic changes in hypoxic cells create sub-optimal conditions for the activity of some DNA repair enzymes (Bindra et al, 2005), and some studies have revealed that ROS and oxidative stress can inactivate the MMR system (Kondo et al, 2001; Chang et al, 2002). It has also been reported that hypoxia and accompanying low pH enrich for MMR-deficient cells (Hardman et al, 2001).

Considering the complex gene expression changes observed under hypoxia, it has been investigated whether alterations in the expression of other DNA repair genes could also play role in hypoxia-induced genetic instability. It has been reported that the

expression of RAD51, a critical mediator of homologous recombination (HR) in mammalian cells, is specifically down-regulated by hypoxia at the mRNA level. Decreased RAD51 protein expression under hypoxia was observed in numerous cell lines, and more interestingly this decrease persisted even during post-hypoxic phase (Bindra et al, 2004). This is especially relevant to solid tumors, which experience fluctuating blood perfusion that results in temporally and spatially varying oxygen tensions.

These data provide evidence that genetic instability may arise from deregulated DNA repair pathways as well as from increased DNA damage.

Evaluating mechanisms underlying the genetic instability

Proposing different experimental protocols and various culture conditions was used in evaluating mechanisms underlying the genetic instability in developing tumors. However, *in vitro* conditions do not exactly mimic the tumor's very complex microenvironment. Even more, different microenvironmental factors may interact with each other synergistically, producing a bigger effect together than each of them alone. Rotin et al. reported that cellular ATP, energy change and cell viability were reduced after 6 hour exposure to hypoxia at pH 6.0. None of them were influenced by hypoxia or acidosis alone (Rotin et al, 1986). Reynolds et al. investigated tumor hypoxia-induced mutations and found that single exposure of the cells to hypoxia increased mutation frequency 3.4 fold above that for the untreated cells. Cells exposed multiple times to hypoxia showed even higher mutation frequencies, indicating cumulative dose-response effect (Reynolds et al, 1996). This is pointing to conclusion that transient exposures to

low oxygen levels found within tumors are mutagenic. While investigating whether tumor microenvironment could influence cellular repair of DNA damage, Yuan et al. noted that they saw only a small decrease in DNA mismatch repair in cells treated with hypoxia alone. However, when cells were exposed to a combination of hypoxia and acidosis, they observed large differences (Yuan et al, 2000), which was in accordance with other studies reporting a synergistic effect of low oxygen and low pH (Rotin et al, 1986; Boyer and Tannock, 1992). The frequency of mutations in cells grown in a tumor was found to be higher than in identical cells grown in culture for an equivalent period of time (Graeber et al, 1994; Reynolds et al, 1996). A different pattern of mutation was also seen in Reynolds experiment, with significantly more deletions and transversions in tumors, while mutations in cultured cells were point mutations, implicating that strand breaks must be produced by tumor microenvironment.

Tumor microenvironment can contribute to mutations in several ways. A summary of the pathways by which hypoxia, specifically, induces genetic instability is shown in Figure 3.1 (adopted from Bindra and Glazer, 2005)

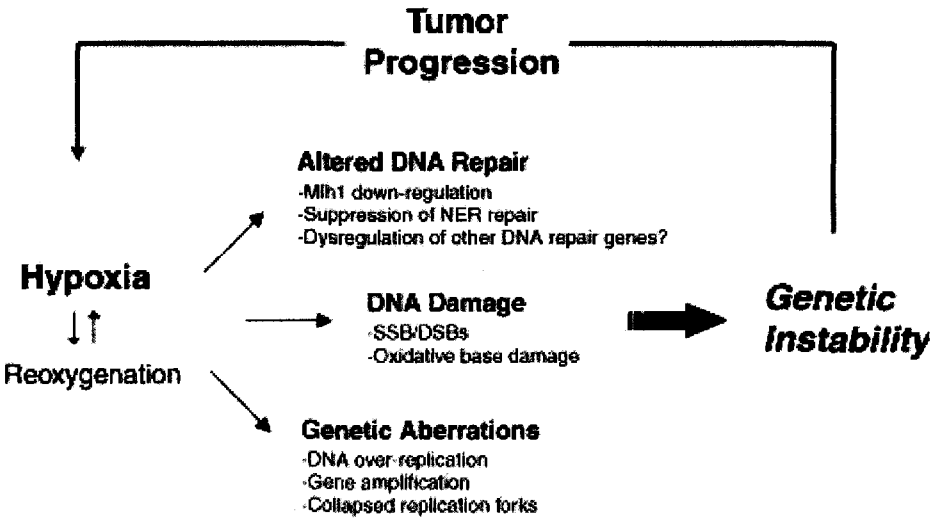

Figure 3.1 Hypoxia, genetic instability and tumor progression. Abbreviations: NER, nucleotide excision repair; SSB/DSBs, Single-strand breaks/double-strand breaks.

BIBLIOGRAPHY

1. Bindra RS, Schaffer PJ, Meng A, Woo J, Maseide K, Roth ME, Lizardi P, Hedley DW, Bristow RG, Glazer PM (2004) Down-regulation of Rad51 and decreased homologous recombination in hypoxic cancer cells. *Molecular & Cellular Biology* 24: 8504-8518

2. Bindra RS, Glazer PM (2005) Genetic instability and the tumor microenvironment: towards the concept of microenvironment-induced mutagenesis. [Review] [79 refs]. *Mutation Research* 569: 75-85

3. Bindra RS, Schaffer PJ, Meng A, Woo J, Maseide K, Roth ME, Lizardi P, Hedley DW, Bristow RG, Glazer PM (2005) Alterations in DNA repair gene expression under hypoxia: elucidating the mechanisms of hypoxia-induced genetic instability. *Annals of the New York Academy of Sciences* 1059: 184-195

4. Boyer MJ, Tannock IF (1992) Regulation of intracellular pH in tumor cell lines: influence of microenvironmental conditions. *Cancer Research* 52: 4441-4447

5. Brison O (1993) Gene amplification and tumor progression. [Review] [228 refs]. *Biochimica et Biophysica Acta* 1155: 25-41

6. Bronner CE, Baker SM, Morrison PT, Warren G, Smith LG, Lescoe MK, Kane M, Earabino C, Lipford J, Lindblom A (1994) Mutation in the DNA mismatch repair gene homologue hMLH1 is associated with hereditary non-polyposis colon cancer. *Nature* 368: 258-261

7. Chang CL, Marra G, Chauhan DP, Ha HT, Chang DK, Ricciardiello L, Randolph A, Carethers JM, Boland CR (2002) Oxidative stress inactivates the human DNA mismatch repair system. *American Journal of Physiology - Cell Physiology* 283: C148-C154

8. Chang DK, Ricciardiello L, Goel A, Chang CL, Boland CR (2000) Steady-state regulation of the human DNA mismatch repair system. *Journal of Biological Chemistry* 275: 18424-18431

9. Cheng KC, Cahill DS, Kasai H, Nishimura S, Loeb LA (1992) 8-Hydroxyguanine, an abundant form of oxidative DNA damage, causes G----T and A----C substitutions. *Journal of Biological Chemistry* 267: 166-172

10. Cuvier C, Jang A, Hill RP (1997) Exposure to hypoxia, glucose starvation and acidosis: effect on invasive capacity of murine tumor cells and correlation with cathepsin (L + B) secretion. *Clinical & Experimental Metastasis* 15: 19-25

11. Eckert KA, Kunkel TA (1993a) Fidelity of DNA synthesis catalyzed by human DNA polymerase alpha and HIV-1 reverse transcriptase: effect of reaction pH. *Nucleic Acids Research* 21: 5212-5220

12. Eckert KA, Kunkel TA (1993b) Effect of reaction pH on the fidelity and processivity of exonuclease-deficient Klenow polymerase. *Journal of Biological Chemistry* 268: 13462-13471

13. Gardner LB, Li Q, Park MS, Flanagan WM, Semenza GL, Dang CV (2001) Hypoxia inhibits G1/S transition through regulation of p27 expression. *Journal of Biological Chemistry* 276: 7919-7926

14. Goncharova EI, Nadas A, Rossman TG (1996) Serum deprivation, but not inhibition of growth per se, induces a hypermutable state in Chinese hamster G12 cells. *Cancer Research* 56: 752-756

15. Graeber TG, Peterson JF, Tsai M, Monica K, Fornace AJ, Jr., Giaccia AJ (1994) Hypoxia induces accumulation of p53 protein, but activation of a G1-phase checkpoint by low-oxygen conditions is independent of p53 status. *Molecular & Cellular Biology* 14: 6264-6277

16. Greenblatt MS, Bennett WP, Hollstein M, Harris CC (1994) Mutations in the p53 tumor suppressor gene: clues to cancer etiology and molecular pathogenesis. [Review] [288 refs]. *Cancer Research* 54: 4855-4878

17. Hammond EM, Denko NC, Dorie MJ, Abraham RT, Giaccia AJ (2002) Hypoxia links ATR and p53 through replication arrest. *Molecular & Cellular Biology* 22: 1834-1843

18. Hammond EM, Dorie MJ, Giaccia AJ (2003) ATR/ATM targets are phosphorylated by ATR in response to hypoxia and ATM in response to reoxygenation. *Journal of Biological Chemistry* 278: 12207-12213

19. Hardman RA, Afshari CA, Barrett JC (2001) Involvement of mammalian MLH1 in the apoptotic response to peroxide-induced oxidative stress. *Cancer Research* 61: 1392-1397

20. Kolodner R (1996) Biochemistry and genetics of eukaryotic mismatch repair. [Review] [85 refs]. *Genes & Development* 10: 1433-1442

21. Kondo A, Safaei R, Mishima M, Niedner H, Lin X, Howell SB (2001) Hypoxia-induced enrichment and mutagenesis of cells that have lost DNA mismatch repair. *Cancer Research* 61: 7603-7607

22. Li CY, Little JB, Hu K, Zhang W, Zhang L, Dewhirst MW, Huang Q (2001) Persistent genetic instability in cancer cells induced by non-DNA-damaging stress exposures. *Cancer Research* 61: 428-432

23. Loeb LA (1991) Mutator phenotype may be required for multistage carcinogenesis. [Review] [63 refs]. *Cancer Research* 51: 3075-3079

24. Luk CK, Veinot-Drebot L, Tjan E, Tannock IF (1990) Effect of transient hypoxia on sensitivity to doxorubicin in human and murine cell lines. *Journal of the National Cancer Institute* 82: 684-692

25. Mihaylova VT, Bindra RS, Yuan J, Campisi D, Narayanan L, Jensen R, Giordano F, Johnson RS, Rockwell S, Glazer PM (2003) Decreased expression of the DNA mismatch repair gene Mlh1 under hypoxic stress in mammalian cells. *Molecular & Cellular Biology* 23: 3265-3273

26. Modrich P, Lahue R (1996) Mismatch repair in replication fidelity, genetic recombination, and cancer biology. [Review] [225 refs]. *Annual Review of Biochemistry* 65: 101-133

27. Moulder JE, Rockwell S (1987) Tumor hypoxia: its impact on cancer therapy. [Review] [242 refs]. *Cancer & Metastasis Reviews* 5: 313-341

28. Nowell PC (1976) The clonal evolution of tumor cell populations. *Science* 194: 23-28

29. Paquette B, Little JB (1994) In vivo enhancement of genomic instability in minisatellite sequences of mouse C3H/10T1/2 cells transformed in vitro by X-rays. *Cancer Research* 54: 3173-3178

30. Probst H, Schiffer H, Gekeler V, Kienzle-Pfeilsticker H, Stropp U, Stotzer KE, Frenzel-Stotzer I (1988) Oxygen dependent regulation of DNA synthesis and growth of Ehrlich ascites tumor cells in vitro and in vivo. *Cancer Research* 48: 2053-2060

31. Reynolds TY, Rockwell S, Glazer PM (1996) Genetic instability induced by the tumor microenvironment. *Cancer Research* 56: 5754-5757

32. Rice GC, Spiro IJ, Ling CC (1985) Detection of S-phase overreplication following chronic hypoxia using a monoclonal anti-BrdUrd. *International Journal of Radiation Oncology, Biology, Physics* 11: 1817-1822

33. Rice GC, Hoy C, Schimke RT (1986) Transient hypoxia enhances the frequency of dihydrofolate reductase gene amplification in Chinese hamster ovary cells. *Proceedings of the National Academy of Sciences of the United States of America* 83: 5978-5982

34. Rice GC, Ling V, Schimke RT (1987) Frequencies of independent and simultaneous selection of Chinese hamster cells for methotrexate and doxorubicin (adriamycin)

resistance. *Proceedings of the National Academy of Sciences of the United States of America* 84: 9261-9264

35. Rockwell S (1992) Use of hypoxia-directed drugs in the therapy of solid tumors. [Review] [90 refs]. *Seminars in Oncology* 19: 29-40

36. Rotin D, Robinson B, Tannock IF (1986) Influence of hypoxia and an acidic environment on the metabolism and viability of cultured cells: potential implications for cell death in tumors. *Cancer Research* 46: 2821-2826

37. Russo CA, Weber TK, Volpe CM, Stoler DL, Petrelli NJ, Rodriguez-Bigas M, Burhans WC, Anderson GR (1995) An anoxia inducible endonuclease and enhanced DNA breakage as contributors to genomic instability in cancer. *Cancer Research* 55: 1122-1128

38. Schlappack OK, Zimmermann A, Hill RP (1991) Glucose starvation and acidosis: effect on experimental metastatic potential, DNA content and MTX resistance of murine tumour cells. *British Journal of Cancer* 64: 663-670

39. Subarsky P, Hill RP (2003) The hypoxic tumour microenvironment and metastatic progression. [Review] [134 refs]. *Clinical & Experimental Metastasis* 20: 237-250

40. Teicher BA (1994) Hypoxia and drug resistance. [Review] [241 refs]. *Cancer & Metastasis Reviews* 13: 139-168

41. Welbourn CR, Goldman G, Paterson IS, Valeri CR, Shepro D, Hechtman HB (1991) Pathophysiology of ischaemia reperfusion injury: central role of the neutrophil. [Review] [50 refs]. *British Journal of Surgery* 78: 651-655

42. Wilkinson D, Sandhu JK, Breneman JW, Tucker JD, Birnboim HC (1995) Hprt mutants in a transplantable murine tumour arise more frequently in vivo than in vitro. *British Journal of Cancer* 72: 1234-1240

43. Young SD, Marshall RS, Hill RP (1988) Hypoxia induces DNA overreplication and enhances metastatic potential of murine tumor cells. *Proceedings of the National Academy of Sciences of the United States of America* 85: 9533-9537

44. Young SD, Hill RP (1990) Effects of reoxygenation on cells from hypoxic regions of solid tumors: anticancer drug sensitivity and metastatic potential.[see comment]. *Journal of the National Cancer Institute* 82: 371-380

45. Yuan J, Glazer PM (1998) Mutagenesis induced by the tumor microenvironment. [Review] [47 refs]. *Mutation Research* 400: 439-446

46. Yuan J, Narayanan L, Rockwell S, Glazer PM (2000) Diminished DNA repair and elevated mutagenesis in mammalian cells exposed to hypoxia and low pH. *Cancer Research* 60: 4372-4376

CHAPTER 4

DOES TUMOR HYPOXIA IMPACT MUTAGENESIS?

ABSTRACT

The impact of tumor hypoxia on local tumor control has long been a concern for solid tumors treated with radiation therapy. More recent work has implied that hypoxia of the primary tumor may also be associated with metastatic spread, perhaps by contributing to genetic instability. It has been proposed that tumor microenvironment, with fluctuating hypoxia, low pH and nutrient deprivation may be responsible for diminished DNA repair and increased mutagenesis. I hypothesized that hypoxia alone could lead to genomic alterations. To investigate the hypothesis I used the A_L mutation assay. A_L cells are human-hamster hybrid cells containing a standard set of CHO-K1 chromosomes and single copy of human chromosome 11. Genetic markers on chromosome 11 have been mapped, including the CD59 gene that encodes for the cell surface antigen, CD59. Wild type $CD59^+$ cells are killed when the culture is treated with a monoclonal antibody to the CD59 antigen and rabbit complement. Mutant $CD59^-$ cells survive and form colonies.

Since the human chromosome is not essential for the viability of the hybrid cell, except for the small segment on the tip of the short arm, mutations ranging from point mutations

to loss of almost the whole chromosome 11 can be detected. We exposed A_L cells to different hypoxic conditions, isolated and cloned $CD59^-$ mutants and performed PCR analysis. Only severe hypoxia caused mutations in this system. Levels of oxygen below 0.1% or less than 0.63mm Hg induced mutations in A_L cells. Qualitative analysis indicated that they were possibly point mutations and/or very small deletions on chromosome 11. Cells were also labeled with monoclonal antibodies against the CD59 surface antigen and analyzed by flow cytometry (FCM). Single mutant cells were sorted from the mutant peak. The resulting clonal populations were analyzed using the same methods to determine if mutated cells were truly negative for CD59. The purified DNA from PCR products of four exons, from both types of mutation assays, was sequenced to check for the characteristics of the hypoxia-induced mutants. Sequencing did not detect any changes in the CD59 gene.

INTRODUCTION

The tumor microenvironment is very specific and differs from that of a normal tissue. As a tumor grows, it develops a chaotic and irregular vascular network and insufficient lymphatic system. This unique physiology results in regions of hypoxia, low pH, high lactate levels, nutrient deprivation and interstitial hypertension among solid tumors (Yuan et al, 2000; Vaupel, 2004).

Genetic instability is a commonly observed aspect of tumors (Yuan and Glazer, 1998). The mechanisms underlying genetic instability have been investigated and an important role was attributed to genetic defects influencing cell cycle regulation and

DNA repair, including p53 mutations, defects in DNA mismatch repair (MMR) genes and genes associated with the nucleotide excision repair (NER) pathway (Mihaylova et al, 2003). In addition to genetic factors, it has been proposed that tumor microenvironment itself may be mutagenic and lead to genomic alterations. The evidence has been provided for increased mutation frequency in cells grown in tumors compared to identical cells grown in culture (Reynolds et al, 1996; Wilkinson et al, 1995). This is supported by data demonstrating that exposure of cells to conditions observed in tumors produces chromosomal changes and increases the frequency of drug resistance (Yuan et al, 2000; Reynolds et al, 1996; Rice et al, 1987). Work on experimental models has shown that exposure to hypoxia, glucose deprivation and acidosis have an effect on invasiveness of murine tumor cells (Cuvier et al, 1997; Dewhirst et al, 1994).The association of tumor hypoxia with enhanced metastatic potential of human soft tissue sarcomas, cervix carcinomas and carcinomas of the head and neck (Brizel et al, 1996, 2001; Hockel et al, 1996, 1998; Rofstad et al, 2000) has been reported. These studies suggest an association with modulating gene transcription. Hypoxia, either alone or followed by reoxygenation, has been associated with various DNA lesions, including single-strand breaks, inhibition of replication initiation and gene amplification (Hammond et al, 2002, 2003; Rice et al, 1986). The genetic changes induced by hypoxia may play an important role in the development of genomic instability and more aggressive phenotypes (Koong et al, 2000; Denko et al, 2000, 2003).

Several studies proposed that tumor microenvironment, with fluctuating and chronic hypoxia, low pH and nutrient deprivation, may be responsible for diminished DNA repair and increased mutagenesis (Yuan et al, 2000; Mihaylova et al, 2003; Reynolds et al,

1996; Kondo et al, 2001). It is not known what type of hypoxia is more important for treatment outcome or what the significance of chronic and acute hypoxia is in the development of metastatic disease. I propose that acute hypoxia may play a more significant role in the tumor microenvironment and that acute hypoxia alone can cause genetic instability. Because acute hypoxia is the result of fluctuations in blood flow and not at the limits of oxygen diffusion away from blood vessels like chronic hypoxia, it is supposed that cells exposed to acute hypoxia have higher energy status than chronically hypoxic cells (Fenton et al, 1995; Kim et al, 1993). They are also less likely to be exposed to acidic pH and more likely to survive the complex process of metastasis (Cairns et al, 2003).

To investigate the role of tumor hypoxia alone in the induction of mutagenesis, I used the A_L cell mutation assay. The human-hamster hybrid A_L cell line was developed by Puck et al. (Puck et al, 1971) by fusion of human fibroblasts and the gly$^-$A (glycine deficient) mutant of the Chinese hamster ovary cells. The hybrid cells contain a standard set of 20 CHO-K1 chromosomes (Kao and Puck, 1968; Kraemer et al, 2000) and a single copy of un-rearranged human chromosome 11, which is not necessary for cell reproduction (Waldren et al, 1979, 1986, 1999). The principal markers of mutation assay are the cell surface antigen CD59 and the CD59, gene that encodes it, located at 11p13.5, (Kraemer et al, 2001). Wild type A_L cells express a glycosylphosphatidylinositol (GPI) bound human CD59 surface antigen and are lysed quantitatively by anti-CD59 monoclonal antibody E7.1 in the presence of rabbit serum complement. Cells that have lost expression of the CD59 antigen are not killed and grow into colonies. Since human chromosome 11 codes for genes that are not essential for the survival of the cell,

mutations ranging from point mutations and small deletions to loss of almost all of chromosome 11 can be detected using this mutation assay (Waldren et al, 1999, 2004; Kraemer et al, 2001; Hei et al, 1988; Zhu et al, 1996).

A_L cells were exposed to different levels of oxygenation and for varying durations to determine if hypoxia alone (without changing nutrients or pH of the medium), could cause mutations.

MATERIALS AND METHODS

Cell culture, media and reagents

The A_L hybrid cell line has been used in mutation analysis and described in detail previously (Waldren et al, 1979, 1986, 1999, 2004; Kraemer et al, 2001; Hei et al, 1988; Zhu et al, 1996). The A_L cells contain the standard set of CHO-K1 chromosomes and a single copy of human chromosome 11. Hybrid A_LN cells were constructed by transfecting the pSV2neo plasmid into human chromosome 11, but no hamster chromosome, to give the A_LN cells the resistance to killing by neomycin (G418 sulfate, purchased from Sigma-Aldrich, St. Louis, MO). Cells grown in medium containing 0.8mg/ml neomycin are killed if they do not express the pSV2neo vector to select against cells that have lost human chromosome 11 (Kraemer et al, 2001; McGuinness et al, 1995). Cells were cultivated in Ham's F-12 medium supplemented with 3% fetal calf serum and 4% newborn calf serum (Hyclone, Logan, UT), HEPES buffer (Sigma-Aldrich, St. Louis, MO) and penicillin/streptomycin 10,000 I.U/ml and 10,000 µl/ml (Mediatech Inc. Cellgro, Hendron, VA). Rabbit serum complement was from Covance

Research Product Inc., Denver, PA., human serum type AB from Sigma, St Louis, MO, and monoclonal antibody E7.1 was provided from Dr. Waldren's lab at Colorado State University. E7.1 was prepared as described (Waldren et al, 1979, 1999). Antiserum from sheep immunized with human erythrocytes was used as a source of antibodies against CD59 antigen.

The A_L mutation assay: principle and protocol

Mutation was measured at the CD59 locus of A_L human-hamster hybrid cells. Mutation was detected as loss of expression of the CD59 cell surface antigen that is encoded by the CD59 gene at 11p13.5. Wild-type cells with the antigen are lysed by monoclonal antibody in the presence of complement. Cells that do not express this antigen are not recognized by the E7.1 antibody and survive to form colonies. Colonies grown after exposure to complement and antibody were used to calculate the number of mutants in surviving cells. Cells were exposed to reduced oxygen levels as a potential mutagen.

A Forma Scientific Water Jacketed incubator with thermal, CO_2, and O_2 control was used to obtain 2.5% and 1% O_2 environments. Cells were maintained in these conditions for 4 or 7 days. An incubator insert chamber [C-274 chamber with PRO-OX Model 110 and PRO-CO_2 (BioSpherix, Redfield, NY)] was used to obtain O_2 levels of 0.1%. To lower oxygen further, an anaerobic chamber BBL™ GasPak™ 100 Jar System, with gas generator envelopes (Fischer Scientific, Houston, TX) was used. This system provided oxygen levels between 0% and 0.1%. Cells in the <0.1% group were exposed for 24 hours. Duration was based on achieving 50% cell survival. Enough cells were plated in

enriched F12 medium to give a surviving population of more than 10^5 cells after exposure to hypoxia (mutagen) (Figure 4.1). The cells were then sub-cultured for 10 days to let them recover from the temporary growth lag and divide as described (Waldren et al, 1979, 1999). Cells were then challenged with 2% rabbit serum as a complement (Covance Research Products Inc., Denver, PA), and 0.5% E7.1, a specific monoclonal antibody against the CD59 antigenic marker (Figure 4.2). Cells with CD59 surface antigens do not survive the complement challenge. Surviving cells formed colonies which were counted as mutant cells. The mutant yield was adjusted for plating efficiency and background mutations.

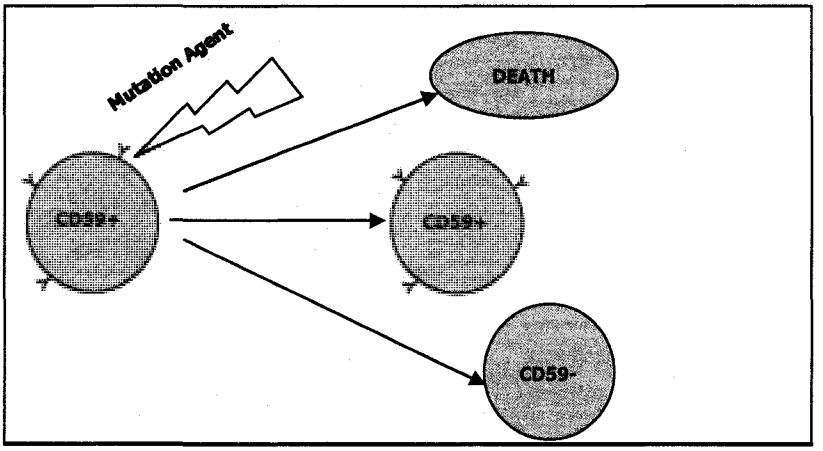

Figure 4.1. Treatment of A_L cells with a mutagen results in survival with wild type CD59, survival with mutated CD59, or death.

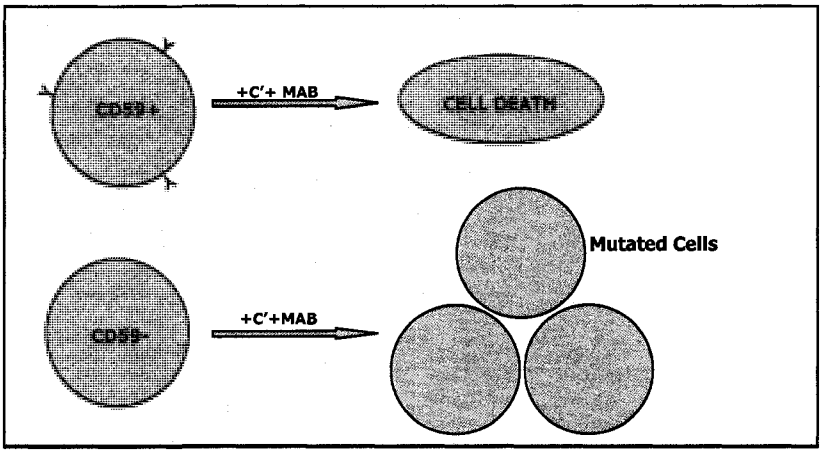

Figure 4.2. Selection of CD59 mutant A_L cells after treatment with CD59 Mab and Rabbit serum; wild type cells are killed, CD59 mutants grow into colonies.

Determination of hypoxic conditions: Survival Curves and A_L mutation assay

A_L cells were first exposed to an environment of 2.5% O_2. 2.5% is less than in the ambient air; however 2.5% or (15.75 mm Hg) O_2 is not considered hypoxic and we used these data for the background mutations level (Figure 4.3). To further decrease oxygen we used the PRO-OX system which allowed us to achieve O_2 concentrations as low as 0.1% (0.63 mm Hg). Cells were exposed to 1%, 0.2% and 0.1% O_2 for 4 or 7 days. The anaerobic chamber was used to obtain severe hypoxia below 0.1% O_2 (less than 0.63 mm Hg). $2X10^5$ cells were plated and placed in the chamber for 1, 3, 24 or 43 hours and a survival curve was constructed to define the optimal time for exposure to hypoxic conditions (Figure 4.4). The subsequent experiment, 24 hours exposure time was used so that at least 10^5 cells survived for challenge with rabbit serum complement and antibody E7.1. To reduce any nonspecific toxicity of the complement, 0.1% human serum was added to the mixture. 7 days after "challenge", colonies were counted as mutated cells.

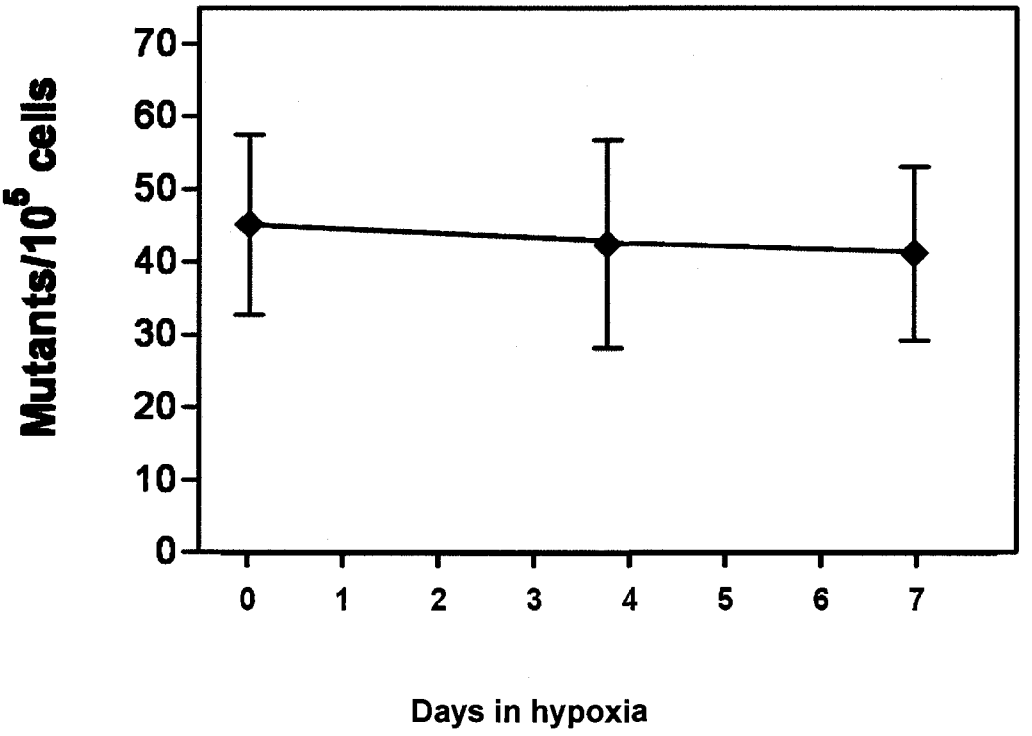

Figure 4.3. Mutant yield for cells exposed to 2.5 % O_2 (15.75 mm Hg). Control cells were grown in normoxic conditions. Presented as mean ± SD for mutants per 10^5 cells without adjusting for background mutations.

The number of mutated cells per 10^5 surviving cells (mutant yield) is the average number of colonies on the plates divided by the plating efficiency (PE) of cells exposed to complement without antiserum, so it is corrected for any nonspecific killing due to complement alone (Waldren et al, 1979; McGuinness et al, 1995). The background mutant yield (adjusted number of colonies grown in untreated plates) was subtracted to give the final mutant yield. Colonies were picked and expanded for PCR analysis.

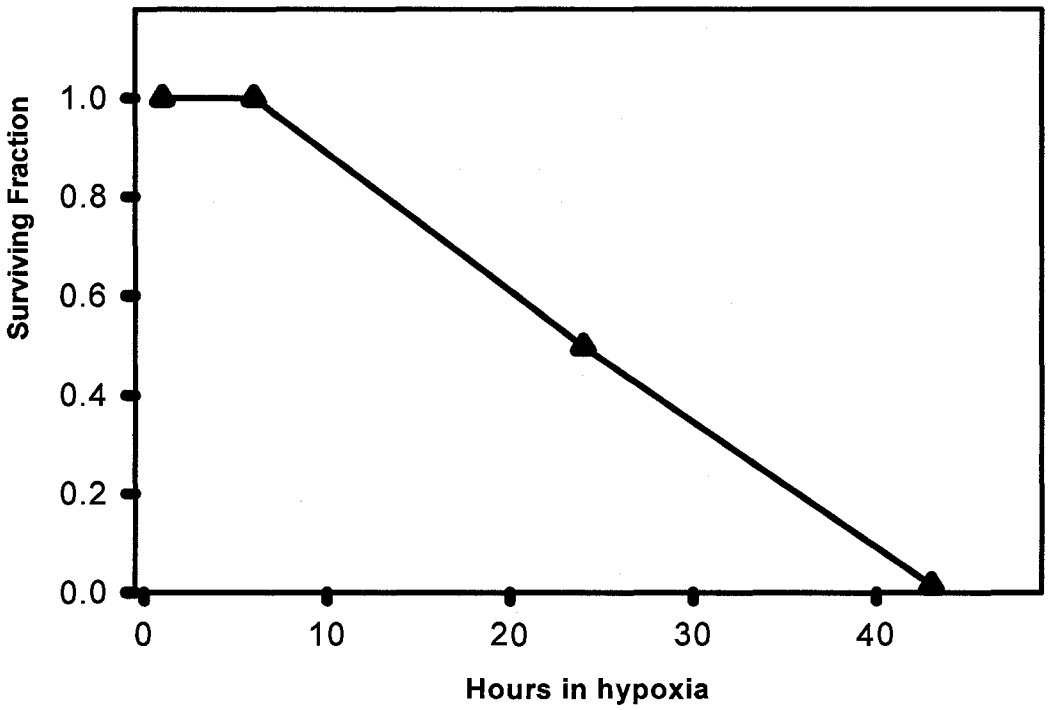

Figure 4.4. Survival curve for CHO A_L cells grown in less than 0.63 mmHg (<0.1% O_2).

PCR and Sequencing Analysis

The mutated cells were cloned and DNA was extracted using DNeasy Tissue Kit (Qiagen, Valencia, CA). DNA concentrations were diluted to 100 μg/ml and the presence or absence of five loci on chromosome 11 was determined by PCR. Five DNA marker genes on chromosome 11 (RAS at 11p15.5, LDHA at 11p15.4, Catalase- CAT at 11p13, Centromere and Apolipoprotein A-1- APO at 11q23-24) were chosen because of their positions relative to the CD59 gene (Figure 4.5), and the availability of PCR primers for the coding regions of these genes (Zhou et al, 1999; Hei et al, 1998).

The primers, synthesized by Macromolecular Resources (Fort Collins, CO) were:

RAS:	Forward GAC GGA ATA TAA GCT GGT GG
	Reverse TGG ATG GTC AGC GCA CTC TT
LDHA:	Forward ATA CAC TTT GGG GGA TCC AAA AGG A
	Reverse AAA AAA TGT TGG ACT AGG CAT GTT C
CAT:	Forward TTA GCG TTC ATC CGT GTA ACC
	Reverse TCC AAT CAT CCG TCA AAA CA
CENTROMERE:	Forward AAT TTC TTC TCC ACC CAC CC
	Reverse TTG CAT GCC ATT GTG GAG
APO:	Forward GCT TCA AGG TCA GCT TCC TG
	Reverse GGA AAC GTT TAT TCT GAG CAC C

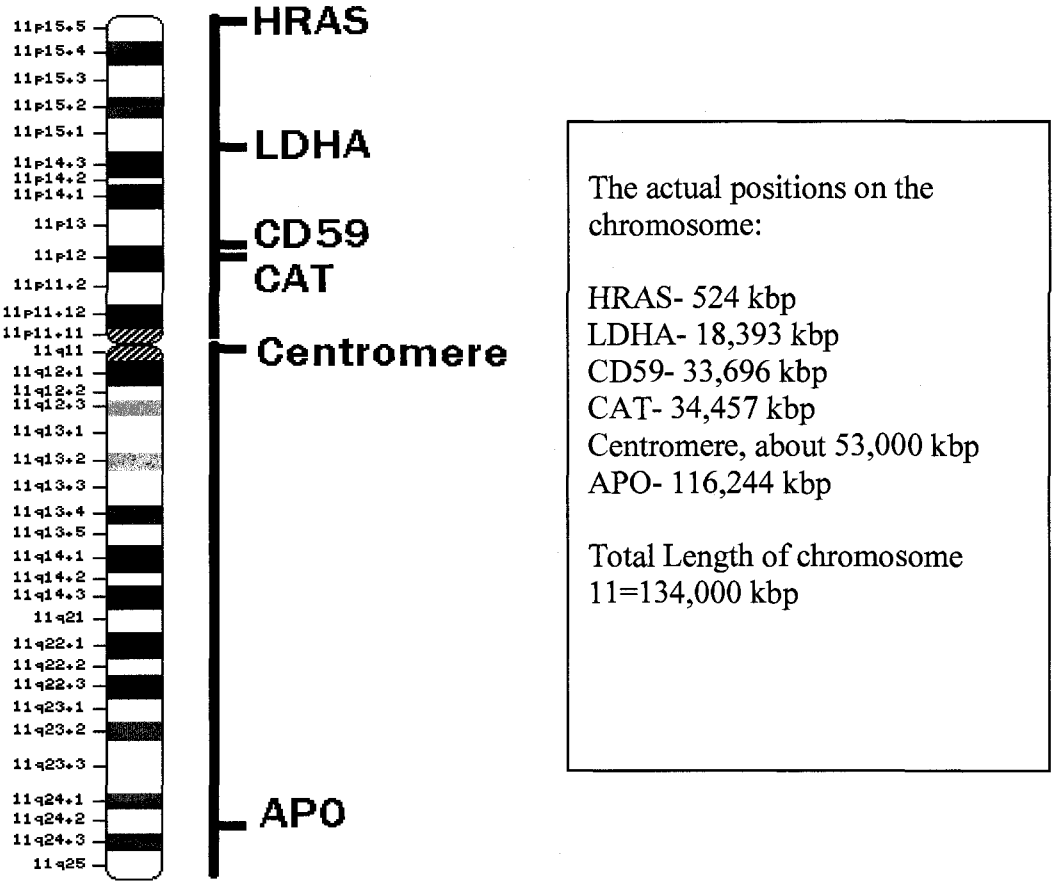

Figure 4.5. Diagram of human chromosome 11, showing the CD59 gene and the relative position of other markers used in the PCR analysis for determination of the extent of the mutations. The two nearest markers to CD59 are separated by about 16 Mbp.

To determine the presence or absence of the four exons of the CD59 gene (Figure 4.6), PCR was done using the following primers obtained from Macromolecular Resources as previously described (Waldren et al, 1999).

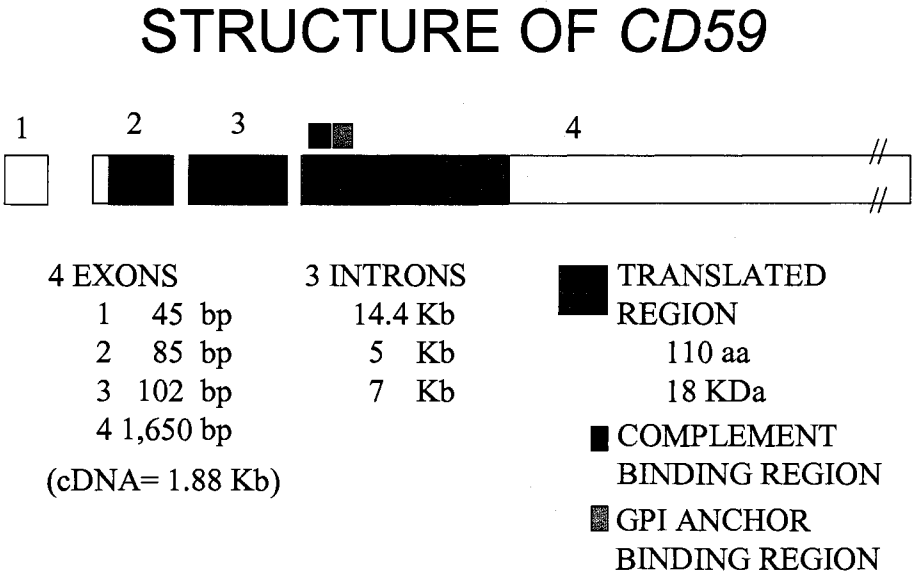

FIGURE 4.6. Structure of the CD59 gene, exons, introns and their sizes in base pairs (bp) and kilo base pairs (Kb). Binding site for complement and GPI anchor are encoded by exon 4 (Courtesy of Diane Vannais). Exon 2 translated region 67 bp, untranslated 18 bp; exon 4 translated region 215 bp, untranslated 1435 (Petranka et al, 1992).

Exon 1: Forward CTG GAG CGA AAG ATT GCG

Reverse: TTC GGG CCT TCT TAC CTG

Exon 2: Forward TTG AGA CAA CCA GCA GTC

Reverse TAA GAA GGG AGT TCA TGG

Exon 3: Forward GGA AGT ATA CCA CAA GTT GC

Reverse GCC TAA TGA GGA TTA CAG TG

Exon 4: Forward ACA AGT GTA TAA CAA GTG TGG

Reverse TCC CTG CAA ACA GGA CTG

Extracted DNA was diluted 1:50 to measure its concentration by spectrophotometry. All samples were diluted to 100 ng/μl using the formula $C_1V_1 = C_2V_2$ (concentration X volume). The PCR reactions of 50 μl were set up using 100 ng of DNA, 5 μl of each primer (10 μM) and 25 μl of Taq PCR Master Mix Kit (Quiagen, Valencia, CA). $MgCl_2$ concentration and annealing temperature were adjusted according to Table 4.1. Amplifications were performed in a MultiBlock PCR System (MBS) Thermal Cycler (Hybaid, Franklin,MA). The thermal protocol was: 95° C, 5 min, each of 30 PCR cycles consisted of denaturation at 94° C for 45 sec, annealing temperature (given in Table 1) for 45 sec, and extension at 72° C for 45 sec. After the last cycle, the samples were incubated at 72° C for an additional 20 min. Samples were analyzed using electrophoresis on 2% agarose gels in TAE and stained with ethidium bromide (0.5 μl/ml). The gels were scanned on a Typhoon 9410 imager (Amersham Biosciences Corp., Piscataway, NJ). The post-PCR reaction products of four exons of CD59 were purified using ExoSAP-IT (USB Corporation, Cleveland,OH) adding 1 μl of cleaning product to the 5 μl of reaction product directly following PCR. After incubation at 37° C for 15 min to degrade remaining primers and nucleotides, the mixture was incubated at 80° C for 15 min to inactivate ExoSAP-IT. DNA sequences were analyzed in both forward and reverse directions using an ABI3100 Genetic Analyzer (Applied Biosystems, Foster City,CA).

The sequenced exon fragments were compared with those in the Genebank database by BLAST analysis.

Table 4.1. PCR program adjustments for amplification of different gene markers.

Gene Marker	Annealing Temp (°C)	MgCl2 (mM)	Product Size (bp)
RAS	55	1.5	63
LDH A	57	3	407
CAT	65	4.5	207
CENTROMERE	62.5	3	130
APO	53	1.5	109
Exon 1	53.5	1.5	87
Exon 2	55	3.5	205
Exon 3	55	3.5	350
Exon 4	55	3.5	401

For DNA sequencing analysis the following programs and web sites were used:

1. For the DNA sequencing chromatogram viewing: FinchTV (Figure 4.7)

   http://www.geospiza.com/finchtv

2. For the DNA assembly: The CAP3 Sequence Assembly Program

   http://pbil.univ-lyon1.fr/cap3php

3. DNA multiple alignments of the nucleotide sequences: ClustalW

   http://www.ebi.ac.uk/clustalw/

   Output format: aln wo/numbers

   Output order: input

   and was done with manual adjustment.

4. DNA sequence editing: Boxshade

http://www.ch.embnet.org/software/BOX_form.html

Output format: RTF_new

Consensus Line: consensus line with letters

Input sequence format: ALN

And for editing also used BioEdit- Biological sequence alignment editor

http://www.mbio.ncsu.edu/BioEdit/bioedit.html

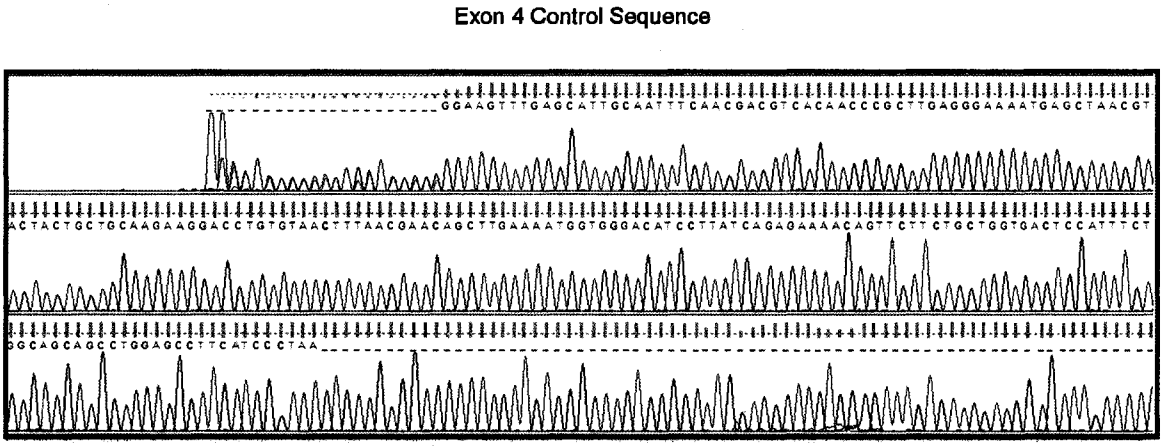

Figure 4.7. Exon 4 of CD59 gene, control sequence from DNA sample depicted on Finch TV, allowing the analysis and comparison of the whole sequence in one view.

Flow Cytometry

Flow cytometric quantification of mutant fractions was done using a CyAn flow cytometer (Dako, Fort Collins, CO) using 488 nm excitation and a 545 nm dichroic long pass and 575 nm band pass filter. 4 X 10^5 A_L cells were plated in six 15 mm Petri dishes,

3 control and 3 for treatment. Cells were placed in the anaerobic chamber for 24 hours for hypoxia treatment as described earlier and then transferred to normoxic conditions in a humidified incubator at 37 ° C. One day after hypoxia treatment marked as day 2, cells were passed (1.5 X 10^5 control cells passed to T75 flasks, 3 X 10^5 treated cells passed to T75 flask). On day 6, 1.5 X 10^5 cells were passed for control and treatment. On day 9, 2 X 10^5 cells were passed. On day 12, 1X10^6 cells were isolated from each of the three controls and treatment replicates. Cells were centrifuged and the pellet was suspended in 1 ml FACS buffer. After the cells were centrifuged a second time, they were suspended in 50 µl of CD59 specific monoclonal antibody conjugated to Phycoerythrin (PE) (1:40 dilution in FACS buffer). Cells were then incubated in a humidified 37° C environment containing 5% CO_2 for 30 minutes.

One ml cold FACS was then added to the cells and they were again centrifuged. Cells were finally suspended in 0.5 ml cold FACS and transferred to flow cytometry sample tubes on ice. 1X10^5 cells from each sample were analyzed on the flow cytometer. Within the PE histogram, the mutant region was defined as cells with fluorescence intensity less than 1% of the mean fluorescence intensity of the positive control peak ($CD59^+$) on a log scale (Figure 4.8).

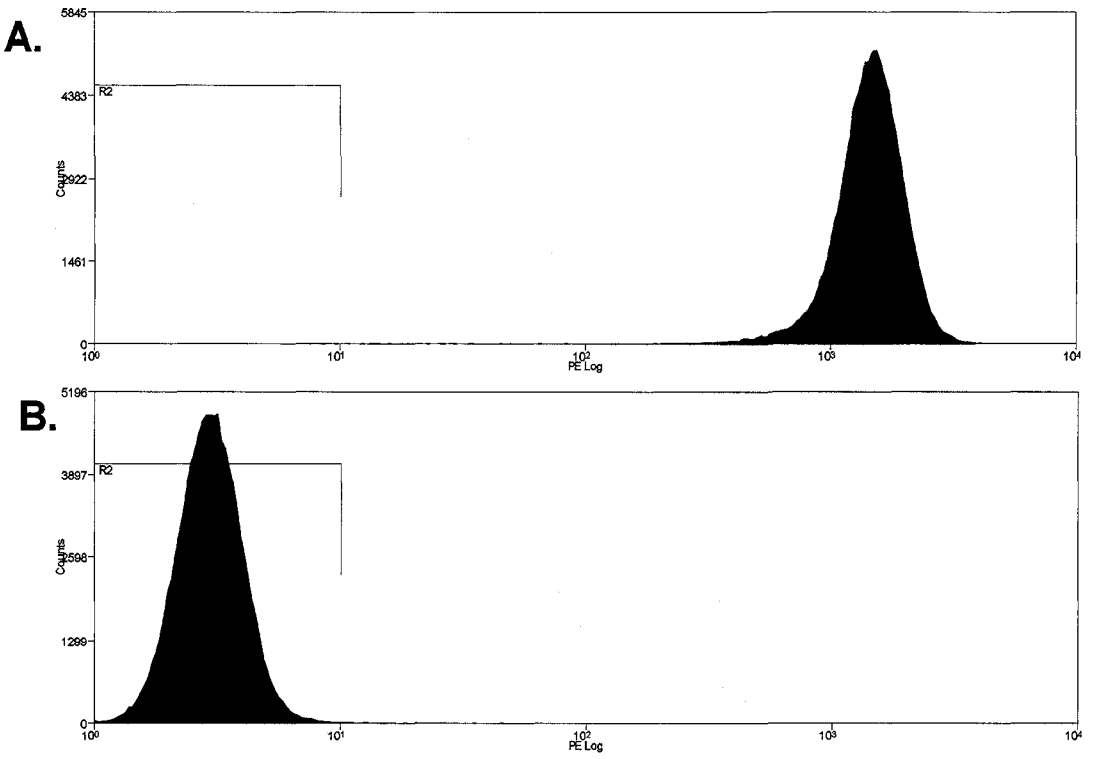

Figure 4.8. A. A_L CD59 positive stock cells. B. CD59 negative cells gated within a region set as 1% of the mean of the positive peak.

Mutant fractions were calculated as mutants per $1X10^5$ cells by subtracting background mutants (control cells) from mutants of the hypoxia treated cells.

Single cells were sorted from the mutant region of hypoxia treated cells on day 12 after treatment using a Dako MoFlo cell sorter (same cell preparation as the flow cytometry analysis). These cells were allowed to form colonies in 96 well plates. After 21 days clones were transferred to T25 plates and expanded. $1X10^6$ cells were isolated and run on the flow cytometer using the previous procedure to determine if cells sorted from the mutant region were truly negative for CD59.

RESULTS

Survival Curves

The cells were exposed to different pO_2 and for various durations to determine the optimum time of exposure for each hypoxia level. As described earlier, I determined the exposure time that gave 50% survival, which left enough surviving cells (more than10^5) to perform the challenge with complement and antibody. Figure 4.4. and Figure 4.9. are examples of the survival curves constructed for two experimental conditions. They show the optimum time of exposure to 0.1% pO_2 is four days, while for the severe hypoxia below 0.1% O_2 optimum it is 24 hours.

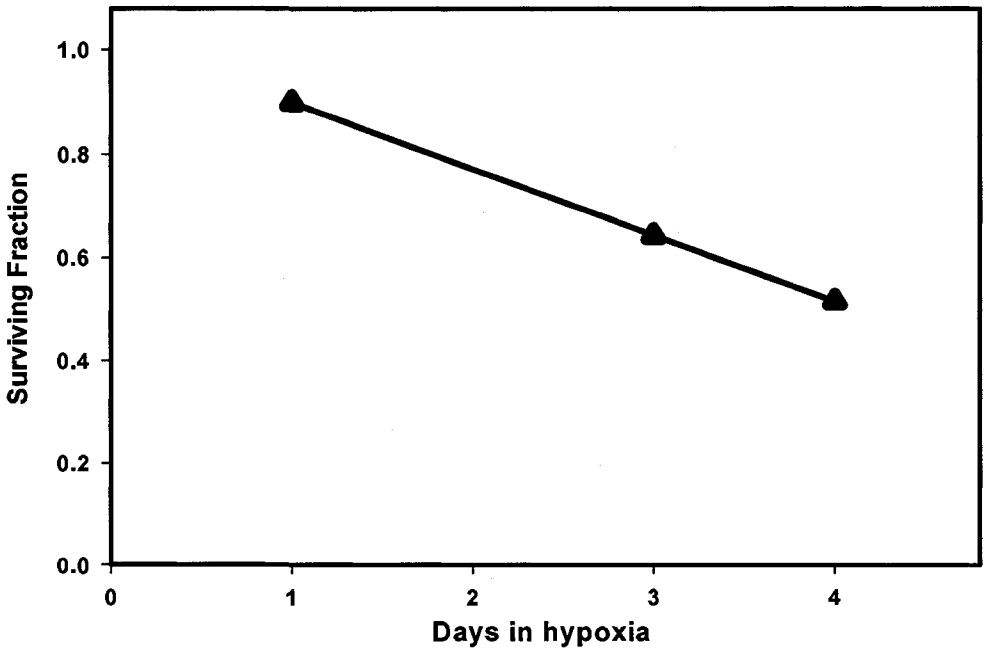

Figure 4.9. Survival curve for A_L cells grown in 0.1% O_2 (0.63 mmHg)

Mutant induction

Cells exposed to 2.5% pO_2 (15.75 mm Hg) were mutated at the rate of 29-58 mutations per 10^5 cells (Figure 4.3). Radiobiological hypoxia is the level of hypoxia that results in attenuated tumor cell death due to radiation, and by definition partial radioresistance begins at oxygen tensions of 10 mmHg (Steen, 1991). Thus, mutants from cells exposed to 15.75 mm Hg were regarded as background mutants. For cells treated with 1% pO_2 , I found inconsistent results in repeated assays and the average number of mutants was no different after four days in this hypoxic condition from the cells kept in standard conditions. For the cells exposed to 1% pO_2 for seven days the average number of mutants per 10^5 cells was 19. Cells grown in 0.1% pO_2 for four days had an average of 17 mutants per 10^5 surviving cells. Significant mutation induction was seen only among the cells exposed to severe hypoxia, pO_2 less than 0.63 mmHg (0-0.1%) for one day. Under these conditions the number of mutants was on average 130 per 10^5 surviving cells (Figure 4.10).

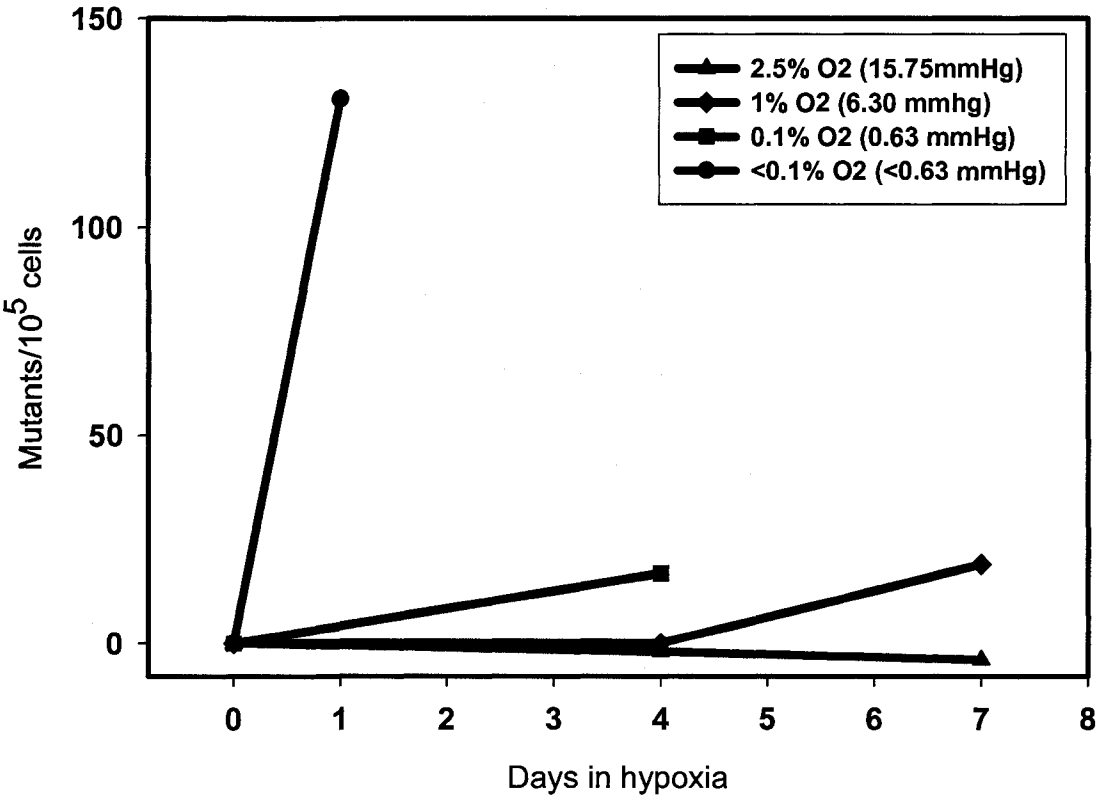

Figure 4.10. Mutant yield for CHO A_L cells treated with different hypoxic conditions. The number of mutants is corrected for background mutants.

Flow Cytometry[1]

The development of flow cytometric analysis of CD59 mutants using the A_L cell line, without the need for a complement-mediated cytotoxicity assay, significantly reduces the time needed for each experiment. The proportions of $CD59^-$ and $CD59^+$ cells can be analyzed in one step by flow cytometry (Ross et al, 2005; Wedemeyer et al, 2001; Zhou et al, 2006).

[1] These experiments were done by Steve Keysar in Dr. Fox's lab

It is very important to have sufficient fluorescence separation between cells expressing the CD59 antigen ($CD59^+$) and mutated $CD59^-$ cells, in order to adequately differentiate and quantify mutants (French et al, 2006). The mutant region was gated as 1% of the mean fluorescence intensity of the positive control peak (Figure 4.11). This gave a 400-fold separation in fluorescence intensity between the two peaks, which is adequate to differentiate $CD59^-$ from $CD59^+$ cells.

Cells were treated with less than 0.1% O_2 for 24 hours, the same as the traditional complement/antibody assay. 10^5 cells were analyzed for each experiment for statistical significance. The number of mutants per 10^5 surviving cells on average was 136, about the same compared to results from complement/antibody assays (Table 4.2).

Flow cytometry histograms from these experiments demonstrate the quantification of CD59 mutants from control cell population and cell population treated with hypoxia (Figure 4.11).

To determine whether these $CD59^-$ cells were really mutants and not just CD59 downregulated and temporarily expressed as mutants, single cells were sortedfrom the mutant region of hypoxia treated cells, allowed to grow into colonies, and after 21 days these cells were analyzed by flow cytometry. Out of 21 clonal populations, 16 fell within the mutant region they were sorted from while 5 clones showed intermediate or normal CD59 expression. This demonstrated that most cells scored as mutants are truly negative for CD59 (Figure 4.12).

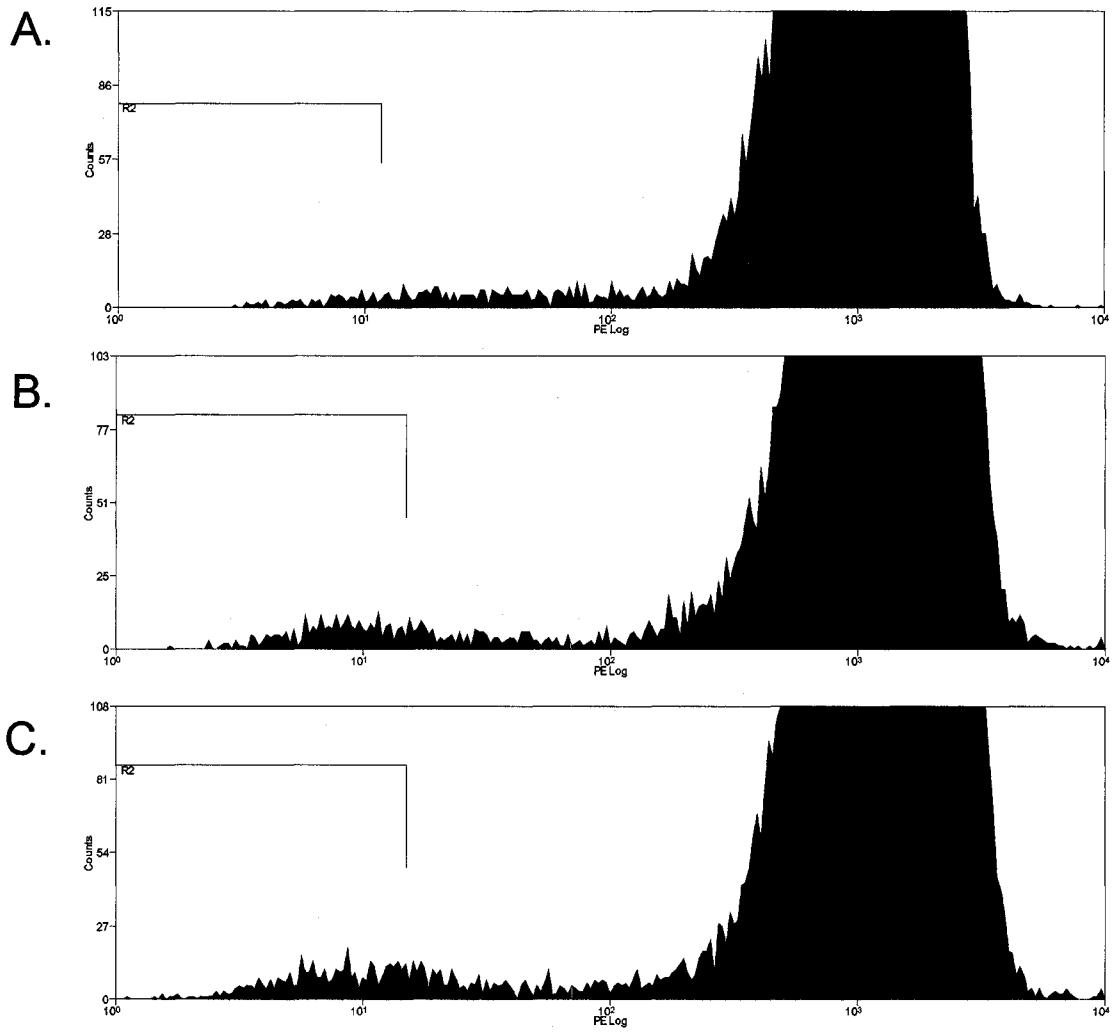

Figure 4.11. A. Control stained cells with gated region set as 1% of the positive peak and used to measure CD59 mutants. C. and B. Day 12 histograms of cells which were hypoxic for 24 hours.

Table 4.2. Flow cytometry analysis of mutants in A_L cells treated with <0.1 % pO_2 (<0.63 mm Hg). Mutant fraction reported as number of mutants per 10^5 surviving cells and after subtracting background mutations.

Experiment 1			Experiment 2			Experiment 3		
Replicate	Control 1	Treatment 1	Replicate	Control 2	Treatment 2	Replicate	Control 3	Treatment 3
A	165	264	A	182	365	A	117	261
B	143	281	B	169	251	B	128	213
C	NA	281	C	NA	404	C	116	260
Average	154	275	Average	176	340	Average	120.33	244.66
SEM	11	5.7	SEM	6.5	45.9	SEM	3.8	15.8
mutant fraction			mutant fraction			mutant fraction		
121			165			124		
P value <0.01								

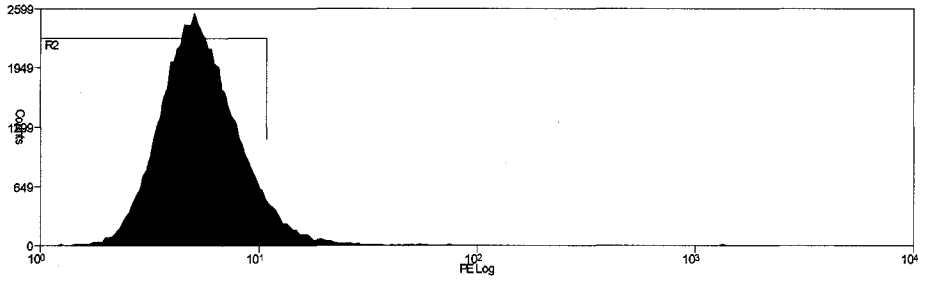

Figure 4.12. Hypoxia clone twenty days after sorting, then stained with monoclonal antibodies against CD59. 95% of the sample falls within the CD59 negative region it was sorted from.

Mutant spectra

To determine the types of mutation that cause the $CD59^-$ phenotype in hypoxia-treated A_L cells, we isolated individual clones and applied PCR. Five marker genes on chromosome 11 were amplified to determine the presence or absence of corresponding PCR products (Figure 4.5). In this study $CD59^-$ mutants retained all five of the human chromosome 11 markers (Figure 4.13). PCR analysis of the CD59 gene was obtained by providing primer pairs for the four exons of CD59 gene. PCR analysis of the four exons of the CD59 gene from $CD59^-$ mutants (Figure 4.14) shows no loss of these markers. As no deletions were detected on the chromosome 11 with the chosen markers, and mutations in the human chromosome were smaller than 27 kb (the size of the CD59 gene) the analyses indicate the induction of point mutations or very small deletions in the A_L cells grown in severe hypoxia.

DNA Sequencing results

The same primers used for the PCR analysis of the four exons of the CD59 gene were utilized to produce DNA sequences for further analysis of the mutants induced by hypoxia. Since exon 1 is a non-coding exon of the gene, only exons 2, 3, and 4 were sequenced. The human reference sequence used was NM_000611.4 (from NCBI website).The analysis did not show mutations in DNA sequences that were examined (Figure 4.15). For exon 4, only one replicate was done because the one direction was unsuccessful, possibly due to inadequate DNA template or primers (Figure 4.16).

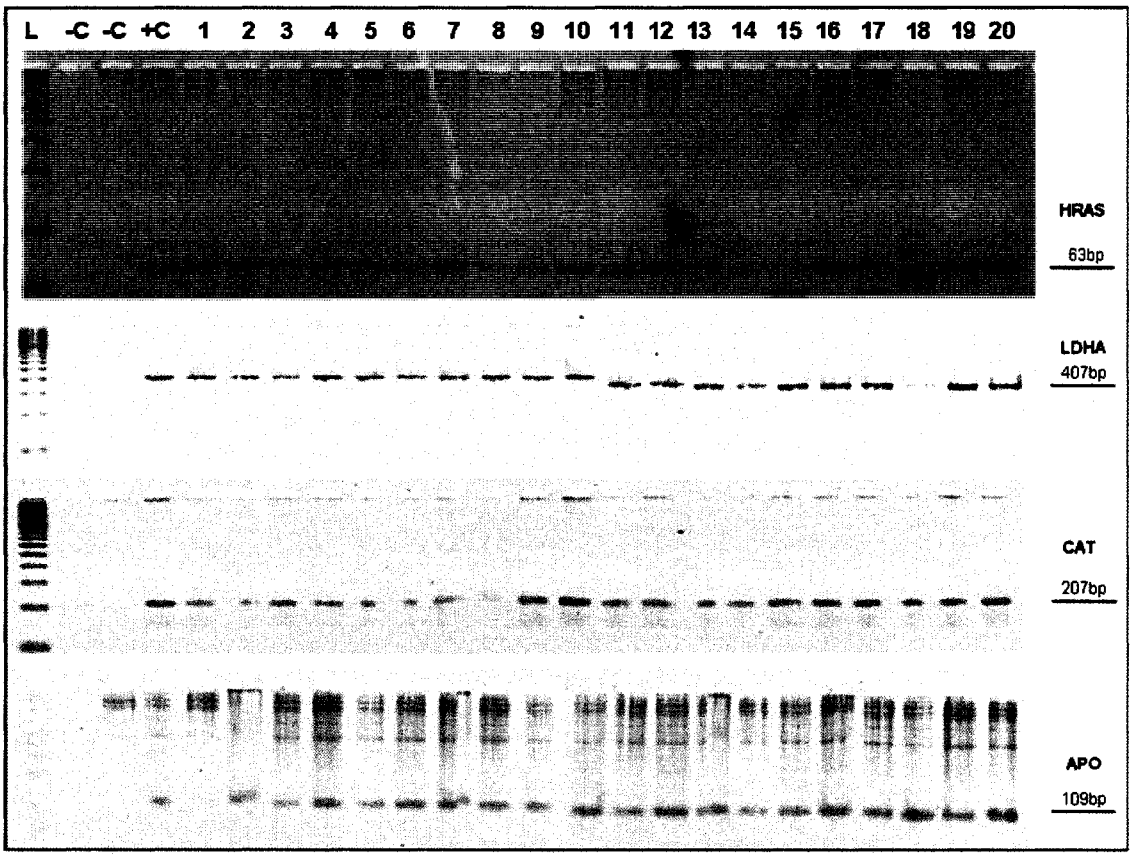

Figure 4.13. Gel electrophoresis of PCR products using DNA from CD59- mutants as templates and primers for RAS, LDHA, CAT, and APO. In each first lane is a size ladder (L), than (-C) are negative controls (no DNA, and CHO cells), next lane as a positive control wild-type CD59+ cells, and 1-20 are CD59-mutants induced by hypoxia. All samples show no loss of these markers.

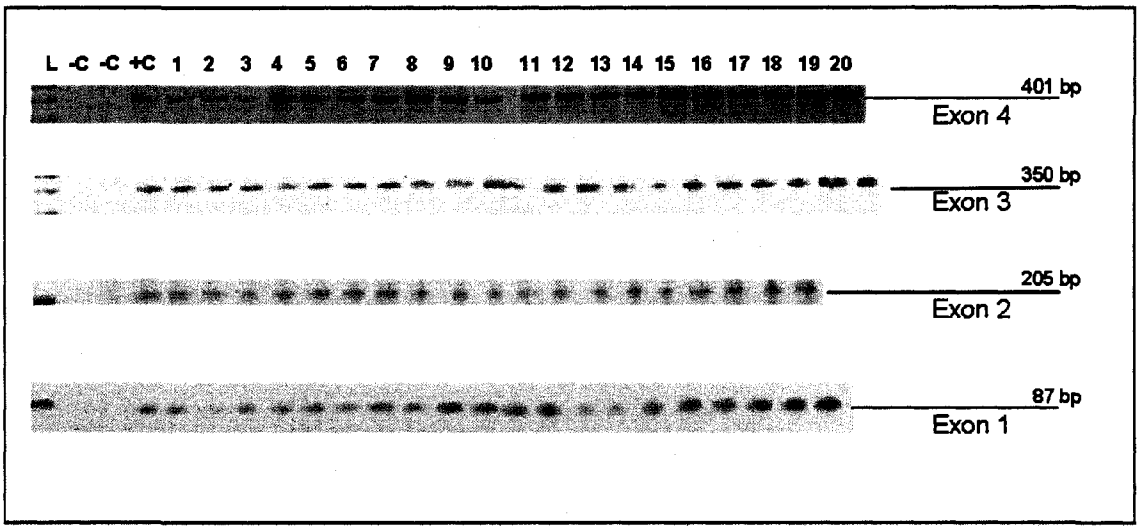

Figure 4.14. Gel electrophoresis of PCR products using DNA from CD59- mutants as templates and primers for four exons of CD59. Gels are done and marked the same as in Figure 4.13. All samples show no loss of these markers.

CD59

Exon 2 (67 bp)

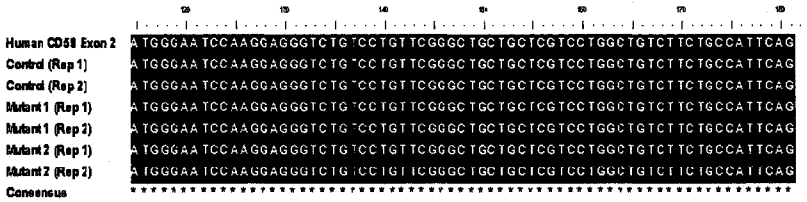

Exon 3 (102 bp)

Figure 4.15. Alignment of human CD59 gene sequences, control DNA sequences and DNA sequences from mutant cells, for double replicas of exon 2 and exon 3. It shows no mutation in depicted sequences.

Exon 4 (218 bp)

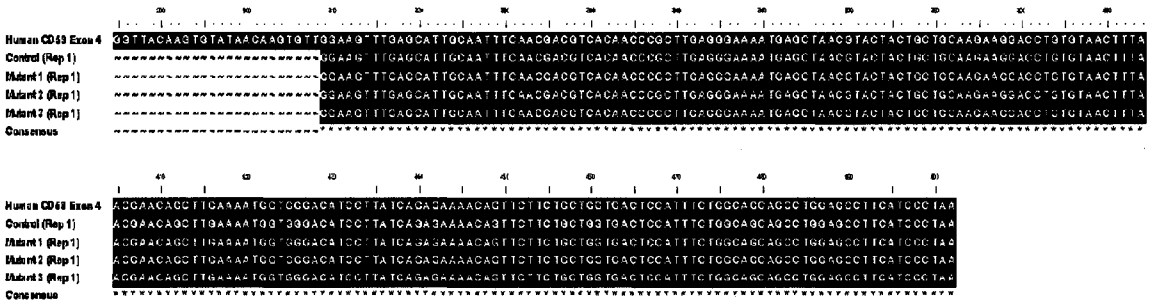

Figure 4.16. Alignment of human CD59 gene sequence, control DNA sequence and DNA sequences from mutant cells, for one replica of exon 4.It shows no mutation in depicted sequences. "~" symbol for unreadable first 24 nucleotides (8 amino acids).

DISCUSSION

The results of this study indicated that exposure to severe hypoxia induces mutations in A_L cells, and there was a quantitative difference in mutant induction depending on the level of the oxygen present. The mutants reported in this study were induced by radiobiological hypoxia at the CD59 locus of A_L cells.

It has previously been reported that tumor microenvironment or conditions mimicking that milieu *in vitro*, are responsible for increased mutations (Reynolds et al, 1996; Wilkinson et al, 1995), increased drug resistance (Yuan et al, 2000; Reynolds et al, 1996; Rice et al, 1987), and are associated with various DNA lesions (Hammond et al, 2002, 2003; Rice et al, 1986). Hypoxia found in human malignant tumors was associated with more clinically aggressive phenotypes (Brizel et al, 1996, 2000; Hockel et al, 1996, 1998; Rofstad et al, 2000; Walenta and Mueller-Klieser, 2004). There is growing evidence that hypoxia induces proteome changes which may lead to the impairment of tumor growth activating anaerobic metabolism, angiogenesis, tissue remodeling, and may promote tumor propagation (Hockel and Vaupel, 2001). Exposure to hypoxic and acidic environments has been shown to induce changes in gene expression. As noted before, tumor microenvironment is characterized by nutrient deprivation, low pH, and hypoxic regions, and each of these factors has been shown to cause changes in cell metabolism and physiology (Yuan and Glazer, 1998; Reynolds et al, 1996). According to work done in this field, there is abundant evidence that tumor microenvironment is associated with the induction of mutagenesis. Tumor microenvironment may induce DNA damage

(Reynolds et al, 1996), and as shown recently, is also associated with deregulation of DNA repair pathways (Yuan et al, 2000; Mihaylova et al, 2003; Bindra et al, 2004).

In this study I evaluated whether hypoxia alone could induce mutations and if so, to what extent. The A_L assay has been proven useful in showing a spectrum of chromosome mutations that can range up to deletions of 140 million base pairs (Waldren et al, 1998). I changed only the oxygen status in the experiments, and kept nutrition and pH of media (pH measurements were between 7.2 and 7.5) the same for all cells, both those exposed to hypoxia and cells in normal conditions. Hypoxia, or hypoxia/reoxygenation, induced mutations in CHO A_L cells that were significant at partial pressure of oxygen less than 0.1% (0.63 mm Hg). These results confirm the reliability of the A_L assay in detecting mutants induced experimentally by different mutagens. Ionizing radiation (Kraemer et al, 2000; Hei et al, 1988; Ueno et al, 2002; Ross et al, 2005) and a variety of chemical agents (Waldren et al, 1999; Zhou et al, 1999; Hei et al, 1998; French et al, 2006), produced mutants that have lost CD59 gene or larger portions of human chromosome 11 (Waldren et al, 1999; Kraemer et al, 2001).

Hypoxia did not produce drastic deletions as some other clastogens did, but induced mutations that in tumor cells may lead to more progressive tumor phenotypes. The difference in mutation induction depending on hypoxia intensity indicates that hypoxia alone, rather than reoxygenation, caused these changes. After the exposure to hypoxic conditions, cells were kept in normoxia while subculturing during the expression period in which the surface expression of CD59 is lost (Hei et al, 1988).

It appears that hypoxia alone can produce only SSBs and a possible explanation for my results may be found in the fact that hypoxia can result in an S-phase arrest (reversible

after reoxygenation) (Hammond et al, 2002). Thus hypoxia is involved in inhibition of initiation of replication, and consequently can not directly cause considerable DNA damage (Bindra and Glazer, 2005). Our results are consistent with the findings that hypoxia can induce point mutations without inducing DSBs (Reynolds et al, 1996; Hammond et al, 2002). In this study, flow cytometry analysis of mutants confirmed that an extremely low level of oxygen is associated with mutation induction. Single cells that were sorted from the mutant region of hypoxia treated cells and allowed to form colonies were subsequently analyzed using the same flow cytometry analysis method. The majority of the clones remained within the mutant region from which they were originally sorted. Only 5 out of 21 clonal populations showed some CD59 expression. This could possibly be due to sorting error, and more experiments could be needed to verify these results. The sorting results demonstrated that most cells scored as mutants were truly negative for CD59.

Since PCR analysis and DNA sequencing analysis that was performed in these experiments did not detect changes in different genes on chromosome 11, or in exons of the CD59 gene, to further exploit hypoxia-produced changes it may be useful to perform analysis of a greater number of mutants, and maybe do better primers design for DNA sequencing. There is a possibility that loss of expression of the CD59 surface antigen can be caused by mutations in the CD59 gene or by mutation in any one of about a dozen CHO genes involved in expression of the GPI anchor that attaches CD59 antigen to the cell surface (Kraemer et al, 2001). Therefore, one of the directions in the future investigations could be analysis of the CHO genes that encode the GPI anchor (Kinoshita et al, 1997; Nakamura et al, 1997).

It has recently been shown that nearly half of ionizing radiation-induced mutants in CD59 also lost the expression of CD90, another gene on chromosome 11 that is anchored by GPI. Direct analysis of the GPI anchor showed that 33% of the double mutants were defective for the GPI anchor (Ross et al, 2007), most likely in the X-linked Pig A gene. It is important to understand the role of hypoxia in tumor development and progression, as well as its role in treatment resistance and importance of its prognostic aspect. This would be beneficial for the possible development of novel therapeutic strategies that, by targeting tumor hypoxia, may influence genomic stability and result in a better prognosis for patients with hypoxic tumors.

BIBLIOGRAPHY

1. Bindra RS, Schaffer PJ, Meng A, Woo J, Maseide K, Roth ME, Lizardi P, Hedley DW, Bristow RG, Glazer PM (2004) Down-regulation of Rad51 and decreased homologous recombination in hypoxic cancer cells. *Molecular & Cellular Biology* 24: 8504-8518

2. Bindra RS, Glazer PM (2005) Genetic instability and the tumor microenvironment: towards the concept of microenvironment-induced mutagenesis. [Review] [79 refs]. *Mutation Research* 569: 75-85

3. Brizel DM, Scully SP, Harrelson JM, Layfield LJ, Bean JM, Prosnitz LR, Dewhirst MW (1996) Tumor oxygenation predicts for the likelihood of distant metastases in human soft tissue sarcoma. *Cancer Research* 56: 941-943

4. Brizel DM, Schroeder T, Scher RL, Walenta S, Clough RW, Dewhirst MW, Mueller-Klieser W (2001) Elevated tumor lactate concentrations predict for an increased risk of metastases in head-and-neck cancer. *International Journal of Radiation Oncology, Biology, Physics* 51: 349-353

5. Brown JM, Giaccia AJ (1998) The unique physiology of solid tumors: opportunities (and problems) for cancer therapy. [Review] [112 refs]. *Cancer Research* 58: 1408-1416

6. Cairns RA, Khokha R, Hill RP (2003) Molecular mechanisms of tumor invasion and metastasis: an integrated view. [Review] [146 refs]. *Current Molecular Medicine* 3: 659-671

7. Cuvier C, Jang A, Hill RP (1997) Exposure to hypoxia, glucose starvation and acidosis: effect on invasive capacity of murine tumor cells and correlation with cathepsin (L + B) secretion. *Clinical & Experimental Metastasis* 15: 19-25

8. Denko N, Schindler C, Koong A, Laderoute K, Green C, Giaccia A (2000) Epigenetic regulation of gene expression in cervical cancer cells by the tumor microenvironment. *Clinical Cancer Research* 6: 480-487

9. Denko NC, Fontana LA, Hudson KM, Sutphin PD, Raychaudhuri S, Altman R, Giaccia AJ (2003) Investigating hypoxic tumor physiology through gene expression patterns. [Review] [86 refs]. *Oncogene* 22: 5907-5914

10. Dewhirst MW, Secomb TW, Ong ET, Hsu R, Gross JF (1994) Determination of local oxygen consumption rates in tumors. *Cancer Research* 54: 3333-3336

11. Fenton BM, Kiani MF, Siemann DW (1995) Should direct measurements of tumor oxygenation relate to the radiobiological hypoxic fraction of a tumor? *International Journal of Radiation Oncology, Biology, Physics* 33: 365-373

12. French CT, Ross CD, Keysar SB, Joshi DD, Lim CU, Fox MH (2006) Comparison of the mutagenic potential of 17 physical and chemical agents analyzed by the flow cytometry mutation assay. *Mutation Research* 602: 14-25

13. Hammond EM, Denko NC, Dorie MJ, Abraham RT, Giaccia AJ (2002) Hypoxia links ATR and p53 through replication arrest. *Molecular & Cellular Biology* 22: 1834-1843

14. Hammond EM, Green SL, Giaccia AJ (2003) Comparison of hypoxia-induced replication arrest with hydroxyurea and aphidicolin-induced arrest. *Mutation Research* 532: 205-213

15. Hei TK, Hall EJ, Waldren CA (1988) Mutation induction and relative biological effectiveness of neutrons in mammalian cells. Experimental observations. *Radiation Research* 115: 281-291

16. Hei TK, Liu SX, Waldren C (1998) Mutagenicity of arsenic in mammalian cells: role of reactive oxygen species. *Proceedings of the National Academy of Sciences of the United States of America* 95: 8103-8107

17. Hockel M, Schlenger K, Aral B, Mitze M, Schaffer U, Vaupel P (1996) Association between tumor hypoxia and malignant progression in advanced cancer of the uterine cervix. *Cancer Research* 56: 4509-4515

18. Hockel M, Schlenger K, Hockel S, Aral B, Schaffer U, Vaupel P (1998) Tumor hypoxia in pelvic recurrences of cervical cancer. *International Journal of Cancer* 79: 365-369

19. Hockel M, Vaupel P (2001) Tumor hypoxia: definitions and current clinical, biologic, and molecular aspects. [Review] [162 refs]. *Journal of the National Cancer Institute* 93: 266-276

20. Kao FT, Puck TT (1968) Genetics of somatic mammalian cells, VII. Induction and isolation of nutritional mutants in Chinese hamster cells. *Proceedings of the National Academy of Sciences of the United States of America* 60: 1275-1281

21. Kim IH, Lemmon MJ, Brown JM (1993) The influence of irradiation of the tumor bed on tumor hypoxia: measurements by radiation response, oxygen electrodes, and nitroimidazole binding. *Radiation Research* 135: 411-417

22. Kinoshita T, Ohishi K, Takeda J (1997) GPI-anchor synthesis in mammalian cells: genes, their products, and a deficiency. [Review] [50 refs]. *Journal of Biochemistry* 122: 251-257

23. Kondo A, Safaei R, Mishima M, Niedner H, Lin X, Howell SB (2001) Hypoxia-induced enrichment and mutagenesis of cells that have lost DNA mismatch repair. *Cancer Research* 61: 7603-7607

24. Koong AC, Denko NC, Hudson KM, Schindler C, Swiersz L, Koch C, Evans S, Ibrahim H, Le QT, Terris DJ, Giaccia AJ (2000) Candidate genes for the hypoxic tumor phenotype. *Cancer Research* 60: 883-887

25. Kraemer SM, Kronenberg A, Ueno A, Waldren CA (2000) Measuring the spectrum of mutation induced by nitrogen ions and protons in the human-hamster hybrid cell line A(L)C. *Radiation Research* 153: 743-751

26. Kraemer SM, Vannais DB, Kronenberg A, Ueno A, Waldren CA (2001) Gamma-ray mutagenesis studies in a new human-hamster hybrid, A(L)CD59(+/-), which has two human chromosomes 11 but is hemizygous for the CD59 gene. *Radiation Research* 156: 10-19

27. McGuinness SM, Shibuya ML, Ueno AM, Vannais DB, Waldren CA (1995) Mutant quantity and quality in mammalian cells (AL) exposed to cesium-137 gamma radiation: effect of caffeine.[erratum appears in Radiat Res 1997 Jan;147(1):120]. *Radiation Research* 142: 247-255

28. Mihaylova VT, Bindra RS, Yuan J, Campisi D, Narayanan L, Jensen R, Giordano F, Johnson RS, Rockwell S, Glazer PM (2003) Decreased expression of the DNA mismatch repair gene Mlh1 under hypoxic stress in mammalian cells. *Molecular & Cellular Biology* 23: 3265-3273

29. Nakamura N, Inoue N, Watanabe R, Takahashi M, Takeda J, Stevens VL, Kinoshita T (1997) Expression cloning of PIG-L, a candidate N-acetylglucosaminyl-phosphatidylinositol deacetylase. *Journal of Biological Chemistry* 272: 15834-15840

30. Petranka JG, Fleenor DE, Sykes K, Kaufman RE, Rosse WF (1992) Structure of the CD59-encoding gene: further evidence of a relationship to murine lymphocyte antigen Ly-6 protein.[erratum appears in Proc Natl Acad Sci U S A 1993 Jun 15;90(12):5878]. *Proceedings of the National Academy of Sciences of the United States of America* 89: 7876-7879

31. Puck TT, Wuthier P, Jones C, Kao FT (1971) Genetics of somatic mammalian cells: lethal antigens as genetic markers for study of human linkage groups. *Proceedings of the National Academy of Sciences of the United States of America* 68: 3102-3106

32. Reynolds TY, Rockwell S, Glazer PM (1996) Genetic instability induced by the tumor microenvironment. *Cancer Research* 56: 5754-5757

33. Rice GC, Hoy C, Schimke RT (1986) Transient hypoxia enhances the frequency of dihydrofolate reductase gene amplification in Chinese hamster ovary cells. *Proceedings of the National Academy of Sciences of the United States of America* 83: 5978-5982

34. Rice GC, Ling V, Schimke RT (1987) Frequencies of independent and simultaneous selection of Chinese hamster cells for methotrexate and doxorubicin (adriamycin) resistance. *Proceedings of the National Academy of Sciences of the United States of America* 84: 9261-9264

35. Rofstad EK, Sundfor K, Lyng H, Trope CG (2000) Hypoxia-induced treatment failure in advanced squamous cell carcinoma of the uterine cervix is primarily due to hypoxia-induced radiation resistance rather than hypoxia-induced metastasis. *British Journal of Cancer* 83: 354-359

36. Ross CD, Lim CU, Fox MH (2005) Assay to measure CD59 mutations in CHO A(L) cells using flow cytometry. *Cytometry Part A: The Journal of the International Society for Analytical Cytology* 66: 85-90

37. Ross CD, French CT, Keysar SB, Fox MH (2007) Mutant spectra of irradiated CHO AL cells determined with multiple markers analyzed by flow cytometry. *Mutation Research* 624: 61-70

38. Steen RG (1991) Characterization of tumor hypoxia by 31P MR spectroscopy. [Review] [40 refs]. *AJR* American Journal of Roentgenology. 157: 243-248

39. Ueno A, Vannais D, Lenarczyk M, Waldren CA (2002) Ascorbate, added after irradiation, reduces the mutant yield and alters the spectrum of CD59- mutations in A(L) cells irradiated with high LET carbon ions. *Journal of Radiation Research* 43 Suppl: S245-S249

40. Vaupel P (2004) Tumor microenvironmental physiology and its implications for radiation oncology. [Review] [55 refs]. *Seminars in Radiation Oncology* 14: 198-206

41. Waldren C, Vannais D, Drabek R, Gustafson D, Kraemer S, Lenarczyk M, Kronenberg A, Hei T, Ueno A (1998) Analysis of mutant quantity and quality in human-hamster hybrid AL and AL-179 cells exposed to 137Cs-gamma or HZE-Fe ions. *Advances in Space Research* 22: 579-585

42. Waldren, C. A, Jones, C, and Puck, T. T. Measurement of mutagenesis in mammalian cells. Proceedings of the National Academy of Sciences of the United States of America 76[3], 1358-1362. 1979.
Ref Type: Generic

43. Waldren, C. A, Correl, L, Sognier, M. A, and Puck, T. T. Measurement of low levels of x-ray mutagenesis in relation to human desease. Proceedings of the National Academy of Sciences of the United States of America 83, 4839-4843. 1986.
Ref Type: Generic

44. Waldren CA, Ueno AM, Schaeffer BK, Wood SG, Sinclair PR, Doolittle DJ, Smith CJ, Harvey WF, Shibuya ML, Gustafson DL, Vannais DB, Puck TT, Sinclair JF (1999) Mutant yields and mutational spectra of the heterocyclic amines MeIQ and PhIP at the S1 locus of human-hamster AL cells with activation by chick embryo liver (CELC) co-cultures. *Mutation Research* 425: 29-46

45. Waldren CA, Vannais DB, Ueno AM (2004) A role for long-lived radicals (LLR) in radiation-induced mutation and persistent chromosomal instability: counteraction by ascorbate and RibCys but not DMSO. *Mutation Research* 551: 255-265

46. Walenta S, Mueller-Klieser WF (2004) Lactate: mirror and motor of tumor malignancy. [Review] [47 refs]. *Seminars in Radiation Oncology* 14: 267-274

47. Wedemeyer N, Greve B, Uthe D, Potter T, Denklau D, Severin E, Hacker-Klom U, Kohnlein W, Gohde W (2001) Frequency of CD59 mutations induced in human-hamster hybrid A(L) cells by low-dose X-irradiation. *Mutation Research* 473: 73-84

48. Wilkinson D, Sandhu JK, Breneman JW, Tucker JD, Birnboim HC (1995) Hprt mutants in a transplantable murine tumour arise more frequently in vivo than in vitro. *British Journal of Cancer* 72: 1234-1240

49. Yuan J, Glazer PM (1998) Mutagenesis induced by the tumor microenvironment. [Review] [47 refs]. *Mutation Research* 400: 439-446

50. Yuan J, Narayanan L, Rockwell S, Glazer PM (2000) Diminished DNA repair and elevated mutagenesis in mammalian cells exposed to hypoxia and low pH. *Cancer Research* 60: 4372-4376

51. Zhou H, Zhu LX, Li K, Hei TK (1999) Radon, tobacco-specific nitrosamine and mutagenesis in mammalian cells. *Mutation Research* 430: 145-153

52. Zhou H, Xu A, Gillispie JA, Waldren CA, Hei TK (2006) Quantification of CD59-mutants in human-hamster hybrid (AL) cells by flow cytometry. *Mutation Research* 594: 113-119

53. Zhu LX, Waldren CA, Vannias D, Hei TK (1996) Cellular and molecular analysis of mutagenesis induced by charged particles of defined linear energy transfer. *Radiation Research* 145: 251-259

CHAPTER 5

CONCLUSIONS

The two sections of this dissertation are concerned with a common feature of the tumor microenvironment: tumor hypoxia. Even though extensively investigated in various experimental settings and tumor models for over 50 years, many unanswered questions remain. The causes and consequences of tumor hypoxia are significant because of its impact on cancer progression and resistance to therapy.

The term tumor hypoxia is still not precisely defined. From the radiation biology perspective, importance is given to the level of oxygen in the tumor that causes tumor cells to become resistant to killing by radiation. This is referred to as radiobiological hypoxia. The level of hypoxia that causes radioresistance is lower than the level necessary to cause other hypoxia-related biological phenomena (such as cell growth, cell survival, and angiogenesis). Tumor cells start developing radioresistance at a pO_2 of 10 mmHg, and are completely resistant at oxygen levels less than 1 mmHg (Steen, 1991). This 10 mmHg benchmark has been used by many authors as the threshold of tumor hypoxia. More recent studies are advocating measurements of tumor oxygen levels less than 5 mmHg as hypoxic, or even below 2.5 mmHg as a more meaningful clinical predictor. This has been applied to clinical studies in human and veterinary medicine.

Furthermore, some authors are defining radiobiological hypoxia at even lower oxygen levels like those of the maximally radioresistant fraction of tumor cells found at $pO_2 < 1$ mm Hg or <0.5 mm Hg (Gulledge and Dewhirst, 1996; Wouters and Brown, 1997, respectively). The confusion about tumor hypoxia thus begins with the understanding of what we consider hypoxic region in tumor: value of pO_2 less than 10, 5, 2.5 mm Hg or less than 1, or 0.5 mm Hg; the oxygen level were cell radioresistance start to develop, progress through that development or when cells are fully resistant to radiation.

Part 1 is an *in vivo* study of changes of oxygen level in tumors after a single dose of radiation treatment. Measuring oxygen partial pressures and other biological parameters in spontaneously developed canine tumors revealed that their microenvironment is very much comparable to the human tumors. We evaluated changes after radiation, but also gained insight in unperturbed tumor microenvironment. Tumor microenvironment is shown to be very complex and tumor hypoxia has to be regarded in that complexity. The classification to perfusion-limited and diffusion-limited oxygen delivery is really oversimplified. Many other parameters are playing a role in the development of tumor hypoxia, and it is important to examine this problem in the complex three-dimensional view as a part of tumor microenvironment. Even more, doing my research with CHO A_L assay and creating the survival curves to determine what the exposure of the cells to hypoxic conditions should be, I demonstrated a role for time. The consequences of different levels of hypoxia were greatly influenced by the time of the exposure, adding the new dimension to the mosaic of hypoxic conditions.

Part 2 is concerned with the role of hypoxia in the induction of mutagenesis and subsequently in genomic instability, which is a hallmark of malignancies. This *in vitro*

study gave us insight in the possible and probable development of the chain of the events that could lead to a more aggressive tumor behavior.

The results of the second study showed that extreme hypoxia may lead to mutagenesis. The results of the first study proved that this level of hypoxia is present in most of the hypoxic regions existing in naturally occurring tumors.

Both of my studies have an implication in the present understanding of tumor treatment failure. The main factors determining disease control after radiation therapy are tumor radioresistance and incidence of tumor metastasis (West et al, 1997; Lyng et al, 2000). Hypoxia may induce genetic instability of tumors leading to increased metastatic potential (Young et al, 1988; Reynolds et al, 1996). The hypoxia-induced radioresistance is dependant on oxygenation at the time of irradiation, relying on changes in biological parameters responsible for the oxygen supply and consumption in the tumor. As stated by Overgaard (2007), among the several thousands of publications about hypoxia and radiation therapy, only about 3% address hypoxia in the therapeutic clinical setting. Therefore, studies of the changes in these parameters after a fraction of radiation during scheduled radiation treatment are needed, and studies performed in a clinical setting must incorporate concepts related to tumor hypoxia into routine clinical use, which is still very limited.

BIBLIOGRAPHY

1. Gulledge CJ, Dewhirst MW (1996) Tumor oxygenation: a matter of supply and demand. [Review] [68 refs]. *Anticancer Research* 16: 741-749

2. Lyng H, Sundfor K, Trope C, Rofstad EK (2000) Disease control of uterine cervical cancer: relationships to tumor oxygen tension, vascular density, cell density, and frequency of mitosis and apoptosis measured before treatment and during radiotherapy. *Clinical Cancer Research* 6: 1104-1112

3. Overgaard J (2007) Hypoxic radiosensitization: adored and ignored. [Review] [74 refs]. *Journal of Clinical Oncology* 25: 4066-4074

4. Steen RG (1991) Characterization of tumor hypoxia by 31P MR spectroscopy. [Review] [40 refs]. *AJR* American Journal of Roentgenology. 157: 243-248

5. West CM, Davidson SE, Roberts SA, Hunter RD (1997) The independence of intrinsic radiosensitivity as a prognostic factor for patient response to radiotherapy of carcinoma of the cervix.[see comment]. *British Journal of Cancer* 76: 1184-1190

6. Wouters BG, Brown JM (1997) Cells at intermediate oxygen levels can be more important than the "hypoxic fraction" in determining tumor response to fractionated radiotherapy. *Radiation Research* 147: 541-550